Salmonid Selection, Evolution, and Historical Abundance Patterns

Curry James Cunningham

A dissertation

submitted in partial fulfillment of the

requirements for the degree of

Doctor of Philosophy

University of Washington

2015

Reading Committee:

Ray Hilborn, Chair

Thomas P. Quinn

Trevor Branch

Program Authorized to Offer Degree:

School of Aquatic and Fishery Sciences

University of Washington

Abstract

Salmonid Selection, Evolution, and Historical Abundance Patterns

Curry J. Cunningham

Chair of the Supervisory Committee:

Dr. Ray Hilborn

School of Aquatic and Fishery Sciences

Pacific salmon represent an important group of species both from both cultural and economic perspectives. Given the importance of salmonids in marine and freshwater ecosystems, as a component of human food security, it is important to understand what natural and anthropogenic factors influence the evolutionary and demographic dynamics of population across their range, and develop quantitative tools to aid in the implementation of sustainable management practices. This dissertation is focused upon: (i) evaluating whether selective predation by brown bears (*Ursus arctos*) depends upon the density of their sockeye salmon (*Oncorhynchus nerka*) prey, (ii) quantifying strength and direction of natural and anthropogenic selection forces and life history tradeoffs that shaping optimal phenotypic distributions for populations of sockeye in Bristol Bay, Alaska, (iii) development of methods for reconstructing salmon run size by partitioning mixed-stock catches while accounting for differences in

availability to harvest within common fishing areas and interception in spatially proximate terminal fishing districts using both age and genetic composition of catch data, (iv) simulation testing of a stage-structured statistical life cycle model for evaluating the natural and anthropogenic drivers of Chinook salmon (*O. tshawytscha*), and (v) an application for the statistical life cycle model to seven populations of fall and spring-run Chinook in the Sacramento River watershed of California.

Introduction

Pacific salmon are culturally and economically important species, forming the foundation of valuable commercial, sport, and subsistence fisheries in many regions. In addition to their importance to humans, salmon are also important sources of nutrients for terrestrial ecosystems (Moore and Schindler 2004) and critical prey items for maintaining sustainable predator populations. Despite the importance of salmon in the United States and globally, many questions still remain regarding their evolutionary ecology, interactions with terrestrial predators, and the natural and anthropogenic factors that influence their survival and abundance over time. Furthermore, there is a need to develop quantitative tools for addressing conservation concerns and aiding in the efficient operation of sustainable fisheries, if the sustainability of salmon populations and the communities relying on them is to be ensured in the future.

Within their range, Pacific salmon traverse a gradient both in latitude and the level of anthropogenic influence exerted on their freshwater spawning habitats. Sockeye salmon (*Oncorhynchus nerka*) spawning in Bristol Bay, Alaska represent one end of this continuum, with minimal human development on, or alterations to, freshwater habitats. The only direct anthropogenic impacts originate from a carefully managed commercial fishery in the region. Chinook salmon (*O. tshawytscha*) native to the Central Valley of California represent the other end of that continuum, with a long history of severely altered freshwater and estuarine habitats, lost access to traditional spawning grounds, and direct impacts from water management (Williams 2006). Contrasting in many ways, salmon populations in these two regions provide an opportunity to understand the ecology of salmon in differing habitats, subject to diverse factors influencing their evolutionary and demographic histories.

This dissertation has a dual focus on: (i) understanding the evolutionary forces shaping the evolutionary trajectory of salmon in habitats which remain unaltered by anthropogenic influence, and (ii) developing quantitative tools to aid in effective management of commercial fisheries and improve understanding regarding the environmental forces driving the demographic trajectory of salmon in heavily altered habitats. The first chapter of my dissertation, *Size-selectivity of Brown Bears Depends on the Density of their Sockeye Salmon Prey*, examines how the size selective nature of predation by brown bears (*Ursus arctos*) on sockeye salmon in a tributary of Bristol Bay is directly influenced by interannual variation in prey abundance. The second chapter of my dissertation, *Selecting for the Phenotypic Optimum: Size-related Tradeoffs Between Mortality Risk and Reproductive Output in Female Sockeye Salmon*, expands upon the first chapter placing the influence of predatory selection within the context of other forms of selection shaping the morphology of sockeye salmon, including fishery selection, the mortality cost of prolonged marine residence required for growth, and physiological relationships between body size and reproductive output. The third chapter of my dissertation, *A General Model for Salmon Run Reconstruction Accounting for Interception and Differential Availability to Harvest,* describes a flexible model for reconstructing salmon brood tables by partition catches in mixed stock salmon fisheries and accounting for interception harvest in proximate terminal fishing districts, using age and genetic composition of catch data. This chapter reports results from an application of this model to data from the commercial sockeye salmon fishery in Bristol Bay. Chapter four, *A Statistical Life Cycle Model for Central Valley Chinook Salmon: A Simulation Study*, describes a stage-structured model for testing hypotheses regarding the strength and direction of influence natural and anthropogenic factors have on the survival of multiple populations of Chinook in the Central Valley of California. This chapter details results of a

simulation study evaluating the level bias and precision in model estimates for parameters of interest, and the influence of observation uncertainty in model predictions. The fifth and final chapter of my dissertation, *Evaluation of Freshwater and Marine Influences on The Survival of Spring and Fall-run Sacramento River Chinook*, presents findings from an application of the statistical model described and tested in Chapter 4, to seven populations of wild and hatchery-reared, spring and fall-run Chinook in the Sacramento River watershed of California.

Chapter 1

Size-selectivity of Predation by Brown Bears Depends on the Density of their Sockeye Salmon Prey

Abstract

Can variation in prey density drive changes in the intensity or direction of selective predation in natural systems? Despite ample evidence of density-dependent selection, the influence of prey density on predatory selection patterns has seldom been investigated empirically. We used 20 years of field data on brown bears (*Ursus arctos*) foraging on sockeye salmon (*Oncorhynchus nerka*) in Alaska to test the hypothesis that salmon density affects the strength of size-selective predation. Measurements from 41,240 individual salmon were used to calculate variance standardized selection differentials describing the direction and magnitude of selection. Across the time series, the intensity of predatory selection was inversely correlated with salmon density; greater selection for smaller salmon occurred at low salmon densities as bears' tendency to kill larger than average salmon was magnified. This novel connection between density-dependence and selective predation runs contrary to some aspects of optimal foraging theory and differs from many observations of density-dependent selection because: 1)

The direction of selection remains constant, while its magnitude changes as a function of density, and 2) Stronger selection is observed at low abundance. These findings indicate that sockeye salmon may be subject to fishery-induced size-selection from both direct mechanisms, and latent effects of altered predatory selection patterns on the spawning grounds resulting from reduced salmon abundance.

Introduction

Selection shapes the phenotypic landscape we observe and the underlying genetic composition of a population through adaptive evolution (Darwin 1874, Rieseberg et al. 2002). While selection may operate on a wide array of morphometric or life history traits, selection is observed to vary greatly in both direction and magnitude over time (Grant and Grant 2002, Siepielski et al. 2009) often resulting from inherent non-stationarity in environmental factors (Bell 2010). This inconsistency in selection over time may help to maintain genetic and phenotypic diversity across generations (Kingsolver and Diamond 2011). However, variation in the strength and direction of selection may also result from changes in demographic qualities of the population under selection (Siepielski et al. 2011), including sex ratio (Jann et al. 2000, Leftwich et al. 2012, Punzalan et al. 2010) and density (Einum et al. 2008, Mueller 1997).

Density-dependence in selection predicts that the fitness of one phenotype relative to another will change with the abundance of conspecifics at any given time. The theoretical basis for this interface between demography and selection comes first from MacArthur (1962), who detailed differences between populations at high and low density and postulated that density itself was dictating selection. While density-dependence may be manifest in selection related to sexual (Conner 1989, Tomkins and Brown 2004, Zeh 1987) or mortality related processes (Milner et al. 1999, Sinervo et al. 2000), the underlying criterion is that there is a change in the distribution of fitness across trait values when the population's density changes. The strength of selection for secondary sexual characteristics including forceps used in courtship and fighting by the male European earwig *Forficula auricularia* (Tomkins and Brown 2004) and size of male pedipalp pincers (chela) associated with combative mate acquisition in pseudoscorpions (Zeh

1987) has been correlated with density. Specifically, high density and increased male-male competition magnify selection for the large phenotype in these appendages. Conversely, selection for an analogous character in the fungus beetle *Bolitotherus cornutus* was strongest under conditions of low abundance, as large horns provided less advantage in mate acquisition at high density (Conner 1989).

Density-dependent selection may also arise from non-sexual processes where mortality rates are linked to individual phenotypic values (Milner et al. 1999). Phenotypes that confer a fitness benefit at high density (K-selected) or at low density (r-selected) should be expected to demonstrate inverse responses in the direction of selection to variation in conspecific density (Mueller 1997, Pianka 1970). Pianka (1970) specifically postulated that (K-selected) traits such as prolonged lifespan, iteroparity, large size at maturity and reduced growth rate, should be favored at high population density. Sinervo et al. (2000) found that selection for two competing morphs of side-blotched lizard *Uta stansburiana* displaying alternative strategies in the tradeoff between fecundity and egg size depended upon population density. Further evidence suggests that selection for the ability of *Drosophila melanogaster* to persist in suboptimal (cadmium-rich) environments depends upon the density of conspecifics inhabiting optimal environments (Bolnick 2001). While numerous examples of density-dependent changes in selection pressure are available from model (Joshi and Mueller 1996) and non-model organisms (Mueller 1997, Reznick and Endler 1982), most such studies were conducted under laboratory settings, or encountered limitations in methodology including uncontrolled environmental variables in inter-population comparisons, lack of replication, or the inability to identify the causal mechanism for selection (see Einum et al. (2008) discussion of Tomkins and Brown (2004)). Furthermore, the presence of density-dependence in patterns of predatory selection has been scarcely evaluated.

Although selective predation and density-dependent predation rate affect prey survival, few studies have evaluated the interaction between these processes. Here we distinguish between density-dependent and frequency-dependent or apostatic selection. Under a frequency-dependent selection regime, the success of a phenotype depends upon the relative frequency of that phenotype within the community (Fitzpatrick et al. 2009, Levin et al. 1988, Partridge 1988). Individuals of the rare phenotype may experience lower (Aditya et al. 2005, Allen and Greenwood 1988, Olendorf et al. 2006) or higher (Shigemiya 2004) risk of predation, representing apostatic and anti-apostatic selection, respectively. In contrast, density-dependent predatory selection refers to variation in the magnitude or direction of selection by a predator in response to prey density. Previous research has evaluated the effect of prey density on predatory selectivity at the species level in the form of prey switching in top trophic level carnivores (Owen-Smith and Mills 2008) and mesocarnivores (Prugh 2005, Randa et al. 2009). However, examples of the interaction between prey density and patterns of phenotypic selection within species by predators are extremely limited, except for the report by Bartell (1982) report of a positive relationship between zooplankton density and size selectivity by the predator, bluegill sunfish (*Lepomis macrochirus*). To evaluate whether predation may become more or less selective as a function of prey density, we quantified patterns of size-selective predation by brown bears (*Ursus arctos*) on mature sockeye salmon (*Oncorhynchus nerka*) in a fully natural setting.

Adult Pacific salmon (*Oncorhynchus spp.*) are ideal for quantitatively testing the hypothesis that the strength of predatory selection is directly affected by prey density for several reasons. First, Pacific salmon are semelparous, completing their life cycle and inevitably dying after re-entering freshwater to spawn (Quinn 2005). This distinctive life history permits

extensive sampling of an entire population of mature individuals, including those killed by predators and those escaping predation and dying of senescence within a given year, allowing selection differentials to be calculated. Second, Pacific salmon cease feeding upon freshwater entry (Gende et al. 2004, Gilhousen 1980), with no somatic growth occurring during the time period when predatory selection is operating. Thus, salmon can be measured for body size throughout the breeding season with no need to correct for daily growth, which would otherwise introduce some error. Third, the primary predator of mature salmon is typically brown and black (*U. americanus*) bears, and the cause of death can be easily and consistently determined from visual analysis of remains for conspicuous bite marks and tissue consumption (Quinn and Buck 2001, Reimchen 2000). Finally, salmon reliably home to natal streams and seldom move amongst streams after initial entry. This site fidelity permits replicate sampling of a single population across years, without the confounding factors affecting the inter-population comparisons often used for evaluating density-dependence in selection (Einum et al. 2008).

Previous research showed that the *per capita* predation rate by brown bears on sockeye salmon was density-dependent (Quinn et al. 2003), and bears tended to kill larger than average salmon within the population (Quinn and Buck (2001); Quinn and Kinnison (1999); Ruggerone et al. (2000); see also Reimchen (2000) for similar results with different salmon and bear species), but the interaction between these processes has not been evaluated. In this study, we used 20 years of data on predation rate and selection for length in a population of sockeye salmon to test the null hypothesis that density does not affect the magnitude or direction of size selection, against two alternative density-dependent hypotheses. First, when salmon density is high, bear predation is more selective as bears have more potential prey to choose among and are not resource limited, whereas at low densities bears might kill salmon indiscriminately with

respect to size because even a small salmon is a valuable prey item. This hypothesis is consistent with the optimal foraging theory advanced by (Emlen 1966) which suggests that indiscriminant patterns of feeding should coincide with resource scarcity, and would be consistent with observations by Gende et al. (2001) indicating that bears preferentially consume energetically rewarding tissues when salmon density is high. Second, bear predation might be more size-selective at low salmon densities. Bears might choose larger, more energetically rewarding, prey when the salmon are scarce and harder to catch or because low prey density permits size variation amongst salmon to be more easily discerned. This hypothesis coincides with MacArthur and Pianka (1966)'s optimal foraging theory which suggests predators will act to maximize energetic intake per unit time when resources are scarce.

Methods

Patterns of selection were evaluated in a population of sockeye salmon spawning in Hansen Creek, a small (2 km) tributary of the Wood River system, in southwest Alaska; see reference map in Carlson and Quinn (2007). This stream is fed by a beaver pond and series of springs resulting in stable flows and clear water that facilitate accurate visual surveys. Sockeye salmon is the only salmon species spawning in the stream, further simplifying analysis of density, predation and selection. Sockeye salmon congregate in Lake Aleknagik at the stream mouth in mid-July, begin entering about 20 July, and by 20 August the breeding season is complete and virtually all salmon have died.

In each of 20 years, 1990-1993 and 1997-2012 (inclusive), total salmon density and length distributions were estimated from daily visual surveys of live and dead salmon within the stream. All dead salmon were counted, identified to sex, and their cause of death was recorded.

Our analysis was restricted to salmon that entered the stream, and excluded those found at the mouth of the stream below the spawning areas (Carlson and Quinn 2007). Data from both tagging (1990-1993) and complete surveys (1997-2012) were analyzed in the same manner with male and female observations pooled in each year. Density in a specific year was calculated as the sum of all individuals found dead in Hansen Creek during daily surveys and the number still alive on the final survey that year (average 6% remaining alive).

The length distributions of individuals killed by bears and those dying of senescence were compared in each year. Length was measured to the nearest mm from the middle of the eye to the posterior boundary of the hypural plate. This measurement avoids the bias caused by the presence of secondary sexual features including elongated jaws in males, and error associated with estimating the length of females whose tails become frayed during nest construction. Mode of death was determined from visual inspection, with puncture wounds and partial consumption indicating that mortality was due to bear predation, and frayed fins, gaunt appearance and degradation of scales indicating mortality was due to senescence post spawning (Quinn and Buck 2001). During the early years (1990-1993), salmon were measured prior to stream entry and individually marked (Ruggerone et al. 2000) and the eventual mode of death for these marked individuals was subsequently recorded. From 1997 onward, regular stream surveys were conducted throughout the spawning season (July - August) during which all observed dead within the stream and surrounding riparian area were categorized by source of mortality, and a subset were measured. In total, 41,240 salmon length measurements were included in this analysis of selection. Individual length measurements were weighted to account for daily differences in the fraction of dead individuals measured. For each sampling day, an individual length observation was multiplied by the inverse of the number of fish measured divided by the

number of observed dead, for each mortality category (senescent or bear killed). Weighting individual length observations in this way accounts for intra-seasonal variation in sampling effort which could lead to bias, given the tendency for larger fish to arrive earlier in the season than smaller fish (Doctor and Quinn 2009, Hendry et al. 1999).

To quantify the magnitude and direction of predatory selection in each year, we calculated variance-standardized selection differentials (SSD), representing the difference in the sockeye salmon length distribution before and after predatory selection:

(1.1) $SSD = \frac{\bar{X}_{post} - \bar{X}_{pre}}{\sqrt{v_{pre}}}$

Variance-standardized selection differentials are a common metric for the relative strength of selection required to cause an observed shift in a phenotypic distribution (Endler 1986, Falconer 1981, Kingsolver et al. 2001). All individuals which were killed by bears plus those that died of senescence comprised the pre-selection group ($\bar{X}_{pre}$), and the individuals that died of senescence, thus surviving predatory selection, comprised the post-selection group ($\bar{X}_{post}$). Only bear-killed and senescent individuals were included as members of the pre-selection group ($\bar{X}_{pre}$), because inclusion of the alternative mortality sources would have meant calculating the effect of all selection from all sources and not predation in isolation, thus obscuring our focus on the effect of the primary predator. Selection differentials were divided by the square root of the variance ($\sqrt{v_{pre}}$) in the pre-selection phenotypic distribution to standardize the value, permitting comparison across years (Kingsolver et al. 2001). Negative SSD values indicated that smaller fish were less likely to be killed than larger fish, thus having greater expected fitness, and higher absolute values indicated stronger selection.

The relationship between annual densities of sockeye salmon and the corresponding standardized selection differentials quantifying length-selective predation was evaluated using

weighted least squares regression (Carroll and Ruppert 1988, Ryan 1997). A weighted regression procedure ensured that each data point (SSD) was attributed an appropriate level of influence; each weight was proportional to the inverse of the pooled variance in the calculated selection differential (Equation 1.2) for that year (Endler 1986).

$$\sigma^2_{pooled} = \sqrt{\frac{n\left[\left(N_{pre}-1\right)\sigma^2_{pre}+\left(N_{post}-1\right)\sigma^2_{post}\right]}{\left(n-2\right)N_{post} * N_{pre}}}$$
$$n = N_{post} + N_{pre} \quad (1.2)$$

$$\text{Predatory Preference} = \bar{x}_{senescent} - \bar{x}_{predator-killed} \quad (1.3)$$

To elucidate the mechanisms driving the observed selection patterns, the average difference in length between senescent and predator-killed salmon was calculated annually. Unlike the SSD (Equation 1.1), which quantifies the shift in length distribution resulting from predatory selection, this metric for "predatory preference" (Equation 1.3) represents the explicit selective behavior of the predator itself.

Results

The available data from 16 consecutive years of stream surveys (1997-2012) included 107,169 carcasses categorized by mode of death, of which 44,202 were measured for length and 37,820 died of senescence or were killed by bears. In both sexes, the proportion of individuals killed by bears was positively correlated with individual length (Figure 1.1). The increase in predation risk with length was significant when evaluated by linear regression for males ($R^2 = 0.938$, $p < 0.001$) and females ($R^2 = 0.926$, $p < 0.001$); predation rate increased from < 20% to > 80% across sex-specific length distributions (Figure 1.1). From an evolutionary perspective,

these data indicated that predation by brown bears favored survival of smaller salmon within the population.

Standardized selection differentials quantifying the observed change in length distribution resulting from predation for the combined sexes in years with tagging (1990-1993, n = 3,420) and survey (1997-2012, n = 37,820) data varied among years but were always negative (mean: -0.237 SDU), indicating that survivors of predation tended to be shorter than the population mean in all years. SSD values ranged from -0.012 (SDU) in 2006 when salmon were abundant (n = 14,952) representing a minimal impact of predatory selection, to a maximum of -0.574 (SDU) in 2001 when salmon were scarce (n = 1,957).

Yearly salmon densities ranged from 1,320 in 2009 to 16,296 in 1999 (mean = 7,505, StDev = 4,869). To investigate the relationship between salmon abundance and selection, linear and curvilinear models describing annual variation in SSD with yearly total in-stream density as the predictor variable were fit to these data. Various transformations were also explored for the density predictor, and model selection was conducted using Akaike's information criterion (Burnham and Anderson 2002). The model with natural log of salmon density as the sole predictor was selected (AIC= -21.18) when compared to a model with untransformed density as the predictor (AIC= -16.84) but the general results were the same in both cases.

Employing the natural log of in-stream density as the predictor for the observed predatory SSD in each year, least squares regression weighted by the reciprocal of the variance in each SSD estimate (Equation 1.2) was significant ($p < 0.001$, $R^2 = 0.55$). Smaller (i.e., more negative) SSD values at low salmon densities indicated that bear predation exerted greater selection favoring the survival of smaller salmon in years when salmon density was low (Figure 1.2, Table 1.1). A t-test with (n-2) degrees of freedom (Endler 1986, Sokal and Rohlf 1981) and $\alpha = 0.05$,

indicated that four of the calculated SSD values were not statistically different from zero, and all four of these values occurred in years of high salmon density (Figure 1.2).

To further examine mechanism of selective predation by bears, the predatory preference (Equation 1.3: difference in mean length between senescent and bear-killed salmon) was plotted against the natural log of salmon density (Figure 1.3). The positive correlation between the predatory preference and density (least squares regression: $p < 0.01$, $R^2 = 0.41$) indicated that the tendency of bears to kill larger than average salmon was especially marked in years with low salmon abundance (Figure 1.3, Table 1.1). This relationship was similar to that described for the interaction between SSD and in-stream density (Figure 1.2, Table 1.1), although less pronounced.

Discussion

Our investigation into the magnitude and direction of selection by brown bears on sockeye salmon strongly indicated a correlation with prey density (Figure 1.2). The significant increase in the standardized selection differential, representing the observed shift in the sockeye length distribution resulting from predatory selection, with greater salmon density revealed greater directional selection (favoring smaller salmon) in years when salmon density was low. Conversely, when sockeye salmon densities were high there was little or no directional selection from bear predation. Phenotypic selection by predation in this case varied in magnitude but not direction, with selection either favoring smaller size in salmon (-SSD value) or not statistically significant, across years and salmon densities.

These findings contrast with many previous examples of density-dependent selection within the literature in three distinct ways. First, the observed interaction between bears and

sockeye salmon represents one of few examples of density-dependent selective predation (see Bartell (1982) for another). The vast majority of documented examples of density-dependent selection arise from either sexual selection (Conner 1989, Tomkins and Brown 2004, Zeh 1987), competition (Bolnick 2001, Joshi and Mueller 1996, Sinervo et al. 2000), or non-predatory mortality (Moorcroft et al. 1996). Second, the intensity of selection was greatest at low population densities. This directly contrasts with findings by Moorcroft et al. (1996) indicating stronger selection across phenotypes and sexes in years of high density, findings by Bolnick (2001) indicating more rapid adaptation to toxic environments as a result of stronger selection in high density treatments, and observations by Zeh (1987) and Tomkins and Brown (2004) detailing stronger selection for secondary sexual characteristics under high abundance (competitive) conditions. However, Conner (1989) found more intense selection under the low density condition. Third, rather than the direction of selection responding to observed fluctuations in density (Moorcroft et al. 1996), the intensity of selection varied in response to density (Figure 1.2).

The consistent direction of selection over time in this population contrasts with the observation that the direction of selection for components of fitness related to survival often vary among years (Siepielski et al. 2011), and speculation by Kingsolver and Diamond (2011) that changes in the direction of selection may be a key process maintaining phenotypic variation. In the case of salmon and bears, one might ask what processes allow large salmon to persist despite consistently negative selection differentials. First, the magnitude of directional selection was correlated with salmon density, which varied by more than an order of magnitude over this time series ($\text{Density}_{\text{min}}$ = 1,320, $\text{Density}_{\text{max}}$ = 16,296, $\sigma_{density}$ = 4,869), and this variation in the magnitude of selection over time should facilitate the persistence of large fish in years of high

salmon density. Additionally, the presence of large phenotypes could be maintained by environmental variability, or positive correlations observed between female fecundity and size (Quinn et al. 1995) and male reproductive success and length (Carlson et al. 2009). Regardless of what factors may limit the evolutionary effect of directional selection, predatory selection consistently favored small size, and the magnitude of this selection was correlated with salmon density.

Standardized selection differentials are commonly used for describing the shift in a phenotypic distribution in response to a selective event (Endler 1986, Kendall et al. 2009, Kingsolver et al. 2001), and it is very important to understand that such a shift (and similar calculated SSD values) may arise under two separate scenarios. First, the selective agent (in this case the predator) may be highly selective with respect to a specific trait but remove only a small proportion of the population (e.g., if bear predation was highly selective with respect to length, but bears killed only a small fraction of the available fish). However, a similar selection differential could result if the mortality agent was only slightly selective with respect to phenotype but exerted a high mortality rate, resulting in a similar shift in the mean of the trait under selection (e.g., if bears showed only weak selection but killed most of the fish). These selection regimes differ mechanistically, though they have the same result from the evolutionary perspective of the prey. Too few studies make this distinction and we encourage those using this metric to report which of these processes was responsible for the patterns of selection differentials observed. Otherwise, it is impossible to determine whether variation in selection differential values resulted from variability in selection or simply variability in exploitation rate. Our finding, that predatory preference (Equation 1.3) also correlated with prey density (Figure 1.3), indicated that shifts in salmon length distributions were not driven merely by density-

dependent variation in predation rate (Quinn et al. 2003), but also by changes in predatory behavior.

In the search for a biologically relevant explanation for the mechanism driving the observed density-dependence in predatory selection, we confronted our results with the literature on optimal foraging theory. Theory predicts that an optimally efficient predator will modify its behavior to maximize energetic intake per unit time, by either reducing the time spent in pursuit of prey or by selectively feeding on items (or individuals) that provide the greatest energetic reward per unit of energy invested in search or capture (Emlen 1966, MacArthur and Pianka 1966). With respect to variation in food abundance or density of prey over time, optimal foraging theory would predict that the predator should become more selective when prey abundance or density is greater (Emlen 1966, MacArthur and Pianka 1966). Emlen (1966) further concluded that predatory selectivity is directly related to predatory satiation, and that animals should necessarily be "… more indiscriminate when starved or when food is scarce". This prediction contrasts with the observed pattern of less selective feeding by bears when salmon density was higher (Figure 1.2). However, MacArthur and Pianka (1966) postulated that efficiency of capture may also affect predatory diet diversity, speculating that increased specialization may be linked to greater difficulty in pursuit. This idea is consistent with our findings that when prey density was low, the predator practiced more specialized (selective) consumption, under the assumption that at low density prey are more difficult to catch (requiring greater energetic expenditure per successful capture).

The observed non-stationarity and density-dependence in predatory selection described here is important from the perspective of salmon ecology because it indicates that reproductive success of phenotypes depends on salmon density on the spawning grounds. Fleming and Gross

(1994) also found that sexual selection on body size varied with density of coho salmon, but in that case smaller males achieved greater mating success in years of higher density. The success of these small males resulted from increased efficacy of their alternative reproductive tactic (sneak fertilization) rather than changes in predation. The importance of evaluating how the direction and magnitude of selection change with density was noted by Einum et al. (2008), as a clear understanding of these processes may provide a more complete understanding of the selection mechanisms shaping an observed phenotypic landscape. Einum et al. (2008) further concluded that salmonids may be ideal subjects for such evaluations of density dependent selection, given the large body of empirical work on their evolutionary ecology. However, Einum et al. (2008) speculated that variation in predation rate might be the critical driver of density-dependent variation in predatory selection, while our results indicate that this variation is also driven by changes in predatory preference (behavior) with respect to salmon size, as a function of density.

Our results strongly suggest that the abundance of the prey population must be considered when evaluating the evolutionary influence of predatory selection. For example, the commercial gillnet fishery that operates in Bristol Bay, Alaska may impose both direct and indirect selection on body size of sockeye salmon. The fishery is managed to allow the estimated carrying capacity of the system for sockeye salmon to be reached each year, with the remaining salmon available for capture (Minard and Meacham 1987). This policy has the effect of reducing the average and variation in density on the breeding grounds. Sockeye salmon returning to Hansen Creek are subject to annual harvest rates between 19% and 86% (mean: 54%) (Kendall et al. 2009). In addition to this exploitation rate, the gillnet fishery is selective for body size (Kendall et al. 2009). Given the relationship between salmon density and predatory

selection demonstrated here (Figure 1.2), the commercial fishery imposes two distinct forms of selection for smaller body size upon the salmon population. In the absence of a large-scale commercial fishery (prior to 1893), returning adult sockeye salmon would have been free from fishing that now tends to catch larger fish at a higher rate than smaller fish. In addition, the breeding ground densities would have been ~54% higher on average than are now observed. Higher in-stream densities would result in less directional selection favoring smaller size, resulting from density-dependent predatory selection. Thus the commercial fishery has resulted in both direct selection for smaller size due to the gear employed and indirect selection from the reduction in salmon density and associated increased selectivity by bears. In the face of future environmental uncertainty and resultant variability in salmon abundance (Hilborn et al. 2003b), a clear understanding of the biological interactions driving evolutionary change within these species is of great importance.

Acknowledgements

We acknowledge the efforts of the faculty, staff and students of the Fisheries Research Institute and the Alaska Salmon Program who have contributed to the extensive data set that we examined, and especially Greg Buck, Chris Boatright, Stephanie Carlson, Harry Rich, Jr., Neala Kendall, and Keith Denton, whose hard work in the field, attention to detail, and invaluable insights have made this possible. Funding for this research was provided by the National Science Foundation, Gordon and Betty Moore Foundation, and the Bristol Bay salmon processing industry.

Figures

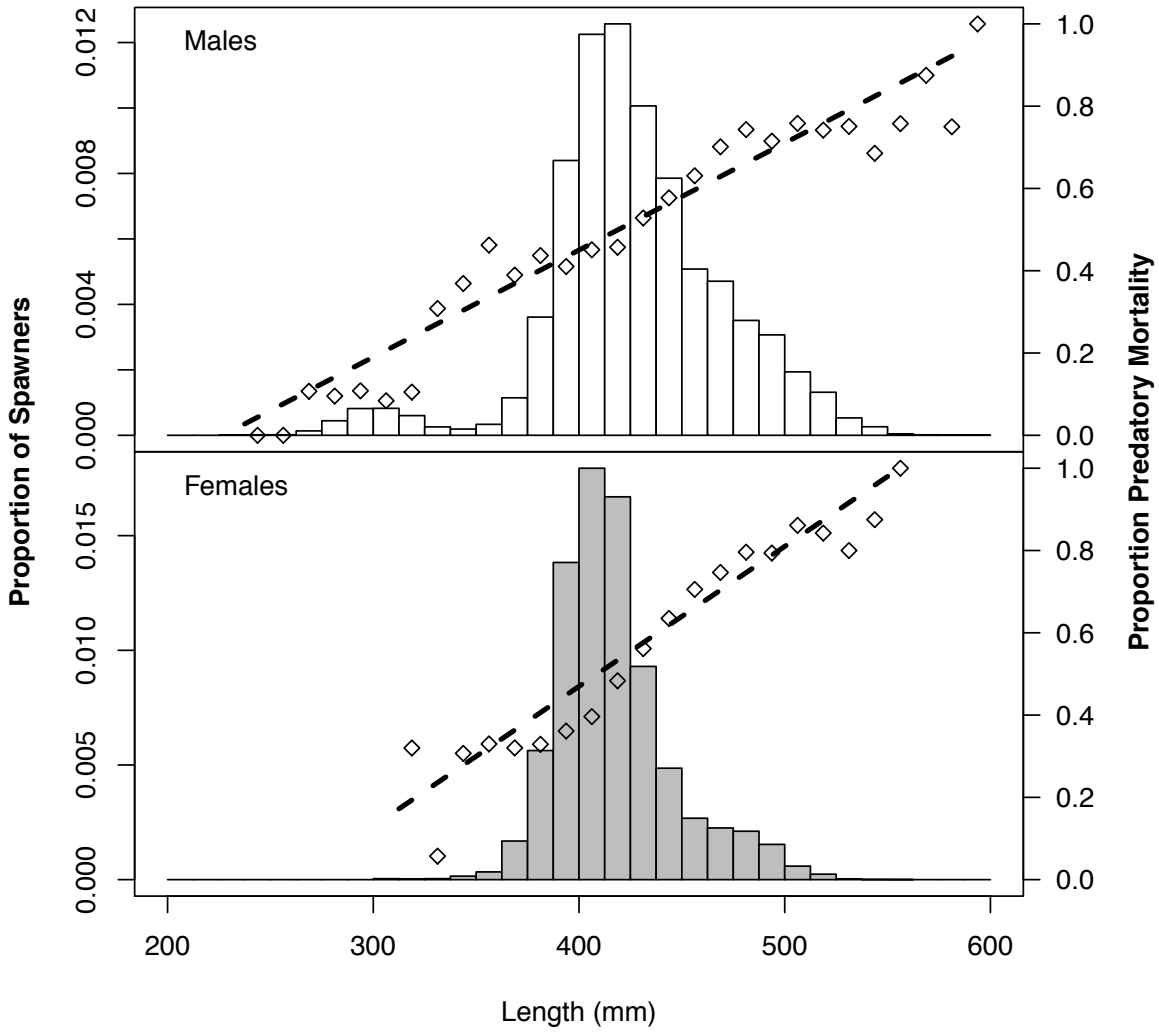

Figure 1.1 Weighted sex-specific length frequency histograms for all dead salmon measured within Hansen Creek from daily stream surveys 1997-2012. Diamonds represent the percentage of each sized category killed by bears. Lengths are in mm and have been binned by 12.5-mm increments, with individuals at the upper and lower end of the length distribution (<200-mm and >600-mm) combined in respective end categories. Line indicates the least squares regression of the proportion killed by bears on length for males (R^2=0.938, $p < 0.001$, n=18,235) and females (R^2=0.926, $p < 0.001$, n=25,967).

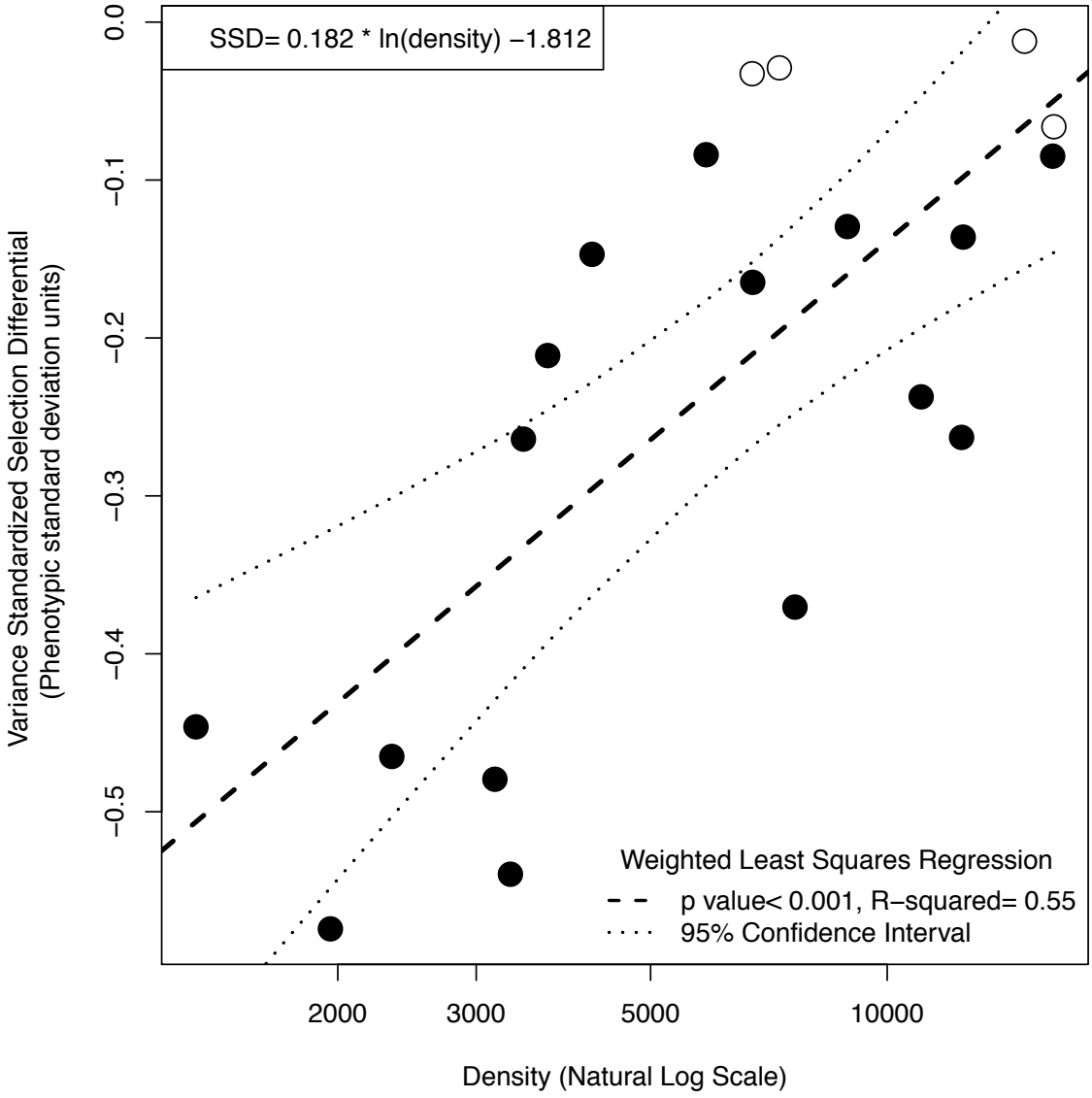

Figure 1.2 Variance-standardized selection differentials calculated for each year plotted against the natural log of in-stream salmon density. The dashed line represents the weighted least squares regression and the dotted line the 95% confidence interval around that regression. Open points designate years in which SSDs were not significantly different from zero (t-test, p-value > 0.05).

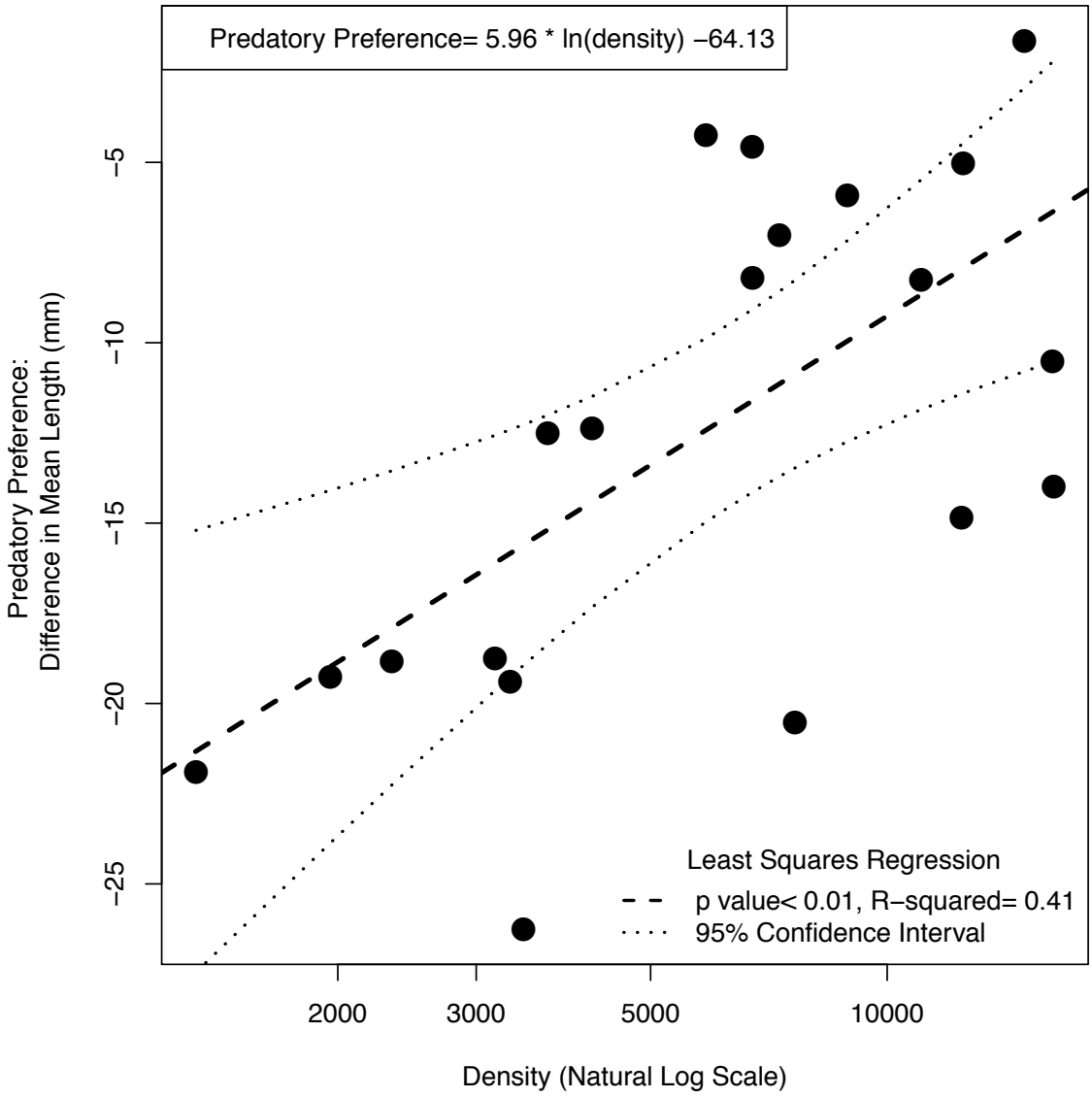

Figure 1.3 Relationship between predatory preference (difference in mean length of natural (senescent) and bear killed salmon, Equation 1.3) and total in-stream salmon density across years (1990-1993 & 1997-2012). Lines indicate least-squares fit of linear model to these data and associated 95% confidence interval.

Tables

Table 1.1 Annual data and derived selection metrics. Numbers of observed mortalities in gray come from years in which tagging data were used to assess selective predation.

Year	Instream density	Variance-standardized selection differential	Predatory preference	Number of measured fish	Observed bear mortalities	Observed natural mortalities
1990	6,733	-0.033	-4.57	773	148	625
1991	16,296	-0.066	-13.99	1,128	165	963
1992	7,292	-0.029	-7.02	943	119	835
1993	4,212	-0.147	-12.38	576	196	380
1997	5,884	-0.084	-4.24	3,094	4,176	1,017
1998	12,436	-0.263	-14.85	7,772	5,878	5,169
1999	16,239	-0.085	-10.52	2,426	2,834	9,578
2000	3,169	-0.479	-18.75	1,886	2,591	302
2001	1,957	-0.574	-19.25	1,368	1,617	77
2002	7,633	-0.370	-20.53	2,477	4,470	2,105
2003	8,899	-0.129	-5.92	2,173	4,506	3,058
2004	2,343	-0.465	-18.83	1,402	1,555	497
2005	3,445	-0.264	-26.25	2,078	1,123	1,261
2006	14,952	-0.012	-1.64	2,514	2,517	11,877
2007	6,744	-0.165	-8.19	3,413	3,182	2,756
2008	3,699	-0.211	-12.51	2,806	1,707	1,820
2009	1,320	-0.446	-21.89	422	993	218
2010	12,494	-0.136	-5.01	1,708	6,689	2,897
2011	11,046	-0.237	-8.26	1,606	7,693	255
2012	3,316	-0.540	-19.39	675	2,739	188

Chapter 2

Selecting for the Phenotypic Optimum: Size-related Tradeoffs Between Mortality Risk and Reproductive Output in Female Sockeye Salmon

Abstract

Selection drives evolutionary changes but is often difficult to quantify and tightly link to phenotypic trait distributions in wild populations. Sampling a single population of sockeye salmon (*Oncorhynchus nerka*) for over a decade, we calculated the expected spawning success for females resulting from: 1) increased fecundity with body length, 2) the mortality cost of prolonged marine residency necessary to achieve large size, 3) size-selective natural mortality on the spawning grounds from biotic (bear and gull predation) and abiotic (stranding) processes, and 4) exploitation by a size-selective commercial fishery. We quantified the size-specific probability of different modes of death and the resultant potential for successful spawning, and then modeled the theoretical relationship between female length and fitness (spawning success) in the population. This optimal distribution closely matched the observed length distribution of the

focal population, when removals by the size-selective commercial fishery were included. We then used a likelihood-based approach to compare competing model predictions to length distributions from other populations in the watershed with different levels of size-selective freshwater mortality, as determined by the physical characteristics of the spawning grounds. This study provides a quantitative framework for assessing female spawning success in wild populations, as represented by the expected number of eggs deposited per spawning female. These results advance previous analyses of natural selection in that predictions for phenotypic distributions were generated and then compared to those observed *in situ*, rather than assuming the adaptive nature of observed distributions.

Introduction

The literature on evolutionary biology is rich with studies quantifying selection in natural populations, including many cases of directional selection on quantitative traits (Endler 1986, Hoekstra et al. 2001, Kingsolver et al. 2001). However, detailed field studies of selection have traditionally been challenged by the difficulty inherent in fully sampling both survivors and mortalities, and directly linking phenotype to relative fitness within a population. Consequently, some studies are conducted in controlled settings (Trexler et al. 1994) which may not fully represent natural conditions, and others can only subsample and approximate the distributions of the survivors and mortalities (Britton and Moser 1982). As Shine et al. (2001) noted, "The problem involves logistics: It is simpler to quantify differential mortality by assessing phenotype distributions in living animals before and after the mortality event than it is to directly observe mortality or measure the attributes of dying versus living animals." In addition, directional selection is often either inconsistent over time (Grant and Grant 2002, Seamons et al. 2007) or opposed by other forms of selection. Furthermore, the signal for selection may often be obscured by co-occurring demographic processes, which are neutral with respect to phenotypic selection. Therefore, many years of sampling may be needed to fully account for variation in selection, and the inclusion non-mortality related processes is necessary to elucidate the true relationship between phenotype and relative fitness for the species of interest.

When selection resulting from mortality-related processes is adequately quantified, the question then becomes whether it is sufficient to shape the observed phenotypic landscape. If fitness is assumed to be proportional to offspring production, in species exhibiting a positive correlation between female body size and fecundity there should also be strong selection for increased body size under what is termed the "fecundity advantage model" (Darwin 1874,

Preziosi et al. 1996). While many taxa including insects (Honek 1993, Leather 1988, Thornhill and Alcock 1983), reptiles (Fitch 1985, Gibbons 1972, Semlitsch and Gibbons 1982), anurans (Crump 1974, Woolbright 1983) and other amphibians (Shine 1979), turtles (Berry and Shine 1980), isopods (Veuille 1980), zooplankton (Gilbert and Williamson 1983), passerine birds (Hughes and Hughes 1986), and some mammals (Clutton-Brock and Harvey 1978) demonstrate increased fecundity with female body size, this relationship is not always sufficient to describe the observed length distribution or degree of sexual size dimorphism exhibited by some species (Shine 1988). From this it may be suspected that tradeoffs associated with the interaction between size and alternative forms of selective pressure may be occurring, in the presence physiological limits on growth.

Tradeoffs causing improved performance in one aspect while decreasing fitness in another can result from fundamental constraints in resource allocation such as the balance between the number and size of eggs or offspring (Elgar 1990, Sinervo and Licht 1991, Smith and Fretwell 1974), or from the balance between advantages and disadvantages of breeding date (Olsson and Shine 1997, Svensson 1997), body size, or other phenotypic traits (Roff 1992, Stearns 1992). For example, delaying maturation to achieve a larger body size may not only confer the benefits of greater egg production (Berrigan 1991), acquisition of better breeding sites or enhanced ability to provision offspring, but also a greater risk of mortality prior to first reproduction. There may also be tradeoffs associated with body size in a given breeding season if mortality is size-selective. Size-related tradeoffs may additionally manifest as increased competitive ability for resources at the cost of increased risk of mortality from a size-selective predator (Hulsmann et al. 2005).

Given the logistic problems in field studies (Shine et al. 2001), tradeoffs associated with age, size and reproductive success can be quantified more easily in semelparous than in iteroparous species. The life history and reproductive biology of Pacific salmon, *Oncorhynchus* spp., is well-documented (Fleming and Reynolds 2004, Quinn 2005), facilitating studies of reproductive success and life history tradeoffs. The combination of anadromy and semelparity means that all individuals surviving to maturity can be sampled, and often occur at high density so the statistical demands for large sample sizes can be met. Moreover, as "capital breeders", all growth occurs prior to reproduction (Fleming and Reynolds 2004) so size distributions can be sampled on the spawning grounds throughout the spawning season without bias from subsequent somatic growth. The primary fitness benefit associated with body size is the number of eggs produced (Beacham and Murray 1993) but larger females also produce larger eggs, yielding larger offspring (Heath et al. 1999, Kinnison et al. 1998) with enhanced ability to compete (Abbott et al. 1985) and survive (Einum and Fleming 2000, Healey 1982). Larger females also dig deeper nests (Steen and Quinn 1999) that are less vulnerable to disturbance by scouring floods after the female has died (Schuett-Hames et al. 2000) or left the site (Lapointe et al. 2000), or disturbance by other females digging their nests (Foote 1990). The very great benefit of size predicted by some models (van den Berghe and Gross 1989) is not necessarily realized, but parentage studies often indicate higher reproductive success by large females (Anderson et al. 2010, Serbezov et al. 2010) (for negative evidence, see for example Dickerson et al. 2005).

The benefits of large size in salmon are countered by the risk of mortality during the marine portion of the life cycle when almost all of the final adult body size is achieved (Quinn 2005). Females maturing at a young age may produce fewer and smaller eggs than those remaining at sea for an additional year prior to maturation, but those remaining at sea risk

mortality and hence a loss of all reproductive potential (Mathews 1968, Ricker 1976). There may be additional risks to large size in freshwater, notably from size-selective predation by bears (Quinn and Buck 2001, Quinn and Kinnison 1999, Reimchen 2000, Ruggerone et al. 2000) and, in some cases, stranding in shallow water (Carlson and Quinn 2007, Quinn and Buck 2001). Despite these risks, previous attempts to quantify the relationship between size and fitness in female salmon have not included the risk of size-selective mortality on the spawning grounds (Holtby and Healey 1986, van den Berghe and Gross 1989) and thus may have overestimated the benefits of large body size.

The purpose of this study was to quantify the tradeoffs in body size and age with respect to successful reproduction, utilizing female sockeye salmon, *O. nerka* (Figure 2.1) as a focal species, and then compare the estimated optimal size with the true length distribution observed in multiple populations. We utilized: 1) extensive multi-year salmon carcass surveys to quantify size-selective mortality on the spawning grounds, 2) data from the Bristol Bay commercial fishery quantifying patterns of size-selective exploitation, 3) estimates of age-specific marine mortality, and 4) data describing the relationship between female fecundity and size, to create a range of competing models predicting fitness as function of body length under a variety of potential selection scenarios. We then compared the focal population's length distribution and those of other salmon populations within the same watershed displaying different habitat-related selection regimes, with expectations of spawning success in the presence or absence of size-selective freshwater and harvest mortality, the observed length-fecundity relationship, and cost of prolonged marine residence, to determine the extent to which size-selective mortality may be shaping the observed phenotypic landscape.

Methods

Study site and survey methods

Data were collected annually from 1997 to 2010 at Hansen Creek, a tributary of Lake Aleknagik in the Wood River system in southwestern Alaska. Hansen Creek has been the site of intensive research on predation by brown bears, *Ursus arctos*, and sockeye salmon reproductive behavior because it is small (2 km long, averaging 10 cm deep and 4 m wide), clear, and resistant to flooding and therefore ideal for surveys and observations (Quinn and Buck 2001, Quinn et al. 2001a, Ruggerone et al. 2000). Hansen Creek is also an ideal study site because sockeye salmon are the only Pacific salmon species spawning there, so observations of predation patterns are not complicated by the presence of other species. Similarly, brown bears are a significant source of mortality, while other mammalian predators that prey on salmon elsewhere (e.g., black bears, *U. americanus*, and wolves, *Canis lupus*) are conspicuously absent. Furthermore, sockeye salmon are known to reliably home to natal streams, with experimental evidence from Quinn et al. (2006) indicating even finer scale homing to the area of incubation within the stream itself, suggesting that salmon spawning within Hansen Creek represent a separate population from others within the Wood River watershed.

Field data collection on Hansen Creek included two main elements: surveys of dead salmon and observations of tagged live salmon. Stream surveys were conducted on each day during the spawning season, which lasts from approximately 20 July to 20 August, from 1997 to 2010 by three or more people on foot. All dead salmon found in the stream and adjacent riparian areas were categorized by sex and mode of death. Salmon in this system may successfully complete spawning and die of senescence or suffer one of three common causes of premature mortality (Quinn and Buck 2001): 1) stranding, primarily at the shallow mouth where the stream

flows into Lake Aleknagik (Carlson and Quinn 2007), but also in shallow reaches of the stream itself, 2) predation by glaucous-winged gulls, *Larus glaucescens* (Mossman 1958), and 3) predation by brown bears. In almost all cases the cause of death could be unambiguously determined. Senescent fish were emaciated, with scars from intra-sexual competition, and females' tails were frayed from digging (Figure 2.1), whereas bear-killed fish had conspicuous bite marks and large amounts of missing tissue, especially in the belly region of females (Gende et al. 2001). Some salmon killed by bears are taken from the stream corridor into the riparian zone (Quinn et al. 2009), which were accounted for in subsequent analyses (see below for details on tagging and analysis). Stranded fish were found dead in shallow water on their sides, and those categorized as gull-killed had well-defined wounds made by the beak of the bird chiseling into the body cavity, typically near the vent or gill plate as the gulls primarily remove and consume the eggs from ripe females.

Body length was measured from the middle of the eye to the hypural bone at the end of the spinal column for all or a subset (46.67% overall) of mortalities observed during a specific survey, depending on the total number of fish present and the condition of the carcasses. After measurement, all carcasses were moved ca. 5-10 m away from the stream: sufficiently far to avoid counting them on subsequent surveys but not far enough to alter the behavior of predators or scavengers. For each length observation a multiplier was calculated to account for the proportion of fish measured on that day and for that mode of death, so overall length distributions would be robust to daily variation in the proportion of fish measured. Sampling of nearby streams was conducted on two or three occasions annually and employed the same categorization and measurement procedure to generate length distributions and estimate predation rate.

The carcass surveys allowed us to determine the overall size distribution of female salmon and the probability that females of a given length would die from one of the four primary causes. We also tagged a subset of the population each year from 1999 to 2010 to determine how long each fish spent in the stream prior to death, and whether they completed spawning or not. Annually, ~ 200 sockeye salmon were encircled in a small-meshed seine in Lake Aleknagik at the mouth of Hansen Creek, measured, and tagged with individually lettered round plastic tags (see Quinn et al. (2001a) for description). Tagging took place on multiple dates and tagged fish migrated into the stream throughout the entire breeding season. A few tagged fish (~ 0.5%) subsequently entered other streams nearby but most entered Hansen Creek and were observed on one or more days prior to death. Live females were categorized as migrating, ripe, partially spawned, or completely spawned based on their behavior and appearance. Migrating fish were actively moving upstream and had not established nest sites; ripe females had established visible nest sites but had not spawned, based on visual assessment of body condition (i.e., full, round belly, absence of scars); partially spawned females were also attending nest sites but their appearance indicated that at least some of their eggs had been spawned. Females classified as completely spawned had the gaunt, slim appearance resulting from the loss of ca. 20% of their body mass during egg deposition (Hendry et al. 1999), and also had frayed fins and scarring caused by nest preparation and defense. Detailed observations of tagged females indicated that nests were fully prepared within a day after selecting a site and spawning completed less than 3 d later (McPhee and Quinn 1998).

Sequential observations of tagged females were used to estimate whether each fish spawned at least some of her eggs prior to death. If the fish was seen alive and categorized as partially spawned or completely spawned on that day, we assumed that it had spawned,

regardless of how it was found dead subsequently. However, fish seen migrating or ripe on one day and dead the next day (e.g., killed or stranded) were assumed to have failed to spawn. For females reaching the stream, the probability of successful spawning was closely related to the number of days seen alive, such that females living > 3 d in the stream all completed spawning. At death, the spawning condition and mode of death were noted; examination of carcasses of fish categorized as senescent confirmed that most eggs had been spawned. In some cases (21.9%), individual salmon were seen repeatedly in the stream, but not recovered at death. The distributions of body size and the number of days alive in the stream before they disappeared closely matched those of salmon killed by bears. Combined with observations of bears taking salmon away from the stream, we concluded that such "missing" salmon had been killed by bears and then removed from the survey area (Quinn et al. 2009). For analysis of in-stream life we treated these salmon as though they had been found killed on the day following their last observation alive. Given the similarity in length distribution between missing and bear killed individuals and their conspicuous absence in subsequent surveys, the assumption that these individuals were killed by bears is sound and inclusion of the data does not bias the results. These tagging data provided direct estimates of the probability that a female had spawned as a function of her mode of death.

To create a length-at-age distribution, we annually collected sagittal otoliths from about 100 females that were measured for length. Examination of these otoliths revealed the number of years spent in the lake prior to seaward migration and the number of years at sea. Virtually all (94.1%) had spent 1 rather than 2 years in the lake, and final body size is determined almost exclusively by marine age (Blair et al. 1993), so our subsequent analyses compared females spending 2 vs. 3 years at sea.

To estimate fecundity as a function of length, 149 females that had stranded at the mouth of the stream, but had not been scavenged by gulls, were collected. Each fish was measured, otoliths were removed for age determination, and the entire mass of eggs was weighed. Subsequently, a subsample of eggs (usually about 100) was removed, weighed, and counted to determine mean egg mass and from that an estimate of total fecundity.

Analytical methods

Average spawning success for females of a given size was calculated using a probabilistic approach incorporating expected egg production, the survival cost of marine residency prior to reproduction, the probability of successfully spawning, given size-selective mortality on the spawning grounds, and the probability of escaping capture in the size-selective commercial fishery which exploits these individuals. Each of the four possible modes of death (MOD) had a length-specific probability of occurrence. Combining the probability of each mode of death with the probability of spawning given a specific mode of death, the total probability of successfully spawning as a function of length was calculated as the summed products of these conditional probabilities (Equation 2.1), and represents the probability of spawning in the presence of size-selective freshwater mortality.

$$(2.1) \quad P(spawning \mid length) = \sum_{MOD} \left[P(MOD \mid length) * P(spawning \mid MOD) \right]$$

However, the largest females on average spend three rather than two years at sea, and therefore incur the risk of mortality during that extra year. To account for this additional mortality risk when comparing life history patterns, we estimated the fitness (spawning success) of females maturing after two years at sea, and then "discounted" the fitness of the females that spent three years at sea when calculating their overall spawning probability. To do so, the empirically

calculated probability of spawning as a function of length was multiplied by the proportion of individuals of that length who return after three years at sea ($p_{length}^{3-ocean}$) and the mortality rate for individuals in the third ocean year ($r_{mortality}^{3-ocean} = 0.42$), as estimated by Mathews (1968) for from high-seas sampling and tagging data (Equation 2.2). The Mathews (1968) estimate for marine mortality (0.42 ± 0.12) between the second and third ocean year was chosen because it was specific to both the species and region of interest.

(2.2) $$P\left(spawning \mid length, age\right) = P\left(spawning \mid length\right) * \left[1 - p_{length}^{3-ocean} * r_{mortality}^{3-ocean}\right]$$

Overall spawning success as a function of length was therefore the cumulative probability of spawning, determined by length dependent freshwater and age dependent marine mortality, and length-specific fecundity (Equation 2.3).

(2.3) $$SS_{length} = P\left(spawning \mid length, age\right) * fecundity_{length}$$

The units for this metric of spawning success are the average number of eggs expected to be deposited, per female of a given length (ED/F). The distribution of length-specific spawning success was the metric for fitness, against which the length distributions observed for the Hansen Creek population and other populations within the same watershed (Wood River) were compared. We use the term spawning success to indicate successful deposition (i.e., spawning) of eggs rather than "reproductive success" as that would imply survival of progeny to some designated age, and we have no data on progeny survival. To further evaluate the influence of selection on salmon phenotypic distributions, we also generated predictions for relative spawning success ($SS_{length}^{relative}$) in the absence of size-selective freshwater mortality across length bins by multiplying the expected fecundity for a given length by the mortality "discount" incurred for an additional year of marine residence (Equation 2.4).

(2.4) $$SS_{length}^{relative} = fecundity_{length} * \left[1 - p_{length}^{3-ocean} * r_{mortality}^{3-ocean}\right]$$

This alternative estimate of relative spawning success permitted comparison to length distributions observed in deeper streams of with little risk of size-selective mortality (Quinn et al. 2001b).

Individuals returning from the ocean to spawn in tributaries of the Wood River system are also exploited by a commercial fishery that is size-selective and removes on average 60% of returning salmon (Kendall et al. 2009). To quantify the impact of this anthropogenic selection we calculated the harvest rate for females in 10 mm length intervals caught in the fishery $\left(hr_{length}\right)$, by comparing length distributions for the catch and those fish escaping the fishery to migrate upstream (see Kendall and Quinn (2009) for details). The expected proportions of individuals for each length avoiding capture in the fishery $\left(1 - hr_{length}\right)$, were then multiplied by our expectations of spawning success (eggs deposited per female) in the presence (Equation 2.3) and absence (Equation 2.4) of size-selective freshwater mortality.

In total five alternative models of increasing complexity describing spawning success as a function of length were created incorporating: 1) the length-fecundity relationship only, 2) the length-fecundity relationship and marine mortality cost (Equation 2.4), 3) the length-fecundity relationship, marine mortality cost and size selective freshwater mortality (Equation 2.3), 4) the length-fecundity relationship, marine mortality cost and size-selective fishery removals, and 5) the length-fecundity relationship, marine mortality cost, size selective freshwater mortality and size-selective fishery removals. These five alternative models predicting spawning success as a function of length were then compared to the observed length distribution of salmon from Hansen Creek and six nearby streams within the same watershed of varying size with known predation rates, using a multinomial likelihood (Equation 2.5) where the number of individuals

from a length bin (n_{length}) and total number of measured fish (N) are data and the proportion of total spawning success at a given length ($\hat{p}_{length}$) are predictions. The Akaike information criterion, corrected for finite sample sizes (AICc, see Burnham and Anderson (2002)), was used to determine which of the five competing models, predicting spawning success as a function of multiple selection processes, most parsimoniously represented the observed length distribution for each stream.

$$\ln\left[L(\theta \mid data)\right] = N * \sum_{length}\left[p_{length} * \ln\left(\hat{p}_{length}\right)\right]$$

(2.5)
$$p_{length} = \frac{n_{length}}{N}$$

$$\hat{p}_{length} = \frac{SS_{length}}{\sum_{length} SS_{length}}$$

Results

From 1997 through 2010, 68,060 dead female sockeye salmon in Hansen Creek were sampled (Table 2.1). Of these, 40.8% were classified as having died of senescence, 40.0% were killed by bears, 12.0% were killed by gulls, and 6.7% stranded, with the remainder dying from other or ambiguous causes. The proportions of salmon dying of these four causes varied among years; stranding was related to ease of access to the stream and hence lake level (Carlson and Quinn 2007), and predation by bears was related to salmon density (Quinn et al. 2003). Of the observed dead, 29,086 were measured for length and indicated the forms of mortality to be markedly size-selective. Gull predation and senescence were most common among smaller females whereas the proportions that were stranded and killed by bears increased with body size (Figure 2.2).

Data from tagged fish indicated that the likelihood of successful reproduction was strongly associated with the observed mode of death because death from stranding, bears, or gulls greatly reduced the in-stream lifespan of female sockeye salmon. Virtually all (99.6%) females that died of senescence (n = 231) were estimated to have spawned whereas only 36.5% of the 564 females killed by bears, 28.0% of the 50 killed by gulls, and 16.7% of the 30 stranded females were estimated to have spawned. Combining the extent of size-selection from the entire data set and the probability of reproduction as a function of mode of death from the data on tagged fish revealed strong overall size-selection. Overall, the probability of reproduction was estimated to decrease with length, exemplified as follows: 360 mm (p = 0.723), 420 mm (p= 0.554), 480 mm (p = 0.286) and 520 mm (p = 0.212).

The positive correlation between female length and fecundity was found to be explained as well by a linear function as by more complex models, therefore the linear model was selected for simplicity (least squares regression equation: $Fecundity_{length} = 11.645 * Length - 1660.958$, $p < 0.001$, $r^2 = 0.265$). In total, a 66.2% increase in fecundity across the sampled length range (360 – 504 mm) was observed. A significant positive correlation was also found between female length and the mass of individual eggs (least squares regression equation: $EggMass_{length} = 2.805e^{-4} * length - 2.334e^{-2}$, $p < 0.001$, $r^2 = 0.304$). Of the females sampled, 16.8% were ocean-age 3 and the remaining 83.2% were ocean-age 2. The ocean-age 3 females were larger on average (463.0 vs 414.9 mm, t = 25.13, df = 335, p < 0.001), produced more eggs (3565 vs 3135, t = 3.16, df = 31, p < 0.005), and produced larger eggs (0.111 vs 0.091 g, t = 10.09, df = 37, p < 0.001) than ocean-age 2 females.

Spawning success, quantified as the expected number of eggs deposited per female (ED/F), was estimated for females of different lengths by combining the probability of successful

reproduction, including marine mortality costs, with the expected fecundity at that length (Equation 2.3), and indicated a broad range of near-optimal lengths (380–410 mm), with lower potential for smaller females (because they produce fewer eggs) and larger females (because they incur a greater mortality risk both at sea and in the stream and are therefore less likely to successfully spawn: (Figure 2.3). The empirically derived fitness curve representing expected female spawning success (ED/F) as a function of length generally matched the observed length distribution for Hansen Creek, however when size-selective removals by the Bristol Bay commercial gillnet fishery were included, the resulting model incorporating all components of selection better represented the observed phenotypic distribution. When spawning success was modeled in the absence of size-selective freshwater mortality (bears, gulls and stranding; Equation 2.4), expected spawning success peaked at lengths near 440 mm, significantly larger than that predicted with removals by mortality sources on the spawning grounds (K-S test, $p < 0.05$). These results strongly suggest that natural and anthropogenic selection, in addition to costs of marine residency, and the relationship between length and fecundity, are together shaping the length distribution in Hansen Creek (Table 2.3).

Comparisons of observed sockeye length distributions in nearby streams within the Wood River system (Figure 2.4) revealed that the median female length in Hansen Creek (413 mm) was similar to that in another comparably small stream (Little Whitefish Creek: 403.5 mm) but females were longer on average in larger streams (Ice Creek: 463 mm, Happy Creek: 447 mm, and Bear Creek: 445) where bear predation rates are lower, and rivers (the Agulukpak River: 454 mm, and Agulowak River: 467 mm) where predation is so rare that it cannot be estimated (see Table 2.2). The lengths for females observed in Hansen and Little Whitefish creeks combined were significantly different from those in Ice, Happy, and Bear creeks and the Agulukpak and

Agulowak rivers, combined (Kolmogorov-Smirnov, $D = 0.447$, $p < 0.001$). Least squares regression indicated a significant negative relationship between predation rate and median body size across populations ($p = 0.006$, $r^2 = 0.804$).

When the five alternative models predicting spawning success were confronted with length data from these seven steams, AICc selection of the best model to describe the observed length distribution in each case showed similar results. The model incorporating size-selective freshwater mortality, fishery removals, the length-fecundity relationship, and mortality costs of prolonged marine residency, most parsimoniously described the length distributions in Hansen and Little Whitefish Creeks (Table 2.3). Conversely, the model predicting spawning success in the absence of size-selection on the spawning grounds and anthropogenic selection resulting from the commercial fishery was more likely to explain the length distributions observed in three of the five larger streams (Bear Creek, Happy Creek, Agulukpak River; Figure 2.4; Table 2.3). The model predicting spawning success based upon the length-fecundity relationship alone best explained the observed length distribution for two of the largest streams: Ice Creek and the Agulowak River (Figure 2.4; Table 2.3). For all streams with the exception of the Agulukpak River, alternative models received little support from the data ($\Delta AICc > 10$). The length distribution of salmon in the Agulukpak River was also well described by a model only incorporating the length-fecundity relationship ($\Delta AICc = 1$).

Discussion

Spawning success depends upon both the probability of surviving to reproductive age and the number of viable offspring that can be produced at that age, summed over their lifespan. Size is a critical predictor for spawning success as mortality is often size-selective (Hansson et al.

2007, Kesavaraju et al. 2007), and offspring production (fecundity or clutch size) increases with maternal size in many species (Berrigan 1991). Our investigation of the variation in female spawning potential (successful egg deposition) as a function of body length, yielded several insights into allometric tradeoffs and correlations between optimal and observed length distributions.

If offspring production were the only factor shaping phenotypic distributions for female sockeye salmon, this fecundity advantage would drive populations toward larger average female body size, and body size would be similar among populations. The "fecundity-advantage model" predicts that for species in which fecundity is variable and correlated with body size, larger females will have higher fitness and contribute more genetic material to subsequent generations (Darwin 1874, Preziosi et al. 1996). This idea has been used to explain large relative sizes in terrestrial taxa including insects and reptiles, as well as aquatic taxa from zooplankton to some fishes (Shine 1988). Under this hypothesis, the observed 66.2% increase in fecundity across the length range in Hansen Creek should drive the median female length upward. However, the observed female length distribution peaked between 400 and 410 mm, suggesting that other selective processes may limit the optimal length.

Excluding anthropogenic selection, our analysis predicted a marked (52%) decline in expected egg deposition per female from the peak of 1941 eggs (at length 400 mm) to just 932 eggs (at length 520 mm), resulting primarily from two factors. First, the probability of surviving in the stream long enough to successfully spawn declined with larger sizes because the rate of premature mortality from bear predation and stranding increased with length (Figure 2.2). In contrast, smaller females were more likely to successfully spawn and then die of senescence (Table 2.1). Second, due to finite limitations on growth capacity, the only way to achieve very

large size was is to spend three rather than two years at sea. The additional year at sea incurs a significant mortality cost (estimated at 0.42 ± 0.12, Mathews 1968), reducing the expected spawning success for individuals pursuing this life history pattern. The result of this tradeoff in timing of maturation is that while older females may be larger and therefore have greater fecundity, the chance of surviving to successfully deposit these eggs is significantly reduced. Analogously, Gross (1985) used the probability of mortality at sea in male coho salmon, *O. kisutch*, to demonstrate that males maturing at an early age (termed jacks) had roughly the same estimated reproductive success as older and larger males. Older males were more successful in courtship than the much smaller jacks but this benefit was counter-balanced by the greater risk of mortality during the extra one or more years spent at sea by the older males.

Overall spawning success thus represents a balance between the fecundity benefit associated with greater length, reduction in spawning probability resulting from lower freshwater survival linked to increased length, and the additional mortality cost of prolonged marine residence. The combination of these counteracting factors caused the predicted peak in spawning success (~400 mm) to occur at a size below that which would be predicted in the absence of size-selective freshwater mortality (~440). The expected peak in female spawning success based on the interaction between natural selective forces, physiological constraints on egg production, and marine mortality costs closely matched the observed length distribution in Hansen Creek (Figure 2.3). Both the length distribution and that of predicted spawning success peaked at around 400 mm but when anthropogenic selection resulting from the commercial fishery was incorporated the predicted peak in spawning success shifted to between 380 and 390 mm. Despite the difference in the predicted optimum, the model incorporating both fishery and natural selection processes found greater support from the Hansen Creek length data because the decline in

predicted spawning success following the peak was better represented by a pattern of increased exploitation with size. In reality, the selectivity curve for female sockeye salmon in the commercial fishery is asymmetrically dome shaped (Kendall et al. 2009), with probability of capture increasing from 0.43 (360 mm) to 0.71 (450 mm), and subsequently decreasing to 0.61 (520 mm), across observed length bins, causing enough of a reduction in predicted spawning success at intermediate and large sizes to accurately describe the Hansen Creek length distribution.

In addition, both the observed length distribution for Hansen Creek and that predicted in the presence of natural and anthropogenic selection exhibited distinctive right skewedness, with a small but non-trivial proportion of individuals (or predicted spawning success) at the upper end of the observed length range. The presence of these large females may result from their success when conditions are optimal (e.g., high lake level, reducing the mortality from stranding (Carlson and Quinn 2007), and few bears or high salmon density, reducing *per capita* predation risk), or changes in growing conditions at sea that affect the age distribution of the salmon (Pyper et al. 1999). The similarity between the predicted female spawning success curve and observed length distribution is not unexpected, given the heritability of length-at-age in salmon and their relatives (median h^2=0.29, Carlson and Seamons (2008)). These results do not conclusively demonstrate that this represents an evolutionary response because many biotic and abiotic factors affect salmon growth and size at maturity. However, these factors would largely affect the other populations in common with the Hansen Creek fish because all the juveniles feed in the same lake system, and have the same growth opportunities at sea, thus the differences in phenotype among populations strongly indicate the action of selection.

When the expected spawning success of females as a function of length was estimated in the absence of size-selective freshwater mortality and fishery selection, the peak in spawning success was ~ 450 mm. This approximated the phenotypic distributions seen in the larger streams within the Wood River system, where the risks of selection from stranding and bear predation are functionally close to zero (Agulukpak River) or significantly reduced (Bear and Happy creeks) (Quinn et al. 2001c). These streams are both wider and deeper than Hansen Creek (Table 2.2). In contrast, females from the other shallow and narrow stream with intense bear predation (Little Whitefish Creek), exhibited a distribution of lengths close to that of Hansen Creek, and the length distribution there was better predicted by a model including both natural and anthropogenic selection. Observed length distributions for Ice Creek and the Agulowak River which represent the largest median size range for sockeye among the populations included in these analyses, were best approximated by the length-fecundity relationship alone. This suggests that size-selective freshwater mortality is unlikely to be affecting these populations, and perhaps more interestingly the phenotypic distributions of these two populations do not appear to be better explained with the inclusion of fishery selection or marine mortality costs. Although all of these streams are in close proximity within the watershed, genetic evidence provided by analysis of single-nucleotide polymorphisms (McGlauflin et al. 2011) and microsatellites (Lin et al. 2008) strongly suggests reproductive isolation between spawning populations and ecotypes, substantiating the idea that differences in selection may be driving phenotypic divergence among these populations.

The observed length distributions of female sockeye salmon in this suite of populations (Figure 2.4) indicated the generality of the findings from Hansen Creek and highlight the influence of size-selective freshwater mortality in shaping observed length distributions. Indeed,

studies on chum salmon (*O. keta*) in British Columbia also found a relationship between body size and size of the spawning stream (Beacham and Murray 1987). The observation that expected spawning success in the absence of size-selective freshwater mortality is lower than that observed for the larger streams with lower bear predation rates is likely explained by differences in the proportion of 3-ocean females at a given length in these populations and that observed in Hansen Creek for which these expectations were generated.

Although potential egg deposition was used as the index of spawning success, there are other advantages to female size including larger eggs (Beacham and Murray 1993, Quinn et al. 1995). In the Hansen Creek population, for example, the average mass of individual eggs increased from 0.089 g for females 400 mm long to 0.117 g for females that were 500 mm long. Larger eggs produce larger fry (Heath et al. 1999), and fry size has been linked to increased survival during juvenile life stages in sockeye salmon (West and Larkin 1987) and other salmon species (Quinn 2005). Moreover, larger females construct deeper nests and so their embryos may be more resistant to streambed scour and disturbance by the digging of other females compared to smaller females (Steen and Quinn 1999). Therefore, if we defined spawning success as the number of surviving offspring, the larger and older females would probably obtain some additional benefits. However, the close correspondence between the modeled and observed distributions of female lengths in Hansen Creek suggests that these benefits are not great. In contrast, (Healey 1987) concluded that the observed mean female size exceeded that estimated from egg production, suggesting that other benefits of size were important.

Contrary to expected patterns of spawning success, there is a conspicuous absence of females returning after a single year at sea to spawn in Hansen Creek. These fish would produce few eggs but be less vulnerable to mortality at sea, harvest in the commercial fishery, and

prespawning mortality from predation by bears and stranding. Male salmonids commonly return to breed at an age younger than the youngest females, and use alternative reproductive tactics, sneaking rather than fighting for access to females (Fleming and Reynolds 2004, Gross 1985, Young 2005). A small fraction (1.7%) of the males in Hansen Creek have spent only one year at sea (Rich et al. 2006), yet females displaying this life history are notably absent, and females < 360 mm are exceedingly rare. Given the high spawning success expected for small females, it is interesting that females do not pursue this strategy. One possible explanation for the observed absence of this life history strategy is that a female the size of 1-ocean males (ca. 300 mm) would produce on the order of 1000 eggs (depending on egg size – number tradeoffs) and this might not be enough for replacement, given the sources of natural and anthropogenic mortality to which the offspring are subjected (Quinn 2005). In addition, these extremely small females may not be large enough to defend spawning territory or dig redds that are deep enough to protect embryos from streambed scour during spring high flow events.

This investigation demonstrated that natural and anthropogenic selection processes may shape phenotypic distributions for species in the wild, and selection processes can be quantified and compared amongst populations to explain trait variation. In attempting to define phenotypic optima for a population it is clear that both size-selective freshwater mortality and fishery selection must be incorporated, as both of these processes are likely influencing the evolutionary trajectory of the salmon populations in this system. Failing to include these factors inflates expectations of optimal size, rendering them inconsistent with observed trait distributions. While natural and anthropogenic selection explain much of the variation in body size among streams, large-scale ocean climate conditions also affect the size of returning salmon from year to year (Pyper and Peterman 1999) and therefore affect the length distributions in these populations.

In addition to the implications of this work for the evolution of body size and life history, it illustrates the benefits of research on abundant, semelparous organisms so that the large sample sizes needed to detect and precisely estimate selection pressure are available. Observational studies of selection in natural systems have traditionally been encumbered by very small sample sizes (often less than 135 individuals), and a lack of temporal replication (Kingsolver et al. 2001). Our work illustrates the need for multiple years of data when studying selection as the major sources of size-selective natural mortality (bear predation and stranding) varied greatly from year to year (Table 2.1). Predation varies with salmon density (Quinn et al. 2003) and stranding with lake level (Carlson and Quinn 2007), which are independent of each other. Thus in many ways the relevant sample size to detect selection is not the number of organisms measured in a given year but the number of years of sampling. While modern molecular techniques for parentage analysis are a useful tool for determining phenotypic optima in salmon (Hauser et al. 2011, O'Reilly et al. 1998), these techniques remain cost prohibitive for analysis of larger populations across multiple years of varying selection patterns. The few cases when a population has been studied over many years (e.g., Seamons et al. 2007) reveal great year-to-year variation, further emphasizing the need for long-term studies. Finally, life history studies on species such as salmon and many other fishes that are subject to commercial or recreational exploitation must account for these removals, though in many cases it may be difficult to do so.

Acknowledgements

Data collection for this project was supported by the Pacific salmon seafood industry, the Gordon and Betty Moore Foundation, and the National Science Foundation's Long Term Research in Environmental Biology, and BioComplexity programs. Assistance in the field was

provided by many staff and students but we especially thank Greg Buck, Harry B. Rich, Jr., Stephanie Carlson, Keith Denton, Chris Boatright, Jackie Carter, and Neala Kendall, who also assisted with analysis of the effects of selective fishing. MC was supported by internships from the Howard Hughes Foundation and the Mary Gates Foundation.

Figures

Figure 2.1 Examples of female sockeye salmon (*Oncorhynchus nerka*) whose mode of death was categorized as: A) senescence, based upon the degradation of fins, gaunt form, body cavity devoid of eggs, and rough appearance of scales and tissue (Stephanie Carlson, photo credit), and B) predation by brown bear (*Ursus arctos*), based on the conspicuous loss of tissue to consumption, specifically in the abdominal region in this case (Curry Cunningham, photo credit).

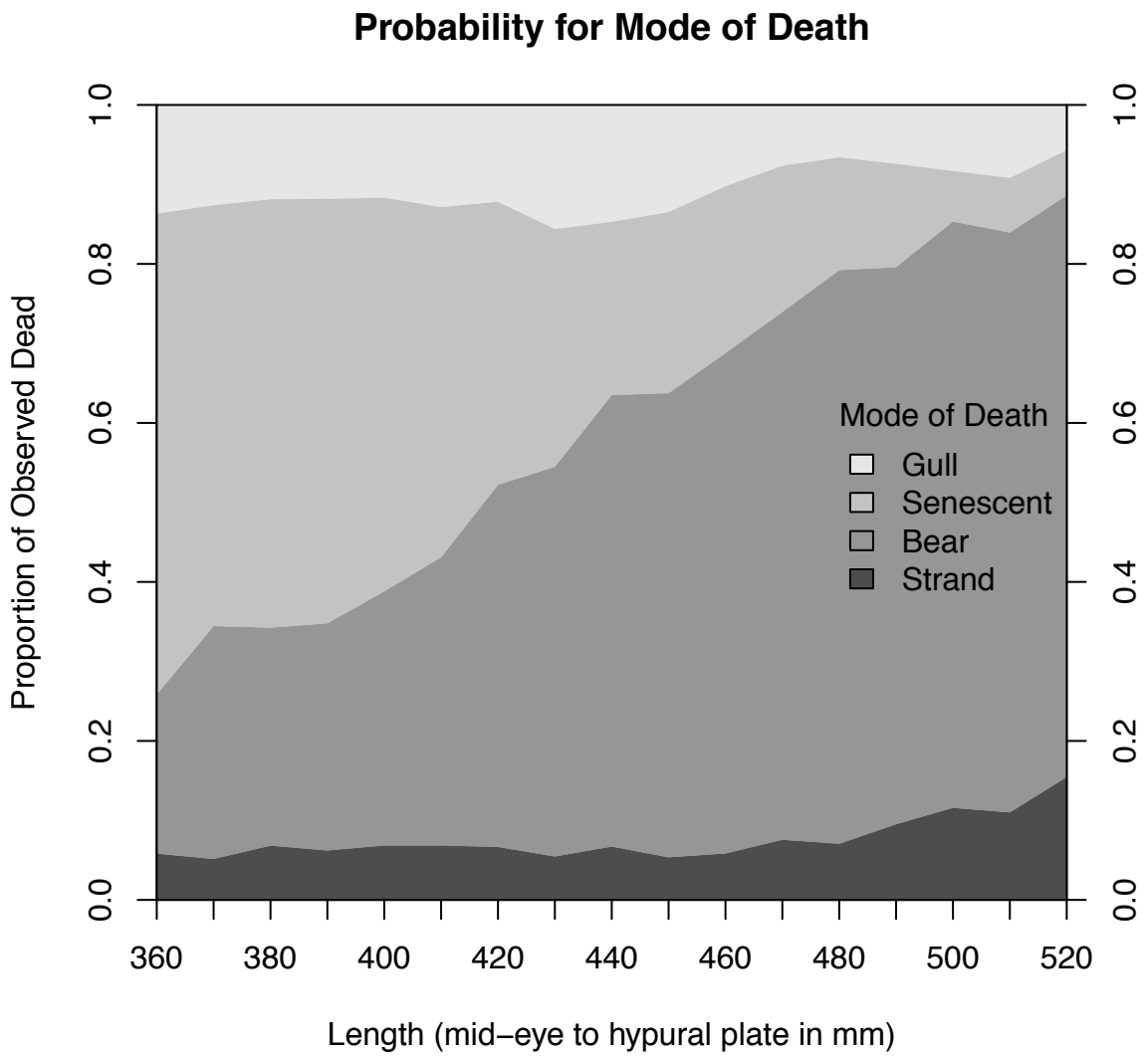

Figure 2.2 Proportion of female sockeye salmon mortalities categorized in each of four modes of death observed in Hansen Creek (1997–2010), as a function of body length.

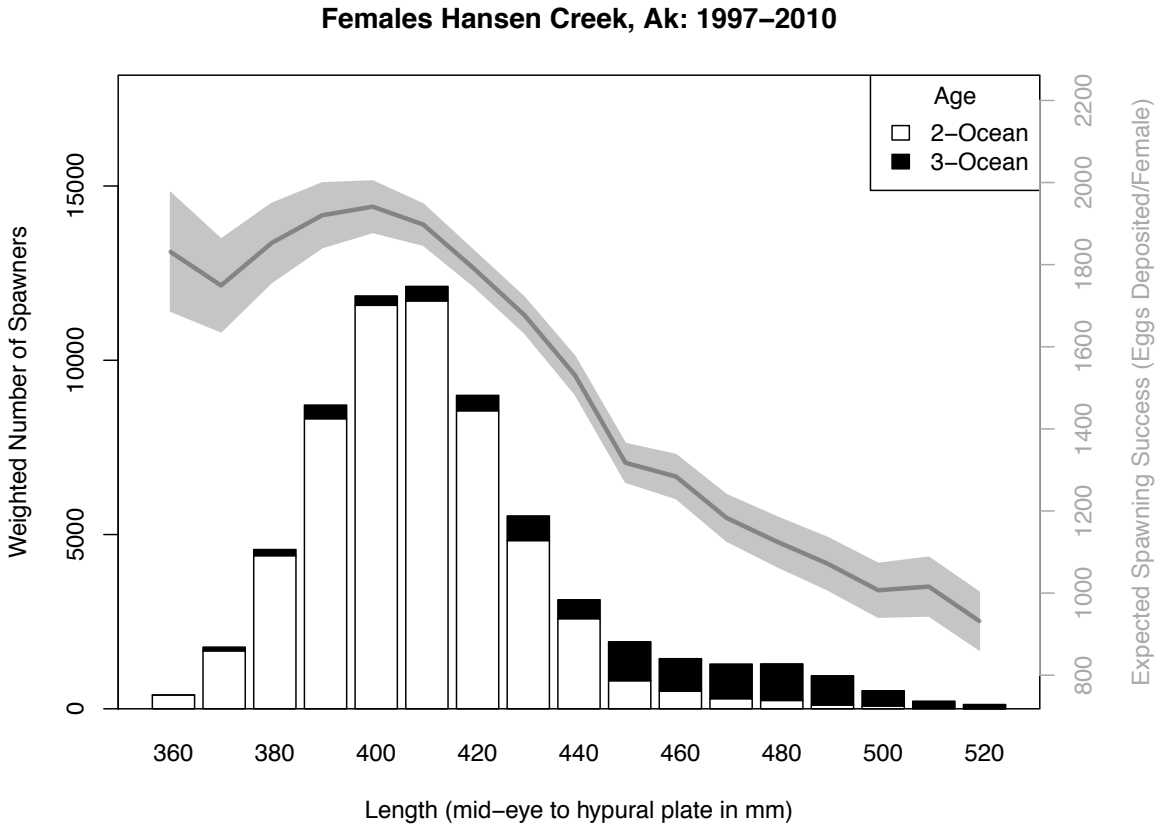

Figure 2.3 Expected female spawning success (eggs deposited per female) in the presence of size-selective freshwater mortality (line and shaded area indicating the median and 95% confidence interval), and weighted length distribution (histogram) for female sockeye in Hansen Creek. Black bars represent the number of fish returning after three years at sea (3-ocean) and white bars the number of 2-ocean fish.

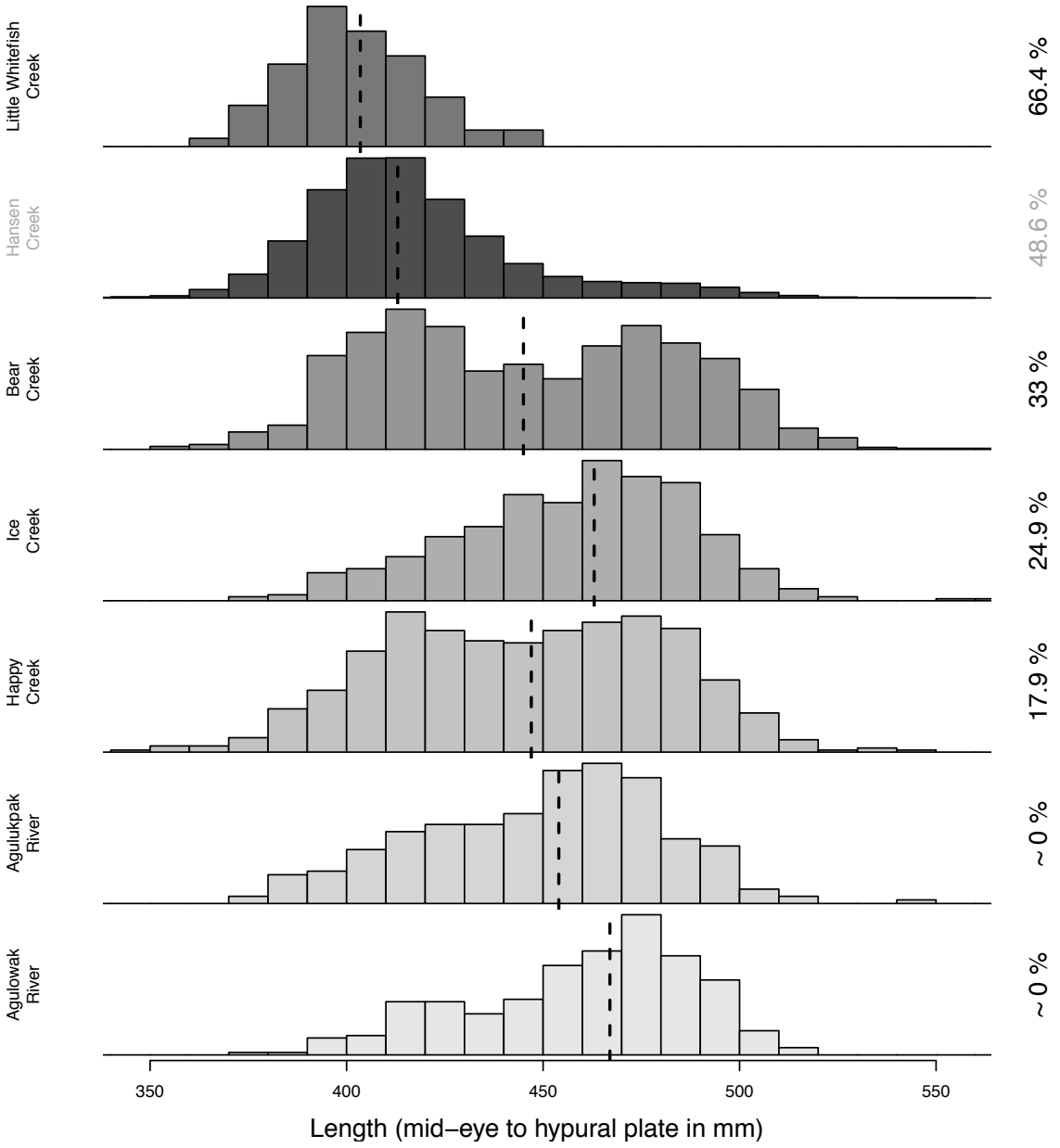

Figure 2.4 Length-frequency histograms for Hansen Creek and nearby sockeye salmon populations in the Wood River system (not reconstructed for fishery removals). Numbers to the right of the histograms indicate the average percentage of fish mortality attributed to bear predation in each population. Dashed vertical lines show the median length for each spawning population. Hansen Creek is highlighted with grey labels.

Tables

Table 2.1 Yearly numbers of dead female sockeye salmon in Hansen Creek, the percent of the sample measured for length, and percent of the entire sample by mode of death. Averages were calculated from annual means (unweighted average) and from all fish. The few fish dying from other or ambiguous causes were omitted.

Year	Total	% Measured	% Senescent	% Bear kill	% Gull kill	% Strand
1997	2,956	62.7%	16.2%	77.7%	0.0%	6.1%
1998	6,904	77.2%	40.2%	49.3%	9.6%	0.9%
1999	10,463	31.3%	60.5%	19.0%	13.7%	3.8%
2000	1,889	66.8%	11.5%	80.9%	3.7%	3.9%
2001	884	88.5%	6.9%	85.4%	4.0%	3.7%
2002	4,689	38.7%	30.4%	55.0%	9.1%	5.4%
2003	6,041	30.3%	31.7%	45.9%	15.7%	6.5%
2004	2,155	74.0%	18.7%	59.6%	16.8%	4.8%
2005	1,986	88.4%	29.5%	35.1%	22.1%	13.3%
2006	13,268	17.8%	62.1%	13.6%	10.2%	14.1%
2007	4,914	63.0%	42.4%	42.0%	6.2%	9.3%
2008	2,642	83.5%	51.2%	40.2%	4.9%	3.7%
2009	682	46.8%	21.1%	70.5%	4.7%	3.7%
2010	8,587	18.8%	20.2%	52.6%	22.9%	4.3%
Total	68,060					
% of all fish			**40.8%**	**40.0%**	**12.0%**	**6.7%**

Table 2.2 Mean and standard deviation of female sockeye salmon lengths (in mm) and rates of bear predation in spawning populations from large rivers (Agulukpak and Agulowak rivers), large streams (Ice, Happy, and Bear creeks), and small streams (Little Whitefish and Hansen creeks) in the Wood River system, Alaska (Marriott 1964, Quinn et al. 2001c) and additional unpublished data.

Population	Mean length (SD)	Median length	Stream width (m)	Stream depth (cm)	Predation rate (%)
Little Whitefish Creek	402.7 (17.2)	403.5	1.7	12.7	66.4%
Hansen Creek	417.7 (28.1)	413.0	3.9	9.8	48.6%
Bear Creek	446.9 (37.5)	445.0	5.1	19.3	33.0%
Ice Creek	458.6 (29.7)	463.0	15.7	42.3	24.9%
Happy Creek	446.0 (34.9)	447.0	4.7	25.2	17.9%
Agulukpak River	450.0 (30.7)	454.0	78.1	78.1	0.0%
Agulowak River	460.9 (28.5)	467.0	77.3	46.6	0.0%

Table 2.3 Results of AICc-based model selection. For each stream, the selection factors which most parsimoniously describe the observed phenotypic distribution are indicated (+), while those factors excluded from the model which received the most support from the data are indicated (-). Selection models incorporating and excluding the influence of marine mortality were equally well supported by the data for the Agulukpak River (ΔAICc < 2), so this factor is indicated (+/-). Possible selection factors include: 1) the relationship between female length and fecundity, 2) the mortality cost associated with prolonged marine residency, 3) size-selective freshwater mortality resulting from predation and stranding in shallow water, and 4) size-selective exploitation by the commercial fishery.

Model Selected	fecundity~length	marine mortality discount	size-selective freshwater mortality	fishery selection
Little Whitefish Creek	+	+	+	+
Hansen Creek	+	+	+	+
Bear Creek	+	+	-	-
Ice Creek	+	-	-	-
Happy Creek	+	+	-	-
Agulukpak River	+	+/-	-	-
Agulowak River	+	-	-	-

Chapter 3

A General Model for Salmon Run Reconstruction Accounting for Interception and Differential Availability to Harvest

Abstract

Traditional methods for partitioning mixed stock catches and reconstructing annual run size primarily utilized age composition data. However, recent advances in molecular genetic techniques have permitted genetic stock identification (GSI) of recent catch samples based on DNA sampled from contemporary catches but also from DNA extracted from historical scale samples obtained years or decades ago for age determination. Traditional methods for run reconstruction used stock-specific differences in age composition to partition mixed stock catches, however these methods do not account for stock-specific differences in availability of fish to harvest within districts and interception rates, the incidental harvest of non-target stocks, in nearby terminal fishing areas. We present a likelihood-based statistical model for salmon run reconstruction which draws inference from both age composition and genetic stock identification data to estimate differential availability of stocks to harvest in mixed stock terminal fisheries and

interception rates amongst proximate fishing districts. This method is applied to data from the commercial sockeye salmon (*Oncorhynchus nerka*) fishery in Bristol Bay, Alaska, to reconstruct annual run size by stock and age class. Results demonstrate that in the absence of genetic data, previous models using only age composition data produced biased estimates of population productivity, underscoring the value of collecting these genetic data.

Introduction

Successful management of commercially exploited species depends upon an accurate understanding of how abundance changes in response to harvest policy. Management of fish resources to achieve maximum sustainable yield (MSY) remains the principal goal, among other social and economic objectives, of fisheries regulation within the United States and in many other countries (Hilborn 2012). To accurately estimate the spawning stock size that is likely to produce MSY, and other fisheries reference points, it is necessary to evaluate the relationship between spawning abundance and the resulting recruitment observed in subsequent years.

Management of commercial for Pacific salmon for MSY targets requires that stock-specific spawner-recruit relationships be quantified. Pacific salmon species (*Oncorhynchus spp.*) return to natal streams with a high degree of fidelity (Fleming and Reynolds 2004, Quinn 2005), significantly simplifying the enumeration of spawning abundance and subsequent recruitment compared to species with oceanic distributions. In salmon populations, recruitment is defined as the number of returning fish that are available to the fishery, i.e. the spawners for the next generation. To estimate recruitment accurately, estimates of catches by population must be combined with in-river estimates of escapement (salmon that escaped the fishery). Available data to quantify spawner-recruit relationships typically include estimates of the catch of that stock

plus the fish migrating upstream past the fishery onto the spawning grounds (termed escapment), as well as the age-composition of the observed run, estimated from scale samples. For salmon stocks exploited by terminal fisheries that target a single stock, acquiring spawner-recruit data is relatively straightforward, although enumeration and collection of age composition information may be costly. However, for fisheries that target a mixture of stocks, each of which is managed separately for MSY, partitioning catches to allocate returning fish among the component stocks poses a significant challenge. Traditionally, some type of "run reconstruction" has been employed to partition catches in mixed-stock fisheries using data available from coded wire tags (Johnson 1990), age-composition (Chasco et al. 2007) or some mix of multiple data types (Flynn et al. 2006, Starr and Hilborn 1988, Templin et al. 1996).

Most recently Branch and Hilborn (2010) used age-composition estimates from commercial fishery catches and upriver escapements collected by the Alaska Department of Fish Game (ADF&G) to apportion catches of sockeye salmon bound for the Igushik, Wood and Nushagak Rivers caught in the same terminal fishery in Bristol Bay, Alaska. Their SYRAH model (Branch and Hilborn 2010) provides a useful tool for partitioning catches in mixed-stock salmon fisheries based upon stock-specific differences in age composition, including estimates of daily returns and arrival timing. However, two difficulties limit its ability to accurately reconstructing age and stock-specific run. First, the SYRAH model did not account for the differing availability of stocks to harvest within mixed-stock fisheries. Differences in availability to harvest are hypothesized to arise from the interaction between stock-specific differences in return migration pathway and the observed spatial heterogeneity in fishing effort within districts. Second, Branch and Hilborn (2010) did not attempt to estimate the harvest rate for fish in multiple discrete fishing areas, resulting from incidental interception. New genetic data reveals

the shortcomings of using age composition as the major source of information for stock separation in Bristol Bay, Alaska.

Bristol Bay sockeye salmon (*Oncorhynchus nerka*) (Fig. 3.1) are a culturally and economically important resource within the state of Alaska providing the basis for vibrant subsistence (Shaw 1998) and commercial fisheries. In 2010, the estimated wholesale value of sockeye caught in the Bristol Bay Commercial fishery was US $390 million, representing about $1/6^{th}$ of the total value of all U.S. seafood exports (Knapp et al. 2013). Although management of the Bristol Bay commercial sockeye fishery restricts fishing effort to spatially explicit terminal fishing areas or districts, in an effort to impose single stock exploitation, there are two principal reasons why these catches must still be partitioned to estimate annual stock-specific returns. First, several terminal fishing districts surround the mouths of multiple river systems and as a result harvest a mixture of stocks during the commercial fishing season. Second, some proportion of returning fish that are caught in specific districts may be bound for spawning grounds in other regions. Evidence for interception comes first from tagging studies conducted in the 1950s and 1960's, which found that a non-trivial number of fish are intercepted in proximate fishing districts (Straty 1975). This phenomenon was more directly demonstrated by Menard and Miller (1997) who analyzed the pattern of scale samples collected from Bristol Bay catches (1983-1995) to estimate average interception rates of 10.0% for Naknek-Kvichak District catches, 24.1% for the Egegik District catches, and 27.0% for the Ugashik District catches. The most compelling evidence and best direct rate estimates for non-natal district interception in Bristol Bay came from genetic stock identification (GSI) of catch samples by Dann et al. (2009), using diagnostic single-nucleotide polymorphisms (SNPs). GSI of commercial fishery samples (2006-2008) by Dann et al. (2009), indicated that catches for select fishing districts, were in

some years comprised of greater than 25%, fish bound for neighboring river systems. Given these findings, it is clear that run reconstruction models must incorporate available genetic data alongside age-composition data, if they are to accurately estimate interception rates, partition mixed stock catches, reconstruct true annual run sizes, and calculate the brood tables necessary to establish sustainable harvest policy. Without properly allocating catches from mixed-stock fisheries and accounting for interception rates, imprecision in brood tables and resulting spawner-recruit relationships will inevitably lead to management goals which are inconsistent with the underlying biology of Bristol Bay sockeye systems, and at best result in foregone yield, and at worst jeopardize the future sustainability of wild sockeye exploitation.

The advent of modern molecular genetic techniques for assigning catches from mixed-stock salmon fisheries back to stocks of origin has proven to be an invaluable tool for resource managers (Shaklee et al. 1999). Development of new putative markers and advances in high-throughput analytical technology have increased the efficacy of these techniques in ecosystems with complex population structure and reduced both the cost and processing time for samples (Hauser and Seeb 2008). Definitive single-nucleotide polymorphisms (SNPs) are utilized as genetic markers to identify the stock composition of catch samples because of their low error rates, high throughput capacities, and the potential to genotype thousands of individuals and dozens of SNP loci (Hauser and Seeb 2008, Smith 2010). Furthermore the development of a comprehensive genetic baseline for Bristol Bay (Habicht et al. 2010) have provided the opportunity to accurately differentiate stocks of management interest from amongst admixture samples. These innovations, paired with techniques for genotyping historical fish scale samples using SNPs (Smith et al. 2011), mean that genetic data are increasingly available for incorporation into modern run reconstruction models. However, for many systems a complete

record of GSI data for commercial fishery catches across time is not available, so it is necessary to utilize both age and genetic composition of catch information to inform the reconstruction of historical returns.

This paper describes the first implementation of a run reconstruction model which partitions catches using both age and genetic composition of catch information, and compare results with those generated using age-based methods traditionally employed by the Alaska Department of Fish and Game (ADFG) (Bernard 1983). This model reconstructs stock-specific brood tables by: (i) partitioning catches in mixed-stock fishing districts where spatial heterogeneity in fishing effort combined with variation in homeward migration pathway drive differences in realized fishing mortality rates amongst stocks, (ii) estimating historical interception rates for stocks in non-natal fishing districts during the spawning migration. Estimates of stock-specific availability to harvest in neighboring fishing districts, age-specific gear selectivity, and realized harvest rates are provided for the Bristol Bay, Alaska commercial sockeye salmon fishery.

Methods

General model description

The objective of this research was to create a generalized run reconstruction model capable of utilizing genetic composition of catch data alongside catch, escapement and age-composition information, to partition commercial fishery catches and reconstruct annual salmon returns. Several aspects of this run reconstruction model differentiate it from previous statistical run reconstruction models. First, while previous run reconstruction models applied to the Bristol Bay commercial fishery (see Branch and Hilborn (2010) and Flynn et al. (2006)) have utilized

comparisons of observed catch and escapement age composition to partition mixed-stock catches within single districts, they have not explicitly addressed the potential for interception in non-natal fishing districts or attempted to account for its effect. The run reconstruction model described here, estimates stock-specific parameters describing the availability of fish from a specific stock to harvest in multiple fisheries, accounting for the effect stock-specific migration pathway variation and interception in non-natal fishing districts.

Second, the current model is designed to reconstruct salmon runs at an annual time scale, with the purpose of generating brood tables that account for interception and stock-specific difference in availability to harvest. Formal run reconstruction models are typically employed to estimate the arrival distribution for salmon stocks in either gauntlet (Starr and Hilborn 1988) or terminal (Branch and Hilborn 2010, Chasco et al. 2007, Schnute and Sibert 1983) fisheries, or for the purposes of "preseason planning" (Cave and Gazey 1994). While many of these "forward" run reconstruction models for Alaskan sockeye salmon commercial fisheries (Branch and Hilborn 2010, Chasco et al. 2007, Flynn et al. 2006) utilize compositional data to partition mixed-stock catches on a daily basis, given that our purpose it to explicitly estimate total seasonal returns by stock we have elected to aggregate data at the seasonal level (see Data section below for methods). Third, previous run reconstruction models for Bristol Bay sockeye salmon utilize age composition data from the four predominant age classes (e.g. 1.2, 1.3, 2.2, 2.3) observed (Flynn et al. 2006), or allow for the contribution of an "other" age class for individuals of particular stocks (i.e. Nushagak River) where alternative age classes are more prevalent (Branch and Hilborn 2010). However, given that complete brood tables for Bristol Bay must account for the contribution of all observed age classes, the current run reconstruction

model structure directly accounts for all 18 potential age classes (0.1, 0.2, 0.3, 0.4, 0.5, 1.1, 1.2, 1.3, 1.4, 1.5, 2.1, 2.2, 2.3, 2.4, 3.1, 3.2, 3.3, 3.4).

Fourth, in addition to estimating age-class specific relative fishing gear selectivity, the current model also estimates an "availability" parameter that represents the stock-specific availability to fishing gear in each fishing district. This represents an improvement over traditional methods for partitioning mixed-stock catches of Bristol Bay sockeye (Bernard 1983, Branch and Hilborn 2010, Flynn et al. 2006) that did not account for the known interception of fish in high seas and South Peninsula, Alaska fisheries.

Bristol Bay

Sockeye salmon returning to Bristol Bay (Figure 3.1) are predominantly bound for eight major river systems, the Igushik, Wood, and Nushagak Rivers on the western side, and the Kvichak, Alagnak, Naknek, Egegik, and Ugashik Rivers on the eastern side. Returning salmon are harvested in four spatially explicit terminal commercial fishing districts between June and August of each year, which are actively managed inseason by emergency order to achieve fixed seasonal escapement goals (Clark et al. 2006). The Nushagak District is a mixed-stock fishery located at the point where the Igushik, Wood, and Nushagak Rivers enter the northwest corner of Bristol Bay (Figure 3.1). The Naknek-Kvichak District is also managed as a mixed-stock fishery harvesting sockeye returning to the Kvichak, Naknek, and Alagnak Rivers and is located at the northeast corner of Bristol Bay. The Egegik and Ugashik Districts are located at the mouths of those rivers respectively and are operated as single-stock fisheries, although GSI data indicate significant proportion of sockeye caught in these districts are bound for other river systems (Dann et al. 2009, Smith 2010).

Four types of data are available to inform reconstruction of annual run sizes by stock and age class: absolute counts in numbers of commercial fishery catches, upriver escapements, age composition of catches and escapements, and stock composition of commercial catches from GSI.

Catch data

Commercial fishing district catches are collected on a daily basis throughout the fishing season for each commercial fishing district. The weight of individual fish are sampled throughout the season by ADFG biologists and used to translate the biomass of observed catches into numbers of fish.

Escapement data

Escapement to the Igushik, Wood, Kvichak, Naknek, Egegik, and Ugashik river systems is counted on a daily basis using elevated towers that visually count the number of sockeye moving upstream. Counts are conducted for 10-minute periods on each side of the river in each hour, 24 hours per day between June and August, and scaled up to daily escapement numbers. Visual enumeration of escapement to the Nushagak River is impossible due to the turbidity of the water, so counts are made using sonar equipment at Portage Creek, Alaska. The escapement counting tower on the Alagnak River has been operated sporadically throughout the period of reconstruction, so a combination of tower counts and end of season aerial survey estimates are used. Given the current objective of reconstructing annual returns by stock, daily catch and escapement data are summed to seasonal totals $C_{d,y}$ and $E_{s,y}$, which are the total catch and escapement respectively for district d and stock s in year y.

Age composition data

Age composition information for both catch and escapement are available from ADFG, dating back to the mid-1960s. Scales are collected from samples of commercial fishery catches and upriver escapements during multiple sampling periods throughout the spawning migration. Scale samples are collected from fishery catches in each commercial fishing district during range of sampling periods which span the duration of the summer fishery, and subsequently aged by ADFG staff. Scales for age identification are collected at escapement enumeration sites by beach seine at multiple points throughout the season. To calculate the seasonal age composition of catches in each district ($p^C_{d,a,y}$), a proportion weighted by the observed catch in each sampling period was calculated as

$$p^C_{d,a,y} = \frac{\sum_{i=1}^{I_{d,y}} P^C_{d,a,i,y} * n^C_{d,i,y}}{\sum_{i=1}^{I_{d,y}} n^C_{d,i,y}} \quad (3.1)$$

$$n^C_{d,i,y} = \sum_{t \in \{D^C_{d,i,y}\}} c_{d,t,y}$$

where, $P^C_{d,a,i,y}$ is the observed proportion of age class a, in catch samples from district d, during sampling period i of year y. $n^C_{d,i,y}$ is the observed catch in by district, sampling period, and year, and represents the sum of daily catches $c_{d,t,y}$ across the set of days in each sampling period i, for each district d in each year y ($D^C_{d,i,y}$). $I_{d,y}$ is the number of catch age composition sampling events by district and year. Seasonal age compositions were calculated in a similar way for escapements

$$p^E_{d,a,y} = \frac{\sum_{i=1}^{I_{s,y}} P^E_{s,a,i,y} * n^E_{s,i,y}}{\sum_{i=1}^{I_{s,y}} n^E_{s,i,y}} \quad (3.2)$$

$$n^E_{s,i,y} = \sum_{t \in \{D^E_{s,i,y}\}} \varepsilon_{s,t,y}$$

as the sum of age composition proportions observed for each sampling event $P^E_{s,a,i,y}$, weighted by the total of daily escapements $\varepsilon_{s,t,y}$ observed during that sampling period $n^E_{s,i,y}$.

Genetic stock identification data

Genetic stock identification data for run reconstructions are available from two sources for different periods of time in Bristol Bay. Genetic stock identification of mixed stock samples of Bristol Bay commercial fishery catches began in 2006 based upon catch samples collected from each of the commercial fishing districts during multiple sampling periods annually, and analyzed by ADF&G Gene Conservation Laboratory (Dann et al. 2009). In addition to genetic stock identification data for recent years (2006 – 2014), data are also available from SNP analysis of archived scale samples collected from Bristol Bay catches conducted by Smith (2010). Until recently, evaluating the genetic composition of mixed stock scale samples has been significantly hindered by the low amounts of template DNA which may be extracted from scales and the potential for contamination from preexisting DNA, with low concentration DNA leading to high rates of PCR failure and errors in genotyping due to allelic dropout (Taberlet et al. 1996). Smith et al. (2011) utilized a novel combination of multiplex preamplification PCR to generate accurate genotypes with low failure and error rates, and amplification of microsatellite loci to detect DNA contamination in scale samples. Using this technique Smith (2010) was able to conduct GSI for Bristol Bay catch samples for a range of years in each commercial fishing

district dating back to the early 1960's, screening for the observed 21% contamination rate in these historical samples. GSI data are available for the Nushagak District in 9 years between 1965 and 1999, the Naknek-Kvichak District in 14 years between 1964 and 2005, the Egegik District in 12 years between 1964 and 2002, and the Ugashik District in 8 years between 1964 and 2002 (Smith 2010). Observed genetic proportions by sampling period were translated into seasonal catch proportions using the same methods described for catch (Equation 3.1) and escapement (Equation 3.2) age composition data.

Model structure

The core of the estimation process within the annual run reconstruction model is the continuous catch equation (Branch and Hilborn 2010, Megrey 1989)

$$\hat{C}_{s,a,d,y} = \hat{N}_{S,a,y}\left(1 - e^{-A_{s,d,y} * S_{k_a,y} * F_{d,y}}\right) \quad (3.3)$$

where $\hat{C}_{s,a,d,y}$ is the estimated catch for stock s, age class a, in district d, of year y, and $\hat{N}_{s,a,y}$ is the stock and age specific number of returning fish by year. $A_{s,d,y}$ is the availability of stock s to harvest in district d, and describes the effect of differences in migration pathway for stocks relative to the spatial distribution of fishing effort in mixed-stock fisheries and the potential for non-target stock interception. $S_{k_a,y}$ is the selectivity of fishing gear by age group k in each year. $F_{d,y}$ is the instantaneous fishing mortality rate for each district in each year.

This formulation of the continuous catch equation differs from both the classic Baranov catch equation (Beverton and Holt 1957, Hilborn and Walters 1992) through the removal of the instantaneous natural mortality rate M. Given that the Bristol Bay commercial salmon fishery operates through terminal exploitation, the natural mortality rate between fishery capture and upriver enumeration of escapement is assumed to be slight compared to removals by the fishery.

This assumption is common amongst previous run reconstruction models (Branch and Hilborn 2010, Chasco et al. 2007, Flynn et al. 2006, Starr and Hilborn 1988). Equation 3.3 also differs from the traditional continuous catch equation because incorporates the $A_{s,d,y}$ term representing stock-specific availability to harvest within each fishing district.

The SYRAH run reconstruction model (Branch and Hilborn 2010) utilized two novel concepts that significantly improved its generality, ease of application to other salmon fisheries, and effectively reduced the number of estimated parameters, which have been included in the current model. The first was the concept of representing fish as age, stock, and arrival date specific groups throughout the model, which greatly increased its generality. The current model likewise employs the group concept, enhancing the applicability of the model structure for use in reconstructing mixed stock catches in other regions with differing stock and age structures. For application to Bristol Bay the run reconstruction model incorporates 54 model groups (3-stocks x 18-age classes) for western Bristol Bay and 90 model groups (5-stocks x 18-age classes) for eastern Bristol Bay, for each of which annual run sizes are calculated in each year. For simplification we have listed these groups in their full array form ($N_{s,a,y}$) however as each stock and age combination is represented as a model group this is equivalent to the representation $N_{g,y}$ within the code for the estimation model.

The second novel concept employed by Branch and Hilborn (2010) was the use of a flexible system of indexing to link model groups and effectively reduce the number of estimated parameters. This system of indexing is equivalent to a lookup table that connects estimated parameter to groups of fish within the model, is used here to reduce the number of estimated gear selectivity and availability parameters. While the full range of model groups includes each of the stock by 18-age class combinations, gear selectivity $S_{k_a,y}$ is linked to the ocean age k of each

age class a. In this way the parameter representing the selectivity of fishing gear for the 2-ocean age class ($S_{k=2,y}$) is indexed to all 2-ocean individuals independent of the duration of their freshwater residency (i.e. 0.2, 1.2, 2.2, and 3.2 age classes), using the k_a pointer vector. The decision to estimate separate selectivity parameters for the distinct ocean age classes only, was predicated on the observation that duration of marine rather than freshwater residency is the primary determinant of size in maturing adults (Quinn 2005), and findings by Kendall et al. (2009) indicating that size is a key determinant of whether or not individual will be retained in the gillnet gear used by Bristol Bay commercial fishery. Separate ocean-age, but stock independent gear selectivity parameters were used for the east and west sides of Bristol Bay. Similarly, the group system of indexing was used to link estimated availability to harvest parameters $A_{s,d,y}$ was indexed to a specific stock in a specific district, while remaining independent of the age class of individuals. In this way, 18 potentially estimated age-specific gear selectivity parameters were reduced to just five.

Model-predicted escapement is calculated by subtracting the sum of predicted stock and age class specific catches from the estimated number of returning individuals

$$\hat{E}_{s,a,y} = \hat{N}_{s,a,y} - \sum_{d=1}^{N_d} \hat{C}_{s,a,d,y} \quad (3.4)$$

where $\hat{E}_{s,a,y}$ is the predicted escapement of stock s and age class a in year y, and N_d is the number of fishing districts which are allowed to intercept or harvest fish of that group.

The fishing mortality rate in each year and district $F_{d,y}$ is not directly calculated from equation 3.3 because no analytical solution exits, therefore repeat iterations of the Newton-Raphson method were used to approximate the solution as suggested first by Sims (1982) and

later evaluated by Restrepo and Legault (1995). This process begins by first determining an analytical solution for each district in each year

$$f_{d,y}^{0} = \ln\left(\frac{\frac{\upsilon_y}{\upsilon_y - \delta_{d,y}}}{\frac{\sum_{s=1}^{N_s}\sum_{a=1}^{N_a} A_{s,d,y} S_{k_a,y} \hat{N}_{s,a,y}}{\upsilon_y}}\right)$$

$$\upsilon_y = \sum_{s=1}^{N_s}\sum_{a=1}^{N_a} \hat{N}_{s,a,y} \tag{3.5}$$

$$\delta_{d,y} = \sum_{s=1}^{N_s}\sum_{a=1}^{N_a} \hat{C}_{s,a,d,y}$$

where, υ_y is the predicted total number of returning fish in year y, $\delta_{d,y}$ is the predicted total catch for each district and year. For $n = 20$ iterations the approximated fishing mortality rate $f_{d,y}$ is updated using the Newton-Raphson method,

$$f_{d,y}^{n+1} = f_{d,y}^{n} + \frac{\delta_{d,y} - \sum_{s=1}^{N_s}\sum_{a=1}^{N_a} \hat{N}_{s,a,y}\left(1 - e^{-A_{s,d,y} * S_{k_a,y} * f_{d,y}^{n}}\right)}{2\sum_{s=1}^{N_s}\sum_{a=1}^{N_a} A_{s,d,y} * S_{a,y} * \hat{N}_{s,a,y} e^{-A_{s,d,y} * S_{k_a,y} * f_{d,y}^{n}}} \tag{3.6}$$

until convergence to $F_{d,y}$.

Likelihoods and penalties

Estimation of run reconstruction model parameters was conducted using maximum likelihood methods. The complete negative log-likelihood is the sum of the negative log-likelihoods of model predicted quantities given the observed data and penalties for scaling model parameters.

$$-\ln\left(L_{total,y}\right) = \sum_{l=1}^{5} -\ln\left(L_{l,y}\right) - \sum_{p=1}^{2} \tau_{p,y} \tag{3.7}$$

In equation 3.7, $L_{l,y}$ are observation error likelihoods for each of the five types of data in each year, and $\tau_{p,y}$ are penalty values for scaling selectivity and availability parameters in each year. Maximum likelihood estimates for model and derived parameters were found by minimizing the total negative log-likelihood.

The likelihood for catch data was assumed to represent a normally distributed observation process

$$\hat{C}_{d,y} = \sum_{s=1}^{N_s}\sum_{a=1}^{N_a}\hat{C}_{s,a,d,y}$$
$$-\ln\left(L_{1,y}\right) = N_d \ln\sigma_C + \frac{1}{2\sigma_C^2}\sum_{d=1}^{N_d}\left(\ln C_{d,y} - \ln\hat{C}_{d,y}\right)^2 \quad (3.8)$$

where $C_{d,y}$ is the catch observed in each district in each year, $\hat{C}_{s,a,d,y}$ is the model-predicted catch, and σ_C is the standard deviation of the observation error distribution. This differed from methods by Branch and Hilborn (2010), which assumed that catch, was observed without error. The likelihood for escapement data was also assumed to represent a normally distributed observation process

$$\hat{E}_{s,y} = \sum_{a=1}^{N_a}\hat{E}_{s,a,y}$$
$$-\ln\left(L_{2,y}\right) = N_s \ln\sigma_E + \frac{1}{2\sigma_E^2}\sum_{s=1}^{N_s}\left(\ln E_{s,y} - \ln\hat{E}_{s,y}\right)^2 \quad (3.9)$$

where $\hat{E}_{s,a,y}$ is the model-predicted escapement for stock s and age class a in return year y, $E_{s,y}$ is the escapement observed for each stock from the tower counts, sonar enumeration, or aerial survey conducted in year y, and σ_E is the standard deviation of the observation error distribution for escapements. In practice, the variance parameters for the catch and escapement observation error distributions σ_C and σ_E tended toward zero during minimization when either estimated

directly from the data or calculated using the analytical solution, so they were fixed at $\sigma_C = 0.5$ and $\sigma_E = 0.1$.

The observation process for the age composition data was assumed to follow a multinomial distribution for samples from both the catch and escapement. The model-predicted age composition proportions of the catch ($\hat{p}^C_{d,a,y}$) and escapment ($\hat{p}^E_{s,a,y}$) are first calculated for each return year.

$$\hat{p}^C_{d,a,y} = \frac{\sum_{s=1}^{N_s} \hat{C}_{s,a,d,y}}{\sum_{s=1}^{N_s}\sum_{a=1}^{N_a} \hat{C}_{s,a,d,y}} \qquad \hat{p}^E_{s,a,y} = \frac{\hat{E}_{s,a,y}}{\sum_{a=1}^{N_a} \hat{E}_{s,a,y}} \tag{3.10}$$

The negative log likelihood of model-predicted seasonal age compositions for the catch $-\ln\left(L_{3,y}\right)$ and escapement $-\ln\left(L_{4,y}\right)$ available from equation 3.11, given the observed weighted seasonal total age composition samples from equations 3.1 and 3.2:

$$-\ln\left(L_{3,y}\right) = -\sum_{d=1}^{N_d}\left[\varepsilon * \sum_{a=1}^{N_a} p^C_{d,a,y} * \ln\left(\hat{p}^C_{d,a,y}\right)\right] \qquad -\ln\left(L_{4,y}\right) = -\sum_{s=1}^{N_s}\left[\varepsilon * \sum_{a=1}^{N_a} p^E_{s,a,y} * \ln\left(\hat{p}^E_{s,a,y}\right)\right] \tag{3.11}$$

where ε is the effective sample size for age composition samples. While alternatives to the likelihood functions for compositional data have been used effectively, including the logit-normal and Dirichlet (Schnute and Haigh 2007) and the robust normal (Fournier et al. 1990, Hilborn et al. 2003a), these likelihood formulations are undefined for composition groups with zero proportions. Therefore the multinomial likelihood was selected given that we are evaluating the full range of potential age classes (18) some of which have very low or zero representation

amongst samples, and its previous use for Bristol Bay sockeye age composition data (Branch and Hilborn 2010, Flynn and Hilborn 2003).

Similar to age composition samples the multinomial likelihood was also used to incorporate GSI data from catch samples and inform estimates of model parameters. The model-predicted proportional representation of stocks in catch samples $\hat{p}^{G}_{d,s,y}$ was first calculated and then used to calculate the likelihood of this prediction given observed data

$$\hat{p}^{G}_{d,s,y} = \frac{\sum_{a=1}^{N_a} \hat{C}_{s,a,d,y}}{\sum_{s=1}^{N_s}\sum_{a=1}^{N_a} \hat{C}_{s,a,d,y}} \tag{3.12}$$

$$-\ln\left(L_{5,y}\right) = -\sum_{d=1}^{N_d}\left[\gamma * \sum_{s=1}^{N_s} p^{G}_{d,s,y} * \ln\left(\hat{p}^{G}_{d,s,y}\right)\right]$$

where γ is the effective sample size for genetic composition of catch data. For estimation the effective sample size for both genetic composition of catch γ and that for age composition ε were fixed at 100 for all years. The decision to fix the effective sample size rather than estimate it iteratively as described by McAllister and Ianelli (1997) was predicated on: (i) the fact that compositional samples represent a weighted sum across multiple sampling events throughout each season, and (ii) better model fits to both types of compositional data were achieve by fixing the effective sample sizes. Trials with alternative effective sample sizes yielded similar fits to the compositional data. Trials with alternative effective sample sizes yielded similar fits to the data, suggesting that estimation is insensitive to the fixed effective sample size.

In addition to the five likelihood functions, the total data likelihood also included two penalty functions for scaling model parameters. To standardize model-estimated gear selectivity parameters to a mean of one, a penalty across all was added to the likelihood

$$(3.13)\quad \tau_{1,y} = 1000\left(\frac{1}{N_k}\sum_{k=1}^{N_k} S_{k,y} - 1\right)^2$$

where N_k is the number of availability age groups and is equal to the number of ocean age classes. A similar penalty was added to the likelihood to ensure that availability parameters for stocks within a district also have a mean of one

$$(3.14)\quad \tau_{2,y} = \sum_{d=1}^{N_d} 1000\left(\frac{1}{N_s}\sum_{s=1}^{N_s} A_{s,d,y} - 1\right)^2$$

where $\tau_{2,y}$ is the total penalty addition to the likelihood function. Both the selectivity parameter penalty $\tau_{1,y}$ and the availability parameter penalty $\tau_{2,y}$ will approach zero as the model converges, and therefore have no contribution to the total log likelihood.

Estimation procedure

The total negative log likelihood $-ln(L_{total,y})$ was minimized separately for each year (1963 – 2014) to obtain estimates of model parameters including the parameter of interest, the reconstructed run size by stock and age class $\widehat{N}_{s,a,y}$. The model was implemented in AD Model builder (ADMB) (Fournier et al. 2012), which calculates the derivative of the objective function with respect to model parameters to minimize the objective function.

Because of the observed separation in return migration pathways for east and west side Bristol Bay stocks (Straty 1975) and resultant low interception rates between east and west side stocks (Dann et al. 2009, Smith 2010), reconstructions were conducted separately for the east and west sides of Bristol Bay (Figure 3.1). In other words the assumption was made that there was no interception of the Igushik, Wood, and Nushagak stocks in the east-side Naknek-Kvichak, Egegik, and Ugashik districts. Similarly, it was assumed that the Kvichak, Alagnak, Naknek, Egegik and Ugashik stocks are not intercepted in the west-side Nushagak district. In

addition, separate gear selectivity parameters were estimated for the east and west sides of Bristol Bay.

Reconstruction of annual returns (1963 – 2014) was conducted in two sequential phases for the east and west sides of Bristol Bay. First, the model was fit to data from years for which full GSI data were available for all districts, to estimate availability parameters for stocks in each district ($A_{s,d,y}$). Subsequently, the model was fit to years for which partial or no GSI data were available. For districts in years where GSI data were not available, the availability by stock for that district was fixed at the mean of availability estimates across years for which data were available, as there appeared to be no temporal trend in estimated availability parameters over time. In this way run size by stock and age class, accounting of interception in non-natal fishing districts and stock-specific availability to harvest in mixed-stock fisheries, for each year 1963 – 2014 inclusive.

After fitting the run reconstruction model to data in each year to reconstruct run size, brood tables were constructed for each stock. Brood tables indicate the observed recruitment by brood year across age classes and are calculated simply lagging age class returns back to their year of conception.

Special harvest area, South Peninsula, and high seas catch allocation

Within the Nushagak, Naknek-Kvichak, Egegik, and Ugashik commercial fishing districts (Figure. 1), there are several fishing areas whose catch was allocated differently within the run reconstruction due to differences between their stock composition and that of the larger fishing districts (Dann et al. 2009). To include catches from these areas with known stock composition differences in the formal run reconstructions would lead to bias in run size estimates (Lowell Fair per comm.). For the Nushagak District these areas included the Wood River Special

Harvest Area (WRSHA) and Igushik River set net catches. The WRSHA is an in-river fishing zone opened periodically to allow for preservation of escapement to the neighboring Nushagak River while still permitting for exploitation of Wood River sockeye. As a result of its location upstream of the main commercial fishing district, catches in the WRSHA are completely comprised of the Wood River Stock. Similarly, Igushik River set net catches are predominantly comprised of the Igushik River stock (Dann et al. 2009) given the location of fishing effort relative to the migration pathway for Wood and Nushagak stocks. Catch from both of these areas were withheld from the formal run reconstruction in each year and allocated post hoc to Wood and Igushik Rivers in proportion to the observed age composition.

Eastern Bristol Bay catches from the Kvichak set net fishery, Alagnak River Special Harvest Area (ARSHA), and Naknek River Special Harvest Area (NRSHA), were withheld from the formal reconstruction and allocated post hoc. Catches from the ARSHA and NRSHA were completely allocated to their respective rivers given minimal potential for interception, while Kvichak set net catches were allocated in proportion to GSI data for that area in each year, or the average of available GSI proportions in years for which data were not available.

Historically there have been two sources of fishing mortality for Bristol Bay sockeye in addition to the commercial fishing districts. These include interception in the South Peninsula commercial fishery and in the high seas salmon fishery. GSI data for the South Peninsula fishery on the Alaska Peninsula suggest a large proportion of sockeye catches are bound for Bristol Bay (Dann et al. 2012). A portion of South Peninsula fishery catches in each year were added into reconstructed run sizes, proportional to the observed distribution of sockeye across Bristol Bay and Togiak, and age composition. Similarly, the high seas salmon fishery that operated through 1987 intercepted sockeye bound for Bristol Bay tributaries, and therefore a portion of these

catches were also added to reconstructed annual run sizes in the same manner as South Peninsula catches.

Results

Model fits to data

A comparison of model-predicted catch in the Nushagak District and escapement to the Igushik, Wood, and Nushagak Rivers with observed data indicates that model predictions are able to capture the high level of interannual variability in these data with significant accuracy (Figure 3.2). For the east side of Bristol Bay, model predictions closely matched the interannual variation in catch, with only slightly lower performance in explaining the observed escapement data (Figure 3.3). All differences between observed and predicted catch and escapement are small in magnitude, relative to the data.

The run reconstruction model's ability to explain the observed variation in age composition over time depended primarily on the age class, and secondarily on whether compositional data were from catch or escapement. For the west side of Bristol Bay, model predictions for age composition proportions across years more closely aligned with the observed proportions in the escapement than Nushagak District catches, but had greater difficulty in fitting to the observed proportions of the 1-ocean age classes (1.1 and 1.2) compared to others (Figure 3.4). This is not unexpected, given the scarcity of the 1-ocean fish in the catch. Similar results were found for the east side of Bristol Bay, with slightly worse fits to observed commercial catch age compositions (Figure 3.5) when compared with samples from upriver escapements (Figure. 3.6). The reconstruction model had more difficulty in explaining interannual variation in the proportion of the 1-ocean age classes in catch samples, compared to other age classes. Biases in

the relationship between predicted and observed age compositions were slight, with fairly consistent under-prediction of the contribution of the 2.2 and 2.3 age classes to Nushagak catches, and over-prediction of the contribution of the 2.2 and 2.3 age classes to the Wood River escapement (Figure 3.4). No temporal trend in deviations between observed and predicted age compositions was observed.

Comparison of predicted genetic composition of catch with GSI data for Nushagak (Figure 3.7), Naknek-Kvichak (Figure 3.8), Egegik (Figure 3.9), and Ugashik (Figure 3.10) Districts, showed that the estimation model fit these data quite well. No significant biases in the estimated contribution of stocks to the catch across years was found in any of the four districts were found. Contrary to a priori expectations, the GSI method (DNA extracted from scale samples by Smith (2010) prior to 2006 or of tissue samples collected by ADF&G more recently), did not influence the model's ability to fit these data despite difference in sample sizes. This is largely due to the assumption of a fixed effective sample size, independent of the year and district.

Parameter estimates

Partitioning of mixed stock catches within the run reconstruction model is based in part upon a comparison of the age composition of district catches, with that of escaping fish that have successfully avoided fishery capture. The selectivity of fishing gear by ocean age class ($S_{k_a,y}$) has been estimated for each year to which the model was fit. Estimates of gear selectivity parameters for the west and east sides of Bristol Bay indicate a pattern of increasing median selectivity for ocean age classes 1-3, with a slight reduction in selectivity for the 4-ocean age group, followed by the highest and most variable selectivity for the 5-ocean age group (Figure 3.11). The large amount of variability in predicted selectivity for the 5-ocean age group is not

unexpected given the rather small contribution of this age class to Bristol Bay returns as a whole (1963-2014 average 0.001%). Despite the observed consistency in the pattern of gear selectivity, the distribution of predicted relative selectivity for the 1-ocean age group is somewhat higher for the west side of Bristol Bay indicating the higher potential for capture of these small individuals in the Nushagak District (Figure 3.11).

Availability to harvest parameters within the run reconstruction model describe the likelihood that a specific stock will be harvested in a particular fishing district, relative to other stocks. In the Nushagak District on the west side of Bristol Bay, the Igushik stock has the lowest availability (median: 0.49), followed by the Nushagak stock (1.05), with the Wood stock predicted to have the highest availability to harvest across years (1.38) (Figure 3.12). Model-predicted availability parameters for the east side of Bristol Bay indicate some interesting patterns in the potential for interception and mixed-stock exploitation. The Naknek-Kvichak is a mixed-stock fishing district targeting the Kvichak, Alagnak, and Naknek stocks. Within this district, the Naknek stock is estimated to have the highest availability to harvest (2.06), with the Kvichak (1.46) and Alagnak (1.37) having a slightly lower relative probability of capture (Fig. 3.13). The availability of the Egegik (0.09) and Ugashik (0.01) stocks to capture were significantly lower in this district (Figure 3.13).

Within the Egegik and Ugashik Districts, the availability of the target stock was significantly higher than that estimated for other stocks. However, the estimated availability of these other stocks was non-zero in many cases, indicating the important influence of interception of non-natal stocks on seasonal catches. Estimated availability parameters for the Egegik District indicate that the Ugashik stock is more likely to be intercepted (0.35), than the Kvichak (0.19), Alagnak (0.1), or Naknek (0.18) stocks. Conversely, within the Ugashik District, the relative

availability of stocks with the exception of Ugashik (4.71) and Egegik (0.22) are exceedingly close to zero (0.01 – 0.02), indicating that the Ugashik is only a significant interceptor of fish bound for Egegik. (Figure 3.13)

Apportioned catch

Model predictions for catch by stock for the Nushagak District indicate the Igushik stock to have represented a minimal proportion (6.1%) of catch across years, followed by the Nushagak stock which is estimated to have comprised 23.5% of catches during this period (Figure 3.14). Historically, the Wood River stock is estimated to have been the single largest contributor to Nushagak District catches, comprising 70.4% on average (Figure 3.14).

Sockeye salmon catch in the Naknek-Kvichak District varied greatly over time, with large catches in 1965, 1970, 1983, and 1995, comprised predominantly of the Kvichak stock (Figure 3.15). However, averaged across the time series the Kvichak stock is estimated to have comprised only 49.7% of catches in the Naknek-Kvichak District, with the Naknek stock estimated to have contributed only slightly fewer at 34.2%. The Alagnak stock is estimated to have represented 10% of historical catches on average, contributing significantly more to the total catch during the period of relatively low Kvichak production between 1996 and 2004 (Figure 3.15). The Egegik and Ugashik stocks are predicted to have been smaller contributors to Naknek-Kvichak District catches at 5.2% and 0.8% on average.

Reconstructed catches in the Egegik District are comprised primarily (77.9%) of the Egegik stock, but interception of sockeye bound for other fishing districts has comprised a significant portion of the catch historically (Figure 3.16). The Kvichak stock is estimated to have been the next largest contributor to Egegik District catches at 10.1% on average, and represented a larger proportion of catches prior to the increase in Egegik production beginning in the early

1980's. Egegik District catch is also predicted to have been comprised of 5.6% Ugashik, 5.3% Naknek, and 1.1% Alagnak sockeye on average.

The pattern in apportioned catch for the Ugashik District is similar to that for the Egegik District, with Ugashik as the target stock comprising the majority, 77.6% on average, of annual catch and the Kvichak stock comprising a larger proportion of catch in years prior to 1980, but only 5.1% on average (Figure 3.17). The neighboring Egegik stock was predicted to comprise 15.3% of Ugashik District catches, which is not unexpected given its geographic proximity. The Alagnak and Naknek stocks were predicted to have been represented rather small proportions of Ugashik District catches at 0.6% and 1.5% respectively.

Comparison of reconstruction methods

To understand how brood tables reconstructed using the current method (Table 3.1 – 3.8), utilizing GSI and age composition data, differ from those reconstructed using age-only methods (Bernard 1983), we compared estimates of brood year productivity for the west (Figure 3.18) and east (Figure 3.19) sides of Bristol Bay. Comparison of reconstructed brood year productivities for the west side of Bristol Bay (Figure 3.18), indicate substantial differences between current model estimates and those generated using age-only methods. Productivity of Igushik stock is estimated to 31.9% lower on average across brood years compared to estimates based on age-only methods. Similarly, productivities were estimated to be an average of 14.7% lower for the Nushagak stock, relative to previous estimates. Conversely, estimates of the productivity of the Wood stock using the current model accounting for stock-specific differences in availability to harvest are 12.3% higher on average. Taken together these results suggest that the productivity of Igushik and Nushagak stocks were over estimated by traditional age-only methods, while productivity of the Wood stock was underestimated on average.

Results of a comparison between brood year productivities estimated using current methods, versus those generated using age-only methods, for the east side of Bristol Bay show greater variability but also some consistent biases. The productivity of the Egegik stock is estimated to be 9.4% lower on average using current run reconstruction methods when compared to those using only age composition data and not accounting for interception amongst districts (Figure 3.19). The pattern of overestimation of productivity for the Egegik stock is fairly consistent across the time series. Updated estimates of productivity for the Kvichak stock are 15% higher on average, although this is largely driven by significant under estimates of productivity using age-only methods in brood years 1972, 1992, and 1996 – 1998. Estimates of productivity for the Alagnak and Ugashik stocks are also estimated to be 15% and 2% on average respectively, although there is significant variation in this pattern over time. Average differences between productivity estimates for the Naknek stock were minimal (0.9% higher), although brood year specific differences range from 28.6% lower to 36.1% higher than those generated using age-only methods.

Discussion

Management of salmon populations based upon the maximum sustainable yield principle depends upon an ability to accurately determine the relationship between spawning abundance and realized recruitment across time. In fisheries where a mixture of stocks are harvested in common fishing districts, estimates of recruitment depend on accurate methods for partitioning mixed-stock catches and allocating those catches them back to their population of origin. Traditional methods for partitioning mixed-stock catches in terminal salmon fisheries with the purpose of reconstructing annual run size have primarily relied on age composition data (Bernard

1983). However, with the advent of modern, efficient, and low cost molecular genetic methods for genetic stock identification of current and historical catch samples, new data are available to inform this process and new run-reconstruction models capable of explicitly estimating the availability of individual stocks to harvest within common and proximate fishing districts are necessary (Smith 2010).

The statistical model described here draws inference from both genetic and age composition data to reconstruct annual run size accounting for both the observed differences in stock-specific availability to harvest, while maintaining the flexibility to be applicable in other salmon fisheries with different stock and age structures. When applied to the commercial fishery for sockeye salmon in Bristol Bay, comparisons of current estimates for stock productivity across time with predictions generated using the age-only methods previously employed for run reconstruction in the region indicated significant differences. For all stocks some difference in predicted productivity rates was observed (Figures 3.18 and 3.19), with consistent biases in four stocks. These comparisons indicated that previous age-only reconstruction methods had significantly overestimated the productivity of the Egegik, Igushik and Nushagak river stocks, while significantly under estimating the productivity of the Wood river stock. By explicitly accounting for the differences in availability to harvest in mixed-stock fisheries and interception rates, updated spawner-recruit information should provide a better foundation for sustainable harvest strategies in the future.

In addition to providing updated data on spawner-recruit relationships for Bristol Bay stocks, the run reconstruction model presented here also provides information about differences in the selectivity of the commercial fishery with respect to the age of returning sockeye. Gear selectivity parameter estimates for Bristol Bay (Figure 3.11) indicated that differences in the

ocean age of sockeye results in differences in realized fishing mortality rate. For sockeye spending one, two, three, and five years at sea, fishery selectivity increased with ocean age, while the selectivity of the 4-ocean age group was predicted to be slightly lower than the 3-ocean age class. This pattern was surprisingly consistent across Bristol Bay, with both the east and west side fishing districts exhibiting the same pattern. Similarity in the pattern of gear selectivity among districts on the east and west sides of Bristol Bay indicates that although the age composition of stocks in these two areas may differ significantly in some cases, the pattern of fishery selectivity for gillnet gear is fairly consistent.

The observed pattern of increasing fishery selectivity with ocean age is consistent with findings by Kendall and Quinn (2009) that realized exploitation rate in the Bristol Bay fishery is largely dependent on the age and size of individuals, and that within a season fishery vulnerability increases with size up to a certain point and then either plateaus or decreases slightly. The pattern of increasing selectivity with ocean-age does suggest that the fishery has imposed strong selection on the age structure of the population over time, reducing survival of older individuals within the population to spawning. Given the positive correlation between the size of female sockeye salmon and fecundity (Cunningham et al. 2013), it is reasonable to question whether this pattern of selection, paired with observed high fishing mortality rates, may have reduced productivity of populations over time. From an evolutionary perspective, the observed heritability of life history traits such as age at maturity (Carlson and Seamons 2008) paired with observed patterns of direction selection in the Bristol Bay fishery provide the mechanistic potential for changes in the age structure of populations over time, with potential deleterious consequences. Changes in yield-determining traits in response selective fishing patterns have been cited as potential drivers of stock collapse (Olsen et al. 2004) and changes in

population productivity (Law 2000) for some species, so concern is warranted as to the potential implications of sustained selection on important life history traits imposed by the Bristol Bay commercial fishery, although the impact of fishery selection may be balanced by other forms of natural and sexual selection (Fleming and Gross 1994, Quinn and Foote 1994).

Gear selectivity parameters for the Bristol Bay commercial fishery were estimated separately for the east and west side districts, however district-specific selectivity parameters were not estimated. While there is potential for the pattern in fishery selectivity to differ amongst districts due to differences in the size of gill net gear employed, the consistency in selectivity patterns observed for east and west side districts suggests that the inclusion of district-specific gear selectivity parameters would have a minimal impact. Alternatively, gear selectivity parameters could be estimated for each of the 18 age classes, rather than simply for the ocean-age groups as currently implemented. However, given that sockeye size is more strongly influenced by duration of marine residency rather than freshwater residency, estimation of separate selectivity parameter for all age classes may be difficult. Both the inclusion of district-specific gear selectivity parameters and parameters for each age class would significantly increase the number of parameters which much be estimated, and would likely be ill advised from the perspective of model parsimony.

Within the current run reconstruction model, the potential for natural mortality occurring between fishing districts and escapement enumeration sites was assumed to be zero. While previous run reconstruction models have both included (Potter et al. 2004) and excluded (Branch and Hilborn 2010, Chasco et al. 2007, Flynn et al. 2006) natural mortality, given that the Bristol Bay commercial fishery operates through terminal fishing districts with short transit times upriver, it is unlikely that the inclusion of natural mortality would greatly influence these results.

However, gill net scaring of sockeye that escape the fishery are observed in 6 – 44% of Bristol Bay sockeye counted as escapement (Baker et al. 2014) leading to increased mortality on the spawning grounds and higher rates of spawning failure (Baker and Schindler 2009). Post entanglement mortality is not accounted for in current run reconstructions, but these differences in condition and survival of sockeye counted as escapement are likely to have a substantial impact on the productivity of individual populations.

Interception of sockeye in non-natal fishing district during return the return migration has traditionally been viewed negatively, given the potential for imprecision in understanding spawner-recruit dynamics and managing for escapement for individual stocks. However, run reconstruction results indicate that interception has accounted for a substantial proportion of Egegik (Figure 3.16) and Ugashik (Figure 3.17) catches in the period of lower productivity prior to 1980. These interception catches may provided a basis for mitigating extremely low catches in districts for fishermen who are unwilling or unable to move to other fishing areas, and through the inclusion of GSI data in run reconstruction models these interception catches can be correctly allocated back to their stock of origin negating the difficulties associated with imprecision in calculating recruitment.

Figures

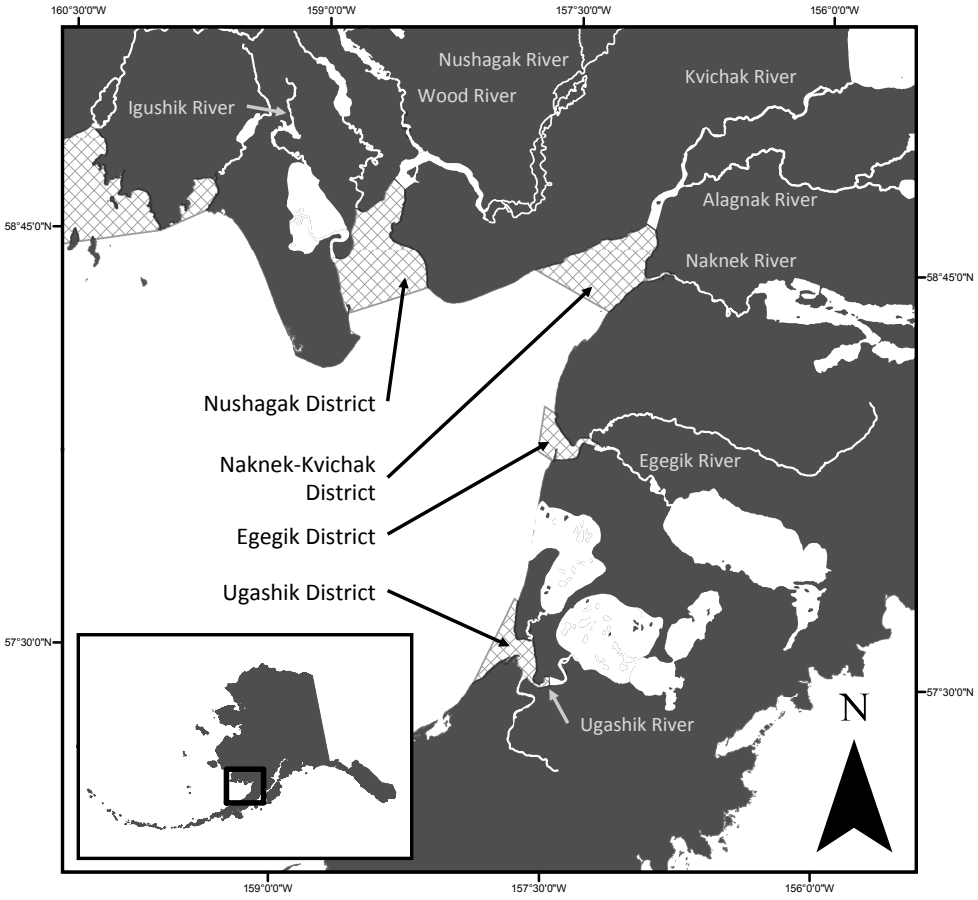

Figure 3.1 Map of Bristol Bay, Alaska. Shaded areas describe boundaries of terminal fishing districts.

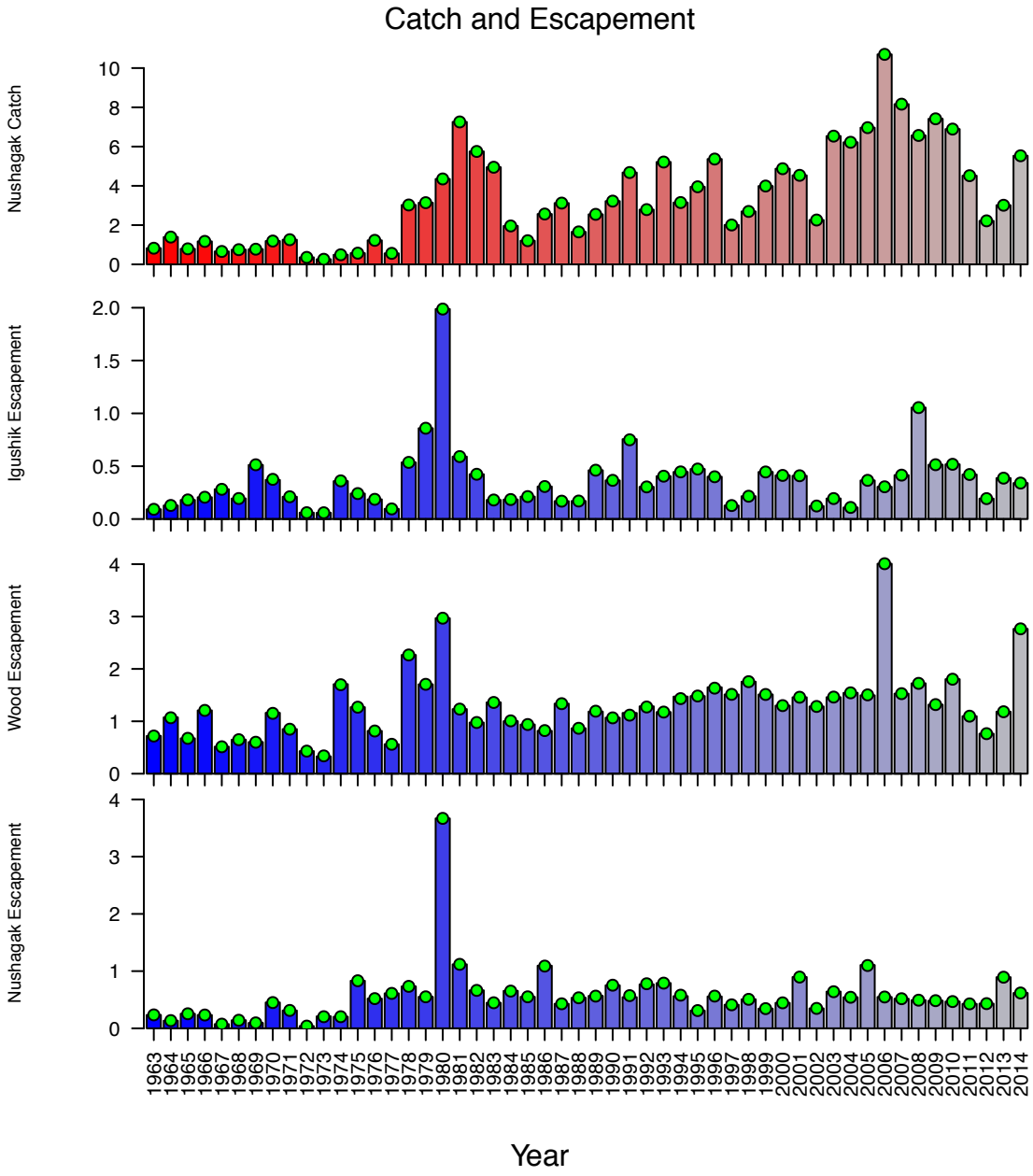

Figure 3.2 Run reconstruction model fit to annual catch and escapement data, for the west side of Bristol Bay in millions of sockeye. Bars are observed catch (red) and escapement (blue), points (green) indicate model predicted values.

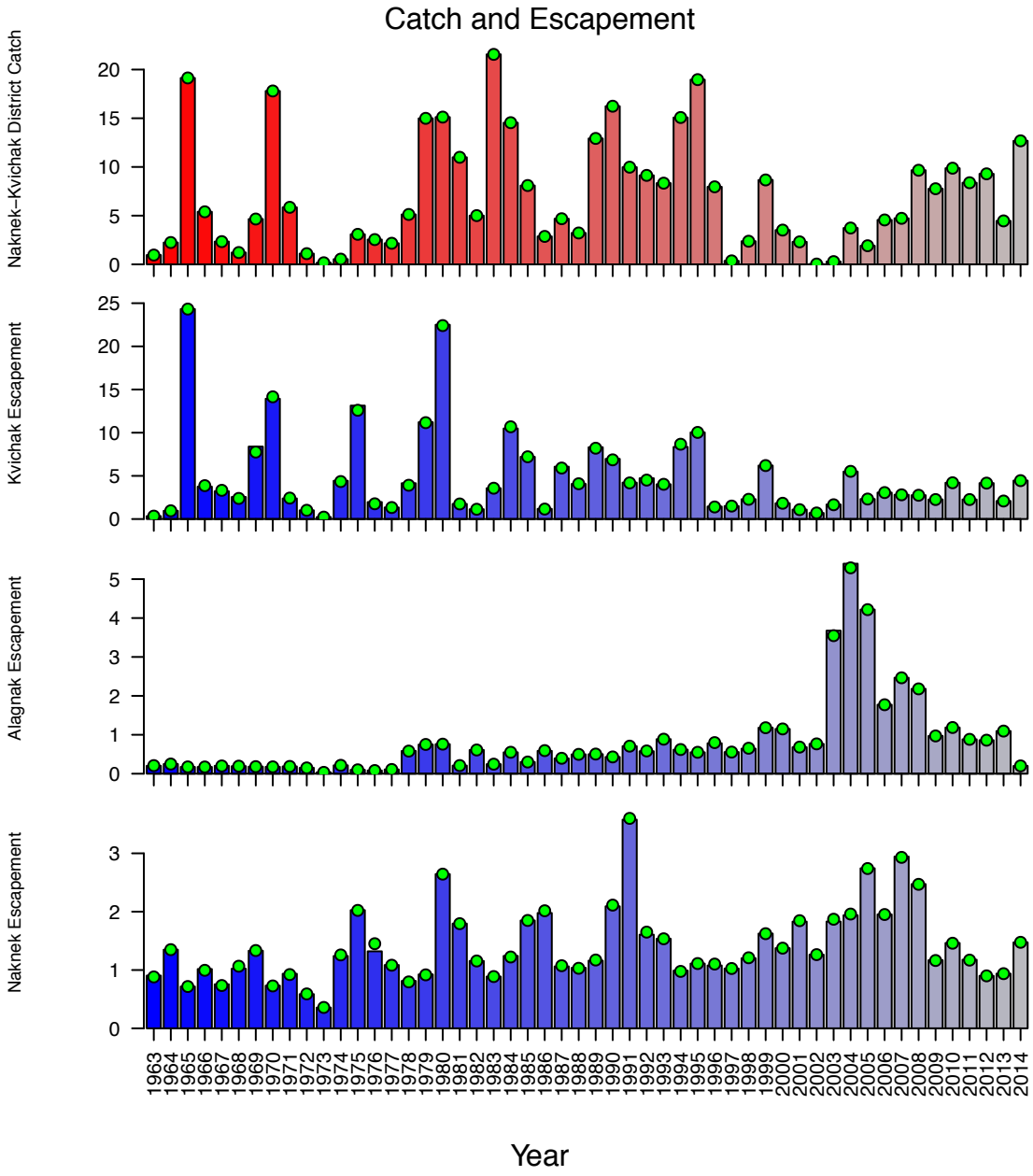

Figure 3.3 Run reconstruction model fit to annual catch and escapement data, for the east side of Bristol Bay in millions of sockeye. Bars are observed catch (red) and escapement (blue), points (green) indicate model predicted values.

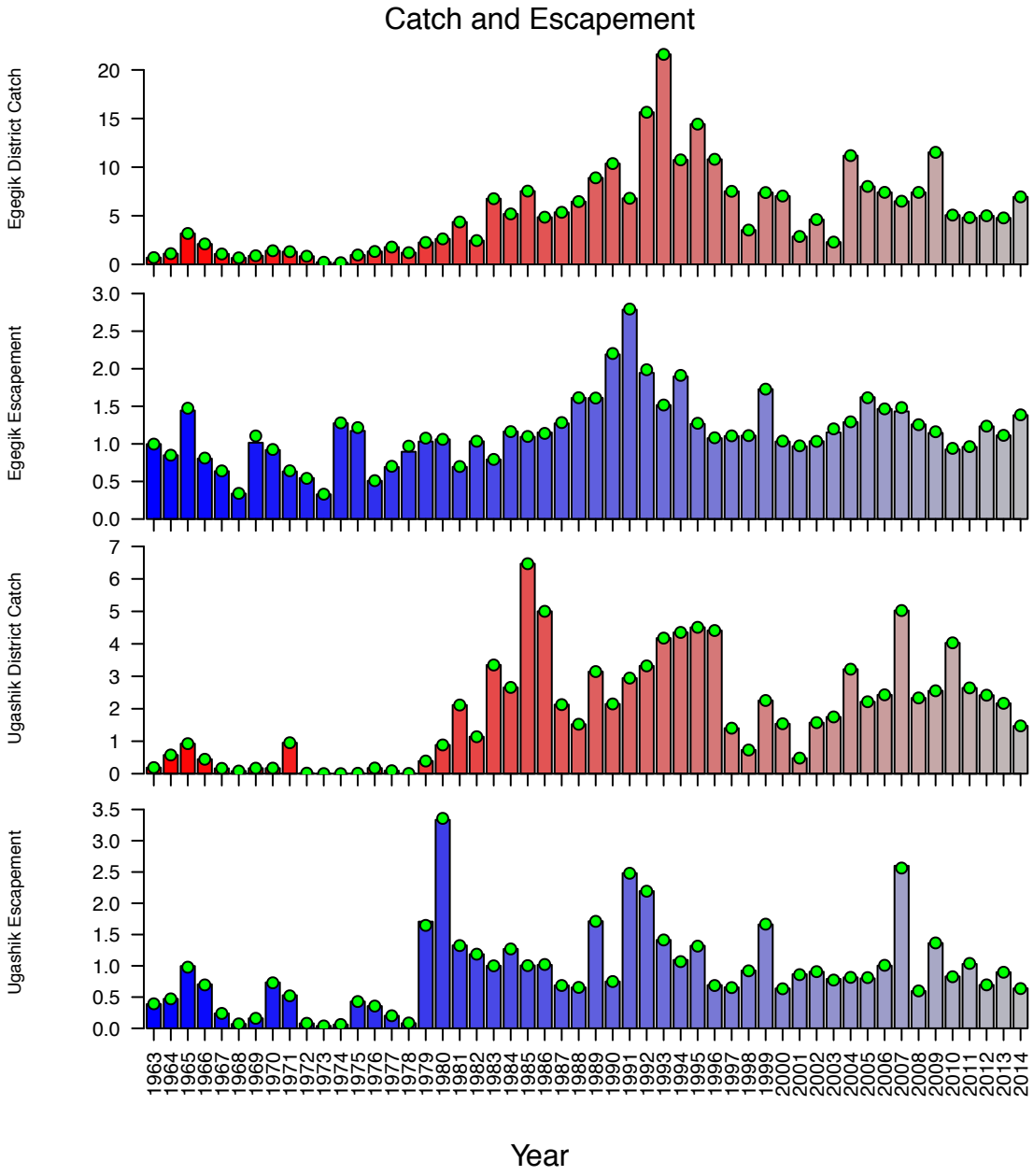

Figure 3.3 cont. Run reconstruction model fit to annual catch and escapement data, for the east side of Bristol Bay in millions of sockeye. Bars are observed catch (red) and escapement (blue), points (green) indicate model predicted values.

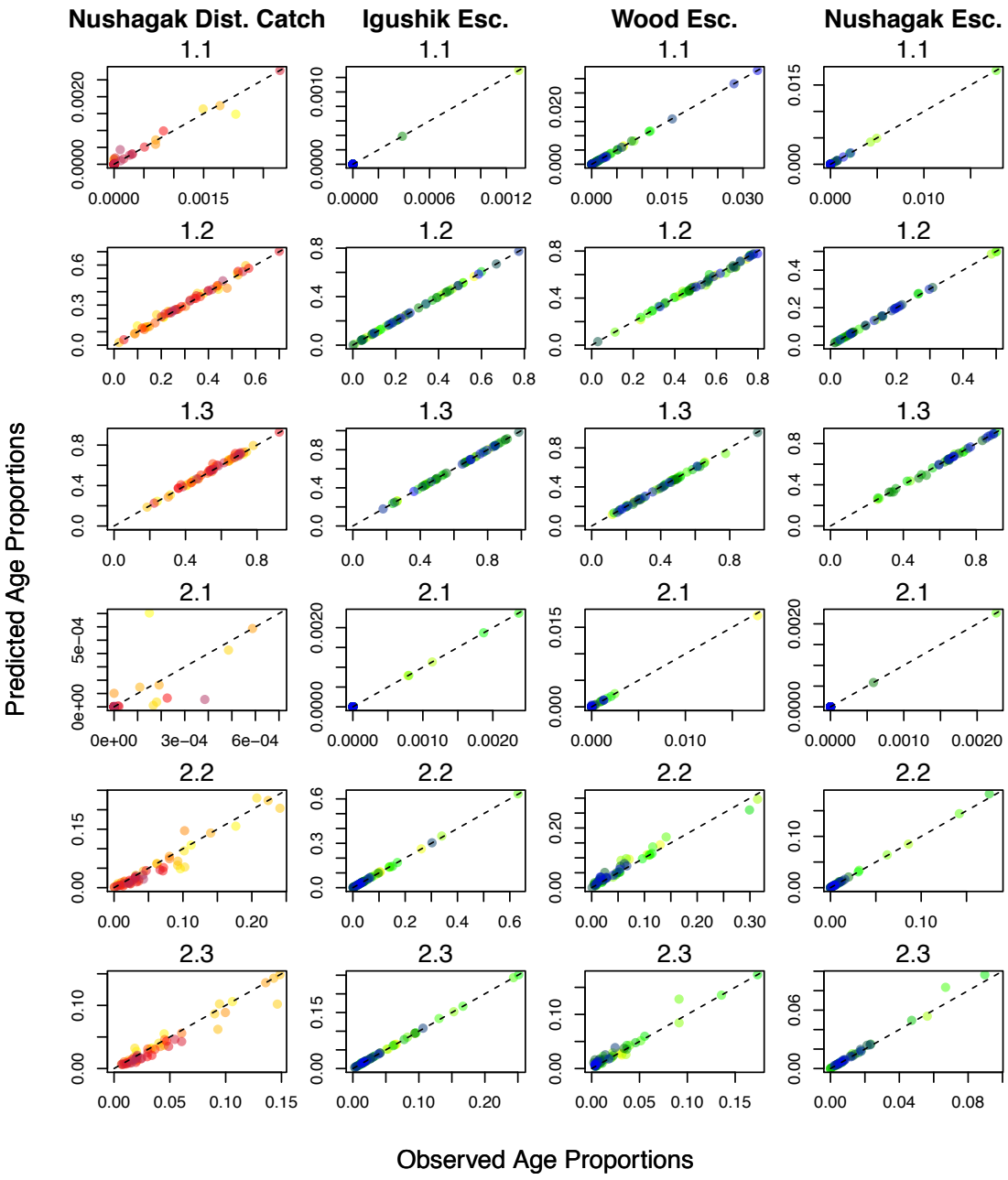

Figure 3.4 Run reconstruction model fit to age composition data from west side of Bristol Bay across years. Individual points describe the relationship between the observed and predicted age composition proportions for district catches and river escapements. Point colors describe the year of reference from 1963 (yellow) to 2014 (red or blue).

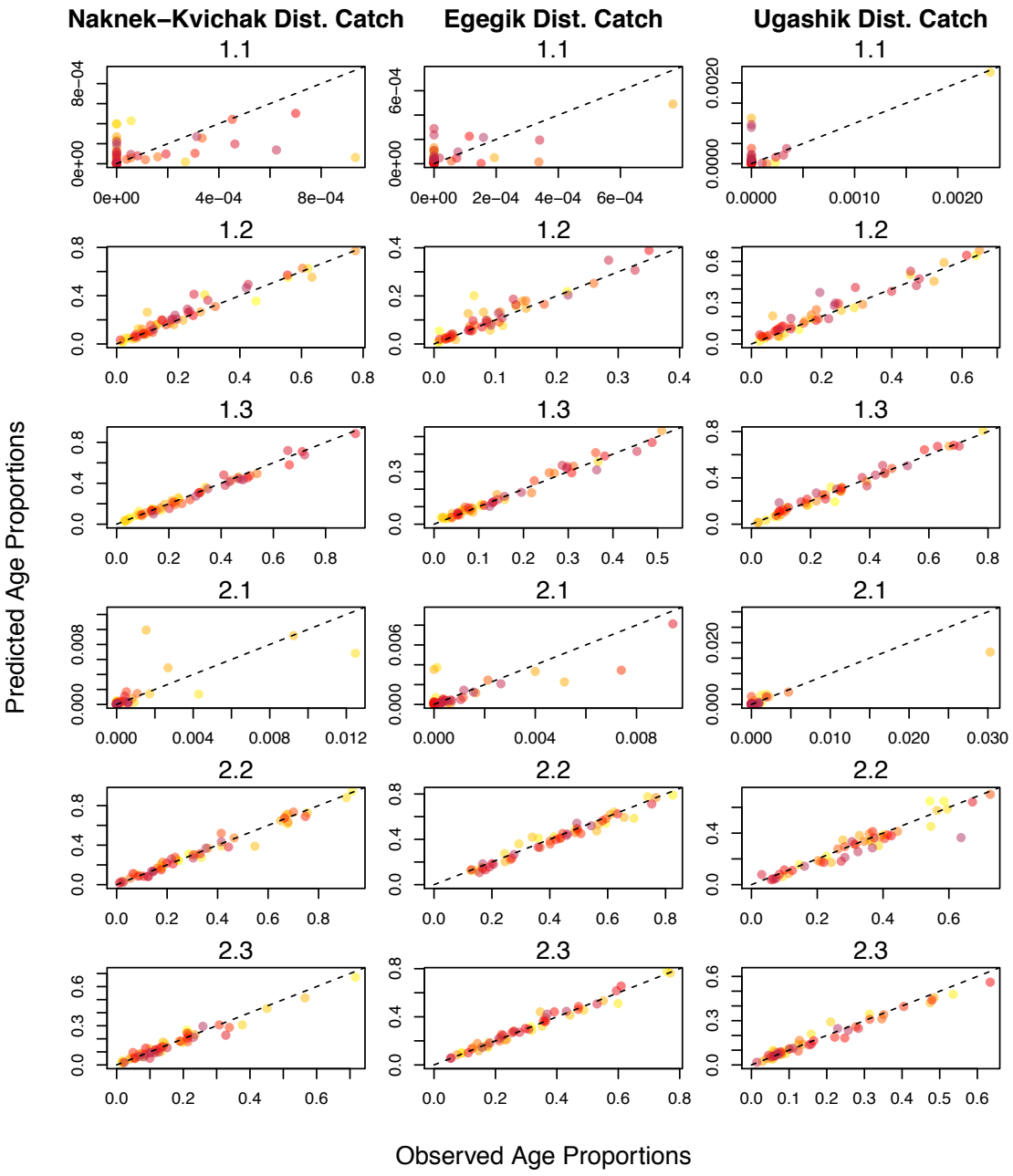

Figure 3.5 Run reconstruction model fit to age composition data from east side of Bristol Bay across years. Individual points describe the relationship between the observed and predicted age composition proportions for district catches. Point colors describe the year of reference from 1963 (yellow) to 2014 (red).

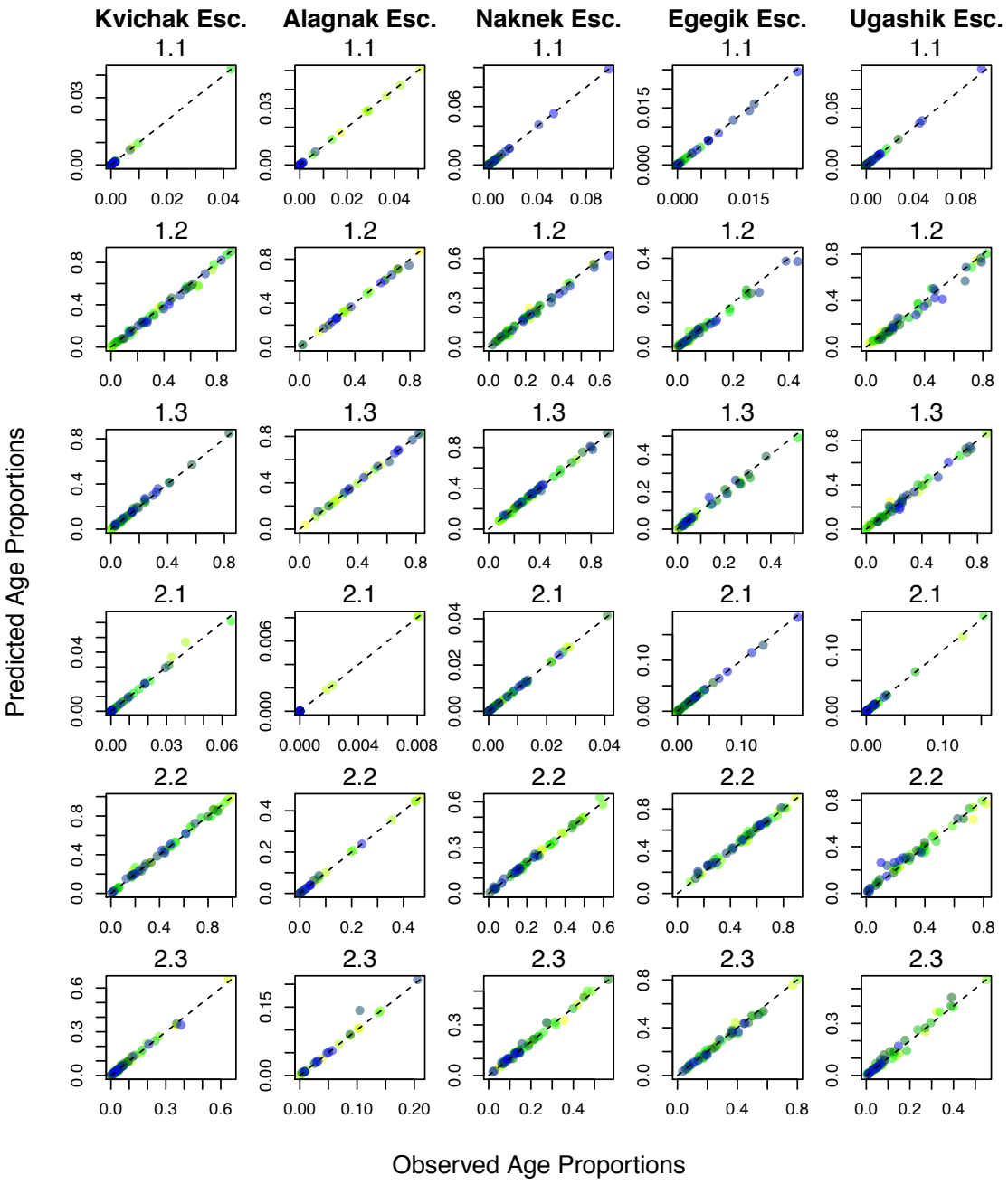

Figure 3.6 Run reconstruction model fit to age composition data from east side of Bristol Bay across years. Individual points describe the relationship between the observed and predicted age composition proportions for river escapements. Point colors describe the year of reference from 1963 (yellow) to 2014 (blue).

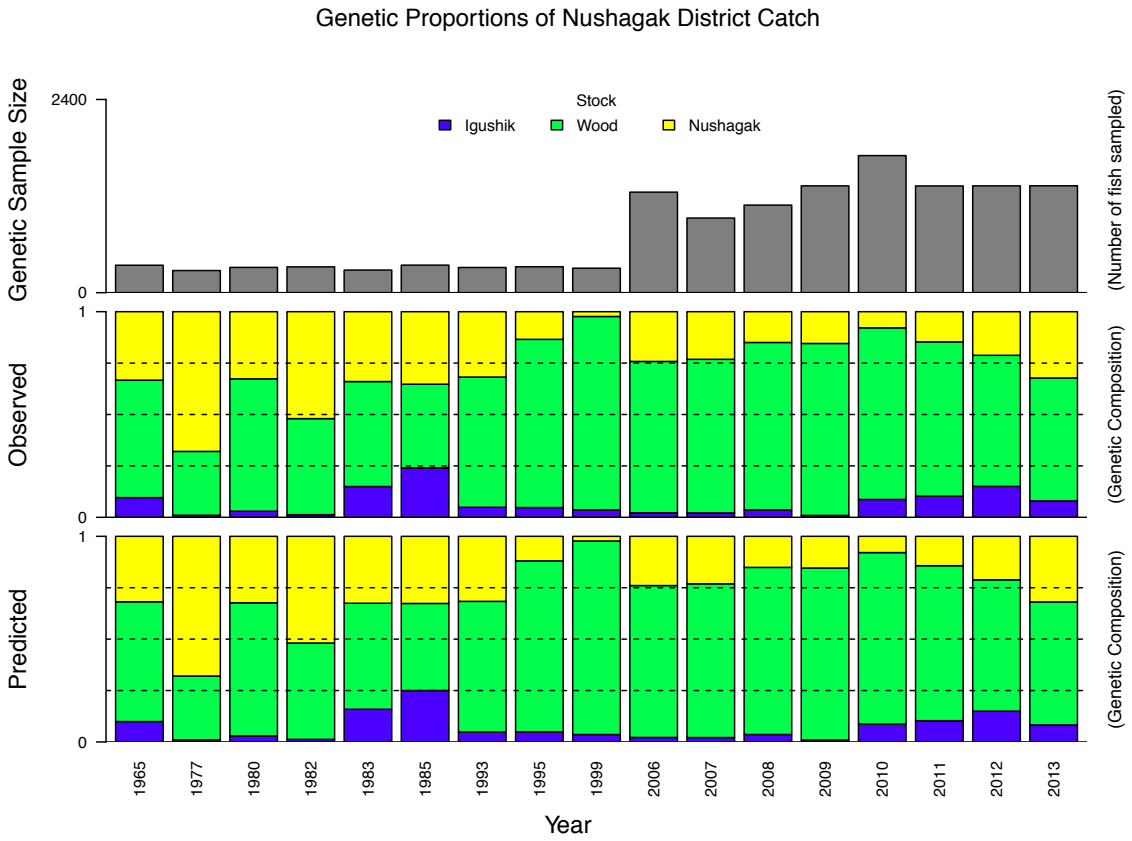

Figure 3.7 Run reconstruction model fit to genetic stock identification data from Nushagak District catches. Genetic sample size, observed proportions, and predicted proportions are listed for each year of GSI.

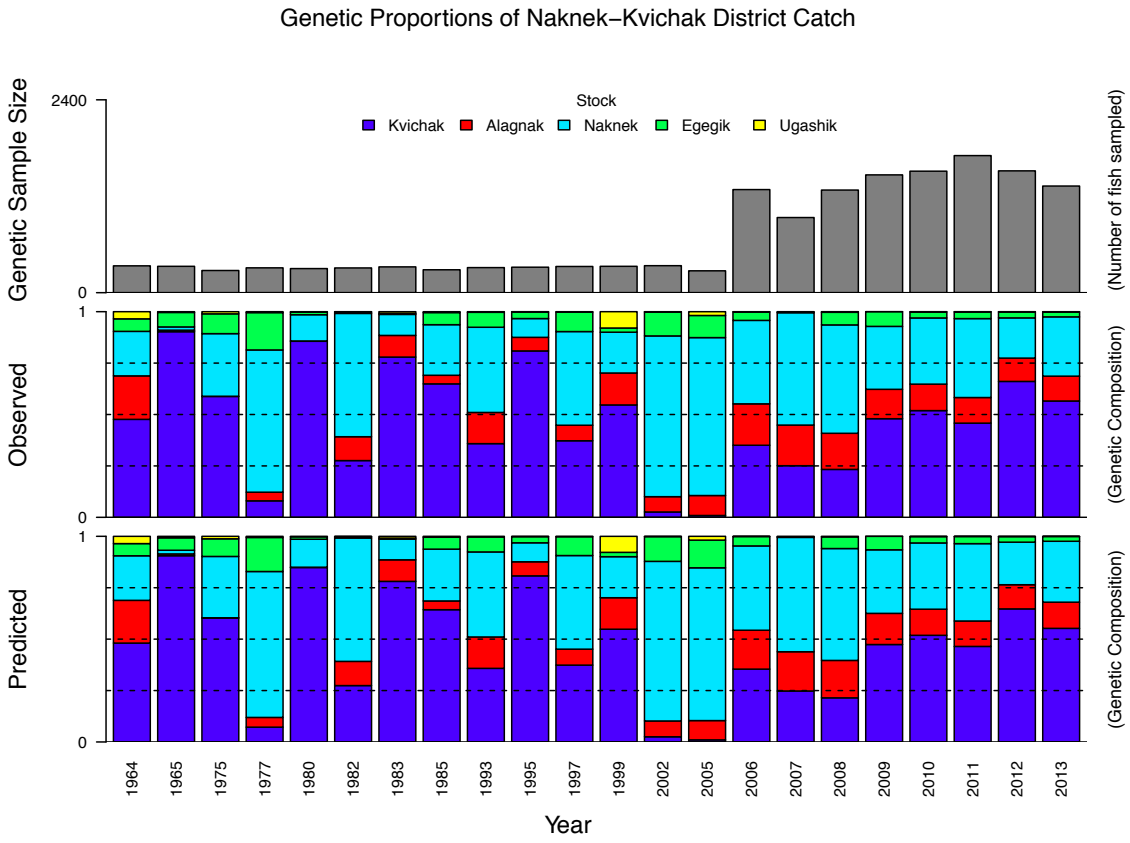

Figure 3.8 Run reconstruction model fit to genetic stock identification data from Naknek-Kvichak District catches. Genetic sample size, observed proportions, and predicted proportions are listed for each year of GSI.

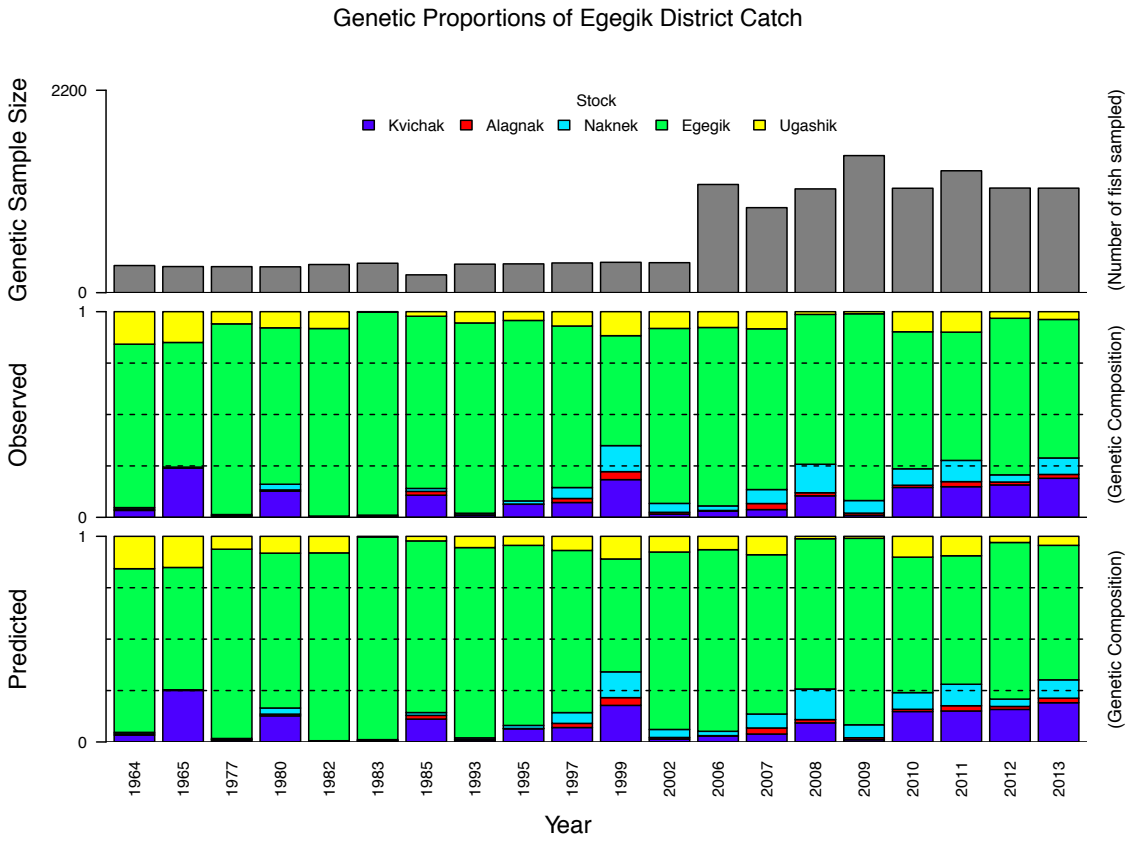

Figure 3.9 Run reconstruction model fit to genetic stock identification data from Egegik District catches. Genetic sample size, observed proportions, and predicted proportions are listed for each year of GSI.

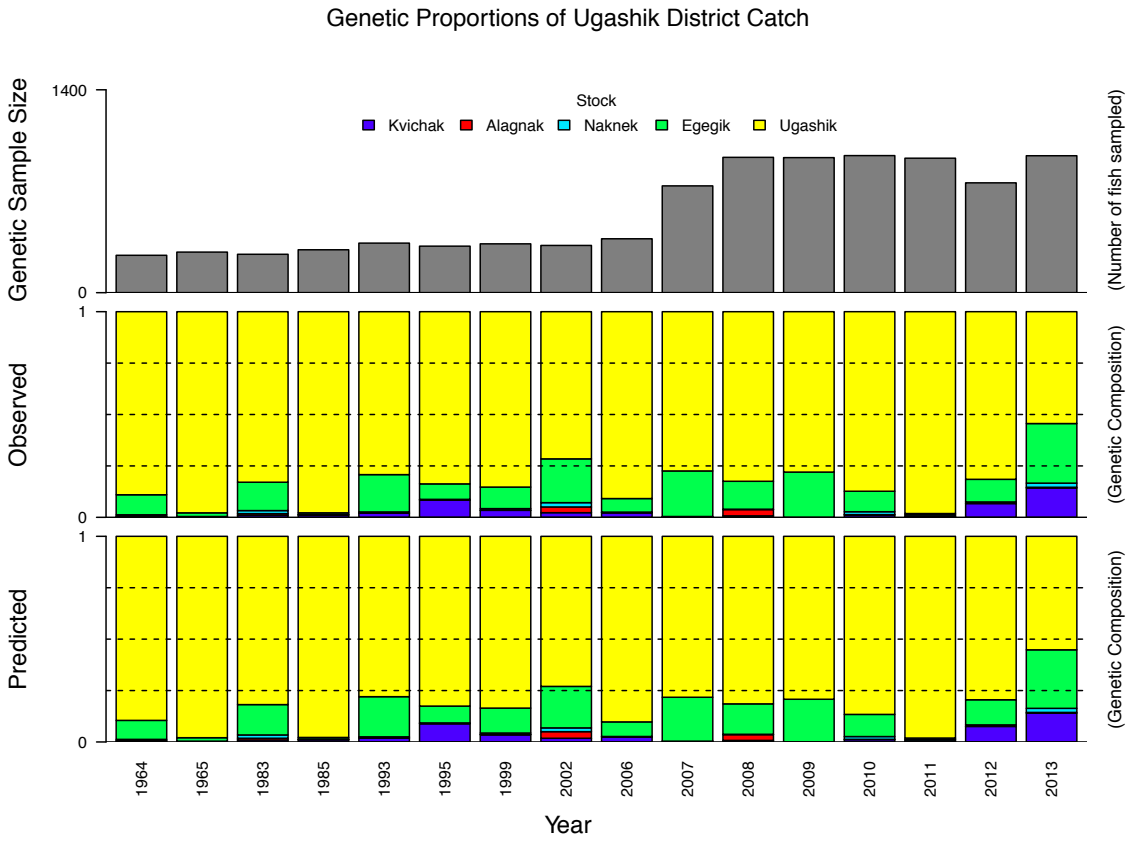

Figure 3.10 Run reconstruction model fit to genetic stock identification data from Ugashik District catches. Genetic sample size, observed proportions, and predicted proportions are listed for each year of GSI.

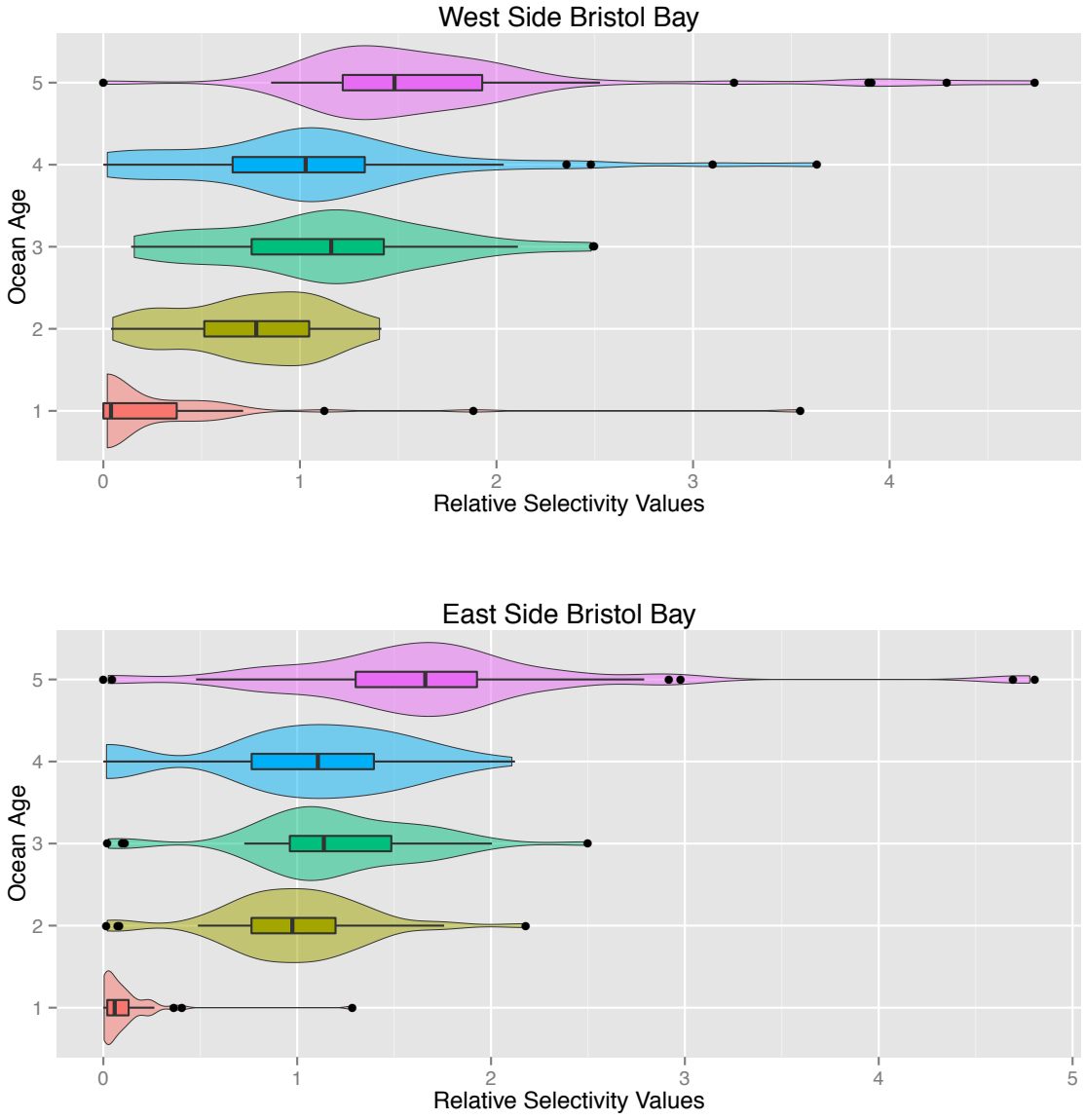

Figure 3.11 Distribution of selectivity parameter values across years, estimated for the West and East sides of Bristol Bay. The distributions of estimated values for ocean age specific selectivity parameters are illustrated as violin plots, with boxplots describing the median, and 50th and 95th percentiles.

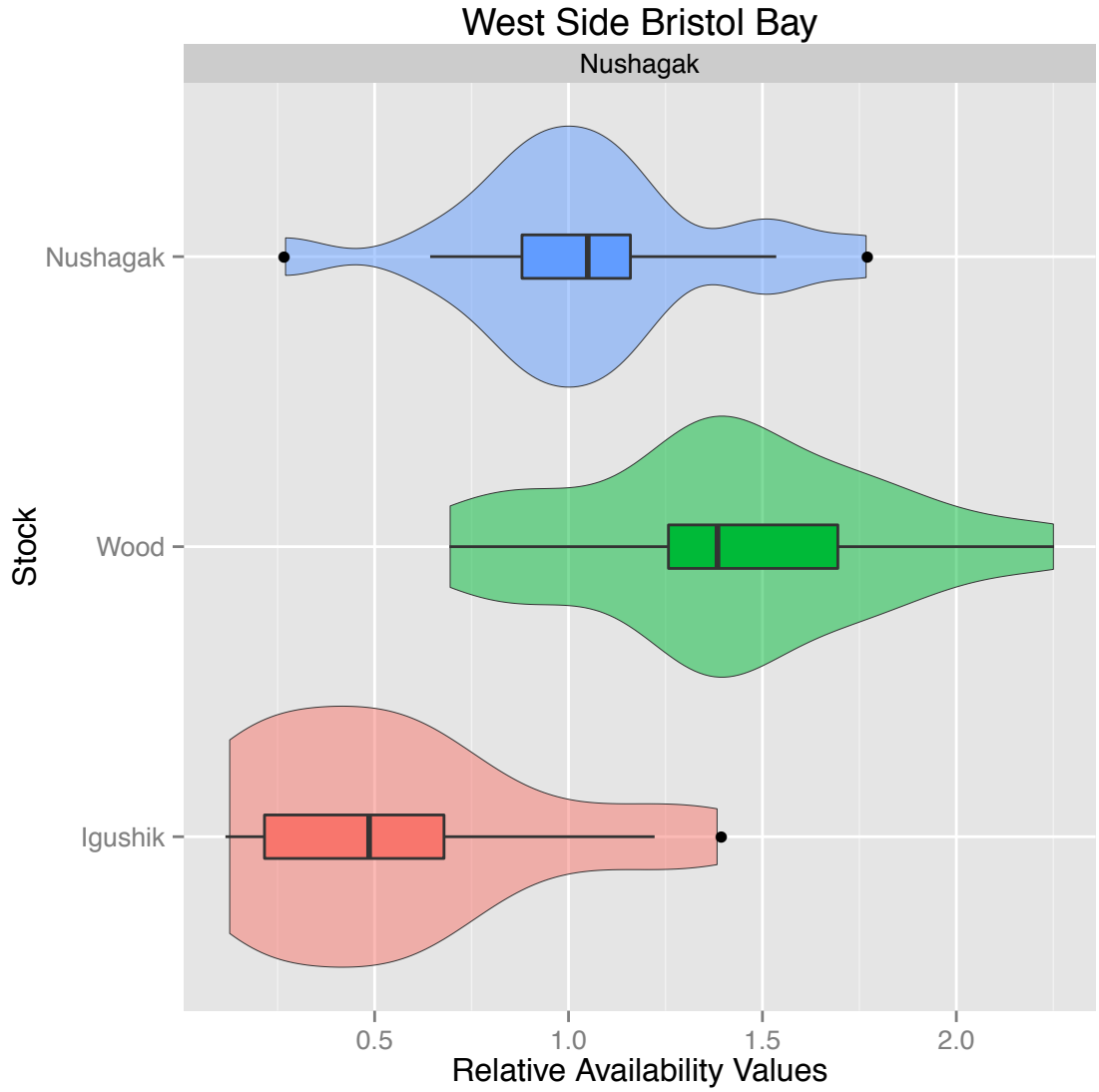

Figure 3.12 Distribution of model estimated availability parameter values for the West side of Bristol Bay. Violin plots describe the distribution, and boxplots the median, 50th and 95th percentiles of estimated values for the availability of stocks to harvest in the Nushagak District.

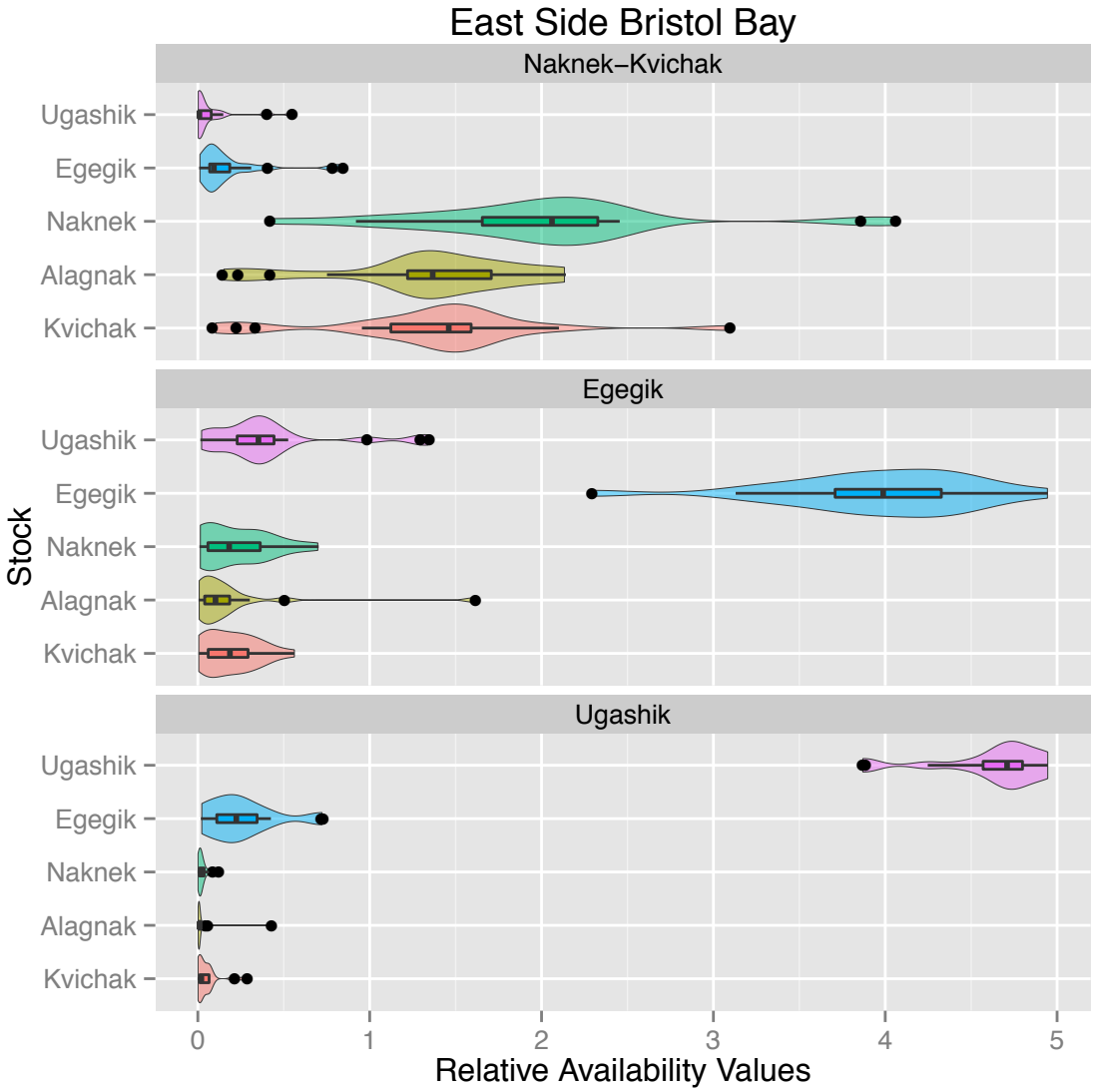

Figure 3.13 Distribution of model estimated availability parameter values for the East side of Bristol Bay. Violin plots describe the distribution, and boxplots the median, 50th and 95th percentiles of estimated values for the availability of stocks to harvest in the Naknek-Kvichak, Egegik, and Ugashik Districts.

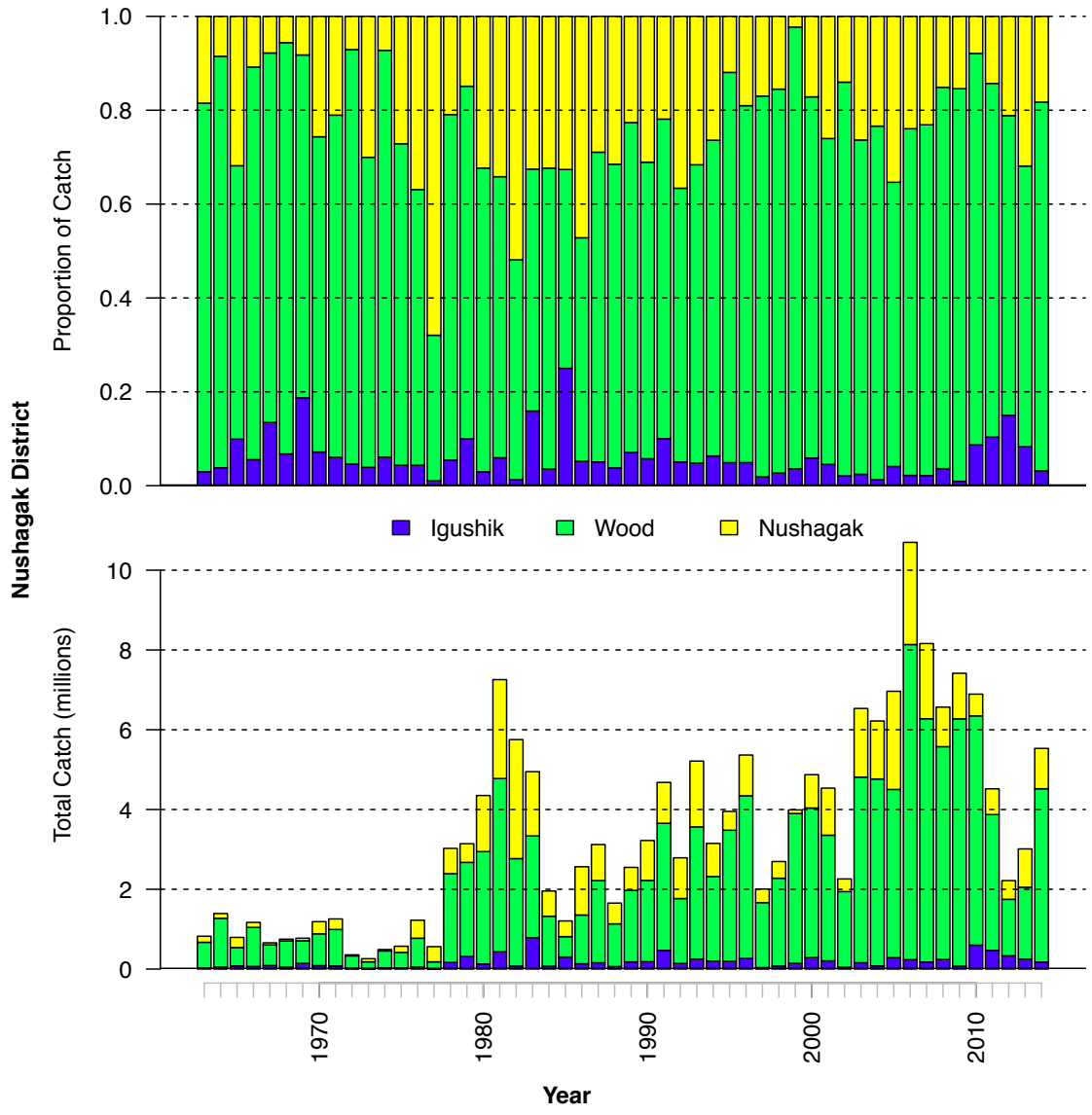

Figure 3.14 Annual catch in the Nushagak District allocated amongst the three stocks represented on the west side of Bristol Bay.

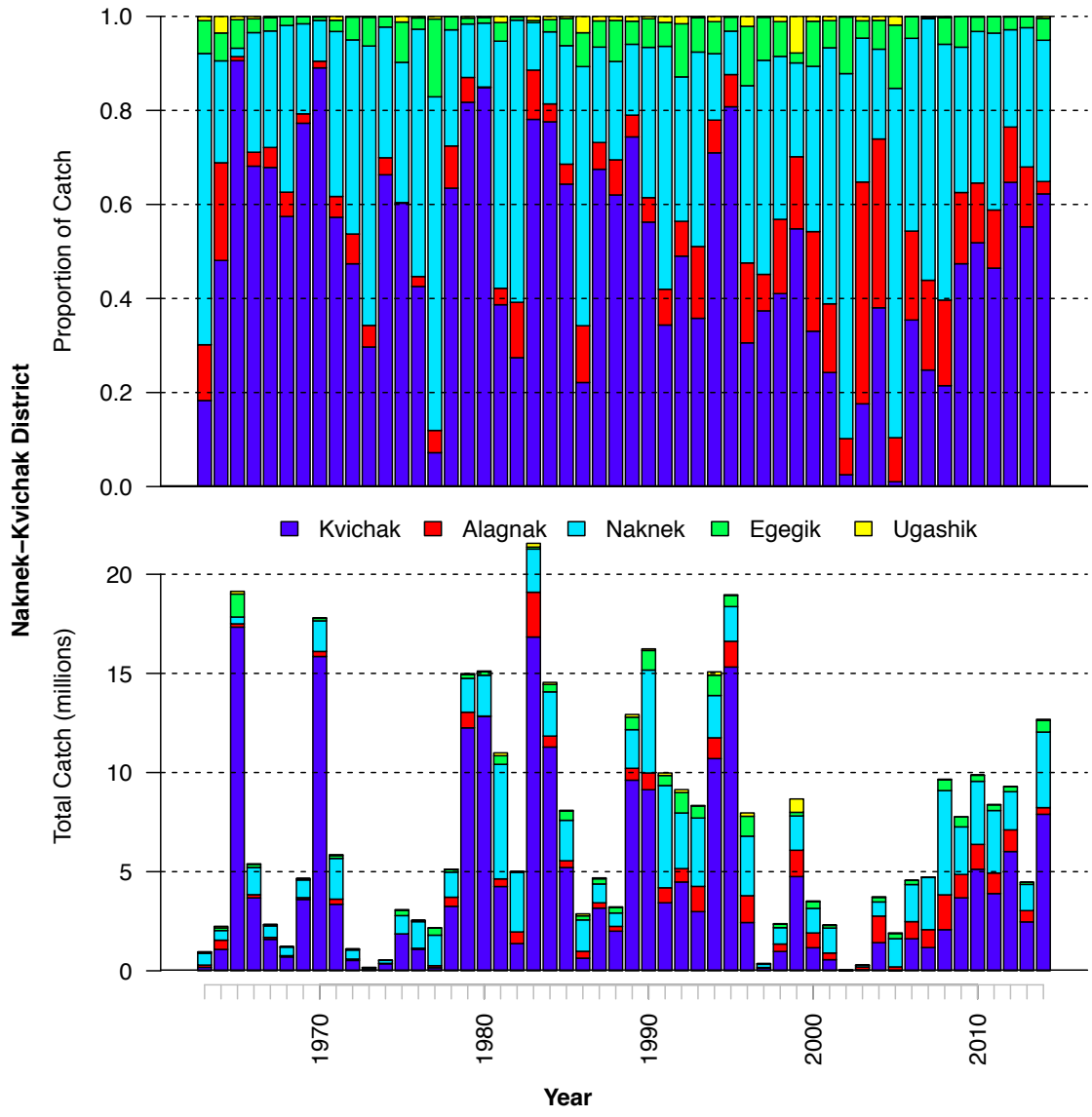

Figure 3.15 Annual catch in the Naknek-Kvichak District allocated amongst the five stocks represented on the east side of Bristol Bay.

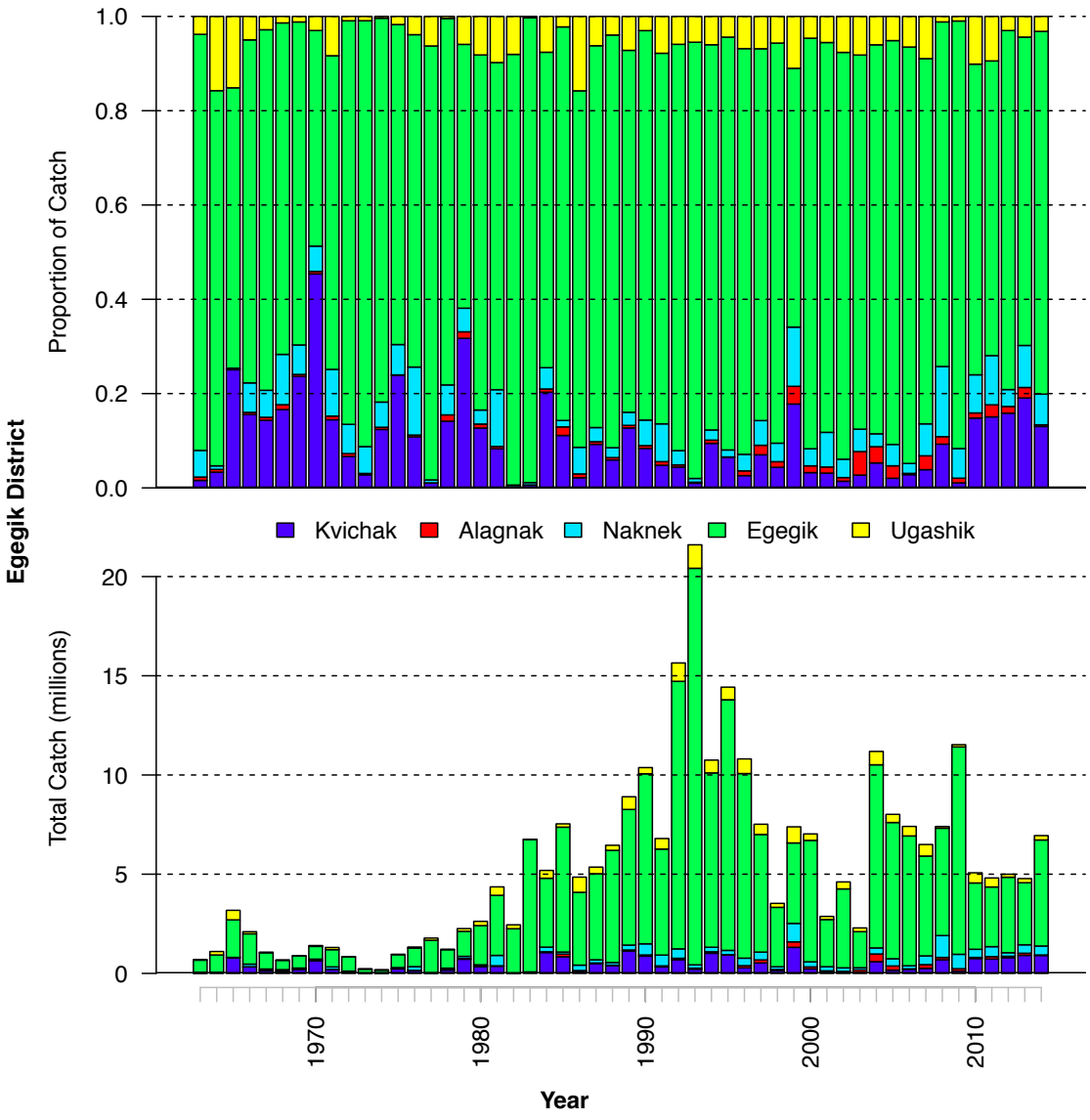

Figure 3.16 Annual catch in the Egegik District allocated amongst the five stocks represented on the east side of Bristol Bay.

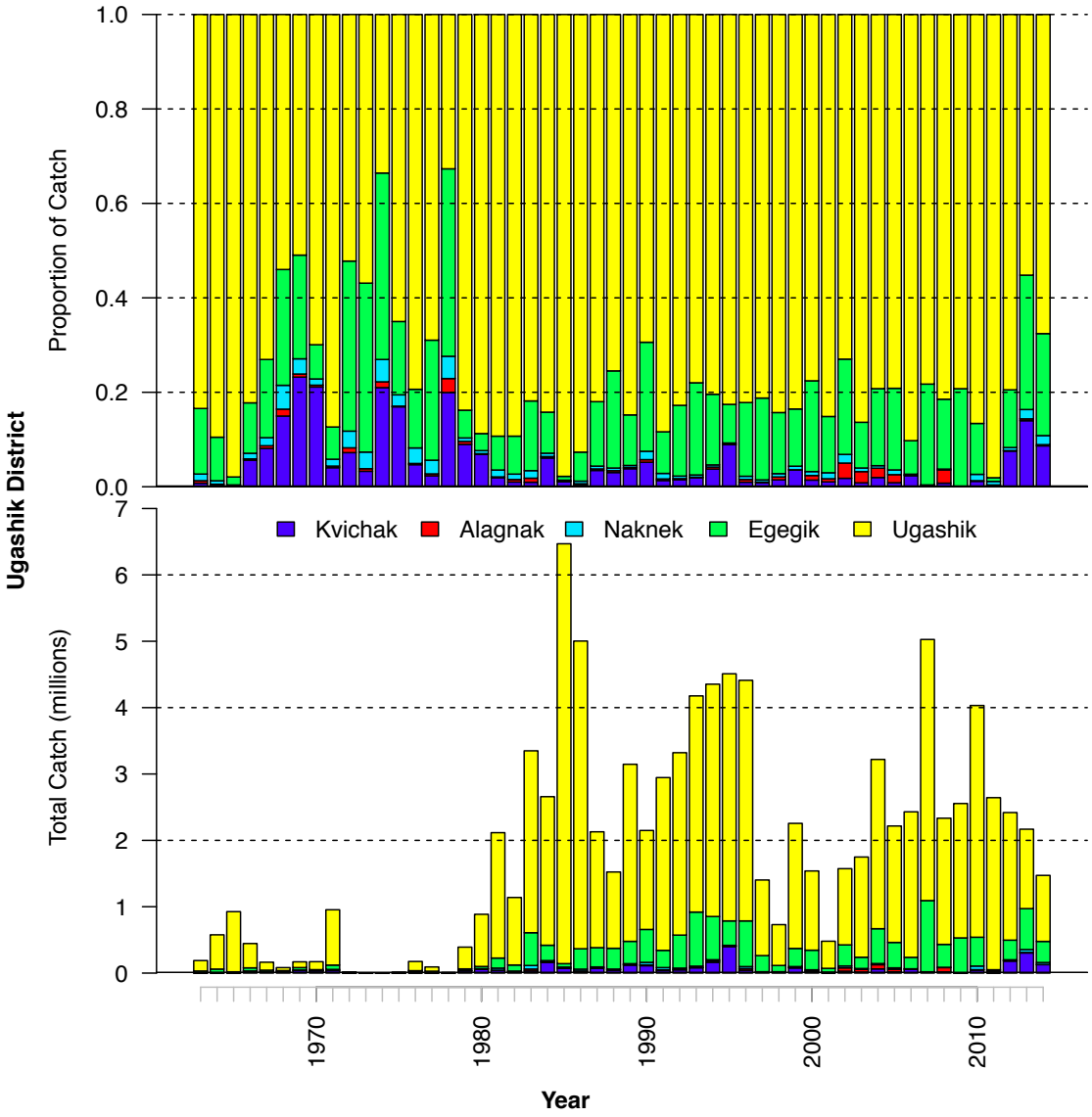

Figure 3.17 Annual catch in the Ugashik District allocated amongst the five stocks represented on the east side of Bristol Bay.

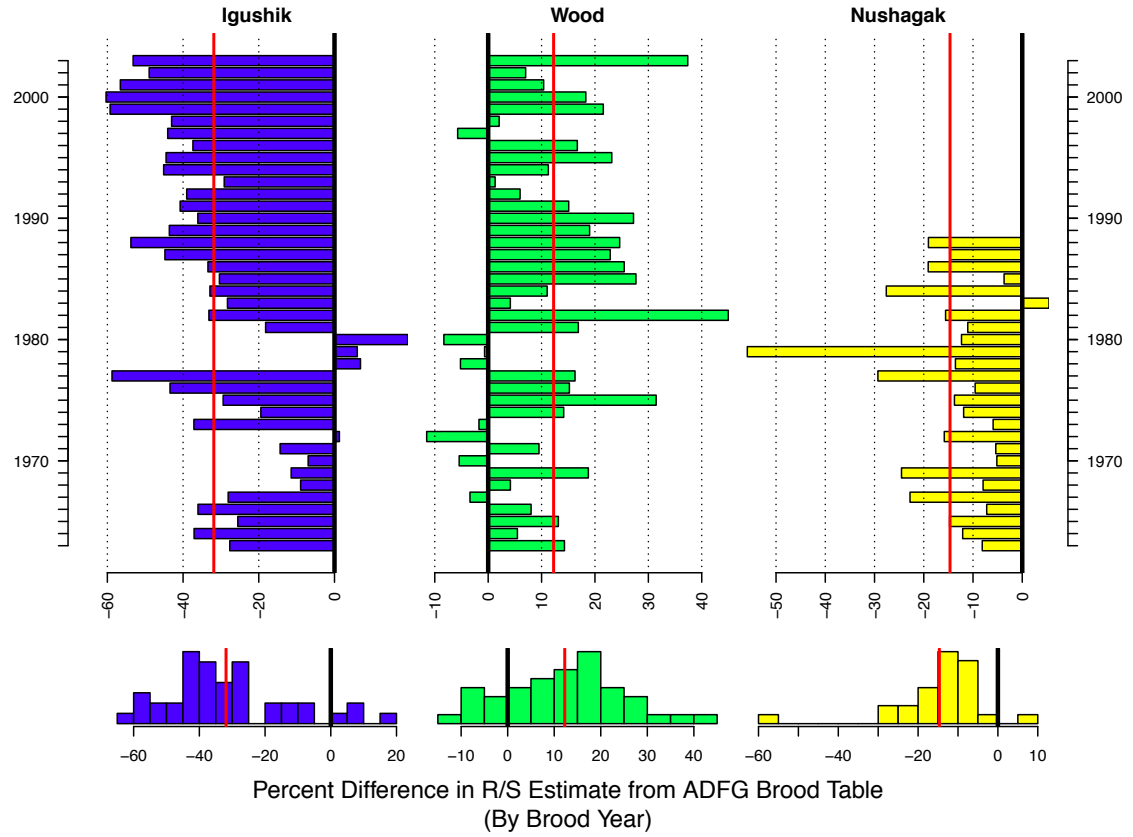

Figure 3.18 Comparison of brood year productivity (recruits/spawner) estimates from the new run reconstruction model employing age and genetic composition of catch ($\hat{P}_{new}$), with previous estimates from Alaska Department of Fish and Game age-based reconstruction methods for the West Side of Bristol Bay ($\hat{P}_{old}$). Difference values are the percent difference between estimation methods: $(\hat{P}_{new} - \hat{P}_{old})/\hat{P}_{old}$. The top row of panels display the differences in productivity estimates by brood year, while the bottom panels provide histograms of difference values. In all panels the red line indicates the mean difference in productivity estimates across brood years.

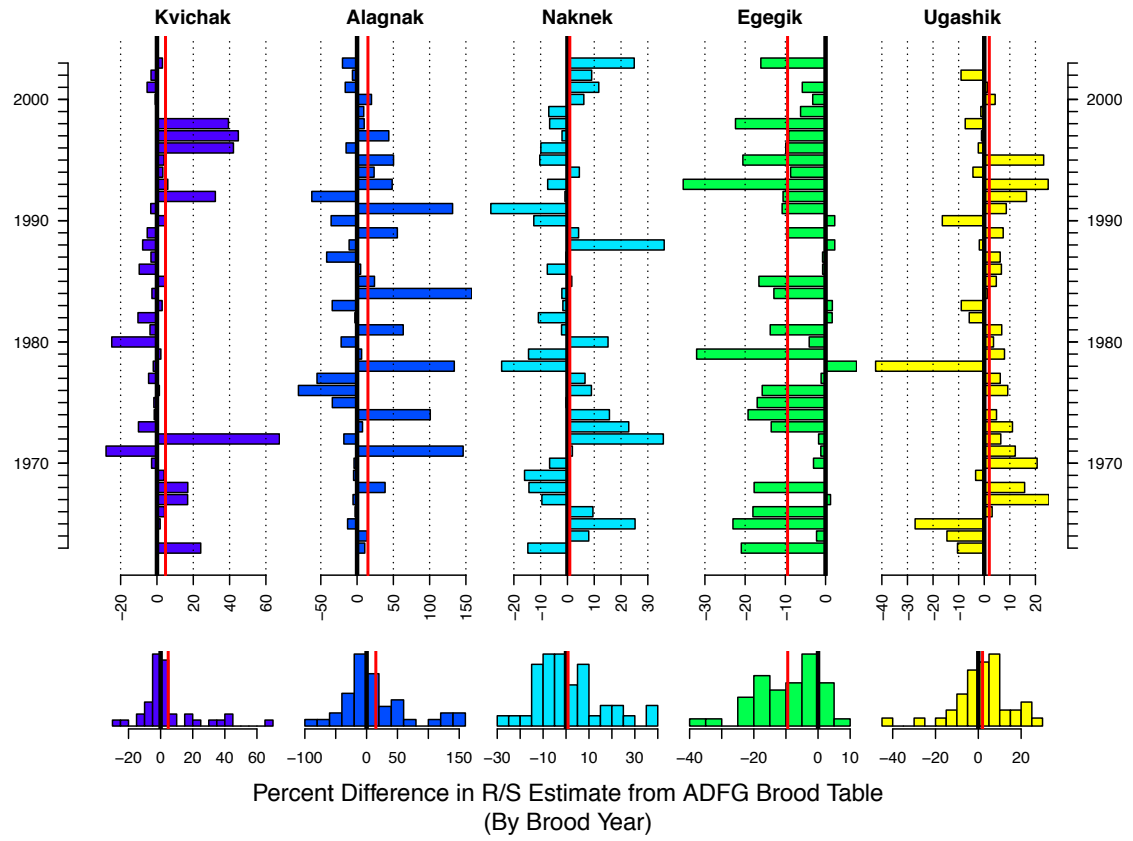

Figure 3.19 Comparison of brood year productivity (recruits/spawner) estimates from the new run reconstruction model employing age and genetic composition of catch ($\hat{P}_{new}$), with previous estimates from Alaska Department of Fish and Game age-based reconstruction methods for the East Side of Bristol Bay ($\hat{P}_{old}$). Difference values are the percent difference between estimation methods: $(\hat{P}_{new} - \hat{P}_{old})/\hat{P}_{old}$. The top row of panels display the differences in productivity estimates by brood year, while the bottom panels provide histograms of difference values. In all panels the red line indicates the mean difference in productivity estimates across brood years.

Tables

Table 3.1 Igushik River brood table.

Brood Year	0.1	0.2	0.3	0.4	0.5	1.1	1.2	1.3	1.4	1.5	2.1	2.2	2.3	2.4	3.1	3.2	3.3	3.4	Escapement	Recruits	R/S
1955	NA	NA	NA	NA	NA	NA	NA	NA	NA	NA	NA	NA	NA	NA	NA	NA	-	NA	NA	NA	
1956	NA	NA	NA	NA	NA	NA	NA	NA	NA	-	NA	NA	NA	-	NA	NA	-	-	NA	NA	NA
1957	NA	NA	NA	NA	-	NA	NA	NA	-	-	NA	NA	9,213	-	NA	-	-	-	NA	NA	NA
1958	NA	NA	NA	-	-	NA	NA	37,357	-	-	NA	14,002	13,488	-	-	-	-	-	NA	NA	NA
1959	NA	NA	0	0	-	NA	75,779	90,589	-	-	0	45,064	16,194	-	-	-	-	-	NA	NA	NA
1960	NA	-	264	-	-	0	41,542	225,973	0	-	106	26,635	29,630	-	-	0	-	-	NA	NA	NA
1961	-	0	78	-	-	-	28,373	253,124	211	-	-	9,653	9,303	-	-	-	-	-	NA	NA	NA
1962	-	-	860	0	-	-	16,811	200,762	0	-	-	5,144	5,541	-	-	-	0	-	NA	NA	NA
1963	-	-	292	0	-	-	196,558	137,346	-	-	-	22,418	11,591	-	-	-	-	-	92,184	368,205	3.99
1964	-	105	507	-	-	-	124,313	325,005	-	-	261	103,991	28,877	-	-	-	-	-	128,532	583,060	4.54
1965	-	0	0	-	-	299	319,406	270,050	0	-	0	168,321	52,842	-	-	-	-	-	180,840	810,920	4.48
1966	-	0	0	0	-	0	54,401	232,637	122	0	0	5,392	8,482	0	-	-	61	-	206,360	301,093	1.46
1967	-	356	430	-	0	-	43,479	59,861	59	-	0	10,884	10,676	-	-	-	-	-	281,772	125,745	0.45
1968	-	452	167	31	-	-	48,450	101,707	888	-	-	513	6,715	-	-	-	-	-	194,508	158,923	0.82
1969	-	-	88	-	-	-	830	107,254	1,387	-	-	278,332	88,831	-	-	-	-	-	512,328	476,722	0.93
1970	-	-	321	-	-	-	36,788	144,568	0	-	299	62,987	42,459	12	-	-	-	-	370,920	287,436	0.77
1971	-	0	1,291	-	-	-	58,279	131,521	197	-	-	39,333	28,794	-	-	-	-	-	210,960	259,415	1.23
1972	-	93	913	61	0	-	93,771	117,097	4,097	-	-	5,306	10,712	-	-	-	-	-	60,018	232,049	3.87
1973	-	0	1,279	866	-	-	17,241	399,007	0	-	-	14,681	18,927	-	-	0	-	-	59,508	452,000	7.60
1974	-	49	1,356	-	-	-	412,983	589,285	1,192	-	1,370	240,733	20,162	-	-	-	-	-	358,752	1,267,130	3.53
1975	-	134	0	-	-	0	543,521	1,835,022	1,199	-	-	119,242	311,785	-	-	-	-	-	241,086	2,810,903	11.66
1976	-	0	0	-	0	-	412,828	741,008	8,897	-	4,261	106,555	80,921	196	-	-	-	-	186,120	1,354,667	7.28
1977	-	-	2,917	0	-	773	174,667	585,308	46,621	-	0	5,600	14,540	-	-	0	-	-	95,970	830,426	8.65
1978	-	-	0	0	-	-	36,011	368,460	73	-	-	146,031	11,700	-	-	-	-	-	536,154	562,275	1.05
1979	-	0	196	0	-	0	611,312	263,565	0	-	-	10,184	11,078	-	-	140	-	-	859,560	896,476	1.04
1980	-	0	0	0	-	-	14,270	353,924	0	-	-	34,537	41,072	-	-	-	-	-	1,987,530	443,803	0.22
1981	-	0	0	0	-	-	243,467	502,783	51,416	-	-	6,742	34,236	-	-	-	-	-	591,144	838,645	1.42
1982	-	0	6,544	0	-	-	50,848	272,741	1,045	-	-	7,067	8,363	-	-	-	-	-	423,768	346,608	0.82
1983	-	1,151	0	27	-	-	105,984	247,075	1,685	-	-	6,211	28,971	-	-	-	-	-	180,438	391,104	2.17
1984	0	0	232	0	-	-	30,298	419,161	3,267	-	-	52,282	16,033	1,680	-	-	-	-	184,872	522,953	2.83
1985	-	0	6,293	0	-	-	395,498	639,188	5,889	-	-	50,116	41,160	809	-	-	-	-	212,454	1,138,951	5.36
1986	-	2,705	8,615	2,213	-	-	157,348	1,497,275	7,475	-	-	9,445	15,520	-	-	-	-	-	307,728	1,700,597	5.53
1987	-	1,607	12,589	0	-	-	75,588	338,281	5,679	-	-	2,145	9,626	0	-	-	-	-	169,236	445,515	2.63
1988	-	0	0	91	-	-	105,973	479,542	1,659	-	-	5,734	21,898	-	-	-	-	-	170,454	614,898	3.61
1989	-	145	2,991	0	-	-	213,200	693,503	5,198	-	-	48,454	28,293	-	-	-	-	-	461,610	991,784	2.15
1990	-	46	3,116	0	-	166	138,198	883,941	2,186	0	-	95,135	106,710	0	-	-	0	-	365,802	1,229,498	3.36
1991	-	0	905	0	-	-	170,953	798,731	2,464	-	-	2,065	8,821	0	-	-	-	-	756,126	983,939	1.30
1992	-	0	2,985	0	-	-	30,018	91,714	323	-	-	5,335	9,187	0	-	0	-	-	304,920	139,561	0.46
1993	-	0	0	0	-	-	100,426	239,151	0	-	-	13,737	4,862	-	-	-	-	-	405,564	358,174	0.88
1994	-	-	0	-	-	-	163,637	435,419	1,001	-	0	42,976	16,920	-	-	-	-	-	445,920	659,953	1.48
1995	-	0	-	-	-	0	376,062	881,256	5,961	-	-	6,531	8,446	-	-	-	-	-	473,382	1,278,256	2.70
1996	-	-	-	-	-	-	77,032	800,393	2,787	-	-	807	5,344	63	-	-	-	-	400,746	886,426	2.21
1997	-	-	1,199	-	-	-	1,927	51,668	1,857	0	-	9,522	33,171	0	-	-	0	-	127,704	99,345	0.78
1998	-	-	-	-	-	0	130,362	393,266	2,298	-	0	2,907	7,521	0	-	-	-	-	215,904	536,354	2.48
1999	-	-	-	-	-	-	60,852	146,840	0	-	67	58,392	96,336	-	-	-	-	0	445,536	362,488	0.81
2000	-	-	-	-	-	0	53,303	660,546	3,360	0	-	12,377	38,294	0	-	-	-	-	413,316	767,881	1.86
2001	-	-	-	366	-	-	31,827	444,415	2,298	-	-	7,838	3,462	-	0	-	-	-	409,596	490,207	1.20
2002	-	-	0	-	-	0	236,714	161,990	4,868	-	-	34,264	10,368	-	-	-	-	-	123,156	448,204	3.64
2003	-	0	-	0	-	0	654,572	1,121,889	423	-	-	1,843	20,330	-	-	-	-	-	194,088	1,799,058	9.27
2004	-	-	0	-	-	0	546,429	646,647	1,186	-	-	12,172	20,819	-	-	-	-	-	109,650	1,227,254	11.19
2005	-	0	-	0	-	0	236,271	1,290,181	2,816	-	-	29,949	62,822	0	574	432	-	-	365,712	1,623,044	4.44
2006	-	-	1,232	-	-	0	196,855	1,000,434	3,115	-	-	23,181	18,067	-	-	-	-	-	305,268	1,242,884	4.07
2007	-	0	0	0	-	-	208,047	623,828	1,175	-	-	20,123	10,416	332	-	-	-	NA	415,452	NA	NA
2008	-	0	0	-	-	0	65,186	618,939	1,859	NA	-	45,489	42,391	NA	-	-	NA	NA	1,054,704	NA	NA
2009	-	0	0	0	NA	-	153,669	470,477	NA	NA	-	47,239	NA	NA	-	NA	NA	NA	514,188	NA	NA
2010	-	-	0	NA	NA	0	420,866	NA	NA	NA	0	NA	NA	NA	NA	NA	NA	NA	518,040	NA	NA
2011	-	549	NA	NA	NA	0	NA	NA	NA	NA	NA	NA	NA	NA	NA	NA	NA	NA	421,380	NA	NA
2012	-	NA	NA	NA	NA	NA	NA	NA	NA	NA	NA	NA	NA	NA	NA	NA	NA	NA	193,326	NA	NA
2013	NA	NA	NA	NA	NA	NA	NA	NA	NA	NA	NA	NA	NA	NA	NA	NA	NA	NA	387,036	NA	NA
2014	NA	NA	NA	NA	NA	NA	NA	NA	NA	NA	NA	NA	NA	NA	NA	NA	NA	NA	340,590	NA	NA

Table 3.2 Wood River brood table.

Brood Year	0.1	0.2	0.3	0.4	0.5	1.1	1.2	1.3	1.4	1.5	2.1	2.2	2.3	2.4	3.1	3.2	3.3	3.4	Escapement	Recruits	R/S
1955	NA	NA	NA	NA	NA	NA	NA	NA	NA	NA	NA	NA	NA	NA	NA	NA	NA	-	NA	NA	NA
1956	NA	NA	NA	NA	NA	NA	NA	NA	NA	-	NA	NA	NA	-	NA	NA	-	-	NA	NA	NA
1957	NA	NA	NA	NA	-	NA	NA	NA	-	-	NA	NA	45,045	-	NA	-	-	-	NA	NA	NA
1958	NA	NA	NA	-	-	NA	NA	451,856	-	-	NA	172,395	26,803	-	-	-	-	-	NA	NA	NA
1959	NA	NA	0	239	-	NA	907,852	458,540	-	-	15,166	316,785	39,543	-	-	-	-	-	NA	NA	NA
1960	NA	-	263	-	-	5,684	1,610,958	942,241	4,277	-	69	96,536	88,896	-	-	0	-	-	NA	NA	NA
1961	-	148	2,736	-	-	-	218,861	1,422,998	871	-	-	13,440	25,286	684	-	-	-	-	NA	NA	NA
1962	-	851	0	504	-	1,739	970,915	422,690	4,124	-	95	109,138	40,572	-	-	-	243	-	NA	NA	NA
1963	-	-	0	0	-	-	591,145	947,041	-	-	659	53,835	39,341	814	-	-	-	-	721,404	1,632,836	2.26
1964	-	0	5,167	-	-	117	492,966	320,746	-	-	910	386,106	80,891	-	-	-	-	-	1,076,112	1,286,903	1.20
1965	-	2,071	2,100	-	-	595	597,032	1,024,258	4,897	-	134	171,819	218,813	-	-	-	-	-	675,156	2,021,719	2.99
1966	-	0	0	0	-	5,584	959,032	1,205,631	5,650	316	223	50,018	64,076	248	-	-	-	-	1,208,682	2,290,780	1.90
1967	-	-	7,435	328	39	1,499	575,431	289,067	653	-	527	81,500	97,783	-	-	-	-	-	515,772	1,054,264	2.04
1968	-	-	5,656	0	-	909	552,272	565,465	4,462	-	-	3,926	21,677	-	-	-	-	-	649,344	1,154,367	1.78
1969	-	-	1,899	-	-	-	60,777	438,024	10,313	-	-	383,878	94,957	-	-	-	-	-	604,338	989,848	1.64
1970	-	-	0	-	-	3,952	1,387,915	1,022,201	0	-	4,459	179,643	49,931	-	-	-	-	-	1,161,964	2,648,102	2.28
1971	-	2,468	19,061	-	-	1,697	444,270	643,532	0	-	-	202,945	111,167	-	-	-	-	-	851,202	1,425,140	1.67
1972	-	1,695	11,223	0	0	1,707	802,386	422,945	34,889	-	-	41,828	22,008	-	-	-	-	-	430,602	1,338,679	3.11
1973	-	645	1,261	0	-	1,245	233,282	1,154,123	0	-	-	44,714	24,991	-	-	0	-	-	330,474	1,460,260	4.42
1974	-	0	12,417	-	-	2,409	3,403,445	1,924,881	8,334	-	4,257	437,456	100,230	-	-	-	-	-	1,708,836	5,893,430	3.45
1975	-	0	0	-	-	30,667	1,796,332	2,809,724	7,864	-	-	548,783	1,097,316	-	-	-	-	-	1,270,116	6,290,687	4.95
1976	-	0	0	-	0	1,967	2,652,958	3,010,833	9,227	-	4,013	617,473	290,716	3,349	-	-	-	-	817,008	6,590,536	8.07
1977	-	-	0	0	-	19,300	1,275,546	2,444,584	0	-	0	55,898	27,016	-	-	1,968	-	-	561,828	3,824,313	6.81
1978	-	-	0	0	-	-	1,274,166	688,659	13,288	-	2,794	1,025,110	113,191	-	-	-	-	-	2,267,238	3,117,207	1.37
1979	-	0	0	10,445	-	16,286	2,360,529	1,708,953	1,419	-	-	31,620	25,417	-	-	-	-	-	1,706,352	4,154,669	2.43
1980	-	0	0	0	-	-	472,216	810,844	1,486	-	-	72,534	114,712	-	-	-	-	-	2,969,040	1,471,792	0.50
1981	-	0	0	2,310	-	-	613,922	1,383,072	0	-	-	69,787	162,822	-	-	-	-	-	1,233,318	2,231,913	1.81
1982	-	0	0	0	-	3,628	533,178	1,388,423	12,821	-	-	125,734	21,586	-	-	-	-	-	976,470	2,085,371	2.14
1983	-	0	1,041	0	-	1,359	1,839,383	1,353,389	2,818	-	-	15,114	113,650	-	-	-	-	-	1,360,968	3,326,753	2.44
1984	155	0	0	1,241	-	382	586,695	1,499,000	16,112	-	-	80,679	34,558	-	-	-	-	-	1,002,792	2,218,822	2.21
1985	-	8,941	16,157	563	-	1,455	1,380,822	1,822,594	3,605	-	-	44,470	24,716	843	-	-	-	-	939,000	3,304,167	3.52
1986	-	3,188	31,947	1,261	-	2,187	1,225,884	2,760,108	20,885	-	-	52,691	78,155	-	-	-	-	-	818,652	4,176,305	5.10
1987	-	18,995	74,929	16,959	-	-	1,579,965	991,109	6,777	-	148	87,905	121,126	0	-	-	-	-	1,337,172	2,897,914	2.17
1988	-	7,723	18,868	4,368	-	1,124	1,850,506	1,935,323	12,680	-	-	90,117	57,212	949	-	-	-	-	866,778	3,978,870	4.59
1989	-	2,349	19,841	0	-	4,110	2,563,487	2,443,447	2,447	-	-	23,864	46,747	-	-	-	-	-	1,186,410	5,106,291	4.30
1990	-	5,651	23,365	5,426	-	1,442	1,122,283	1,824,009	4,644	911	1,436	301,351	264,540	0	-	-	619	-	1,069,440	3,555,678	3.32
1991	-	0	8,271	0	-	12,307	2,739,167	3,167,633	65,018	-	-	51,077	66,660	132	-	-	-	-	1,159,920	6,110,265	5.27
1992	-	8,953	77,658	6,088	-	1,295	2,380,886	1,931,609	0	-	-	85,259	45,424	1,182	-	770	-	-	1,286,250	4,539,123	3.53
1993	-	13,405	1,681	4,109	-	-	1,710,296	1,233,241	2,588	-	-	138,581	163,437	-	-	-	-	-	1,176,126	3,267,339	2.78
1994	-	-	0	-	-	10,892	2,990,517	2,383,374	2,874	-	489	400,066	99,116	-	-	-	-	-	1,471,890	5,887,328	4.00
1995	-	419	-	-	-	7,336	4,452,435	3,217,087	9,319	-	-	117,398	40,742	-	-	-	-	-	1,482,162	7,844,736	5.29
1996	-	-	-	-	-	-	3,104,643	4,383,745	21,333	-	-	2,900	17,323	-	-	-	-	-	1,649,598	7,529,945	4.56
1997	-	-	-	-	-	-	204,615	584,427	25,529	0	-	194,836	227,699	181	-	-	29	-	1,512,396	1,237,317	0.82
1998	-	-	749	-	-	2,776	3,038,334	3,535,682	5,315	-	900	148,017	134,874	314	-	-	-	-	1,755,768	6,866,961	3.91
1999	-	1,095	-	-	-	725	2,291,700	2,609,475	8,219	-	448	399,867	309,514	-	-	-	-	35	1,512,426	5,621,078	3.72
2000	-	-	-	-	-	4,297	3,280,676	3,230,094	46,358	0	-	112,748	540,380	0	-	-	-	-	1,300,026	7,214,553	5.55
2001	-	-	-	0	-	-	2,176,259	5,092,621	13,504	-	-	561,580	62,794	-	1,356	-	-	-	1,458,732	7,908,115	5.42
2002	-	-	18,986	-	-	44,386	5,920,956	2,140,999	0	-	-	242,412	46,759	-	-	-	-	-	1,283,682	8,414,497	6.55
2003	-	0	-	0	-	4,138	5,460,152	3,280,112	73,578	-	-	38,275	114,808	-	-	-	-	-	1,459,782	8,971,062	6.15
2004	-	-	0	-	-	10,784	4,001,428	4,737,761	29,830	-	-	119,736	137,805	-	-	-	-	-	1,543,392	9,037,345	5.86
2005	-	0	-	3,315	-	0	2,659,363	3,888,578	9,582	-	-	235,506	87,671	299	-	-	-	-	1,496,550	6,884,315	4.60
2006	-	-	1,566	2,347	-	40,677	4,545,217	3,009,281	16,447	-	2,334	180,699	47,258	-	-	-	-	-	4,008,102	7,845,825	1.96
2007	-	742	0	0	-	2,506	1,421,241	1,027,026	1,253	-	-	172,159	31,566	-	-	-	-	NA	1,528,086	NA	NA
2008	-	678	1,003	-	-	0	1,297,522	1,702,753	19,842	NA	-	41,302	80,868	NA	-	-	NA	NA	1,724,676	NA	NA
2009	-	0	0	0	NA	1,789	1,361,180	2,204,457	NA	NA	1,627	221,827	NA	NA	-	NA	NA	NA	1,319,232	NA	NA
2010	-	-	6,198	NA	NA	41,822	4,927,412	NA	NA	NA	1,236	NA	NA	NA	NA	NA	NA	NA	1,804,344	NA	NA
2011	-	-	NA	NA	NA	10,402	NA	NA	NA	NA	NA	NA	NA	NA	NA	NA	NA	NA	1,098,006	NA	NA
2012	-	NA	NA	NA	NA	NA	NA	NA	NA	NA	NA	NA	NA	NA	NA	NA	NA	NA	764,211	NA	NA
2013	NA	NA	NA	NA	NA	NA	NA	NA	NA	NA	NA	NA	NA	NA	NA	NA	NA	NA	1,183,348	NA	NA
2014	NA	NA	NA	NA	NA	NA	NA	NA	NA	NA	NA	NA	NA	NA	NA	NA	NA	NA	2,764,614	NA	NA

Table 3.3 Nushagak River brood table.

Brood Year	0.1	0.2	0.3	0.4	0.5	1.1	1.2	1.3	1.4	1.5	2.1	2.2	2.3	2.4	3.1	3.2	3.3	3.4	Escapement	Recruits	R/S
1955	NA	NA	NA	NA	NA	NA	NA	NA	NA	NA	NA	NA	NA	NA	NA	NA	NA	-	NA	NA	NA
1956	NA	NA	NA	NA	NA	NA	NA	NA	NA	-	NA	NA	NA	-	NA	NA	-	-	NA	NA	NA
1957	NA	NA	NA	NA	-	NA	NA	NA	0	-	NA	NA	0	-	NA	-	-	-	NA	NA	NA
1958	NA	NA	NA	0	-	NA	NA	311,993	0	-	NA	65,872	38,995	-	-	-	-	-	NA	NA	NA
1959	NA	NA	39,870	3	-	NA	0	0	602	-	0	169,011	41,625	-	-	-	-	-	NA	NA	NA
1960	NA	0	51,366	3,589	-	34,663	0	213,741	2,225	-	-	47,670	188,107	-	-	12,801	-	-	NA	NA	NA
1961	-	6,980	51,759	0	-	0	210,436	22,240	0	-	-	166,547	8,210	-	-	-	-	-	NA	NA	NA
1962	-	11,314	19,634	10,665	-	1,451	31	0	22,925	-	-	66,348	20,282	-	-	-	0	-	NA	NA	NA
1963	-	0	40,442	38,789	-	0	0	0	226	-	-	124,685	10,698	-	-	-	-	-	234,821	214,841	0.91
1964	-	13,964	9,661	1,351	-	0	0	51,330	-	-	-	15,074	1,963	-	-	-	-	-	134,853	93,342	0.69
1965	-	2,117	13,934	-	-	0	86,140	672,474	0	-	0	5,089	0	-	-	-	-	-	255,794	779,754	3.05
1966	-	4,968	83,443	1,061	-	670	91,353	520,071	0	0	0	0	0	0	-	-	-	-	233,578	701,566	3.00
1967	-	9,148	26,640	-	0	2,290	118,677	47,474	4,048	-	7,843	4,510	6,403	-	-	-	-	-	74,003	227,033	3.07
1968	-	0	0	7,854	-	0	35,190	293,845	2,760	-	-	0	4,530	-	-	-	-	-	142,360	344,179	2.42
1969	-	-	97,507	5,026	-	-	4,815	66,889	4,045	-	-	36,821	278,589	-	-	-	-	-	95,805	493,692	5.15
1970	-	2,654	3,370	0	-	-	127,285	12,169	3,442	-	486	745,793	93,565	-	-	-	-	-	452,892	988,764	2.18
1971	-	1,211	9,601	-	-	3,816	1	807,916	2,596	-	1	28,355	157,501	-	-	-	-	-	312,699	1,010,999	3.23
1972	-	3,598	75,229	887	128	0	71,034	863,255	0	-	-	46,130	87,718	-	-	-	-	-	39,851	1,147,980	28.81
1973	-	4,046	25,302	1,816	-	-	0	1,231,778	12,062	-	-	61,562	43,019	-	-	605	-	-	210,601	1,380,189	6.55
1974	-	1,112	0	0	-	-	0	70	0	-	0	347,528	34,914	-	-	-	-	-	204,190	383,623	1.88
1975	-	15,231	16,604	13,548	-	33,598	622,880	4,934,293	95,363	-	-	154,757	108,875	-	-	-	-	-	832,093	5,995,149	7.20
1976	-	6,033	62,381	0	2,596	-	190,047	3,422,923	57,970	-	0	203,260	406,715	0	-	-	-	-	520,303	4,351,924	8.36
1977	-	-	16,136	63,770	-	0	21,274	3,028,330	92,537	-	7,964	0	6,077	-	-	0	-	-	611,588	3,236,089	5.29
1978	-	0	345,825	133,718	-	-	89,106	933,192	0	-	-	11,883	0	-	-	-	-	-	734,040	1,513,725	2.06
1979	-	72,863	529,084	0	-	0	430,997	767,683	45,526	-	-	0	0	-	-	-	-	-	551,272	1,846,153	3.35
1980	-	22,436	523,065	34,504	-	-	19,768	312,947	8,820	-	-	167,393	121,331	0	-	-	-	-	3,669,136	1,210,266	0.33
1981	-	30,304	101,602	8,931	-	-	250,006	1,576,925	5,804	-	-	2,612	0	573	-	-	-	-	1,118,873	1,976,757	1.77
1982	-	82,470	420,279	34,031	-	1,195	125,109	594,091	71,345	-	-	0	6,628	-	-	-	-	-	664,580	1,335,148	2.01
1983	-	115,055	502,453	111,520	-	276	233,673	543,194	17,210	-	-	5,890	19,467	-	-	-	-	-	446,845	1,548,738	3.47
1984	0	10,147	218,564	26,533	-	0	46,771	432,523	20,858	-	-	3,962	1,890	-	-	-	-	-	655,739	761,247	1.16
1985	-	85,591	533,285	63,475	-	-	63,478	638,819	18,464	-	-	2,858	10,900	0	-	-	-	-	551,319	1,416,870	2.57
1986	-	94,281	803,990	54,040	-	-	98,020	791,155	200,174	-	-	0	50,092	820	-	-	-	-	1,095,241	2,092,574	1.91
1987	-	174,615	667,893	217,691	-	-	32,994	660,535	122,522	-	-	15,735	11,517	1,955	-	-	-	-	429,182	1,905,456	4.44
1988	-	53,520	450,950	110,430	-	-	206,199	1,651,453	72,229	-	-	5,343	7,214	-	-	-	-	-	534,460	2,557,339	4.78
1989	-	87,497	463,980	19,981	-	-	105,904	693,606	22,475	-	-	1,126	3,920	-	-	232	-	-	567,863	1,398,722	2.46
1990	-	108,080	588,590	113,335	-	-	37,828	292,042	8,433	0	-	13,239	21,791	5,910	-	-	0	-	752,513	1,189,247	1.58
1991	-	13,534	138,116	4,627	-	401	124,515	1,073,215	124,084	-	189	2,430	10,371	0	-	-	-	-	544,748	1,491,482	2.74
1992	-	102,933	340,638	1,047	-	-	130,535	567,660	56,242	-	-	9,027	4,493	0	-	0	-	-	768,816	1,212,574	1.58
1993	-	41,501	49,450	0	-	-	48,386	828,615	102,422	-	-	773	3,132	-	-	-	-	-	790,927	1,074,278	1.36
1994	-	1,504	28,616	-	-	207	70,182	277,738	7,774	-	0	5,625	34,269	-	-	-	-	-	563,334	425,915	0.76
1995	-	2,076	-	-	-	563	62,891	925,449	186,962	-	-	13,338	7,199	-	-	-	-	-	311,136	1,198,477	3.85
1996	-	-	-	-	-	-	363,788	1,857,241	99,273	-	-	4,811	10,398	-	-	-	-	-	557,057	2,335,512	4.19
1997	-	-	-	-	-	-	37,572	423,105	27,112	3,142	-	4,075	49,296	0	-	-	0	-	412,591	544,302	1.32
1998	-	-	-	-	-	0	154,934	2,237,869	207,961	-	0	7,352	57,380	0	-	-	-	-	507,532	2,665,496	5.25
1999	-	-	-	-	-	-	88,031	1,540,403	77,948	-	0	13,098	34,236	-	-	-	-	0	344,972	1,753,716	5.08
2000	-	-	-	-	-	0	240,485	3,299,220	389,773	1,084	-	5,167	16,590	4,222	-	-	-	-	446,286	3,956,541	8.87
2001	-	-	-	6,429	-	-	256,405	2,525,696	258,150	363	-	5,094	24,507	-	0	-	-	-	897,112	3,076,644	3.43
2002	-	-	38,496	-	-	0	192,085	1,783,792	68,193	-	-	30,928	7,787	-	-	-	-	-	349,155	2,121,281	6.08
2003	-	8,269	-	18,884	-	0	396,387	1,230,046	192,828	-	-	0	16,901	-	-	-	-	-	642,093	1,863,316	2.90
2004	-	-	55,992	-	-	0	160,719	1,156,550	72,574	-	-	4,828	13,032	-	-	-	-	-	543,872	1,463,695	2.69
2005	-	4,273	-	8,550	-	2,387	303,869	826,261	36,706	-	-	7,976	19,987	0	-	-	-	-	1,106,703	1,210,008	1.09
2006	-	-	6,070	1,429	-	0	95,890	976,883	93,034	-	-	5,166	6,533	-	-	-	-	-	548,410	1,185,006	2.16
2007	-	4,215	51,951	9,733	-	1,034	30,183	669,684	54,735	-	-	0	6,392	-	-	-	-	NA	518,041	NA	NA
2008	-	0	9,581	-	-	1,273	158,802	1,802,731	143,521	NA	-	4,634	13,881	NA	-	-	NA	NA	492,546	NA	NA
2009	-	976	11,203	3,432	NA	627	97,615	1,271,629	NA	NA	-	5,007	NA	NA	-	NA	NA	NA	484,149	NA	NA
2010	-	-	4,975	NA	NA	0	213,895	NA	NA	NA	0	NA	NA	NA	NA	NA	NA	NA	468,696	NA	NA
2011	-	-	NA	NA	NA	0	NA	NA	NA	NA	NA	NA	NA	NA	NA	NA	NA	NA	428,191	NA	NA
2012	-	NA	NA	NA	NA	NA	NA	NA	NA	NA	NA	NA	NA	NA	NA	NA	NA	NA	432,438	NA	NA
2013	NA	NA	NA	NA	NA	NA	NA	NA	NA	NA	NA	NA	NA	NA	NA	NA	NA	NA	894,148	NA	NA
2014	NA	NA	NA	NA	NA	NA	NA	NA	NA	NA	NA	NA	NA	NA	NA	NA	NA	NA	618,477	NA	NA

Table 3.4 Kvichak River brood table.

Brood Year	0.1	0.2	0.3	0.4	0.5	1.1	1.2	1.3	1.4	1.5	2.1	2.2	2.3	2.4	3.1	3.2	3.3	3.4	Escapement	Recruits	R/S
1955	NA	NA	NA	NA	NA	NA	NA	NA	NA	NA	NA	NA	NA	NA	NA	NA	NA	-	NA	NA	NA
1956	NA	NA	NA	NA	NA	NA	NA	NA	NA	-	NA	NA	NA	-	NA	NA	0	-	NA	NA	NA
1957	NA	NA	NA	NA	-	NA	NA	NA	1,413	-	NA	NA	203,661	-	NA	0	0	-	NA	NA	NA
1958	NA	NA	NA	-	-	NA	NA	32,838	6,053	-	NA	139,962	59,115	-	-	0	0	-	NA	NA	NA
1959	NA	NA	-	-	-	NA	236,514	0	0	-	951	208,489	5,451	0	-	2,236	0	-	NA	NA	NA
1960	NA	-	-	-	-	-	1,017,277	456,190	3,128	-	889,149	47,748,183	6,282,092	-	-	11,625	4,061	-	NA	NA	NA
1961	-	1,602	0	-	-	-	415,245	201,593	0	-	0	2,307,309	647,560	0	-	5,316	2,311	-	NA	NA	NA
1962	-	-	0	-	-	0	107,817	133,173	0	-	1,970	4,720,118	534,851	-	-	8,963	0	-	NA	NA	NA
1963	-	-	606	-	-	-	31,231	80,023	0	-	113	925,528	336,813	-	-	0	13,902	-	338,760	1,388,216	4.10
1964	-	-	0	-	-	3,244	2,288,423	288,371	3,941	-	111,882	2,613,881	446,099	-	-	6,606	1,068	-	957,120	5,763,515	6.02
1965	-	-	-	-	-	23,983	10,321,864	299,793	0	-	485,629	33,528,681	1,159,447	0	-	1,292	0	-	24,325,926	45,820,689	1.88
1966	-	4,763	0	0	-	3,429	524,322	885,878	0	-	16,342	4,568,771	517,436	1,122	-	0	0	-	3,755,185	6,522,062	1.74
1967	-	-	14,745	968	-	-	342,819	321,956	65	-	2,299	991,239	109,957	-	-	0	-	-	3,216,208	1,784,048	0.55
1968	-	1,788	0	-	-	-	300,687	38,561	4,514	-	-	104,011	176,512	0	-	7,305	1,946	-	2,557,440	635,324	0.25
1969	-	-	748	-	-	0	149,287	321,597	-	-	6,124	4,476,992	546,728	0	-	12,149	0	-	8,394,204	5,513,626	0.66
1970	-	-	-	-	-	611	45,471	40,280	-	-	28,962	15,247,973	0	-	-	0	575	-	13,935,306	15,363,872	1.10
1971	-	-	-	-	-	0	321,013	653,575	-	-	45,182	919,844	95,529	0	-	1,142	0	-	2,387,392	2,036,285	0.85
1972	-	-	0	-	-	4,360	1,971,913	142,305	10,886	-	0	886,252	232,955	-	-	0	0	-	1,009,962	3,248,671	3.22
1973	-	0	1,204	0	-	-	531,509	1,048,800	0	-	2,634	252,857	351,748	-	-	14,490	0	-	226,554	2,203,241	9.73
1974	-	0	0	-	-	14,322	6,047,999	1,845,015	0	-	319,232	16,927,229	616,516	-	-	14,093	0	-	4,433,844	25,784,407	5.82
1975	-	-	-	-	-	6,365	5,468,931	1,305,049	-	-	314,282	29,958,382	382,348	0	0	3,654	-	-	13,140,450	37,439,011	2.85
1976	-	0	16,621	-	-	5,347	5,940,228	675,758	3,355	-	37,502	3,806,686	230,826	0	-	-	0	-	1,965,282	10,716,323	5.45
1977	-	6,590	4,899	-	-	36,699	2,024,758	718,010	0	-	2,130	174,744	121,674	-	-	0	0	-	1,341,144	3,089,502	2.30
1978	-	-	0	-	-	1,122	1,613,301	1,063,136	0	-	15,273	1,372,783	987,655	0	-	0	1,957	-	4,149,288	5,055,228	1.22
1979	-	2,381	0	0	-	53,985	18,868,217	2,470,065	0	-	69,687	17,920,528	3,664,847	0	-	0	-	-	11,218,434	43,049,711	3.84
1980	-	-	0	-	-	1,374	2,539,067	1,385,016	2,963	-	13,603	8,290,979	364,127	0	-	0	-	-	22,505,268	12,597,129	0.56
1981	-	-	5,260	-	-	-	745,192	188,993	0	-	0	962,156	147,129	0	-	0	0	-	1,754,358	2,048,731	1.17
1982	-	-	0	0	-	0	492,711	385,798	4,844	0	531	514,154	111,109	0	-	0	0	-	1,134,840	1,509,147	1.33
1983	-	-	0	0	-	909	9,266,210	2,994,862	4,091	-	2,975	1,110,949	386,091	8,088	-	0	0	-	3,569,982	13,774,175	3.86
1984	-	0	1,184	0	-	0	2,578,404	1,438,287	0	-	46,565	17,556,989	1,662,891	0	0	0	0	-	10,490,670	23,284,320	2.22
1985	969	3,827	6,640	-	-	7,558	1,051,189	958,922	3,134	-	36,957	14,848,955	1,382,720	8,513	-	1,295	1,079	-	7,211,046	18,311,756	2.54
1986	-	1,587	22,024	371	-	0	652,824	868,041	22,539	-	0	1,539,168	1,007,382	0	-	0	0	-	1,179,322	4,113,937	3.49
1987	-	28,969	55,108	6,575	-	7,292	4,714,523	2,193,713	3,167	-	32,602	4,275,758	329,014	0	-	0	0	-	6,065,880	11,646,723	1.92
1988	-	8,516	23,767	981	-	6,196	3,035,544	1,958,030	1,920	-	17,855	3,697,594	453,823	0	-	0	0	-	4,065,216	9,204,227	2.26
1989	-	31,825	59,837	1,909	-	3,333	1,860,267	1,072,267	0	-	146,440	18,332,312	3,276,252	0	-	12,478	0	-	8,317,500	24,796,919	2.98
1990	-	5,137	7,655	0	-	2,740	1,635,341	890,663	0	-	82,331	22,043,353	1,626,522	1,146	-	0	0	-	6,970,020	26,294,888	3.77
1991	-	0	2,556	0	-	1,129	2,192,134	1,181,519	12,039	-	1,939	1,008,333	237,176	0	-	0	0	-	4,222,788	4,636,825	1.10
1992	-	3,449	3,727	0	-	-	651,475	300,919	0	-	2,137	752,668	162,197	0	-	0	0	-	4,725,864	1,876,573	0.40
1993	-	-	0	2,570	-	230	1,088,225	873,002	4,931	-	679	683,808	478,384	-	-	0	0	-	4,025,166	3,131,830	0.78
1994	-	0	0	-	-	1,849	2,023,264	1,062,178	119	0	47,942	3,920,081	249,058	111	-	0	0	-	8,355,936	7,304,603	0.87
1995	-	-	-	20	-	17,601	7,737,408	2,107,239	8,040	-	0	677,565	97,969	1,515	-	0	18	-	10,038,720	10,647,375	1.06
1996	-	-	-	-	-	-	548,460	1,687,279	9,756	0	-	24,701	30,144	79	-	63	0	10	1,450,578	2,300,492	1.59
1997	-	-	93	-	-	-	159,978	146,338	726	-	19	348,003	187,060	156	0	314	0	-	1,503,732	842,686	0.56
1998	-	-	-	-	-	74	379,112	439,050	18,322	-	638	348,018	95,634	0	-	0	0	-	2,296,074	1,280,847	0.56
1999	-	18	-	-	-	370	1,015,499	282,916	12,451	-	51,078	5,817,918	215,761	33	-	1,537	33	-	6,196,914	7,397,614	1.19
2000	-	-	22	-	-	20	1,888,515	1,310,018	1,300	-	0	746,171	331,310	0	-	52	0	-	1,827,780	4,277,407	2.34
2001	-	-	25	0	-	-	635,233	1,774,193	9,337	0	1,456	737,948	702,240	0	-	0	0	-	1,095,348	3,860,432	3.52
2002	-	-	0	-	-	3,394	2,351,273	983,112	645	-	2,380	119,114	10,541	0	-	0	-	-	703,884	3,470,460	4.93
2003	-	9,830	-	0	-	3,840	3,196,747	1,227,644	9,523	-	0	31,645	127,900	0	-	0	-	-	1,686,804	4,607,129	2.73
2004	-	-	0	-	-	-	4,857,596	2,876,962	0	-	0	2,615,328	573,679	0	-	0	0	-	5,500,134	10,923,565	1.99
2005	-	-	-	0	-	4,311	1,267,168	2,085,082	9,034	-	0	4,570,381	1,856,830	1,153	-	0	0	-	2,320,332	9,793,959	4.22
2006	-	-	0	0	-	2,912	3,702,072	2,849,294	1,869	867	0	1,246,886	743,851	3,542	-	288	556	-	3,068,226	8,552,138	2.79
2007	-	-	1,141	1,763	-	0	1,600,069	1,827,536	12,915	-	24,401	6,963,759	2,430,694	14,926	-	0	0	NA	2,810,208	NA	NA
2008	-	-	5,388	0	-	-	2,669,164	1,949,792	24,321	NA	2,520	1,241,288	364,443	NA	-	1,279	NA	NA	2,757,912	NA	NA
2009	-	-	-	-	NA	-	726,549	786,071	NA	NA	11,703	7,159,075	NA	NA	-	NA	NA	NA	2,266,140	NA	NA
2010	-	-	301	NA	NA	3,076	5,784,437	NA	NA	NA	88,117	NA	NA	NA	NA	NA	NA	NA	4,207,410	NA	NA
2011	-	-	NA	NA	NA	4,659	NA	NA	NA	NA	NA	NA	NA	NA	NA	NA	NA	NA	2,264,352	NA	NA
2012	-	NA	NA	NA	NA	NA	NA	NA	NA	NA	NA	NA	NA	NA	NA	NA	NA	NA	4,164,444	NA	NA
2013	NA	NA	NA	NA	NA	NA	NA	NA	NA	NA	NA	NA	NA	NA	NA	NA	NA	NA	2,088,576	NA	NA
2014	NA	NA	NA	NA	NA	NA	NA	NA	NA	NA	NA	NA	NA	NA	NA	NA	NA	NA	4,458,540	NA	NA

Table 3.5 Alagnak River brood table.

Brood Year	0.1	0.2	0.3	0.4	0.5	1.1	1.2	1.3	1.4	1.5	2.1	2.2	2.3	2.4	3.1	3.2	3.3	3.4	Escapement	Recruits	R/S
1955	NA	NA	NA	NA	NA	NA	NA	NA	NA	NA	NA	NA	NA	NA	NA	NA	NA	-	NA	NA	NA
1956	NA	NA	NA	NA	NA	NA	NA	NA	NA	-	NA	NA	NA	-	NA	NA	0	-	NA	NA	NA
1957	NA	NA	NA	NA	-	NA	NA	NA	-	-	NA	NA	13,499	-	NA	0	0	-	NA	NA	NA
1958	NA	NA	NA	-	-	NA	NA	13,120	-	-	NA	20,219	8,577	-	-	0	0	-	NA	NA	NA
1959	NA	NA	-	-	-	NA	331,300	338,122	0	-	0	286,854	50,739	0	-	773	1,312	-	NA	NA	NA
1960	NA	-	-	-	-	-	121,361	116,448	0	-	0	166,915	43,429	-	-	0	0	-	NA	NA	NA
1961	-	0	727	-	-	4,469	50,293	232,931	0	-	0	6,139	0	0	-	0	0	-	NA	NA	NA
1962	-	-	0	-	-	11,965	110,266	104,885	0	-	-	1,626	22,573	-	-	813	0	-	NA	NA	NA
1963	-	-	0	-	-	-	231,002	151,684	0	-	415	30,953	819	-	-	0	0	-	203,304	414,873	2.04
1964	-	-	0	-	-	6,377	97,650	90,731	-	-	1,880	112,243	73,018	-	-	0	0	-	248,700	381,900	1.54
1965	-	-	-	-	-	8,480	110,323	88,348	5,497	-	510	29,040	17,531	0	-	0	0	-	175,020	259,729	1.48
1966	-	0	0	0	-	9,662	304,544	229,248	0	-	-	13,317	8,812	-	-	0	0	-	174,336	565,584	3.24
1967	-	-	461	0	-	5,830	260,360	52,163	0	-	2,325	59,200	9,010	-	-	0	-	-	202,626	389,349	1.92
1968	-	411	0	-	-	8,143	182,414	52,504	2,130	-	-	685	2,904	0	-	0	0	-	193,872	249,192	1.29
1969	-	-	0	-	-	0	1,354	54,757	-	-	-	108,529	15,545	0	-	0	0	-	182,490	180,185	0.99
1970	-	-	-	-	-	0	78,027	58,491	-	-	0	8,320	803	-	-	0	0	-	177,060	145,642	0.82
1971	-	-	-	-	-	1,233	28,838	56,204	-	-	-	30,123	207,343	0	-	0	1,012	-	187,302	324,752	1.73
1972	-	-	0	-	-	1,462	70,320	27,572	0	-	0	0	0	-	-	24,814	0	-	151,188	124,168	0.82
1973	-	0	0	3,099	-	-	0	6,687	1,378	-	-	350,600	0	-	-	67,512	83,665	-	35,280	512,940	14.54
1974	-	0	1,911	-	-	-	722,581	0	1,867	-	0	1,551,297	0	-	-	0	13,252	-	214,848	2,290,909	10.66
1975	-	-	-	-	-	-	0	467,275	-	-	0	0	492,798	0	62,201	0	-	-	100,480	1,022,274	10.17
1976	-	0	77,257	-	-	0	0	157,897	0	-	1	0	94,649	14,903	-	-	0	-	81,822	344,709	4.21
1977	-	0	3,287	-	-	163,394	0	689,175	0	-	-	0	145,046	-	-	0	1,758	-	108,911	1,002,659	9.21
1978	-	-	0	-	-	-	561,752	1,026,219	15,371	-	-	512,955	0	15,971	-	42,750	0	-	584,970	2,175,018	3.72
1979	-	-	1,045	0	-	-	947,783	81,155	13,786	-	16,623	1,047,577	801	131	-	0	0	-	750,210	2,108,901	2.81
1980	-	-	4,640	-	-	-	0	371,067	23	-	0	264,709	187	0	-	0	0	-	759,645	640,625	0.84
1981	-	-	0	-	-	-	186,206	1,006,317	343	-	0	265	2,803	0	-	0	0	-	209,636	1,195,933	5.70
1982	-	-	5,982	0	-	0	3,699	737,911	292	0	0	3,975	2,386	0	-	0	0	-	610,215	754,244	1.24
1983	-	-	11,675	0	-	6,465	55,502	435,210	1,009	-	0	3,383	9,327	0	-	0	1,807	-	245,361	524,378	2.14
1984	-	511	6,138	1,460	-	0	424,788	1,178,009	23,705	-	0	11,695	677,661	4,144	0	0	2,745	-	549,194	2,330,856	4.24
1985	0	0	33,827	-	-	6,209	238,006	795,093	569	-	0	13,592	680,128	0	-	0	832	-	300,977	1,768,255	5.88
1986	-	0	0	2,282	-	0	189,792	949,026	301	-	0	6,595	1,028,061	0	-	0	8,374	-	586,959	2,184,432	3.72
1987	-	0	0	0	-	0	92,094	407,723	664	-	0	3,495	361,803	0	-	1,327	0	-	393,236	867,107	2.21
1988	-	0	0	-	-	0	48,809	669,891	19,078	-	0	594,239	11,579	0	-	0	0	-	496,307	1,343,595	2.71
1989	-	0	0	1,216	-	0	786,804	1,311,729	12,494	-	0	602,114	12,239	1,719	-	0	0	-	501,738	2,728,315	5.44
1990	-	-	2,798	218	-	89,307	229,300	1,178,449	4,403	-	0	17,357	2,317	0	-	0	1,584	-	430,338	1,525,732	3.55
1991	-	0	0	0	-	17,251	1,117,956	2,317,591	93	-	0	3,285	54,187	0	-	2,585	0	-	707,852	3,512,948	4.96
1992	-	0	34,889	824	-	0	45,877	158,473	259	-	0	1,075	2,117	0	-	0	0	-	577,940	243,513	0.42
1993	-	-	10,418	-	-	0	16,460	944,038	76	-	0	219,052	318,454	0	-	0	0	-	887,336	1,508,499	1.70
1994	-	0	1,553	-	-	578,953	41,924	702,957	11,156	0	0	2,172	262,100	130	-	7,930	0	-	618,464	1,608,876	2.60
1995	-	-	-	23	-	0	2,079,632	1,872,901	1,969	-	0	6,521	7,178	85	-	0	21	-	550,068	3,968,331	7.21
1996	-	-	0	-	-	-	80,961	1,261,737	206,075	0	0	2,934	14,186	92	-	74	0	274	782,213	1,566,334	2.00
1997	-	-	109	-	-	5,782	12,773	641,113	41,820	-	22	102,505	658,290	10,235	0	369	0	-	556,193	1,473,019	2.65
1998	-	-	-	-	-	11,510	19,420	2,468,197	167	-	8,081	281,313	62,440	0	-	0	0	-	643,110	2,851,126	4.43
1999	-	21	-	-	-	0	816,823	1,229,261	544	-	92	657,881	1,076,097	9,407	-	0	63	-	1,182,180	3,790,191	3.21
2000	-	-	26	288	-	2,061	5,601,880	4,139,039	23,113	-	0	45,160	104,315	0	-	100	0	-	1,150,815	9,915,981	8.62
2001	-	-	321	0	-	40,207	134,552	1,158,282	9,690	0	35	40,378	81,492	0	-	0	0	-	680,850	1,464,957	2.15
2002	-	-	5,510	-	-	29	1,617,936	1,509,339	3,996	-	0	60,266	37,101	0	-	0	-	-	766,962	3,234,177	4.22
2003	-	-	-	0	-	0	2,529,847	3,707,507	122,281	-	0	5,779	21,763	0	-	0	-	-	3,676,146	6,387,177	1.74
2004	-	-	0	-	-	1,837	870,940	1,395,698	15,411	-	0	111,642	152,569	0	-	0	0	-	5,396,592	2,548,096	0.47
2005	-	-	-	0	-	0	758,941	1,840,684	7,543	-	0	163,695	128,197	589	-	0	0	-	4,218,990	2,899,649	0.69
2006	-	-	0	0	-	1,341	683,084	1,619,461	955	0	0	62,057	153,787	0	-	147	132	-	1,773,966	2,520,964	1.42
2007	-	-	0	0	-	1,621	515,085	1,171,173	396	-	0	519,852	139,217	154	-	0	0	NA	2,466,414	NA	NA
2008	-	-	147	0	-	826	533,367	1,366,237	2,629	NA	0	91,018	35,221	NA	-	0	NA	NA	2,180,502	NA	NA
2009	-	-	-	-	NA	-	416,486	244,071	NA	NA	264	133,874	NA	NA	-	NA	NA	NA	970,818	NA	NA
2010	-	-	154	NA	NA	0	473,677	NA	NA	NA	366	NA	NA	NA	NA	NA	NA	NA	1,187,730	NA	NA
2011	-	-	NA	NA	NA	183	NA	NA	NA	NA	NA	NA	NA	NA	NA	NA	NA	NA	883,794	NA	NA
2012	-	NA	NA	NA	NA	NA	NA	NA	NA	NA	NA	NA	NA	NA	NA	NA	NA	NA	861,747	NA	NA
2013	NA	NA	NA	NA	NA	NA	NA	NA	NA	NA	NA	NA	NA	NA	NA	NA	NA	NA	1,095,950	NA	NA
2014	NA	NA	NA	NA	NA	NA	NA	NA	NA	NA	NA	NA	NA	NA	NA	NA	NA	NA	200,500	NA	NA

Table 3.6 Naknek River brood table.

Brood Year	0.1	0.2	0.3	0.4	0.5	1.1	1.2	1.3	1.4	1.5	2.1	2.2	2.3	2.4	3.1	3.2	3.3	3.4	Escapement	Recruits	R/S
1955	NA	NA	NA	NA	NA	NA	NA	NA	NA	NA	NA	NA	NA	NA	NA	NA	NA	-	NA	NA	NA
1956	NA	NA	NA	NA	NA	NA	NA	NA	NA	-	NA	NA	NA	225	NA	NA	0	-	NA	NA	NA
1957	NA	NA	NA	NA	-	NA	NA	NA	452	-	NA	NA	563,156	-	NA	813	0	-	NA	NA	NA
1958	NA	NA	NA	-	-	NA	NA	140,335	98	-	NA	597,028	101,204	-	-	1,666	2,793	-	NA	NA	NA
1959	NA	NA	-	-	-	NA	486,708	230,913	0	-	7,813	532,280	266,999	0	-	0	0	-	NA	NA	NA
1960	NA	-	113	-	-	-	1,072,773	286,245	0	-	4,347	549,353	1,443,356	1,605	-	2,522	0	-	NA	NA	NA
1961	-	0	0	-	-	-	112,176	971,787	7,771	-	4,331	330,857	721,523	0	-	0	3,444	-	NA	NA	NA
1962	-	-	0	-	-	170	130,455	262,141	1,575	-	5,809	396,108	303,501	-	-	6,576	0	-	NA	NA	NA
1963	-	-	0	-	-	-	141,944	416,187	0	-	23,215	700,970	418,190	-	-	6,330	0	-	905,358	1,706,836	1.89
1964	-	-	0	-	-	743	342,531	256,174	-	-	34,421	1,275,540	309,692	-	-	4,430	0	-	1,349,604	2,223,531	1.65
1965	-	-	-	-	-	12,877	634,432	600,345	0	-	37,064	854,535	515,515	0	-	0	0	-	717,798	2,654,768	3.70
1966	-	0	0	0	-	13,371	918,493	2,573,070	3,000	-	2,025	209,618	485,528	519	-	0	0	-	1,016,445	4,205,622	4.14
1967	-	-	0	0	-	-	352,459	522,757	0	-	3,787	330,689	342,019	457	-	0	-	-	755,640	1,552,168	2.05
1968	-	0	0	-	-	3,585	126,410	202,857	257	-	-	88,011	216,580	0	-	611	0	-	1,023,222	638,312	0.62
1969	-	-	0	-	-	0	45,889	240,153	-	-	4,366	837,021	1,007,865	0	-	2,051	6,434	-	1,331,202	2,143,778	1.61
1970	-	-	-	-	-	597	161,583	281,376	-	-	17,756	1,549,928	504,895	-	-	17,444	1,726	-	732,502	2,535,306	3.46
1971	-	-	-	-	-	225	349,684	630,688	1,478	-	17,309	1,777,140	1,537,578	25,170	-	1,979	9,172	-	935,754	4,350,422	4.65
1972	-	-	0	-	-	2,938	228,954	397,108	5,084	-	35,046	359,615	676,509	2,647	-	3,618	3,690	-	586,518	1,715,207	2.92
1973	-	0	1,257	0	-	-	610,280	715,809	0	-	255	564,689	850,378	-	-	0	0	-	356,676	2,742,669	7.69
1974	-	0	0	-	-	1,544	253,899	393,360	0	-	1,832	1,103,750	880,690	-	-	7,439	0	-	1,241,058	2,642,513	2.13
1975	-	-	-	-	-	1,029	456,699	1,630,147	-	-	11,804	1,539,430	1,547,266	4,744	0	4,586	-	-	2,026,686	5,195,705	2.56
1976	-	0	0	-	-	4,277	1,013,493	4,461,321	24,292	-	4,423	1,950,161	1,520,144	10,680	-	-	2,941	-	1,320,750	8,991,732	6.81
1977	-	0	4,313	-	-	4,429	788,791	2,456,928	74,909	-	-	145,844	242,959	1,394	-	0	1,493	-	1,085,856	3,721,059	3.43
1978	-	-	0	-	-	393	490,174	949,602	2,206	-	9,731	631,141	704,090	0	-	958	0	-	813,378	2,788,295	3.43
1979	-	-	0	0	-	8,951	1,389,279	1,322,934	5,030	-	5,950	761,179	463,047	0	-	6,049	1,498	-	925,362	3,963,916	4.28
1980	-	-	0	-	-	803	1,059,833	1,629,612	11,979	-	17,349	1,341,149	859,933	1,477	-	0	-	-	2,644,698	4,922,134	1.86
1981	-	-	0	-	-	4,917	770,379	2,359,153	18,479	-	5,842	592,347	928,049	4,335	-	0	0	-	1,796,220	4,683,500	2.61
1982	-	-	0	0	-	5,079	163,761	926,020	27,213	684	-	221,369	469,143	7,450	-	0	0	-	1,155,552	1,820,719	1.58
1983	-	-	0	0	-	0	176,012	547,077	5,761	-	7,647	344,686	370,620	0	-	0	0	-	888,294	1,451,803	1.63
1984	-	0	0	0	-	241	504,531	802,905	11,970	-	30,073	1,525,063	1,508,076	1,420	0	0	0	-	1,242,474	4,384,278	3.53
1985	0	0	1,481	3,654	-	2,051	802,849	3,232,301	54,457	-	29,205	1,576,311	1,398,709	37,784	-	0	8,610	-	1,849,938	7,147,411	3.86
1986	-	0	5,477	0	-	7,133	1,820,705	6,641,769	437,077	709	2,362	1,209,214	2,469,231	41,218	-	0	0	-	1,977,645	12,634,896	6.39
1987	-	2,601	14,558	3,047	-	0	366,144	1,237,224	117,645	-	2,429	611,602	3,105,993	10,933	-	0	0	-	1,061,806	5,472,177	5.15
1988	-	0	0	-	-	-	351,616	1,105,709	18,312	-	31,289	769,987	692,581	3,191	-	0	0	-	1,037,862	2,972,686	2.86
1989	-	0	0	0	-	1,174	356,238	795,431	0	-	4,340	1,333,842	513,440	0	-	2,404	0	-	1,161,984	3,006,870	2.59
1990	-	-	0	0	-	0	624,332	869,546	4,968	-	48,018	1,448,355	813,436	16,030	-	0	0	-	2,092,578	3,824,685	1.83
1991	-	2,135	0	0	-	10,015	427,160	3,509,444	62,276	-	2,276	137,991	421,595	1,437	-	0	0	-	3,578,508	4,574,329	1.28
1992	-	0	5,579	0	-	-	157,494	746,815	11,801	-	474	280,285	261,958	0	1,600	3,486	0	-	1,606,650	1,469,491	0.91
1993	-	-	0	-	-	119	349,586	1,110,393	23,595	-	14,293	424,747	748,754	-	-	0	0	-	1,535,658	2,671,487	1.74
1994	-	0	0	-	-	4,898	497,096	745,786	1,607	0	16,689	715,250	367,018	2,656	-	0	0	-	990,810	2,351,000	2.37
1995	-	-	-	268	-	8,512	2,373,542	3,074,289	67,471	-	480	114,668	167,592	3,283	-	0	243	-	1,111,140	5,810,346	5.23
1996	-	-	-	-	-	1,324	334,193	5,453,703	105,202	0	-	48,123	370,295	2,617	-	851	0	135	1,078,098	6,316,443	5.86
1997	-	-	1,260	-	-	-	94,944	878,522	14,909	-	6,804	803,235	1,554,577	2,112	0	4,247	0	-	1,025,664	3,360,610	3.28
1998	-	-	-	-	-	1,008	583,437	1,895,432	17,590	-	1,476	538,146	727,396	0	-	0	0	-	1,202,172	3,764,484	3.13
1999	-	243	-	-	-	-	693,625	1,357,184	14,515	-	7,508	688,479	899,604	1,108	-	0	1,108	-	1,625,364	3,663,375	2.25
2000	-	-	301	-	-	2,952	1,175,274	6,650,001	93,073	-	0	439,966	539,376	0	-	2,055	0	-	1,375,488	8,902,997	6.47
2001	-	-	331	1,492	-	-	475,095	3,425,105	55,151	3,169	10,531	478,834	901,823	0	-	0	0	-	1,830,360	5,351,531	2.92
2002	-	-	0	-	-	48,389	1,691,664	4,136,648	87,654	-	1,843	278,282	209,666	20,557	-	0	-	-	1,263,918	6,474,702	5.12
2003	-	-	-	0	-	8,998	4,066,808	7,723,581	256,748	-	0	243,366	537,622	4,967	-	1,600	-	-	1,831,170	12,843,690	7.01
2004	-	-	0	-	-	-	941,940	1,416,406	15,928	-	3,328	913,012	654,532	1,381	-	0	0	-	1,939,674	3,946,527	2.03
2005	-	-	-	0	-	36,689	1,231,247	2,213,378	23,298	-	10,562	744,102	859,728	3,944	-	0	2,560	-	2,744,622	5,125,508	1.87
2006	-	-	0	0	-	50,379	1,601,297	1,758,457	32,828	0	18,811	668,709	486,457	1,777	-	25	22	-	1,953,228	4,618,763	2.36
2007	-	-	0	0	-	17,531	1,760,600	1,496,502	30,446	-	14,250	613,820	477,552	26	-	0	0	NA	2,945,304	NA	NA
2008	-	-	25	0	-	22,966	564,127	1,505,351	8,784	NA	13,097	352,555	681,281	NA	-	0	NA	NA	2,472,690	NA	NA
2009	-	-	-	-	NA	5,422	455,151	950,565	NA	NA	6,497	420,988	NA	NA	-	NA	NA	NA	1,169,466	NA	NA
2010	-	-	26	NA	NA	99,957	3,733,825	NA	NA	NA	37,330	NA	NA	NA	NA	NA	NA	NA	1,463,928	NA	NA
2011	-	-	NA	NA	NA	81,485	NA	NA	NA	NA	NA	NA	NA	NA	NA	NA	NA	NA	1,177,074	NA	NA
2012	-	NA	NA	NA	NA	NA	NA	NA	NA	NA	NA	NA	NA	NA	NA	NA	NA	NA	900,312	NA	NA
2013	NA	NA	NA	NA	NA	NA	NA	NA	NA	NA	NA	NA	NA	NA	NA	NA	NA	NA	938,160	NA	NA
2014	NA	NA	NA	NA	NA	NA	NA	NA	NA	NA	NA	NA	NA	NA	NA	NA	NA	NA	1,474,428	NA	NA

Table 3.7 Egegik River brood table.

Brood Year	0.1	0.2	0.3	0.4	0.5	1.1	1.2	1.3	1.4	1.5	2.1	2.2	2.3	2.4	3.1	3.2	3.3	3.4	Escapement	Recruits	R/S
1955	NA	NA	NA	NA	NA	NA	NA	NA	NA	NA	NA	NA	NA	NA	NA	NA	NA	-	NA	NA	NA
1956	NA	NA	NA	NA	NA	NA	NA	NA	NA	-	NA	NA	NA	-	NA	NA	15,612	-	NA	NA	NA
1957	NA	NA	NA	NA	-	NA	NA	NA	-	-	NA	NA	706,516	-	NA	89,606	77,749	-	NA	NA	NA
1958	NA	NA	NA	-	-	NA	NA	62,982	88	-	NA	1,064,196	290,239	-	-	28,637	1,946	-	NA	NA	NA
1959	NA	NA	-	-	-	NA	50,461	155,085	782	-	2,487	1,246,563	635,809	130	-	10,515	20,304	-	NA	NA	NA
1960	NA	-	-	-	-	-	213,842	340,500	0	-	397	4,134,128	2,347,789	-	-	43,857	38,324	-	NA	NA	NA
1961	-	0	0	-	-	-	47,269	104,164	0	-	0	383,656	916,276	0	-	27,632	8,496	-	NA	NA	NA
1962	-	-	0	-	-	0	3,547	19,755	0	-	405	716,891	309,637	-	-	27,596	15,425	-	NA	NA	NA
1963	-	-	1,025	-	-	-	2,667	85,597	0	-	2,264	513,647	298,367	-	-	82,831	7,475	-	997,602	993,872	1.00
1964	-	-	0	-	-	229	61,058	36,450	-	-	5,946	1,534,887	222,304	-	-	72,732	4,276	-	849,576	1,937,882	2.28
1965	-	-	-	-	-	0	24,284	10,867	1,594	-	24,472	1,485,854	811,266	1,013	-	6,338	22,797	-	1,444,608	2,388,485	1.65
1966	-	0	177	0	-	-	145,854	550,528	1,040	-	105	563,055	781,194	-	-	9,642	6,675	-	804,246	2,058,271	2.56
1967	-	-	1,901	0	-	-	56,673	188,696	0	-	470	748,745	630,902	1,833	-	669	1,542	-	636,864	1,631,431	2.56
1968	-	0	1,006	-	-	-	20,399	46,666	0	-	-	90,534	200,828	8,546	-	0	9,076	-	338,654	377,056	1.11
1969	-	-	0	-	-	0	8,738	103,338	-	-	3,358	1,090,569	1,178,715	0	-	371,010	0	-	1,015,554	2,755,728	2.71
1970	-	-	-	-	-	0	106,127	81,045	-	-	0	565,760	0	-	-	415,534	34,119	-	919,734	1,202,584	1.31
1971	-	-	-	-	-	0	21,238	0	-	-	3,282	1,289,361	1,266,965	0	-	55,646	64,037	147	634,014	2,700,676	4.26
1972	-	-	0	-	-	0	0	72,018	186	-	0	1,532,500	1,234,294	-	-	56,930	13,973	-	546,402	2,909,902	5.33
1973	-	0	0	0	-	-	35,038	75,611	0	-	438	585,165	724,246	-	-	23,869	7,319	-	328,842	1,451,686	4.41
1974	-	1,443	0	-	-	-	49,638	88,787	0	-	12,430	1,666,319	561,290	-	-	58,939	2,462	-	1,275,630	2,441,308	1.91
1975	-	-	-	-	-	-	55,085	151,116	-	-	7,279	2,234,183	580,804	1,090	0	8,921	1,690	-	1,173,840	3,040,169	2.59
1976	-	148	0	-	-	0	381,107	452,344	586	-	53,443	2,772,401	820,445	0	-	-	0	-	509,160	4,480,475	8.80
1977	-	0	0	-	-	2,322	823,006	1,935,491	11,696	-	1,846	628,139	698,975	-	-	58,420	7,714	-	692,514	4,167,610	6.02
1978	-	-	0	-	-	-	387,998	422,635	860	-	6,741	6,590,350	2,484,585	0	-	13,141	8,594	-	895,698	9,914,904	11.07
1979	-	-	0	6,465	-	2,849	657,110	219,731	0	-	2,251	1,973,576	1,176,405	1,571	-	0	-	-	1,032,042	4,039,957	3.91
1980	-	-	23,353	-	-	4,870	706,929	2,450,675	4,963	-	22,072	4,057,646	948,962	0	364	4,766	-	-	1,060,860	8,224,600	7.75
1981	-	-	0	-	-	-	593,701	432,117	3,248	-	45,162	2,884,091	1,471,877	0	-	6,296	7,620	-	694,680	5,444,111	7.84
1982	-	-	897	0	-	1,760	1,215,776	1,931,668	6,506	0	11,571	1,691,663	1,558,433	0	-	22,309	1,032	-	1,034,628	6,441,614	6.23
1983	-	-	0	3	-	2,415	1,282,101	2,555,258	6,403	-	7,320	3,488,493	3,448,747	16,762	-	13,745	8,377	-	792,282	10,829,622	13.67
1984	-	0	1,314	0	-	484	398,897	639,629	5,628	-	85,897	5,260,591	5,138,764	8,683	1,922	213,884	37,133	-	1,165,345	11,792,825	10.12
1985	0	437	144	-	-	437	427,083	783,057	2,772	-	34,431	4,033,588	1,104,000	0	-	4,127	10,934	-	1,095,192	6,401,009	5.84
1986	-	0	2,040	0	-	1,429	2,423,619	3,251,084	68,379	-	10,940	4,069,668	4,211,869	56,104	-	95,138	39,003	-	1,152,180	14,229,272	12.35
1987	-	1,256	2,372	0	-	0	700,407	4,226,110	134,575	-	69,644	8,875,890	11,467,511	44,152	5,644	154,958	66,152	-	1,273,553	25,748,671	20.22
1988	-	0	2,320	-	-	1,182	296,386	1,050,429	5,754	-	106,453	11,128,647	6,468,032	3,865	-	258,258	162,944	-	1,612,745	19,484,271	12.08
1989	-	0	0	0	-	-	199,358	251,553	4,117	-	37,847	5,203,932	4,249,920	436	2,168	190,062	28,421	-	1,611,566	10,167,814	6.31
1990	-	-	0	0	-	0	396,193	730,898	5,087	-	74,425	8,837,133	5,984,620	32,458	3,001	13,136	19,351	-	2,191,582	16,096,303	7.34
1991	-	4,455	742	312	-	1,478	1,212,942	2,876,328	25,216	-	19,243	3,225,540	2,574,044	136	-	9,063	7,970	-	2,786,925	9,957,467	3.57
1992	973	1,242	10,947	1,620	-	65	240,059	531,833	2,780	-	39,134	4,580,933	3,194,004	9,436	2,399	38,979	19,352	-	1,945,632	8,673,758	4.46
1993	-	-	0	-	-	0	117,645	329,685	1	-	30,559	801,758	654,747	-	-	1,218	3,878	-	1,517,000	1,939,491	1.28
1994	-	131	0	-	-	7,738	249,901	494,915	2	0	67,695	3,817,731	3,301,571	21,873	-	26,840	7,829	-	1,897,977	7,996,226	4.21
1995	-	-	-	0	-	3,568	1,500,682	2,697,814	18,705	-	3,072	1,728,403	1,540,145	13,866	-	11,318	14,791	-	1,266,692	7,532,365	5.95
1996	-	-	-	-	-	367	412,770	1,386,030	21,928	0	3,505	542,746	1,749,105	3,087	2,450	30,409	9,140	0	1,076,460	4,161,538	3.87
1997	-	-	1	-	-	-	17,156	177,699	12	-	18,771	3,493,279	2,069,036	2,144	9,876	233,787	40,681	-	1,104,004	6,062,442	5.49
1998	-	-	-	-	-	1	20,244	75,987	2	-	12,649	490,651	654,417	954	89	15,146	56	-	1,110,938	1,270,197	1.14
1999	-	0	-	-	-	-	162,160	396,161	205	-	171,815	9,216,012	3,036,121	2,298	-	18,606	10,957	-	1,728,397	13,014,334	7.53
2000	-	-	0	-	-	542	1,303,938	2,432,023	32,474	-	25,313	3,547,120	4,601,497	22,681	-	18,938	8,209	-	1,032,138	11,992,735	11.62
2001	-	-	0	1,677	-	-	292,693	811,140	24	0	47,730	1,592,534	2,157,264	0	-	953	518	-	968,872	4,904,532	5.06
2002	-	-	246	-	-	27,683	1,474,478	2,376,879	3	-	45,941	1,137,703	526,236	333	-	547	-	-	1,036,092	5,590,048	5.40
2003	-	-	-	0	-	19,116	2,102,688	2,616,815	28,087	-	41,425	1,921,231	2,368,749	5,182	-	5,013	2,019	-	1,152,120	9,110,326	7.91
2004	-	-	0	-	-	23,592	2,783,108	3,847,253	0	-	39,793	6,212,797	1,761,770	359	2,255	26,572	7,358	-	1,290,144	14,704,858	11.40
2005	-	-	-	0	-	4,342	505,400	214,446	77	-	36,681	2,862,199	2,471,900	6,203	739	32,837	12,651	-	1,621,734	6,147,475	3.79
2006	-	-	0	0	-	7,767	153,695	256,668	1,869	0	121,107	1,604,779	1,364,367	0	318	29,895	9,955	-	1,465,158	3,550,421	2.42
2007	-	-	0	0	-	8,763	56,843	435,468	55	-	71,973	3,367,158	2,475,172	7,794	2,174	16,867	19,308	NA	1,432,500	NA	NA
2008	-	-	1,018	0	-	318	630,729	1,166,220	1,527	NA	58,246	1,203,460	1,263,315	NA	1,239	1,504	NA	NA	1,259,568	NA	NA
2009	-	-	-	-	NA	5,484	327,784	707,838	NA	NA	94,595	4,540,417	NA	NA	7,772	NA	NA	NA	1,146,276	NA	NA
2010	-	-	1,135	NA	NA	7,912	939,009	NA	NA	NA	267,897	NA	NA	NA	NA	NA	NA	NA	927,054	NA	NA
2011	-	9,259	NA	NA	NA	35,696	NA	NA	NA	NA	NA	NA	NA	NA	NA	NA	NA	NA	961,200	NA	NA
2012	-	NA	NA	NA	NA	NA	NA	NA	NA	NA	NA	NA	NA	NA	NA	NA	NA	NA	1,233,900	NA	NA
2013	NA	NA	NA	NA	NA	NA	NA	NA	NA	NA	NA	NA	NA	NA	NA	NA	NA	NA	1,113,630	NA	NA
2014	NA	NA	NA	NA	NA	NA	NA	NA	NA	NA	NA	NA	NA	NA	NA	NA	NA	NA	1,382,466	NA	NA

Table 3.8 Ugashik River brood table.

Brood Year	0.1	0.2	0.3	0.4	0.5	1.1	1.2	1.3	1.4	1.5	2.1	2.2	2.3	2.4	3.1	3.2	3.3	3.4	Escapement	Recruits	R/S
1955	NA	NA	NA	NA	NA	NA	NA	NA	NA	NA	NA	NA	NA	NA	NA	NA	-	NA	NA	NA	
1956	NA	NA	NA	NA	NA	NA	NA	NA	-	NA	NA	NA	-	NA	NA	0	-	NA	NA	NA	
1957	NA	NA	NA	NA	-	NA	NA	NA	997	-	NA	NA	40,843	-	NA	0	0	-	NA	NA	NA	
1958	NA	NA	NA	-	-	NA	NA	165,552	-	-	NA	440,004	53,021	-	-	0	0	-	NA	NA	NA	
1959	NA	NA	-	-	-	NA	27,692	60,777	649	-	3,694	248,741	152,271	0	-	0	3,087	-	NA	NA	NA	
1960	NA	-	-	-	-	867	937,286	391,312	962	-	5,926	1,997,877	531,780	-	-	1,452	0	-	NA	NA	NA	
1961	-	0	10,770	-	-	68	329,872	484,229	1,166	-	1,262	273,290	119,789	266	-	0	43	-	NA	NA	NA	
1962	-	-	699	-	-	241	77,487	149,928	79	-	754	158,144	20,233	-	-	0	0	-	NA	NA	NA	
1963	-	-	0	-	-	-	10,884	21,608	2,126	-	49	77,497	20,578	-	-	0	0	-	388,254	132,741	0.34
1964	-	-	102	-	-	134	18,938	8,226	-	-	10,590	220,163	16,285	-	-	0	294	-	472,770	274,733	0.58
1965	-	-	-	-	-	0	47,512	51,187	549	-	2,815	212,640	76,458	0	-	1,794	0	-	996,612	392,954	0.39
1966	-	373	407	117	-	101	772,416	1,554,969	228	-	-	42,250	17,326	-	-	0	0	-	704,436	2,388,187	3.39
1967	-	-	0	0	-	-	98,166	54,844	0	-	0	42,254	34,932	114	-	42	-	-	238,830	230,351	0.96
1968	-	0	0	-	-	-	16,985	10,063	0	-	-	13,508	4,394	138	-	0	0	-	70,896	45,088	0.64
1969	-	-	0	-	-	111	4,548	5,661	-	-	319	52,668	24,458	0	-	1,479	0	-	160,380	89,243	0.56
1970	-	-	-	-	-	0	3,709	2,799	-	-	206	303,316	0	-	-	44,928	751	-	735,024	355,709	0.48
1971	-	-	-	-	-	0	193,376	0	-	-	-	573,773	165,880	1,723	-	85	966	-	529,752	935,802	1.77
1972	-	-	0	-	-	0	0	87,271	0	-	0	145,198	39,458	-	-	1,744	2,499	-	79,428	276,170	3.48
1973	-	0	4,467	0	-	-	26,045	6,764	322	-	-	21,377	37,294	-	-	6,039	0	-	38,988	102,308	2.62
1974	-	0	0	-	-	-	9,986	8,385	0	-	14,010	660,052	65,474	-	-	0	0	-	61,854	757,907	12.25
1975	-	-	-	-	-	1,088	1,565,299	578,240	-	-	5,169	1,608,268	365,466	790	0	1,513	-	-	429,336	4,125,834	9.61
1976	-	1,672	0	-	-	0	2,328,527	1,705,028	8,660	-	61,272	1,352,579	341,624	0	-	-	1,667	-	356,308	5,801,029	16.28
1977	-	0	11,008	-	-	792	642,643	1,822,598	5,813	-	-	230,133	138,885	1,279	-	0	0	-	201,520	2,853,151	14.16
1978	-	-	7,170	-	-	-	245,524	336,577	4,513	-	3,163	343,912	253,589	0	-	0	0	-	82,435	1,194,448	14.49
1979	-	-	0	0	-	22,988	3,310,049	786,900	23,149	-	10,427	1,672,861	649,600	4,903	-	0	-	-	1,706,904	6,480,877	3.80
1980	-	-	5,236	-	-	1,117	1,405,682	2,168,620	14,429	-	35,830	3,340,378	1,090,174	1,322	-	118	-	-	3,335,284	8,062,907	2.42
1981	-	241	4,923	-	-	862	1,742,848	3,026,316	3,536	-	6,623	2,261,027	928,975	840	-	176	0	-	1,327,699	7,976,367	6.01
1982	-	-	4,886	1,156	-	4,612	325,144	680,769	8,558	0	266	543,063	788,766	2,660	-	0	0	-	1,185,551	2,359,880	1.99
1983	-	-	11,993	728	-	0	733,445	252,188	2,966	-	3,616	562,322	221,150	0	-	683	0	-	1,001,364	1,789,090	1.79
1984	-	1,456	9,752	0	-	74	479,070	605,045	12,416	-	50,449	3,868,234	500,562	0	0	0	2,285	-	1,270,318	5,529,343	4.35
1985	271	1,890	8,788	-	-	446	646,672	807,662	2,117	-	1,021	878,033	470,692	5,839	-	0	0	-	1,006,407	2,823,431	2.81
1986	-	5,097	48,360	47	-	555	459,133	2,678,224	77,767	-	791	1,927,760	1,925,184	17,548	-	1,780	0	-	1,015,582	7,142,245	7.03
1987	-	5,013	7,801	0	-	97	856,287	1,811,272	13,745	-	11,200	1,998,161	2,421,039	39,037	-	0	441	-	686,894	7,164,093	10.43
1988	-	569	7,709	-	-	1,792	470,674	795,859	19,276	-	33,262	2,017,127	2,182,730	1,267	-	6,050	8,074	-	654,412	5,544,390	8.47
1989	-	3,611	8,149	0	-	5,841	928,095	407,094	10,738	-	13,860	2,510,021	1,024,234	872	-	0	0	-	1,713,287	4,912,515	2.87
1990	-	-	10,683	1,407	-	973	374,148	787,736	2,495	-	12,544	2,004,254	662,351	1,553	-	0	0	-	749,478	3,858,144	5.15
1991	-	443	264	0	-	6,839	2,062,760	3,857,895	19,160	-	420	452,463	276,451	3,835	-	0	0	-	2,482,016	6,680,530	2.69
1992	-	4,730	59,369	1,048	-	6,373	322,814	839,634	691	-	9,210	935,931	940,403	27,504	-	0	1,345	-	2,194,927	3,149,052	1.43
1993	-	1,082	2,503	-	-	1,969	408,154	391,193	29,347	-	5,034	273,268	244,609	-	-	0	417	-	1,413,454	1,357,576	0.96
1994	-	0	1,013	-	-	19,401	260,810	521,884	8,351	97	7,829	596,037	168,483	2,368	-	0	96	-	1,095,068	1,586,369	1.45
1995	-	2,857	-	0	-	10,259	3,802,898	1,732,446	31,441	-	0	130,252	63,083	784	-	0	0	-	1,321,108	5,774,021	4.37
1996	-	-	-	-	-	-	260,720	1,052,662	1,086	140	-	31,822	9,139	346	-	1	0	0	692,167	1,355,916	1.96
1997	-	-	1	-	-	-	283,854	648,117	11,954	-	2,867	1,657,938	419,619	2,117	0	5	0	-	656,641	3,026,473	4.61
1998	-	-	-	-	-	1,238	179,230	303,091	4,403	-	21	524,932	235,098	0	-	465	0	-	924,853	1,248,478	1.35
1999	-	0	-	-	-	3,671	1,255,334	908,027	4,849	-	24,648	1,185,693	289,650	3,134	-	0	1	-	1,662,042	3,675,007	2.21
2000	-	-	0	-	-	2,249	1,866,458	2,344,874	25,678	-	397	44,468	76,025	0	-	2	0	-	638,420	4,360,152	6.83
2001	-	-	0	419	-	629	399,404	1,426,191	53,711	335	2,010	131,676	118,875	373	-	0	0	-	866,368	2,133,622	2.46
2002	-	-	7,592	-	-	7,745	2,070,087	2,123,295	9,790	-	242	257,067	24,481	0	-	13	-	-	905,584	4,500,313	4.97
2003	-	17,191	-	559	-	10,960	4,843,226	1,397,088	11,712	-	0	37,722	51,471	0	-	0	-	-	790,202	6,369,928	8.06
2004	-	-	483	-	-	12,621	1,250,399	1,461,936	2,888	-	374	1,171,779	359,826	0	-	0	0	-	815,104	4,260,305	5.23
2005	-	-	-	927	-	664	839,102	2,295,455	6,203	-	1,960	1,168,235	930,654	2,703	-	1,476	0	-	799,612	5,247,378	6.56
2006	-	-	2,976	356	-	67,054	1,059,585	1,081,722	7,464	0	21,803	957,471	223,880	0	-	0	0	-	1,003,158	3,422,310	3.41
2007	-	-	0	0	-	41,832	1,274,071	931,275	3,133	-	13,582	699,628	175,698	0	-	0	0	NA	2,599,186	NA	NA
2008	-	-	2,826	1,329	-	7,971	1,047,919	1,610,686	2,380	NA	1,654	306,234	71,645	NA	-	0	NA	NA	596,332	NA	NA
2009	-	-	-	-	NA	8,820	349,269	413,774	NA	NA	2,264	535,038	NA	NA	-	NA	NA	NA	1,364,338	NA	NA
2010	-	-	1,320	NA	NA	11,268	840,238	NA	NA	NA	7,449	NA	NA	NA	NA	NA	NA	NA	830,886	NA	NA
2011	-	1,198	NA	NA	NA	67,614	NA	NA	NA	NA	NA	NA	NA	NA	NA	NA	NA	NA	1,029,853	NA	NA
2012	-	NA	NA	NA	NA	NA	NA	NA	NA	NA	NA	NA	NA	NA	NA	NA	NA	NA	695,018	NA	NA
2013	NA	NA	NA	NA	NA	NA	NA	NA	NA	NA	NA	NA	NA	NA	NA	NA	NA	NA	898,110	NA	NA
2014	NA	NA	NA	NA	NA	NA	NA	NA	NA	NA	NA	NA	NA	NA	NA	NA	NA	NA	640,158	NA	NA

Chapter 4

A Statistical Life Cycle Model for Central Valley Chinook Salmon: A Simulation Study

Abstract

The utility of life cycle models in addressing questions regarding the impacts of natural and anthropogenic factors on the survival of Pacific salmon (*Oncorhynchus spp.*) and the potential outcomes of management actions are becoming widely accepted. Recent reviews of federal biological opinions of water management strategies in California's Central Valley, have suggested that life cycle models are a necessary part of future policy decisions for Chinook salmon, *O. tshawytscha*. Among the types of life cycle models, estimation models provide significant benefits over mechanistic models, given their ability to estimate important demographic parameters and functional relationships between survival for species of concern and the environment, rather than specifying these relationships based on information from other systems or laboratory studies. In this chapter I describe a stage-structured life cycle estimation model for Chinook salmon in the Central Valley, which is applicable to multiple populations within this system and capable of estimating the effect of competitive interactions among populations. In addition, results of a simulation study used to test the efficacy of the estimation

model presented, detailing the level of bias and precision in model estimates under different levels of observation uncertainty and when alternative parameters are estimated.

Introduction

Chinook salmon (*Oncorhynchus tshawytscha*) in California's Central Valley have exhibited significant variability in realized survival and severe declines in abundance in recent years, leading to the complete extirpation of some populations (Gustafson et al. 2007), and extreme management actions including the complete closure of commercial and sport fisheries in recent years. Despite the need to understand the environmental and anthropogenic factors affecting variation in survival and resultant abundance over time for Chinook in the region, the causes for observed declines are not clear and quantitative tools are needed for evaluating the causal factors. A wide range of approaches have been used to assess the freshwater and marine processes affecting the survival and population dynamics of Central Valley salmonids. Kope and Botsford (1990) analyzed correlations between environmental and anthropogenic covariates and recruitment dynamics of Central Valley Chinook populations, to identify significant factors that are linked to variation in productivity in both the freshwater and marine portions of the lifecycle. Zeug et al. (2011) analyzed the effect of habitat loss, barriers to migration, and multivariate flow regime descriptors on the probability of extirpation for Central Valley Chinook, using logistic regression models. In addition, several studies have utilized data from paired releases of juvenile Chinook to evaluate the influence environmental covariates, using quasi-likelihood (Newman and Rice 2002) and Bayesian hierarchical (Newman and Brandes 2010) models. Acoustic telemetry data for juvenile Central Valley Chinook have been utilized to evaluate differences in survival and travel time as a function of tidal, water routing measures, and the abundance of predators before and after removals (Cavallo et al. 2012). Telemetry data have also been utilized effectively to inform mark-recapture models that estimate survival probabilities for juvenile

Chinook in the system as a function of water routing and fish movement patterns (Perry et al. 2010), and the influence of environmental covariates on reach-specific survival (Michel 2010).

While these studies provide valuable insights into the drivers of realized survival for Central Valley Chinook populations, many relate only to a single life stage or habitat type, or do not account for the full range of potential survival influences throughout the Chinook life cycle (Zeug et al. 2012). Complete life-cycle models, describing trends in survival and abundance as a function of environmental factors experienced throughout marine and freshwater portions of the life cycle are required to evaluate the effect of potential stressors at multiple stages, and identify population bottlenecks. Resource managers and the scientific community alike are increasingly turning to life-cycle models as a means for evaluating potential responses by salmon populations to management actions (Ruckelshaus et al. 2002). Furthermore, several recent discussions in the scientific and legal communities have pointed to life-cycle models as necessary tool for addressing concerns over future sustainability of salmonid populations and understanding the impact of management actions. Reviewing salmonid recovery efforts on the West Coast, Good et al. (2005) recommended the use of life-cycle models in addressing recovery potential of federally listed salmon and steelhead stocks. In addition, in 2009 the National Marine Fisheries Service provided a Biological Opinion (NMFS 2009) on the Operations and Criteria Plan (OCAP) for the Central Valley Project and State Water Project that outlined water export and use strategies for the Sacramento – San Joaquin Delta for these two water user groups. In the NMFS (2009) report, the potential impacts of export and management strategies were reviewed with respect to their impacts on Endangered Species Act listed Sacramento River winter-run Chinook and Central Valley spring-run Chinook, among other species. Reviews of the NMFS (2009) biological opinion by the National Research Council (NRC 2010) and CALFED (Anderson et al.

2009), both suggested increased use of life-cycle modeling to direct future biological opinions on the execution of Central Valley water management. More recently, court decisions have questioned the validity of actions taken as a result of the NMFS (2009) biological opinion, citing the lack of complete life-cycle modeling.

Life-cycle models track individuals or groups of organisms through spatially or temporally explicit stages, and describe survival through these stages as functions of habitat or demographic factors over time. Typically this type of model is utilized to understand how populations will respond to changes in the environment they experience at different points in life cycle, elucidate population bottlenecks and areas of density-dependent compensation, or weight the impact of alternative management actions. Life-cycle models generally fall into two categories, mechanistic models and statistical models. Mechanistic models utilized data from laboratory or field experiments, other systems, literature on the species of interest, or best professional judgment, to specify the functional relationship between environmental factors and survival. Mechanistic life-cycle models have been used effectively for evaluating the population dynamics of salmonids in many areas along the West Coast. The Interactive Object-oriented Salmon Simulation (IOS) model was utilized to evaluate the relative impact of alternative water flow, temperature and water export scenarios on Sacramento River winter-run Chinook (Cavallo et al. 2011, Zeug et al. 2012). Tracking the survival of daily cohorts of Chinook down the Sacramento River and into the marine environment, IOS relies on generalized additive models linking stage-specific survival to environmental factors, fit to data from laboratory experiments (Beacham and Murray 1989, Murray and McPhail 1988) and in-river survival estimates (Michel 2010, Zeug et al. 2012). The Shiraz model was designed to evaluate anthropogenic and habitat effects on production of Chinook in the Snohomish River basin of Puget Sound, Washington

(Scheuerell et al. 2006). Shiraz represents stage-specific survival as a series of Beverton-Holt mortality functions, which are influenced by the abundance of conspecifics and linked to environmental covariates through specified functional relationships (Scheuerell et al. 2006). Shiraz-type models employing the same mechanistic structure have also been employed to evaluate the efficacy of spring-run Chinook habitat restoration alternatives in the Columbia River basin (Honea et al. 2009), and understand the potential impacts of Chinook habitat restoration alternatives for the Snohomish River basin in the fact of climate change (Battin et al. 2007). The SALMOD model (Bartholow et al. 2001) tracks cohorts of individuals through life stages, with user-specified responses to hydrologic scenarios, and employs a mechanistic structure similar to Shiraz but allowing for greater spatial and temporal complexity.

Statistical life-cycle models utilize time-series of abundance data to inform estimates of demographic parameters and relationships between stage-specific survival and environmental covariates. These statistical life-cycle models are fundamentally different from mechanistic models, because they attempt to estimate functional relationships between survival and environmental factors directly from the available data, rather than specifying these relationships *a priori* based upon values from literature, experiments, other systems, or expert opinion. Within the Central Valley, statistical life-cycle models have been used effectively to estimate magnitude and direction of effects on species of concern. Maunder et al. (2015) used a simple state-space population dynamics model to estimate factors impacting survival of longfin smelt (*Spirinchus thaleichthys*) in the San Francisco Bay-Delta. OBAN (Hendrix et al. in prep) is a Bayesian stage-structured estimation model that has been utilized to estimate the effects of various environmental covariates on the survival of endangered winter-run Chinook in the Sacramento River.

There are several principal benefits of statistical over mechanistic life cycle modeling approaches. First, absolute abundance, survival, or survey data are used to directly estimate demographic parameters and functional relationships linking stage-specific survival to environmental covariates. Second, estimation life-cycle models may be used as hypothesis testing frameworks, where the weight of evidence from the data are utilized to determine the most parsimonious set of explanatory covariates with the best predictive potential, information theoretic approaches or AICc criteria (Burnham and Anderson 2002). Third, estimation models can directly quantify the uncertainty in model parameters, which may be propagated forward when making predictions for future trends in survival and abundance under alternative environmental and water management scenarios. In a report detailing the findings of a working group evaluating existing life-cycle models for Central Valley Chinook, Rose et al. (2011) describe the important aspects of future life-cycle models utilized to NMFS biological opinions. Rose et al. (2011) concluded that life-cycle models for Central Valley Chinook must: (i) be designed to address a specific question rather than being general explorations of life history, (ii) balance complexity in model components and spatial and temporal structure with the suitability in addressing pertinent conservation questions, based upon the principle of model parsimony, (iii) move beyond modeling a single cohort or population, a shortcoming in previous life-cycle modeling exercises in the region, (iv) base stage structure on the specific geography of the system, rather than implementing generalized spatial boxes, (v) incorporate the dynamics of marine ecosystems, (vi) allow for density-dependence and permit understanding of how density-dependence propagates through the whole life cycle, and (vii) be transparent with respect to model assumptions, utilization of data, and methods for calibration and validation.

Based upon these recommendations, we have designed a flexible estimation model for Sacramento River Chinook populations capable of evaluating alternative hypotheses for natural and anthropogenic factors influencing survival throughout freshwater and marine portions of the Chinook life cycle. When fit to available juvenile and adult indices of abundance, the model estimates the direction and magnitude of influence from a range of environmental covariates, as well as demographic parameters describing stage-specific maximum survival rate and capacity. The estimation structure allows for multiple populations to be explicitly modeled with independent and combined responses to environmental covariates, and has the potential to estimate competitive interactions between co-migrating and co-rearing populations. Within the model structure it was necessary to explicitly allow for density-dependent compensation because Zabel et al. (2006) found density-dependence in the egg-to-smolt transition for Snake River spring and summer-run Chinook, and Weber and Fausch (2005) found that the growth of wild Sacramento River Chinook was adversely impacted by the presence of hatchery-produced fish.

While estimation life-cycle models have been created for species of concern in the Central Valley (see Maunder et al. (2015) and Hendrix et al. (in prep)), these previous analyses have not gone through an explicit process of model validation through simulation testing. Simulation testing is recognized within the stock assessment literature as a critical component of the development process for reliable estimation models, and is the key to understanding the accuracy, and potential biases in, parameter estimates. Simulation-estimation study designs have been used to evaluate whether natural mortality and spawner-recruit relationship parameters are reliably estimated given the level of information provided by differing catch histories (Magnusson and Hilborn 2007), as well as the impact of time-varying natural mortality on assessment model predictions (Johnson et al. 2014). Simulation-estimation studies have also

evaluated the effect of abundance and age composition data quality on parameter estimates (Chen et al. 2003), the importance of length composition data on integrated assessment model results (Wetzel and Punt 2011), and the influence of the quantity and quality of length and age composition data on assessment model predictions for parameters of interest across life histories (Ono et al. 2014). Given the need to fully explore the ability of our life-cycle model to reliably estimate parameters of interest, along with the level of uncertainty and potential level of bias in parameter estimates, we have created a simulation-testing framework comprised of: (i) an operating model that generates time-series of abundance data with lognormally distributed observation uncertainty in response to user-specified values for model parameters, and (ii) the stage-structured maximum likelihood estimation model.

This paper describes the structure of an estimation model for evaluating alternative hypotheses regarding the factors affecting survival of Sacramento River Chinook, and discusses its flexibility and potential application. In addition, results of simulation testing of the stage-structured estimation model are presented. The simulation study was designed to address four important questions regarding the estimation model:

(i) How does the level of observation uncertainty in data provided to the estimation model influence the bias and accuracy of predicted values for model parameters?

(ii) How well estimated are initial spawning abundances prior to the beginning of the abundance time series?

(iii) How well estimated is potential effect of competitive interactions between two populations?

(iv) How well estimated are stage-specific maximum survival rates and capacities for stages beyond the first model stage without abundance indices in addition to adult spawning abundance?

Methods

To test alternative hypotheses regarding the natural and anthropogenic drivers of survival throughout the life cycle of Sacramento River Chinook, a stage structured maximum likelihood estimation model was created. A Bayesian version of the model was also created for application to real Chinook data for the Sacramento River watershed, but will be presented in Chapter 5. In order to validate the estimation model, a simulation study was conducted where a simple operating model was used to generate time-series of abundance data with uncertainty, based upon user specified values for life-cycle model parameters. Five case studies were designed to test the bias and precision of estimation model predictions for specific parameters. The estimation model, operating model, and simulation study design are discussed below.

Estimation model

The population dynamics model tracks cohorts of Chinook from specific brood years forward in time across sequential model stages. Chinook abundance is represented by $N_{y,s,p}$ or the number of individuals from brood year y, surviving to stage s, of population p. The abundance of Chinook from brood year y and population p, surviving to the end of the current stage s, is dependent upon the year, stage, and population specific survival rate $SR_{y,s,p}$ in Equation 4.1.

(4.1) $$N_{y,s,p} = N_{y,s-1,p} * SR_{y,s,p}$$

Survival though the spatio-temporally explicit life stages is described by a Beverton-Holt transition function (Moussalli and Hilborn 1986). The Beverton-Holt equation, while traditionally used in the evaluation of spawner-recruit data (Beverton and Holt 1957), provides a useful approximation for survival of individuals from one model stage to the next, and has been used in a wide range of life-cycle models for Chinook (see Scheuerell et al. (2006), Honea et al. (2009), Battin et al. (2007), Hendrix et al. (in prep)). The year, population, and stage-specific survival rate ($SR_{y,p,s}$) is calculated as:

$$SR_{y,s,p} = \frac{p_{y,s,p}}{1 + \frac{p_{y,s,p} * \sum_{i=1}^{Npop} \alpha_{p,i,s} * N_{y,s-1,i}}{K_{y,s,p}}} \quad (4.2)$$

where $p_{y,s,p}$ is the productivity parameter and $K_{y,s,p}$ is the rearing capacity, of each stage (Figure 4.1).

In this formulation (Equation 4.2) the year, stage, and population-specific productivity parameter ($p_{y,s,p}$) represents the maximum survival rate in the absence of density-dependent compensation. Conversely, the year, stage, and population-specific capacity parameter ($K_{y,s,p}$) describes the total number of individuals that can potentially survive through the model stage. However, given evidence for competitive interactions between Chinook populations within the Sacramento watershed (Weber and Fausch 2005) equation 4.2 also includes an interaction effect ($\alpha_{p,i,s}$), which describes how many individuals of the focal population p are displaced with respect to the stage capacity ($K_{y,s,p}$) for each individual of another population i. In this way, no interaction effect amongst populations for a specific stage may be specified with a zero value for all elements of $\alpha_{p,i,s}$, except $\alpha_{p,i=p,s}$ the focal population. Positive, non-zero values indicate that the abundance of other populations (i) results in a reduction in overall rearing capacity for the

focal population (p), and therefore reduced survival at high abundance levels which approach the stage-specific capacity ($K_{y,s,p}$). Specifying $\alpha_{p,i,s}$ elements equal to one create a situation where capacity is shared across populations with symmetric impacts on capacity.

The productivity ($p_{y,s,p}$) capacity ($K_{y,s,p}$) parameters in the population dynamics model are time varying and assumed to change in response to inter-annual variation in the environmental covariates under evaluation. The productivity parameter for population p, of brood year y, in stage s is a function of the basal productivity $\beta_{s,p,0}$, or the average maximum survival rate for members of that population in the current stage across years, and the sum of environmental covariate c values at time t ($X_{t,c}$) multiplied by their respective coefficients ($\beta_{s,p,c}$), which describe the influence of each covariate on stage and population-specific productivity $p_{y,s,p}$ (Equation 4.3).

$$p_{y,s,p} = \frac{1}{1+\exp\left(-\beta_{s,p,0} - \sum_{c=1}^{Nc_{s,p}} \beta_{s,p,c} * X_{t,c}\right)} \quad (4.3)$$

$$t = y + \delta_c$$

In this equation δ_c is the covariate-specific temporal reference that describes the difference between the brood year y and the year in which the cohort will interact with that covariate. Within the model structure, δ_c is used as a pointer to ensure that the covariate value for the correct year is used when tracking each cohort forward in time. The variable $Nc_{s,p}$ is the number of productivity covariates linked to each population in each stage. The overall productivity parameter value ($p_{y,s,p}$) is a logit transformation of the additive effects of the basal productivity rate and covariate effects, which ensures that its value is smoothly scaled between 0 and 1 (Equation 4.3).

The capacity parameter for each population's brood year specific cohort in each stage ($K_{y,s,p}$) is likewise a function of a basal, or average, stage and population specific capacity across years ($\gamma_{s,p.0}$) and the additive effects of capacity-related covariates ($Y_{t,k}$) and the population-specific coefficients ($\gamma_{s,p.k}$) describing the magnitude and direction of influence each holds (Equation 4.4).

$$K_{y,s,p} = \exp\left(\gamma_{s,p,0} + \sum_{k=1}^{Nk_{s,p}} \gamma_{s,p,k} * Y_{t,k}\right) \quad (4.4)$$

$$t = y + \delta_k$$

The capacity parameter ($K_{y,s,p}$) is described in natural log space for ease of estimation and to ensure it is bounded within the set of positive values, where k is the covariate reference number and δ_k is the temporal reference for the offset from the brood year for each covariate, indicating when the population interacts with each specific covariate in the life cycle.

For populations of Chinook salmon occupying the same habitats and subject to the same environmental covariates, it may be reasonable to assume that a shared response in survival to a particular covariate has been exhibited historically. For this reason we have further allowed for a coefficient describing the effect of a particular covariate to be shared across populations. In this way several productivity ($\beta_{s,c}$) capacity ($\gamma_{s.k}$) coefficients may be common across a subset of populations. This reduces model complexity, increases parsimony, and improves the estimability of coefficients describing the effect of covariates for which a common survival response across populations is biologically defensible.

Predictions for survival $SR_{y,s,p}$ and resultant abundance $N_{y,s,p}$ of cohorts of Chinook are tracked forward in time across spatio-temporal model stages in the same manner (Equations 4.2, 4.3, 4.4) independent of whether the stage is in the freshwater or marine portion of the life cycle

and the ontogenetic status of individuals (Figure 4.1). However, for the final three model stages representing the 1st, 2nd, and 3rd years in the ocean, it is necessary to account for both the maturation process and marine harvest when tracking the number of individuals entering the next stage. Harvest mortality is assumed to occur after the annual mortality event, but prior to maturation. Catch by calendar year t, population, and stage ($C_{t,p,s}$) is the number of surviving individuals multiplied by the population specific harvest rate observed in each year ($hr_{t,p}$), scaled by the stage (i.e. ocean age) specific catchability coefficient (ε_s). Annual catch is calculated as:

$$
\begin{aligned}
& C_{t,p,s} = N_{y,s,p} * SR_{y,s,p} * \left(hr_{t,p} / \varepsilon_s\right) \\
& t = y + \rho_s \\
& \varepsilon_s = \{0,0,0,0,1.54,1.0\}
\end{aligned} \tag{4.5}
$$

where ρ_s is the temporal offset for model stages that indicates the difference between the brood year y and the calendar year t, and ensures that the proper annual harvest rate is referenced. Annual harvest rate estimates were obtained from the Pacific Fishery Management Council (PFMC).

For the three ocean stages, the number of individuals of a cohort moving to the next stage is governed by the survival rate ($SR_{y,s,p}$), annual catch estimate ($C_{t,p,s}$), and the maturation probability (ϕ_s).

$$
\begin{aligned}
& N_{y,s+1,p} = \left(N_{y,s,p} * SR_{y,s,p} - C_{t,p,s}\right) * \left(1 - \phi_s\right) \\
& \phi_s = \{0,0,0,0.1,0.942,1\} \\
& t = y + \rho_s
\end{aligned} \tag{4.6}
$$

While the cohort specific survival rate varies over time, the maturation probability (ϕ_s) is assumed to be temporally invariant. From equation 4.6 the number of individuals of a cohort advancing to the next ocean stage is the number in the previous stage ($N_{y,s,p}$) that have survived,

less the proportion that matures and begins homeward migration. The return abundance ($R_{y,s,p}$) is the number of individuals from a cohort that survived marine and harvest mortality, and have initiated the maturation process and migrate into freshwater to spawn (Equation 4.7).

$$R_{y,s,p} = \left(N_{y,s,p} * SR_{y,s,p} - C_{t,p,s}\right) * \phi_s \quad (4.7)$$

The predicted number of spawning adults of each population in each calendar year t ($\hat{A}_{t,p}$) is the sum of returning individuals ($R_{y,s,p}$) across stages or equivalently ocean age classes

$$\hat{A}_{t,p} = \sum_{s=1}^{Nstage} R_{y,s,p} \quad (4.8)$$
$$t = y + \rho_s$$

where ρ_s is again the temporal offset between the brood year y and calendar year t.

A principal goal in creation of this statistical life-cycle model was to include populations of both hatchery and wild origin in the Sacramento watershed. Depending on whether a wild-type or hatchery-type life history is assumed for each population the next cohort ($N_{y,s=1,p}$) is calculated based upon either the predicted number of spawning adults and an assumed fecundity value of 2000 eggs/individuals (Equation 4.9) or the recorded releases from hatchery facilities in calendar year t (Equation 4.10).

$$N_{y,s=1,p} = \hat{A}_{t=y,p} * fec \quad (4.9)$$

$$N_{y,s=1,p} = RH_{t=y,p} \quad (4.10)$$

To estimate the value for model parameters including basal productivities ($\beta_{s,p,0}$) and capacities ($\gamma_{s,p.0}$) for each population in each stage, and coefficients describing the direction and magnitude of influence each environmental covariate has on either productivity ($\beta_{s,p,c}$) or capacity ($\gamma_{s,p.k}$) for individual populations or shared amongst populations ($\beta_{s,c}$ and $\gamma_{s,k}$), the model is fit to available abundance data. We employ a likelihood-based approach to compare

abundance predictions with available data and estimate model parameter values (Hilborn and Mangel 1997). Predicted adult spawning abundances are calculated (Equation 4.8) as part of the population dynamics model. In addition the estimation model structure has the flexibility to also include juvenile indices of absolute abundance to inform parameter estimates. Predicted juvenile abundance collected at a particular site that generally coincides with the end of stage s are calculated as

$$\hat{J}_{t,j,s} = \sum_{j \in \{n_t\}} N_{y,s,p=j} \qquad t = y + \rho_s \tag{4.11}$$

where n_j is the set of populations for which juvenile abundance indices are available.

Model predicted adult spawning abundances are compared to empirical data, and model parameters are estimated by maximizing the likelihood of the model given the observed data,

$$L_A\left(\Theta \mid A_{t,p}\right) = \prod_{p=1}^{n_p} \prod_{t=1}^{n_t} \frac{1}{\hat{\sigma}_p \sqrt{2\pi}} \exp\left[-\frac{\left(\ln(A_{t,p}) - \ln(\hat{A}_{t,p})\right)^2}{2\hat{\sigma}_p^2} \right] \tag{4.12}$$

where $A_{t,p}$ and $\hat{A}_{t,p}$ are the observed and predicted adult spawning abundances and n_p and n_t and the number of populations and number of years of adult abundance data respectively. The likelihood of the model parameters, given the adult abundance data, assume that observation error of log transformed abundances are normally distributed, with the standard deviation of the observation error distribution ($\hat{\sigma}_p$) equal to the maximum likelihood estimate (Equation 4.13).

$$\hat{\sigma}_p = \sqrt{\sum_{t=1}^{n_t} \frac{\left(\ln(A_{t,p}) - \ln(\hat{A}_{t,p})\right)^2}{n_t}} \tag{4.13}$$

Under these same assumptions, the observation error likelihood of the model parameters Θ, given juvenile abundance data (Equation 4.11) are calculated as

(4.14) $$L_J\left(\Theta \mid J_{t,j,s}\right) = \prod_{j\in\{n_j\}}\prod_{t=1}^{n_{t,j}} \frac{1}{\hat{\omega}_j\sqrt{2\pi}} \exp\left[-\frac{\left(\ln(J_{t,j,s}) - \ln(\hat{J}_{t,j,s})\right)^2}{2\hat{\omega}_j^2}\right]$$

where $n_{t,j}$ is the set of of juvenile abundance indices, and $J_{t,j,s}$ and $\hat{J}_{t,j,s}$ are the observed and model-predicted juvenile abundance indices. The maximum likelihood estimate for the standard deviation of the normal observation error distribution is also used for the juvenile abundance data.

(4.15) $$\hat{\omega}_j = \sqrt{\sum_{t=1}^{n_{t,j}} \frac{\left(\ln(J_{t,j,s}) - \ln(\hat{J}_{t,j,s})\right)^2}{n_{t,j}}}$$

The total data likelihood is the sum of the negative log of the likelihood of the juvenile and adult abundance data.

(4.16) $$LL_T = -\ln\left(L_A\right) - \ln\left(L_J\right)$$

Model parameter values that minimized the total negative log likelihood (LL_T) were found using AD Model Builder (Fournier et al. 2012). AD Model Builder (ADMB) is a software platform allowing complex non-linear minimizations for models containing a large number of parameters while also permitting profile likelihoods or posterior distributions for parameters of interest to be estimated. ADMB was selected as the software design platform for this estimation model because of its flexibility, computational efficiency, and ability to reliably sample a complex multivariate likelihood surface. In addition to its benefits as a fast and stable optimization tool for fitting statistical models to data, ADMB also estimates uncertainty in and correlations between model parameters based on their derivative structure.

Operating model

The operating model is an integral component of this simulation study designed to test the efficacy of the estimation model with respect to potential bias and precision in predictions for specific parameters of interest. The operating model is mechanistic and stage-structured, and is used to generate input data for the estimation model, created with known parameter values. The operating model generates abundance data for two simulated Chinook populations over a hypothetical 1967 – 2010 time series. For simplicity we will refer to simulated populations as P1 and P2, although they could theoretically represent any of the Sacramento River Chinook populations. The operating model contains six model stages through which abundance and survival of each population is tracked, as a function of the time varying productivity and capacity parameters. The six simulated life stages are: (i) fry rearing in upstream sections of the Sacramento River tributaries, (ii) the Sacramento – San Joaquin Delta, (iii) the nearshore and estuary region extending from San Francisco Bay to the Gulf of Farallon, and three stages representing survival, harvest mortality, and maturation in the marine environment. Both the maturation schedule (ϕ_s) and age-specific scaling factor (ε_s) for fishing mortality are fixed and assumed time-invariant. Observed harvest rates for the 1967 – 2010 time period were utilized for consistency. Each of the populations was assumed to exhibit the wild-spawning life history, with associated fixed fecundity rate.

The basal productivity rate for the first model stage, representing average egg to smolt maximum survival rate, was fixed at -1 (logit transformed: 26.9% survival) for P1 and -3 (logit transformed: 4.7% survival) for P2 to provide contrast between the abundance time series. Basal productivities were fixed at 0 for the remaining life stage, equivalent to a 50% survival rate. The assumption of 50% survival in the Sacramento – San Joaquin Delta is consistent with estimates

by Perry et al. (2010) of 35 – 54% survival, and acoustic tracking estimates by Michel (2010) of 52.6% survival. Both P1 and P2 were assumed to be capacity limited in only the first stage of the life cycle, wherein a capacity of e^{15} or slightly more than 3 million individuals is imposed for each population separately. Capacities for subsequent stages were assumed high so as to impose no density-dependent compensation later in the life cycle.

Responses by the two populations in the operating model, to environmental covariates were specified through coefficients describing the population-specific effects on either the productivities or capacities for particular stages. The true time series of environmental covariate data were utilized to ensure a realistic level of contrast within the covariate time-series, as the level of contrast in model inputs can influence precision of model parameter estimates (Magnusson and Hilborn 2007). Population P1 was simulated with productivities influenced by four covariates, impacting survival in the upstream (1st), Sacramento – San Joaquin Delta (2nd), nearshore (3rd), and first marine (4th) stages. The productivity covariates for P1 are listed below, with the specified values of their coefficients in parenthesis:

i) **yolo.wood.peak.streamflow (+3):** water flow into the Yolo Bypass that provides valuable off-channel rearing habitat for juvenile Chinook (Sommer et al. 2001a, Sommer et al. 2001b).

ii) **fall.dayflow.export (-2):** the Dayflow data metric quantifying the total amount of water exported from the Sacramento – San Joaquin Delta, primarily by the Central Valley Project and Stage Water Project for agricultural and urban use (CDWR 2014).

iii) **upwelling.south.early (+1):** nearshore upwelling of nutrient-rich deep waters in the nearshore region south of San Francisco Bay, prior to the period when juvenile Chinook enter the ocean.

iv) **pdo.early (+2):** average of monthly Pacific Decadal Oscillation index (Hare and Mantua 2000, Mantua and Hare 2002) values January – March, during the first year in the ocean.

Population P1 was also simulated with a single covariate influencing rearing capacity in the second (Sacramento – San Joaquin Delta) life stage:

i) **keswick.discharge (+2):** January – March average discharge (cfs^{-1}) from Keswick Dam during juvenile rearing.

Covariate effects on productivity for P2 similarly encompasses the upstream, Sacramento – San Joaquin and nearshore life stages:

i) **freeport.sed.conc (-0.5):** average concentration of sediment measured between February – April of the year of outmigration, measured at Freeport, California by USGS.

ii) **fall.dayflow.expin (-2):** average ratio of delta exports to inflow during March – May of the juvenile outmigration year (CDWR 2014).

iii) **farallon.temp.late (-3):** average temperature of nearshore waters recorded at the Farallon Islands July – December of the outmigration year.

iv) **upwelling.south.early (+2.5):** nearshore upwelling of nutrient-rich deep waters in the nearshore region south of San Francisco Bay, prior to the period when juvenile Chinook enter the ocean.

One environmental covariate was also specified to influence capacity in the delta life stage for P2:

i) **fall.dayflow.yolo (+3):** average water flow out of the Yolo Bypass during February – April of the outmigration year (CDWR 2014).

Coefficients for all other covariate effects were set to zero for both populations, indicating no influence on either stage productivities or capacities.

Differing levels of lognormally distributed observation uncertainty were added to abundance trends generated by the operating model. In each of 100 replicate simulations an independent random deviate was introduced to the index of adult abundance

$$O_{t,p} = A_{t,p} * e^{\nu} \qquad (4.17)$$
$$\nu \sim N(0, \sigma_{\nu})$$

where $A_{t,p}$ is the adult spawning abundance in each year for each of the two populations generated by the operating model, $O_{t,p}$ is the observed abundance data with lognormally distributed observation uncertainty, and σ_{ν} is the standard deviation of the observation error distribution. Four representative levels of observation uncertainty were specified, with σ_{ν} equal to 0.1 (low observation uncertainty), 0.3, 0.5, and 0.8 (high observation uncertainty).

Simulation study cases

The simulation study to test the efficacy of the estimation model in discerning the parameter values specified to the operating model was conducted as four specific test cases. Each case represented a specific question to be addressed by the simulation study. For all cases, 100 replicate observed abundance trends were generated with randomly distributed observation

uncertainty, for each of the four levels of observation uncertainty (i.e. σ_v values). Parameter values not estimated were fixed at the true values specified to the operating model.

Case 1: What is the influence of the level of observation uncertainty on model estimates of coefficients and basal productivities and capacities?

In case 1, the influence of observation uncertainty on the ability of the estimation model to capture the true values of coefficients describing environmental covariate influences ($\beta_{s,p,c}$ $\gamma_{s,p,k}$), and basal productivities $\beta_{s=1,p,0}$ and capacities $\gamma_{s=1,p,0}$ for the first model stage. In addition, the efficacy of the maximum likelihood estimate for the standard deviation of the observation error distribution σ_v was compared to the true value specified to the operating model.

Case 2: Is the estimation model capable of estimating adult abundance in years prior to the start of abundance data?

In this case, the estimation model attempted to estimate the initial spawning abundances in 1967-1969, the years prior to when adult abundance data were provided to inform the estimation model. These years provide the initial spawning abundances which seed the first few years in the abundance time series and are therefore of importance, but are potentially poorly informed by the available data.

Case 3: Is the estimation model capable of estimating an interaction effect amongst populations?

Case 3 evaluated whether an interaction effect, representing the level of competition between co-rearing or co-migrating populations, may be estimated from the data when specified in the operating model. An interaction effect ($\alpha_{p,i,s}$, equation 4.2) indicates the asymmetric

reduction in stage-specific rearing capacity for population p imposed by each member of population i. Within the operating model data were simulated with a value of $\alpha_{p=1,i=2,s=1} = 2$, which indicates that within the life stage representing the upper Sacramento River and tributaries (1nd stage), each member of P2 displaces the potential rearing capacity of P1 by 2 individuals. The level of bias and precision in model estimates of alpha were evaluated at each of the four levels of observation uncertainty.

Case 4: Is the estimation model capable of estimating basal productivities and capacities for stages beyond the first stage without additional indices of abundance?

In the final case, the efficacy of the estimation model in estimating stage-specific productivities and capacities for later life stages was evaluated. The estimation model attempted to estimate basal productivity and capacity in the 2nd model stage representing the Sacramento – San Joaquin Delta, where capacity is unlikely to be limiting giving the specified value, and no additional indices of abundance beyond adult spawning abundance were provided. The effect of attempting to estimate the basal productivity $\beta_{s=2,p,0}$ and capacity $\gamma_{s=2,p,0}$ parameter on the estimability of other model parameters was evaluated at the four differing levels of observation uncertainty.

Results

The purpose of this chapter was twofold. First, to describe the design of a flexible stage-structured statistical life-cycle model for evaluating alternative hypotheses about the natural and anthropogenic drivers of survival for multiple populations of Sacramento River Chinook, which was capable of estimating the level of competition between co-rearing and co-migration Chinook populations at various life stages. Second, to conduct a simulation study to evaluate the efficacy

of the estimation model in correctly assessing the true values for demographic parameters. The simulation study utilized an operating model which tracked the abundance of two hypothetical Chinook populations through a series of life stages with user specified effects of environmental covariates on stage-specific Beverton-Holt survival and capacity parameters. By simulating data with known demographic parameters, introducing observation uncertainty into indices of adult abundance, and subsequently fitting the estimation model to these data, the level of potential bias and precision in parameter estimates was identified. Four alternative test cases were utilized to determine the estimability of specific parameters of interest, each at four levels of potential estimation uncertainty. For each test case, and each level of observation uncertainty, the estimation model was fit to 100 abundance time series generated with randomly distributed observation errors in each time step.

Case study 1 was designed as a base case to evaluate whether the estimation model was able to predict the true parameter values specified to the operating model across differing levels of observation uncertainty. The parameters directly estimated from the data included the coefficients describing the influence of environmental covariates on productivity $\beta_{s,p,c}$ and capacity $\gamma_{s,p,k}$ at various stages of the life cycle, the basal or average productivity (maximum survival rate) $\beta_{s=1,p,0}$ and capacity $\gamma_{s=1,p,0}$ in the first stage representing survival from egg to entry into the delta. Figure 4.2 displays the results from case 1 for P1, with the true values for parameters specified to the operating model as red lines, and estimation model predictions for these parameters across the 100 replicate simulations presented as boxplots. Results for the four alternative levels of introduced observation uncertainty are plotted in different colors, with the lowest level of observation uncertainty in red and the highest in purple (Figure 4.2). For P1, coefficients for productivity-linked covariates are reliably estimated without significant bias with

the exception of the coefficient describing the influence of upwelling.south.early under high observation uncertainty (Figure 4.2). The true value for the upwelling.south.early coefficient was 1.00, however the estimated value across simulations under the high observation uncertainty conditions was positively biased with a mean of 1.18 and standard deviation of 0.52, compared with means of 1.00, 1.02, and 1.02, when σ_v values of 0.1, 0.3, and 0.5 were assumed. Estimates of the covariate describing the effect of keswick.discharge on capacity in the first stage are unbiased independent of the level of observation uncertainty. With respect to estimates of basal capacity and productivity across simulations, no significant biases are observed in estimated values with the exception of simulations under high observation uncertainty. With high observation uncertainty ($\sigma_v = 0.8$), the model estimates of basal productivity demonstrated a slight positive bias with the average of parameter estimates -0.80 (0.48), relative to the true value of -1.00 specified to the operating model. Conversely, under high observation uncertainty model estimates of basal capacity in the first stage show an exceedingly small negative bias 14.94 (0.31), compared with the true value of 15.00. The maximum likelihood estimate for the standard deviation of the observation error distribution $\hat{\sigma}_p$ show a substantial negative bias, with estimates of 0.09 (0.01), 0.27 (0.04), 0.44 (0.06), and 0.73 (0.09) for the four levels of uncertainty respectively.

Despite the minimal bias in parameter estimates across different levels of observation uncertainty, there are significant differences in the precision of model estimates (Figure 4.2). For all estimated parameters, the level of precision decreases with increased observation uncertainty. Differences in the precision of parameter estimates across differing levels of observation uncertainty are parameter specific with the coefficient of variation for the parameter describing the effect of upwelling.south.early on productivity in the nearshore stage increases from 0.06 to

0.44 between the low and high observation uncertainty cases, and the cv of the parameter describing capacity in the first model stage increasing from 0.002 to 0.02. While the relative reduction in the precision of parameter estimates with increasing observation uncertainty depends largely upon the parameter, the pattern is consistent across parameters. The relative precision of parameter estimates measured as the cv across replicate simulations under high observation uncertainty is lowest for the parameter describing basal (average) productivity in the first model stage with cv = 0.60.

Results of simulation testing of the estimation model for P2 are similar in some respects to those for P1, with a reduction in estimated parameter precision with increased observation uncertainty (Figure 4.3). A positive bias was found in estimates of both the basal productivity and capacity parameters in the first stage and a negative bias in estimates of the coefficient describing the effect of upwelling.south.early on productivity in the nearshore stage, but only under high levels of observation uncertainty in both cases. Similar to results for P1, the maximum likelihood estimate for the standard deviation of the observation error distribution was negatively biased across all levels of observation uncertainty specified to the operating model. A consistent negative bias and low level of precision were observed for estimates of the coefficient describing the effect of fall.dayflow.yolo on capacity in the delta stage, across all levels of observation uncertainty. When the correlation amongst time series of environmental covariates was for P2 was evaluated (Figure 4.4), a relatively strong negative correlation between the fall.dayflow.yolo and fall.dayflow.expin covariates was found. This correlation in the covariate values across time is likely contributing to imprecision and bias in estimates of the coefficient describing the effect of fall.dayflow.yolo.

With the exception of the capacity linked covariate for P2, most model parameters are able to be estimated with suitable precision under low to moderate levels of observation uncertainty and with limited bias. However, significant reductions in the precision of parameter estimates should be expected at higher levels of observation uncertainty.

Case 2 evaluated the reliably of estimates for the spawning abundances 1967 – 1969 prior to the beginning of the abundance data time series was. Simulation-estimation results for P1 indicated that while the spawning abundance in 1967 was able to be estimated with only a small negative bias across all levels of observation uncertainty, estimates of spawning abundance in 1968 and 1969 were completely unreliable, with exceedingly large positive biases across all across all levels of observation uncertainty, and extremely large imprecision for all but the lowest levels of observation uncertainty (Figure 4.5). Case 2 results for P2 were similar, with high imprecision for initial spawning abundance estimates at all but the lowest level of observation uncertainty (Figure 4.6). For both P1 and P2, the inability to estimate initial spawning abundance parameters had little effect on the level of precision and bias for other estimated and derived parameters. The inability to estimates initial spawning abundances largely results from the fact that these parameters have little impact on the total likelihood, only influencing the first few spawning abundances after 1970 that are compared with data through the observation likelihood.

Case 3 focused on evaluating whether the magnitude of competition between the two simulated populations, manifest as reduced capacity P1, and can be reliably estimated. Results indicate that the true value interaction parameter $\alpha_{p,i,s} = 2.0$ can be estimated (Figure 4.7). Under the two lowest levels of observation uncertainty interaction parameter estimates were unbiased, however when the standard deviation of the observation error distribution was set as

0.5 and 0.8 estimates were positively biased, with mean estimates of 2.57 and 3.62 respectively across the 100 simulations. Precision of interaction parameter estimates decreased at higher levels of observation uncertainty, with CV's of 0.8 and 1.37 for the two highest levels. Bias and precision in estimates of coefficients describing environmental covariate effects on stage-specific survival rates was minimally altered by the inclusion of the interaction effect, however estimates of the basal productivity parameter for P1 in the first model stage became somewhat less precise at high levels of observation uncertainty in this case.

Case 4 evaluated the effect of attempting to estimate a basal (average) productivity and capacity for the delta stage in addition to the earlier upstream stage. Estimates of the basal productivity in the first stage became less precise and negatively biased for P1 under high levels of observation uncertainty, when basal productivity in the second stage was estimated (Figure 4.8). Interestingly, estimates of basal productivity for the second stage showed substantially higher precision than those for that of the first stage, but an associated positive bias. Observed levels of bias and imprecision in estimates of the basal productivity in both stages were significantly lower under low to moderate levels of observation uncertainty. Estimates of basal capacity for P1 in the second (delta) stage were hugely imprecise at all but the lowest level of observation uncertainty. Conversely, estimates of basal capacity in the first model stage showed only a slight positive bias and minimal increase in imprecision, even at the highest levels of observation uncertainty. Results indicated that estimates for coefficients describing the influence of environmental covariates on stage-specific productivities became less precise with the estimation of basal productivities and capacities for both stages, reductions in precision were substantially larger under the highest level of uncertainty and most substantial for covariates

linked to survival in stages before or during the delta (2nd) stage in for which the additional basal productivity and capacity parameters were estimated.

Case 4 results for P2 were similar to those observed for P1, with significant decreases in precision of estimates for coefficients describing the effects of environmental covariates on stage-specific productivity most severe for covariates linked to the first two model stages, while those linked to productivity in later stages remaining relatively unaffected by the estimation of additional basal productivity and capacity parameters (Figure 4.9). Simulation-estimation results for P2 also indicated that the precision of estimates for basal productivity in both the first and section stages increased markedly under high levels of observation uncertainty (Figure 4.9), while for P1 the level of precision in estimates of basal productivity in the first stage was less effected (Figure 4.8).

Discussion

Results of simulation testing of the stage structured life cycle estimation model provided valuable insights, useful when using the estimation model to estimate the influence of environmental factors on survival of Sacramento River Chinook populations. The precision with which model parameters may be estimated largely depends on the level of observation uncertainty in the data. This is not surprising, given that a reduction in the performance of the estimation model should be expected with the introduction of greater uncertainty in the data to which it is fit. Ono et al. (2014) likewise found that reductions in the quality of data provided to a stock assessment estimation model, stock synthesis, lead to less precise estimates for parameters of interest. However, increased observation uncertainty rarely lead to increased bias in parameter estimates, with the possible exception of slight increases in the level of positive bias

in estimates of the basal capacity parameter for P2 (Figures 4.3 and 4.6). Despite increased imprecision, at low to moderate levels of observation uncertainty estimates of coefficients describing the effect of environmental covariates on stage-specific productivities can be estimated with suitable precision and lack of bias. Conversely, estimates for coefficients describing the influence of environmental covariates on stage-specific capacities may be difficult to estimate, exhibiting consistently biases and high levels of imprecision if significant correlations between covariates exist. Estimates of the influence of fall.dayflow.yolo on capacity of the delta stage for P2 are a prime example (Figures 4.3 and 4.6). Furthermore, given the difference in basal productivity rates P1 abundances came closer to capacity limits and were therefore subject to greater density dependent compensation, when compared with P2 whose average abundance was lower across years and simulations. This suggests that for populations such as P2 that do not frequently approach basal capacities for limiting stages, the influence of capacity-linked covariates may more difficult to estimate.

Results indicated significant difficulty in estimating initial spawning abundances prior to the beginning of the time series of data (Figures 4.5 and 4.6). This largely arises from the minimal impact of these parameters on the total data likelihood. Furthermore, given capacity limitations in subsequent stages and years, there is the potential for strong positive bias in these estimates as additional abundance will not be realized in the abundance of future cohorts, if they exceed early stage capacities. In future application of this estimation model it is likely best to fix these parameters at locally weighted averages of the time series, given their minimal influence on future population dynamics, however this may not be necessary as their estimation has little impact on bias or precision of other model parameters. Despite difficulty in estimating initial spawning abundances, parameters describing the competitive interactions amongst populations

may be estimated without bias across all levels of observation uncertainty, although the precision of these estimates is significantly reduced at high levels of uncertainty (Figure 4.7). It should be recognized however, that if this parameter is not well informed by the data, either due to changes in its value over time as a function of habitat characteristics or changes in the timing of outmigration through altered hatchery practices, estimation of this parameter may adversely impact the precision with which other model parameters are estimated. However, estimates of coefficients describing the impact of environmental covariates on stage-specific productivities, key parameters of interest from a management perspective, were only moderately impacted by its inclusion. The stage in which the competitive interaction is assumed to take place should be carefully considered when designing the model and be based upon the known biology of the populations involved and in what stages of the life cycle competition may reasonably be expected to occur. Furthermore, given the parameterization of the interaction effect (Equation 4.2), if the recipient population p exists at levels well below its assumed or estimated capacity, it may be very difficult to estimate $\alpha_{p,i,s}$ given that it influences capacity only and thus density-dependent compensation at high abundance levels, rather than overall survival rate. Alternative parameterizations of equation 4.2 might include the interaction parameter in the numerator, so as influence survival rate independent of density.

Finally, results of this simulation study indicate that attempting to estimate basal productivity $\beta_{s,p,0}$ and capacity $\gamma_{s,p,0}$ parameters for multiple stages can be very difficult in situations where high levels of observation uncertainty in abundance indices are suspected (Figures 4.8 and 4.9). It is important to note however that although untested in this study, the inclusion of additional indices of abundance, likely in the form of rotary screw trap (Poytress et al. 2014) or trawl (Newman and Rice 2002) juvenile abundance estimates, may be able to help

partition mortality between subsequent model stages. By further partitioning mortality between model stages, estimates of basal productivity and capacity parameters, and coefficients describing the influence of environmental covariates earlier in the life cycle, may be better informed.

Two potential sources of uncertainty not addressed in the current simulation study are worthy of future research. The first is the potential for a mismatch between the operating model and the estimation model through the inclusion of a covariate effect on survival within the operating model that is not considered in the estimation model. There is large potential for this to occur as not all hypothesized covariates may be easily included in the estimation model, given an inability to identify a biologically defensible mechanistic explanation for it's effect or the availability of a complete time series of data for a specific covariate. It is likely that a "missing" covariate would bias the estimated value of the coefficients for other covariates with which it is highly correlated, but this remains unknown. The second is the potential for process uncertainty alongside observation uncertainty in the system. Process uncertainty may result from temporal variability in covariate effects, either random or due to persistent and directional changes in the ecosystem. While the process uncertainty inherent in the system will be explained by the current estimation model as additional observation uncertainty, for some systems it may be possible to estimate both process and observation uncertainty using a stage-structured state-space model, as was done by Maunder et al. (2015) for Delta Smelt in the Sacramento-San Joaquin Delta.

Finally, despite the recognition that life-cycle models are necessary for evaluating potential impacts of alternative water management strategies on species of concern in the Central Valley (NRC 2010, Rose et al. 2011) and the potential benefits of estimation over mechanistic life-cycle models, none of the current estimation models for these species (see Hendrix et al. (in

prep) and Maunder et al. (2015)) have undergone evaluation through simulation testing. Testing of models to understand the level of precision and potential for bias in parameter estimates, is fundamentally important for understanding the reliability of predictions based upon the model for the likelihood of outcomes from potential management actions.

Figures

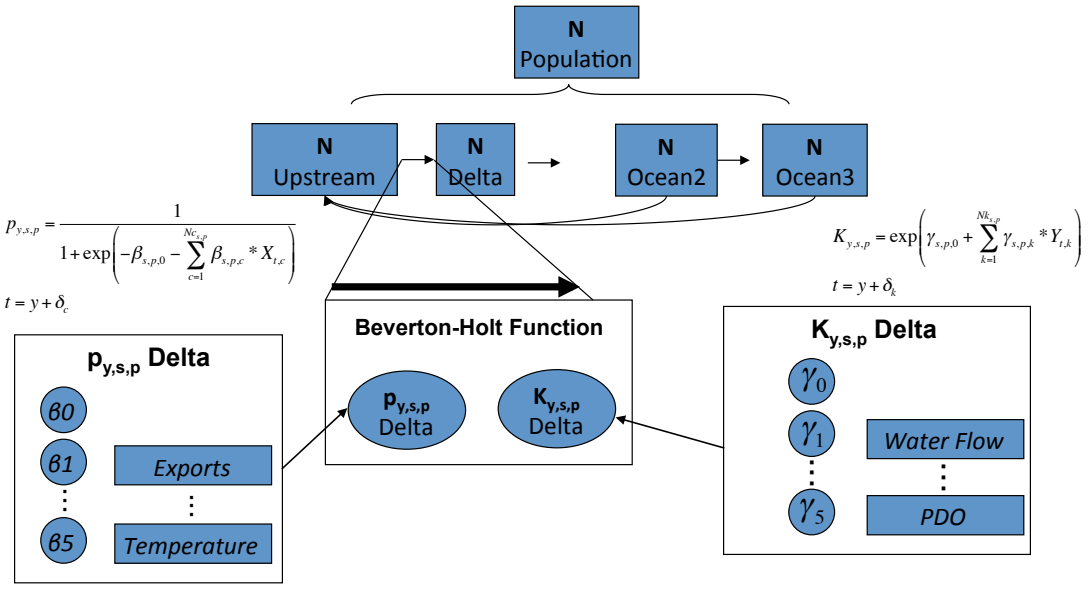

Figure 4.1 Schematic diagram of stage structured life cycle estimation model. Survival between stages is governed by a Beverton-Holt survival function of time varying stage-specific productivity $p_{y,s,p}$ and rearing capacity $K_{y,s,p}$ parameters. Productivity and capacity parameters are logit and log transformed linear functions of basal (average) productivities and capacities, as well as coefficients describing the influence of environmental covariates.

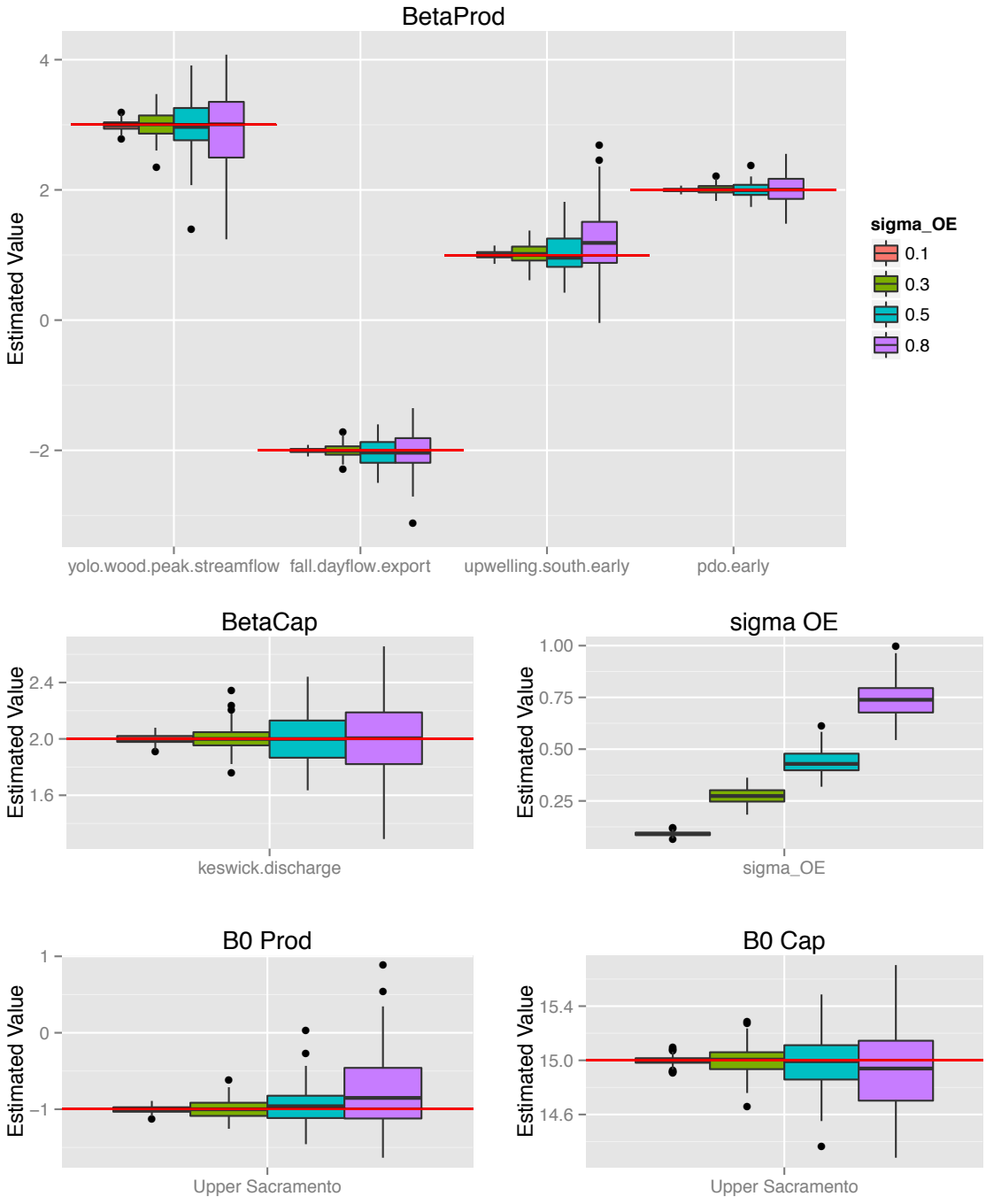

Figure 4.2 Results of case 1 for P1. Boxplots illustrate the distribution of estimates for model parameters across replicate 100 simulations. Boxplots of differing colors show results under different levels of observation uncertainty. Red lines depict the true values for parameters.

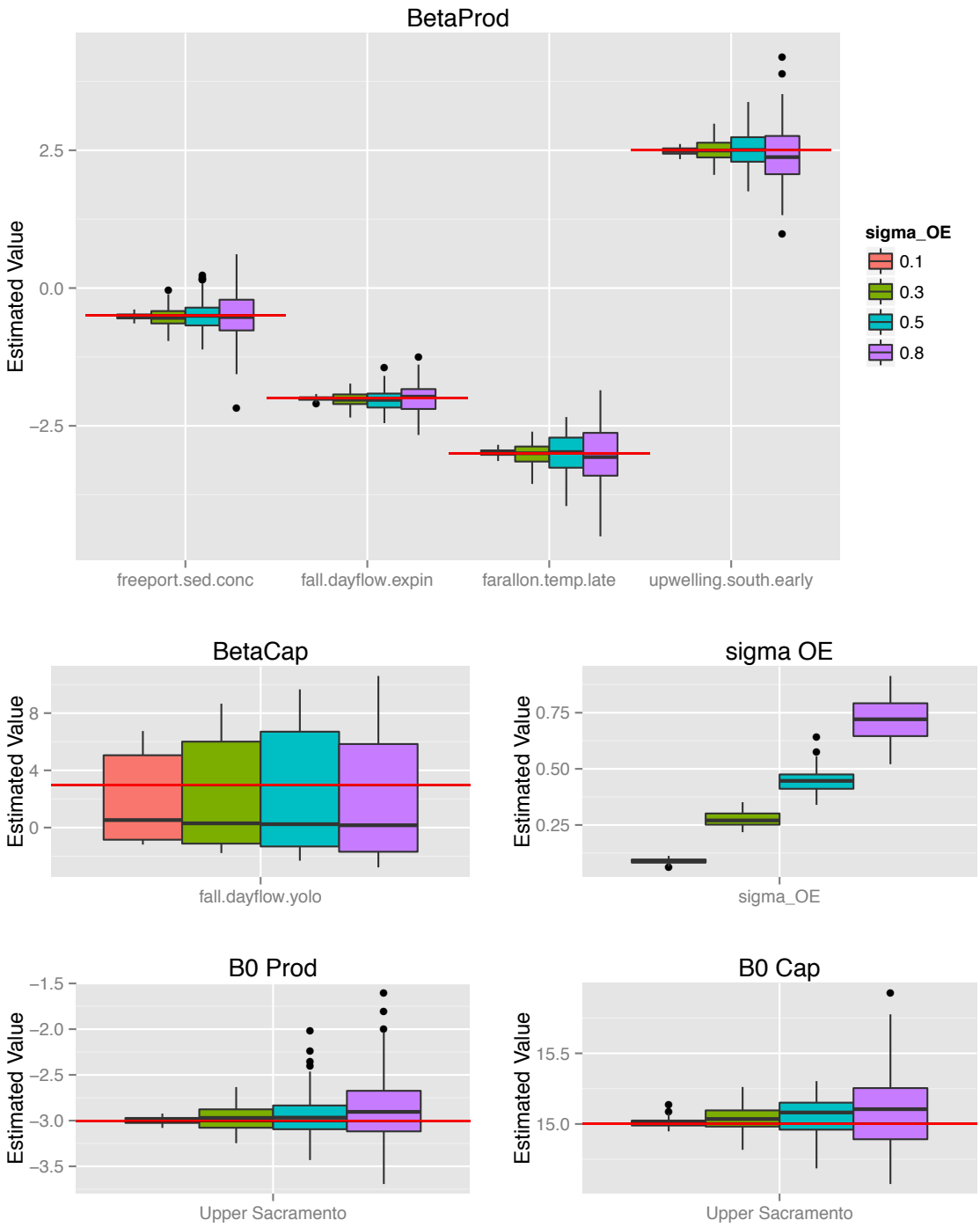

Figure 4.3 Results of case 1 for P2. Boxplots illustrate the distribution of estimates for model parameters across replicate 100 simulations. Boxplots of differing colors show results under different levels of observation uncertainty. Red lines depict the true values for parameters.

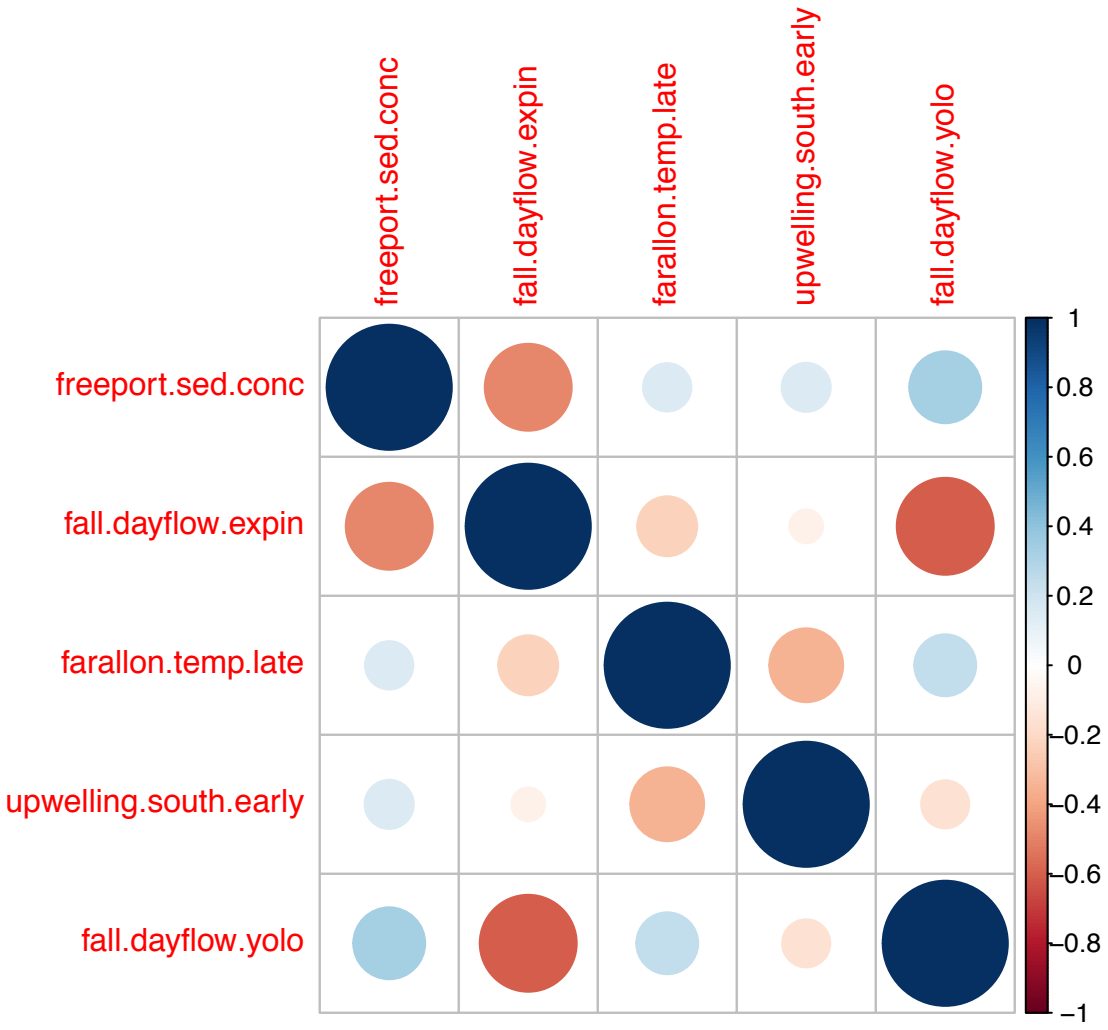

Figure 4.4 Correlation plot for P2 covariate values across time. A somewhat strong negative correlation $\rho = -0.6$ is observed between the fall.dayflow.expin and fall.dayflow.yolo covariates. The size of circles indicates the strength of correlation, and the color the direction.

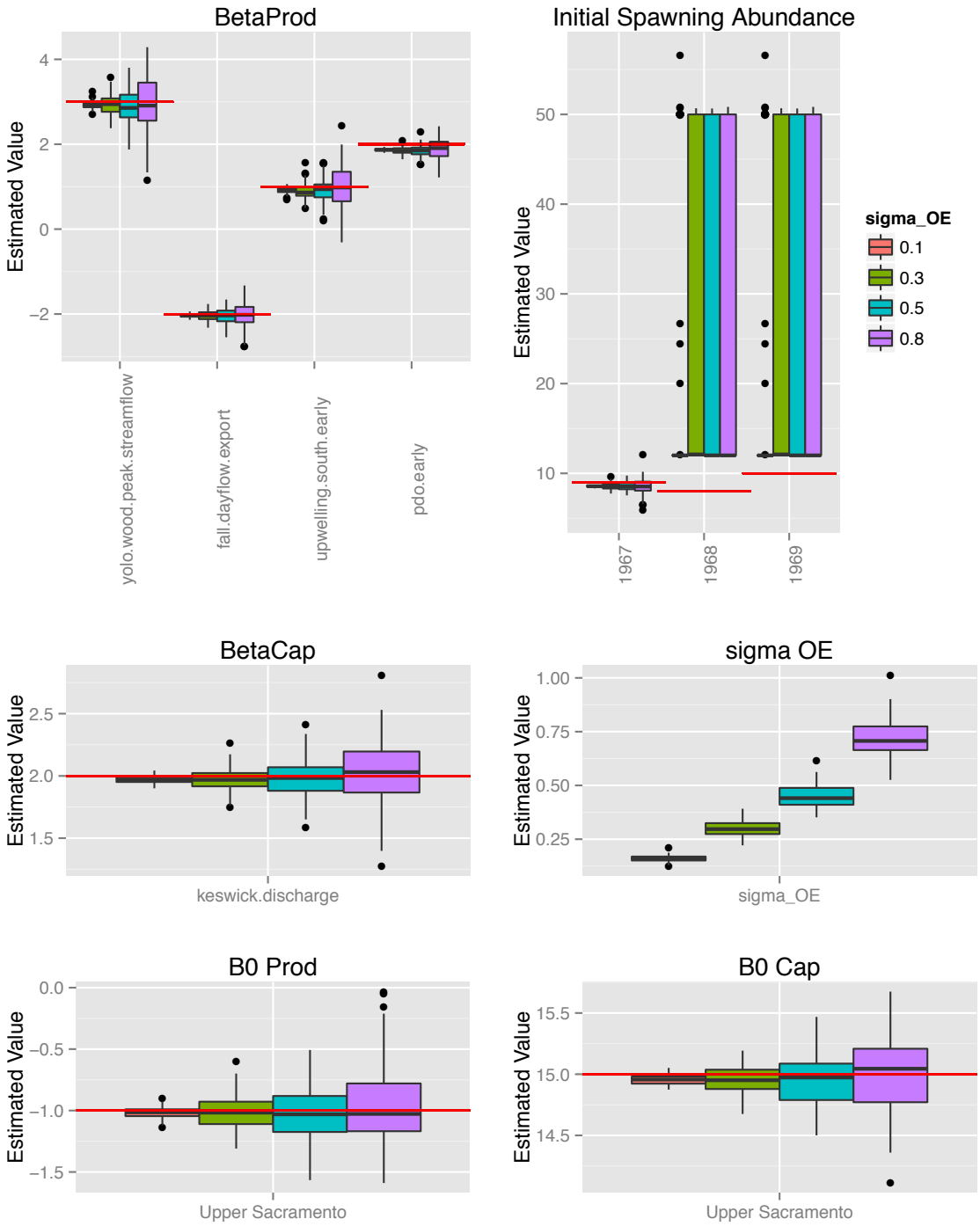

Figure 4.5 Results of case 2 for P1. Boxplots illustrate the distribution of estimates for model parameters across replicate 100 simulations. Boxplots of differing colors show results under different levels of observation uncertainty. Red lines depict the true values for parameters.

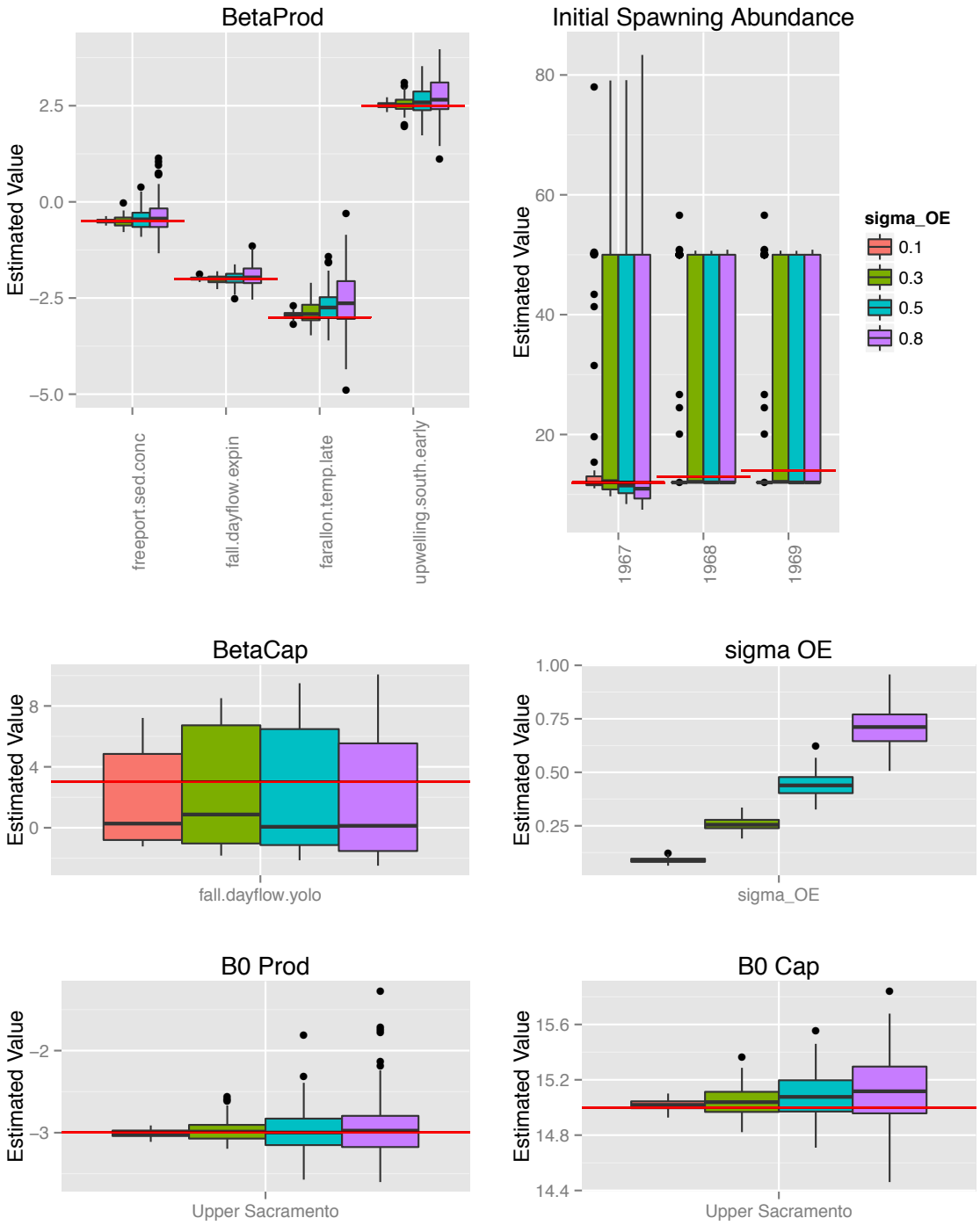

Figure 4.6 Results of case 2 for P2. Boxplots illustrate the distribution of estimates for model parameters across replicate 100 simulations. Boxplots of differing colors show results under different levels of observation uncertainty. Red lines depict the true values for parameters.

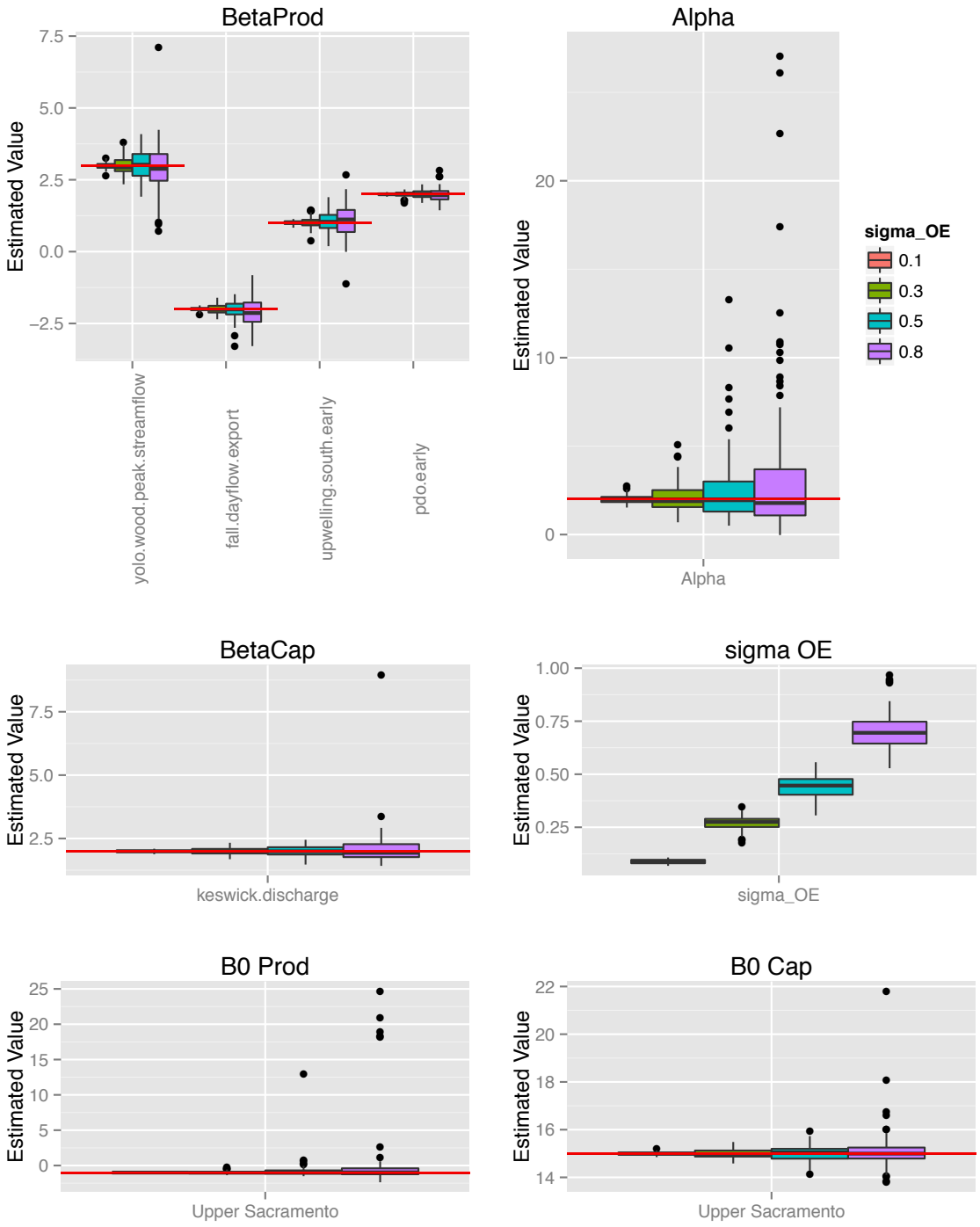

Figure 4.7 Results of case 3 for P1. Boxplots illustrate the distribution of estimates for model parameters across replicate 100 simulations. Boxplots of differing colors show results under different levels of observation uncertainty. Red lines depict the true values for parameters.

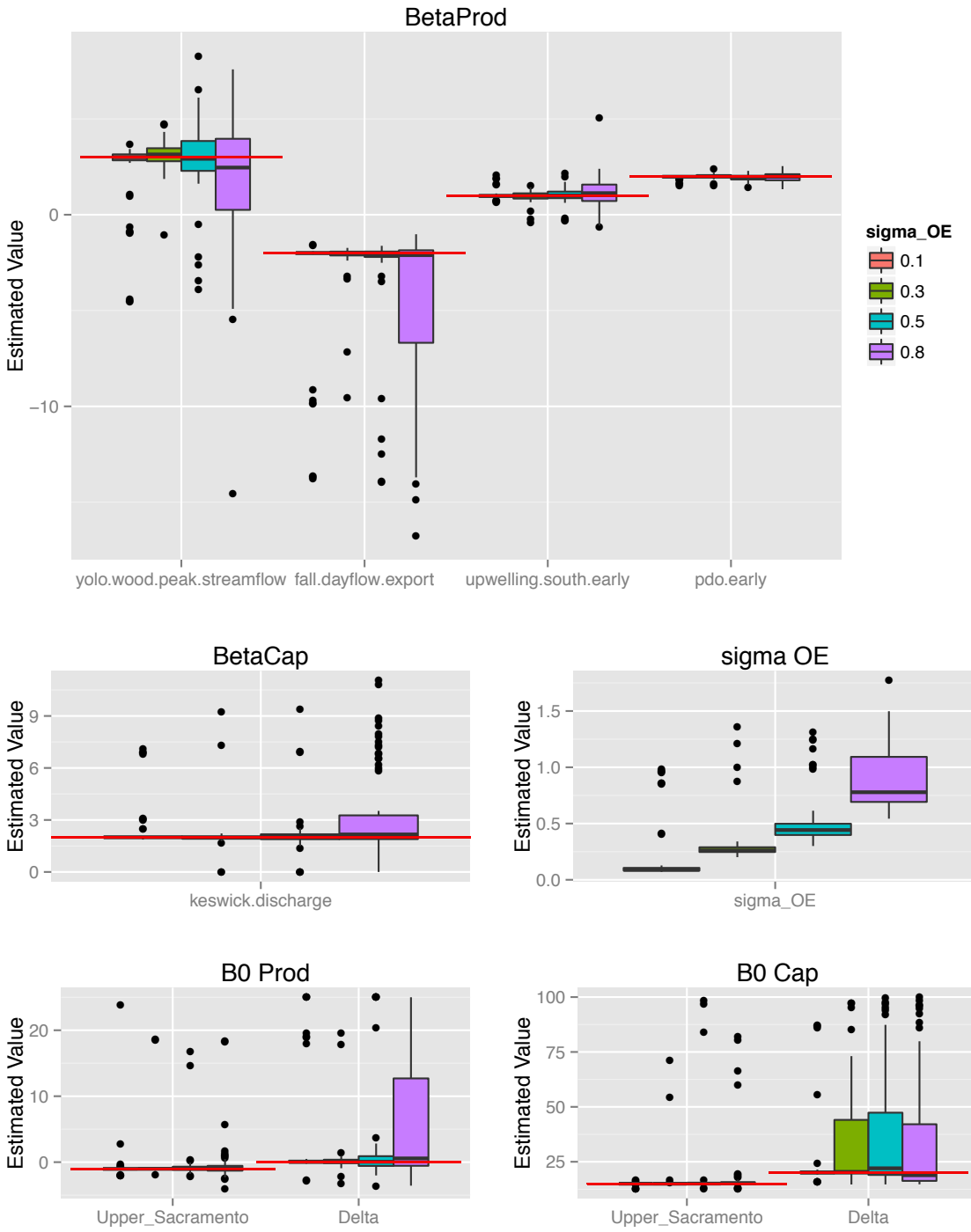

Figure 4.8 Results of case 4 for P1. Boxplots illustrate the distribution of estimates for model parameters across replicate 100 simulations. Boxplots of differing colors show results under different levels of observation uncertainty. Red lines depict the true values for parameters.

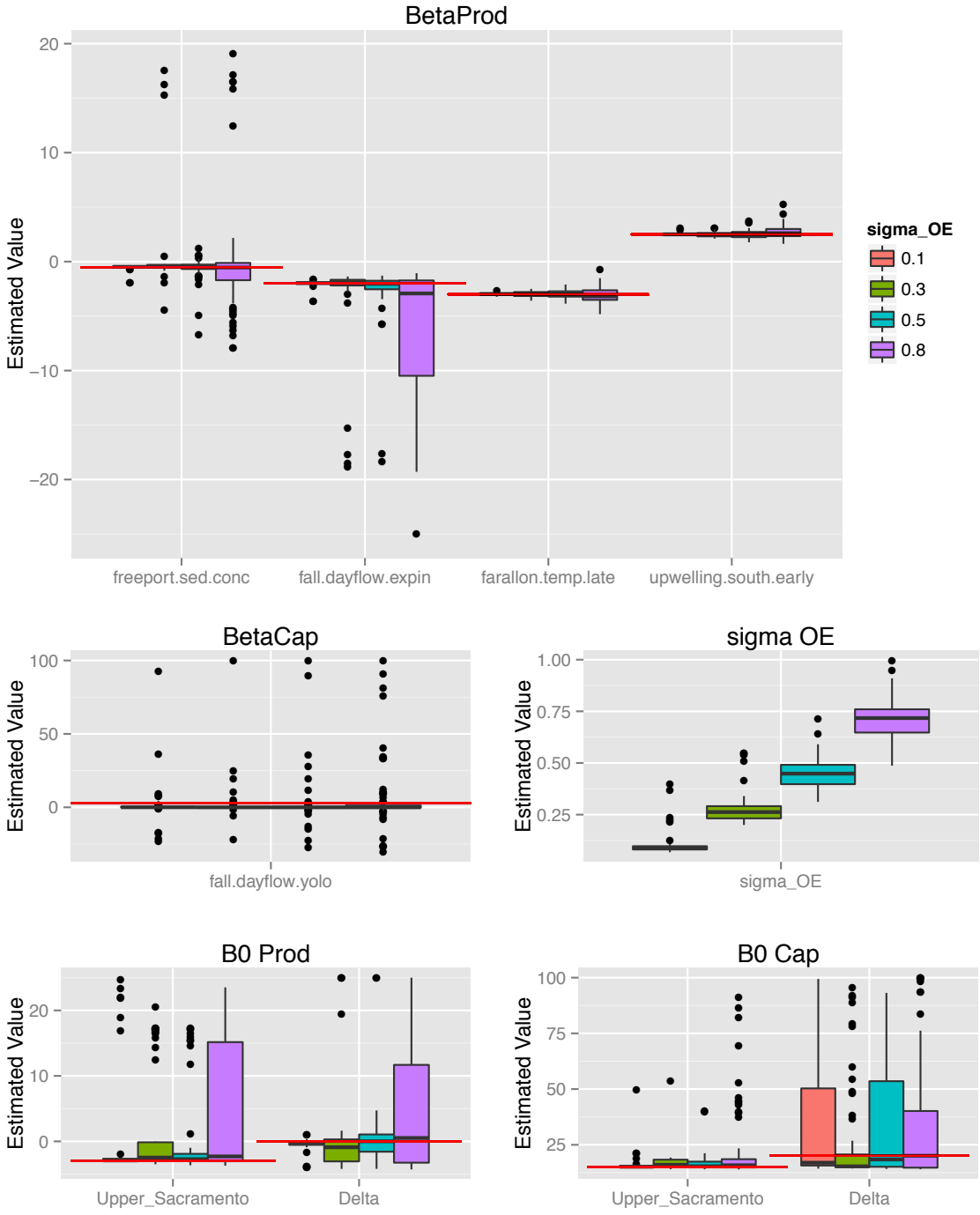

Figure 4.9 Results of case 4 for P2. Boxplots illustrate the distribution of estimates for model parameters across replicate 100 simulations. Boxplots of differing colors show results under different levels of observation uncertainty. Red lines depict the true values for parameters.

Chapter 5

Evaluation of Freshwater and Marine Influences on The Survival of Spring and Fall-run Sacramento River Chinook

Abstract

Chinook salmon (*Oncorhynchus tshawytscha*) populations native to the Central Valley of California have exhibited high variability and significant reductions in abundance in the recent past, leading to the listing of several populations under the Federal Endangered Species Act. Despite concern over the viability of Central Valley Chinook in the future, few studies have attempted to evaluate the full range of potential drivers of survival throughout the entire life cycle. We used a stage-structured statistical life-cycle model fit to adult and juvenile abundance data, using maximum likelihood and Bayesian methods, to evaluate the direction and magnitude of survival impacts from a range of natural and anthropogenic factors on spring and fall-run Sacramento River Chinook. In addition we employed information theoretic approaches paired with a novel method for exploring potential alternative models to identifying the most parsimonious set of explanatory environmental factors. We found support for environmental impacts of 14 variables including flow, temperature, sediment concentration, export inflow

ratios, exports, ocean upwelling, wind stress curl and Pacific Decadal Oscillation (PDO, an integrated climate index). The three environmental drivers most strongly associated fall-run Chinook recruitment were the ratio of Sacramento-San Joaquin Delta exports to inflows, spring upwelling south of the Farallon Islands, and the gross delta water channel depletion. The three most important factors affecting spring-run Chinook recruitment were smolt body size at Chipps Island, Sacramento-San Joaquin Delta water export levels, and sediment concentration in lower sections of the Sacramento River. Overall recruitment of spring and fall-run Chinook in the Sacramento River is influenced by the both natural and anthropogenic factors, in both freshwater and marine portions of the life cycle.

Introduction

The native home range for Chinook salmon (*Oncorhynchus tshawytscha*) extends from California throughout the north Pacific to areas of Russia and Japan, providing the foundation for valuable commercial and subsistence fisheries. Within this range, the status of individual populations of Chinook salmon varies from healthy to critically endangered and at risk for extinction. Spawning abundance of Chinook salmon in California's Central Valley has declined substantially during the period of historical record (Lindley et al. 2009). These declines in abundance have resulted in the listing of both winter and spring-run Chinook by state and federal agencies (Lindley et al. 2004). Exceedingly low returns in 2007 and 2008 of the fall-run component of the Sacramento River Chinook stock complex, once the most abundant, forced the Pacific Fisheries Management Council to issue a complete moratorium on commercial and recreational fishing during the 2008 – 2009 season, costing an estimated $225 million and 2,263 lost fishing jobs (California 2008). While a report evaluating the potential causes of the fall-run Chinook collapse by Lindley et al. (2009) suggested that nearshore ocean conditions could be the proximate cause of the observed low returns, there is still considerable uncertainty regarding what has driven trends in survival and the abundance of Central Valley Chinook historically.

A wide range of hypotheses regarding potential anthropogenic and natural drivers of survival for Central Valley Chinook have been presented by various user groups and scientific organizations. However statistical methods for weighing these alternative hypotheses throughout the entire life cycle have been largely absent. Reviews of the NMFS (2009) biological opinion on potential water export management operations in the Sacramento – San Joaquin Delta by both the National Research Council (NRC 2010) and CALFED (Anderson et al. 2009) suggested that future biological opinions should rely on life-cycle models for evaluating potential impacts of

management actions. Statistical approaches are needed for evaluating the impact of a wide range of natural and anthropogenic factors, and using the weight evidence from the data to determine the important drivers of survival for Central Valley Chinook. Furthermore, these methods need to be capable of evaluation multiple populations and allowing for competitive interactions amongst populations given the large contribution of hatchery-reared fall-run Chinook produced within Sacramento River watershed.

The goal of this chapter was evaluate the environmental drivers of survival for Chinook salmon populations spawning in the Sacramento River, CA watershed, in a statistically rigorous manner. More generally, our purpose was to assess a range of factors hypothesized to affect survival, including natural and anthropogenic factors involving biotic and abiotic processes. To achieve this goal we implemented the stage-structured statistical population dynamics model detailed in Chapter 4. When fit to available juvenile and adult spawning abundance data, this model estimates the direction and magnitude of influence that a range of factors, or environmental covariates, have on survival through specific portions of the Chinook life cycle. The population dynamics model is currently used to explore the environmental drivers of survival for four fall-run populations including: 1) Mainstem Sacramento wild-spawning Chinook, 2) Battle Creek Coleman National Fish Hatchery Chinook, 3) Feather River Hatchery Chinook, and 4) American River Nimbus Hatchery Chinook, as well as three spring-run populations including: 5) Deer Creek, 6) Mill Creek, and 7) Butte Creek, wild-spawning Chinook.

The stage-structured population dynamics model used here complements and expands upon previous analyses of interactions between environmental factors and survival of Chinook salmon populations of the Sacramento River watershed in several ways. First, while many

previous analyses have modeled the survival or productivity of single components of the Sacramento River Chinook stock complex (Lindley and Mohr 2003, Newman and Brandes 2010, Newman and Rice 2002, Zeug et al. 2012), or the fall (Newman and Rice 2002), late-fall (Newman and Brandes 2010), or winter (Lindley and Mohr 2003, Zeug et al. 2012) Sacramento Chinook runs in isolation, the current population dynamics model is applied to multiple populations of both spring-run and fall-run Chinook and evaluates interactions between these populations at points in the life cycle where co-rearing and co-migration occurs. Second, the current population dynamics model approximates both wild and hatchery type life histories, utilizing historical records of hatchery releases from the Coleman National Fish Hatchery on Battle Creek, the Feather River Hatchery, and the Nimbus Fish Hatchery on the American River compiled by Huber and Carlson (in review). Third, we have utilized estimates of stray rates between hatcheries and wild populations of fall-run Chinook available from the proportional coded wire tagging program (Kormos et al. 2012, Palmer-Zwahlen and Kormos 2013), to reconstruct spawning abundance data in the presence of straying, prior to fitting the estimation model. Fourth, in contrast to previous analyses that primarily evaluated survival variation in either the freshwater or marine portions of the Chinook life cycle, our model incorporates both marine and freshwater stages, permitting the testing of competing hypotheses for putative survival influences in all habitats utilized by Sacramento River Chinook. Fifth, previous stage-structured population dynamics models used to evaluate the interaction between environmental factors and the survival of Sacramento Chinook including Zeug et al. (2012) defined these interactions based upon a priori information or findings from other systems or laboratory experiments, our model is statistical in nature, estimating the effects of the hypothesized environmental drivers of survival based upon observed variation in adult and juvenile

abundance. The result is a flexible multi-stock, stage-structured, statistical, population dynamics model that estimates the influence of natural and anthropogenic environmental factors on survival of Chinook salmon throughout their life cycle, using both Bayesian and Maximum Likelihood methods.

To identify the critical drivers of Chinook survival, we used several statistical techniques to evaluate the relative importance of environmental variables on the survival including both information theoretic approaches and Bayesian approaches. Due to the large number of potential explanatory covariates, or alternative hypotheses, and the inability to fit all combinations of these covariates, we used the Akaike Information Criterion for small sample size (AICc) and a novel method for exploring the model space.

Methods

The Data

To estimate the effect of various environmental covariates as well as basal productivity and capacity for the seven populations in specific life stages, the estimation model was conditioned on different types of data available for the Sacramento River system. The first type of data was time-series of explanatory environmental covariates. For each environmental covariate being evaluated for influence on survival, we needed a record of its value over time as a model input. Covariate data were z-standardized (Zar 2010) based upon the mean and standard deviation of the time-series (Equation 5.1).

$$X_{t,i} = \frac{x_{t,i} - \sum_{t=1}^{Nt} x_{t,i} / Nt}{\sigma_i} \quad (5.1)$$

In this way, the ith covariate at time t ($x_{t,i}$) is transformed into units of standard deviations from the time-series mean for each year in the set of length Nt, rather than untransformed values that span many orders of magnitude among covariates. By transforming covariate data into the same units, the coefficients describing the influence of individual covariates were more readily comparable and estimable.

Potential covariates were chosen for evaluation within the estimation model based upon first principals and a valid biological rationale for why each might be expected to influence either survival rate or stage-specific capacity. Covariates were developed came from a wide range of sources, including a review of the pertinent literature and expert opinion, and were created using data from the period of time throughout the year over which they were expected to exhibit the greatest influence (Table 5.1).

We also needed time-series of abundance data for the populations included in the multi-stock population dynamics model. Estimates of the number of adult Chinook returning to natural spawning grounds and hatcheries are available from the GrandTab database (CDF&W 2014) for all seven populations evaluated as part of this study. However, since the Central Valley Constant Fractional Marking Program (CFM) was initiated in 2007, it has been possible to estimate the contribution of hatchery-origin Chinook to the spawning abundance observed on wild spawning grounds and the contribution of wild-origin Chinook production to observed returns to regional hatcheries (Kormos et al. 2012). Historical abundances for the seven Chinook populations were reconstructed to account for straying between hatcheries and natural spawning grounds, using the average of the estimated proportion of observed adult Chinook straying in 2010 (Kormos et al. 2012) and 2011 (Palmer-Zwahlen and Kormos 2013). Average (2010-2011) proportions of observed adult abundance that were comprised of hatchery and wild individuals in each

population (Table 5.2), were used to reconstruct historical abundances for the fall-run spawning populations. For example, to reconstruct the fall-run wild Sacramento mainstem population spawning abundance, each year 24% of the observed spawning abundance was remove and reallocated to the Coleman National Fish Hatchery (Battle Creek) adult abundance, while 11% of the observed Battle Creek hatchery (CNFH) abundance was removed as wild migrants into the hatchery (Figure 5.1).

Adult abundances for the four fall-run Chinook populations were reconstructed using the methods detailed above for years 1967 – 2010 (Figure 5.2). Existing adult abundance estimates reported by CDF&W (2014) for the spring-run populations included in our analyses (i.e. Deer, Mill, and Butte Creeks) were assumed to be minimally impacted by hatchery straying and therefore unaltered (Figure 5.2).

Estimates of juvenile Chinook abundance in Sacramento River system were also used to inform estimates of model parameters. The inclusion of additional abundance indices to which the estimation model is fit, confers a greater ability to partition mortality between life stages and more precise estimation of the strength and magnitude of influence from environmental covariates. Poytress et al. (2014) have used available trap efficiency information to calculate absolute abundance indices for juvenile Chinook passing Red Bluff Diversion Dam, partitioned by race. Fall-run juvenile Chinook abundance estimates from 2002 forward were assumed to be comprised predominantly of two populations, the wild Sacramento Mainstem population and the Battle Creek (CNFH) Hatchery population. Therefore, model estimates of the combined abundance of these two populations were compared to the estimates provided by Poytress et al. (2014) in likelihood calculations.

The third type of data required by the estimation model was historical hatchery releases. As constructed, the estimation model allows for specification of the wild or hatchery life-history type for each population. Three of the seven populations currently in included in our analysis are of hatchery origin, therefore annual hatchery release numbers were required for the Battle Creek (CNFH) Hatchery, Feather River Hatchery, and American River (Nimbus) Hatchery populations. Huber and Carlson (in review) have digitized historical hatchery reports. For the three hatchery populations included in our analysis, we have used these hatchery release data in place of the functional relationship between spawning abundance and fecundity assumed for the wild spawning populations. Figure 5.2 shows hatchery release numbers from Huber and Carlson (in review) for each of the three fall-run hatchery populations. Hatchery release practices have differed among facilities and over time, with on-sight releases, releases in the Sacramento-San Joaquin delta, releases in San Francisco Bay, and many locations in between (Huber and Carlson in review), however hatchery release location was not specifically considered in this analysis.

The fourth type of data required for these analyses were annual estimates of harvest rate by population. Harvest rate estimates are available from the U.S. Fish and Wildlife Chinookprod database. For each population of interest, this database uses both the abundance estimates from the Grandtab (CDF&W 2014) database and ocean harvest numbers from the Pacific Fishery Management Council (PFMC) to calculate harvest rates in the marine and in-river regions. For our purposes, we have calculated the total harvest rate by stock and year as the sum of ocean ($C_{t,p}^{ocean}$) and in-river catch ($C_{t,p}^{in-river}$), divided by the total abundance including observed escapement ($E_{t,p}$) and catches for that population (p) in that year (t) (Equation 5.2).

$$hr_{t,p} = \frac{C_{t,p}^{ocean} + C_{t,p}^{in-river}}{E_{t,p} + C_{t,p}^{ocean} + C_{t,p}^{in-river}} \quad (5.2)$$

In our analysis we have identified the Sacramento-San Joaquin Delta stage (2nd) and nearshore stage (3rd) as points of possible competition and therefore capacity interactions within the model. Fall-run and spring-run juvenile Chinook are assumed to compete with members of their own run within these two stages of the life cycle and therefore shared capacities are assumed, with symmetric interactions (i.e. $\alpha_{p,i,s}$ elements equal to 1).

The basal capacity parameters for a population ($\gamma_{s,p.0}$, see Equation 4.4), or group of interacting populations, for which $\alpha_{p,i,s} > 0$ (Equation 4.2), represent the maximum rearing capacity for that population in that stage over time in the absence of influence from environmental covariates. For populations that are currently well below historical abundance levels, or for populations without subsequent juvenile abundance estimates, it is often difficult to estimate these basal stage capacity values. However, auxiliary information may be used to inform these stage-specific capacities. Recent work has resulted in monthly juvenile Chinook salmon capacity estimates for the Sacramento River mainstem and the Sacramento-San Joaquin Delta (Hendrix et al. 2014). In place of estimating stage capacities for: 1) Sacramento River mainstem-spawning wild fall-run Chinook in the upstream stage (1st), 2) mainstem-spawning wild, Battle Creek (CNFH) hatchery, Feather River Hatchery, and American River (Nimbus) Hatchery, populations in the Sacramento-San Joaquin Delta stage (2nd), and 3) Deer, Mill, and Butte Creek populations in the Sacramento-San Joaquin Delta stage (2nd), we have used capacity estimates available from NOAA in-stream Chinook capacity modeling (Hendrix et al. 2014). The average of estimated monthly capacities in the Sacramento mainstem for the period between January and April in each year, was used for as the input capacity for mainstem-spawning wild fall-run population. The average of estimated monthly Sacramento – San Joaquin Delta rearing

capacities for the March – May and February – April periods, were used as the input capacities for the fall-run and spring-run populations in that stage, respectively.

Capacity estimates for the Sacramento-San Joaquin Delta from NOAA in-stream Chinook habitat capacity modeling were only available after 1980 (Hendrix et al. 2014). Given that our population dynamics model begins in year 1967, we assumed a fixed capacity for the period prior to 1980. NOAA Delta capacity estimates correlate most directly with water year type, therefore the average of estimated capacities for the fall-run and spring-run populations by water year type were calculated and used in place of actual capacity estimates prior to 1980. These average capacities by water year type and Chinook run type were used in years prior to 1980 based on the reported water year.

Estimation model structure

The method we employed for modeling the salmon life cycle as a series of sequential, spatially-explicit, stage-specific Beverton-Holt transition functions that relate density-dependent survival to habitat covariates is similar to those successfully used to address conservation questions regarding other Chinook salmon populations along the West Coast. The Shiraz model developed by Scheuerell et al. (2006), employed to evaluate anthropogenic and habitat effects on production of Chinook in the Snohomish River basin of Puget Sound, Washington, was one of the first to specify interactions between habitat variables and the productivity and capacity parameters of the Beverton-Holt functions describing survival though life stages. Subsequently, Battin et al. (2007) and Honea et al. (2009) employed stage-structured models governed by linked Beverton-Holt transition functions to evaluate the influence of climate change, hydrologic variability, and habitat restoration on populations of Chinook salmon in the Columbia River

basin. All three of these analyses used a Shiraz-type approach by linking habitat and climate covariates to stage-specific survival.

However, the model we have designed for evaluating the environmental drivers of survival for Chinook salmon in the Sacramento River differs from the Shiraz-type models described above (Battin et al. 2007, Honea et al. 2009, Scheuerell et al. 2006) in several fundamental ways. First, the model used in these analyses is statistical in nature. Whereas Scheuerell et al. (2006), Honea et al. (2009), and Battin et al. (2007), all specify the relationships between environmental covariates and the productivity and capacity parameters of the Beverton-Holt function for each stage, based upon *in situ* observations, laboratory experiments, or expert opinion, the estimation framework we have created for the analysis of the drivers of Sacramento River Chinook survival estimates these relationships directly from the abundance data. Second, estimation of the relationships between environmental covariates and the Beverton-Holt productivity and capacity parameters, provides both point estimates of the effect of each covariate and estimates of uncertainty. By estimating both the value for coefficients describing covariate effects, as well as their uncertainty, we can discern which covariates have the largest influence, and also which covariates have had a consistent influence historically. Finally, by estimating the value of coefficients describing the magnitude and direction of influence each environmental covariate has on stage-specific productivity or capacity, our method allows for the propagation of estimation uncertainty in those relationships forward when those model parameters are used to predict future abundance trends under alternative climate, marine productivity, or water use scenarios.

When fitted to available abundance data the ADMB stage-structured population dynamics model provides estimates of model parameters, uncertainty in those parameter

estimates, and the Hessian matrix for model parameters from which the parameter covariance matrix may be derived. However, with 37 separate environmental covariates to be tested as competing hypotheses it was necessary to define metrics for model fit and parsimony. We use the Akaike Information Criterion corrected for small sample sizes (AICc) (Burnham and Anderson 2002) as a metric for model parsimony (Equation 5.4).

$$AICc = 2LL_T + 2p + \frac{2p(p+1)}{n-p-1} \quad (5.4)$$

AICc balances the degree to which a model is able to explain the variability in data (LL_T) against the number of parameters estimated (p) and number of data used in estimation (n), and provides a basis for model selection. The second statistic used to evaluate model fit is the mean absolute percent error in model predictions (Equation 5.5).

$$MAPE_p = \frac{\sum_{t=1}^{n} \left| \frac{\hat{A}_{t,p} - A_{t,p}}{A_{t,p}} \right|}{n} \quad (5.5)$$

Uncertainty – AICc selection and MCMC methods

To test a range of hypotheses regarding which environmental covariates influence the survival of seven populations of Sacramento River Chinook, we constructed a stage-structured statistical population dynamics model. When fit to available adult and juvenile abundance data, this model estimates the magnitude and direction of influence that a set of environmental covariates has on two components of Chinook survival, life-stage specific productivity (maximum survival) rates and capacities. In the process of fitting population dynamics models to data as part of our analysis, there were two sources of uncertainty that we considered directly. The first was structural uncertainty, or uncertainty in the subset of environmental covariates that best represent the processes driving changes in abundance over time. The second is estimation

uncertainty, or uncertainty in our ability to identify the true direction and magnitude of impact each environmental covariate imposes on Chinook survival. To address structural uncertainty in our analysis, we used a process of forward stepwise model building, based upon AICc criteria, with replication to ensure complete evaluation of model space, or the range of potential models that may be used to describe trends in abundance over time. This process allowed us to define the "best" model or subset of potential environmental covariates (hypotheses) for describing observed population dynamics. To address the second type of uncertainty in our analysis, estimation uncertainty, we employed Markov Chain Monte-Carlo estimation methods to quantify the probability distributions for the coefficients describing the effect of each environmental covariate on survival.

Stepwise AICc Model Selection

In total 37 separate environmental covariates were identified by the study team as potential drivers of interannual variation in Sacramento Chinook survival. Describing the effects of these 37 environmental covariates on separate populations in the form of either population-specific effects or common influences on groups of populations, resulted in a total 59 covariate-by-population effects, whose influence on survival may be estimated based on their ability to explain observed Chinook abundance data. Each of these 59 covariate-by-population effects represents an alternative hypothesis to be tested in our analysis.

Hypotheses for covariate-by-population effects on Chinook survival may be compared to a "null" model that attempts to explain variation in the time-series' of observed juvenile and adult abundance data based on only observed ocean harvest rates, hatchery release numbers, estimated productivities (maximum survival rates) for populations in the first life-stage, and annual capacities specified by the juvenile capacity modeling (Hendrix et al. 2014). The null

model represents the base case without any influence from environmental covariates. Competing models incorporating alternative combinations of covariate effects were compared based on their AICc values to define a "best-fit" model for generating predictions for future abundance trends.

With a total of 59 independent covariate-by-population effects to be tested for their ability to explain variation in historical Sacramento Chinook survival, the number of possible combinations of these effects, or potential models, is quite large. It becomes unrealistic to fit every possible model permutation to the available data and compare AICc values. Therefore we used a method for exploring the model space, or the range of potential models incorporating different combinations of these effects, which involved a forward stepwise model building with AICc as the selection criteria. Forward stepwise model building begins first by fitting the null model, without any covariate effects, to the available data. Second, a covariate is selected at random from amongst the set of 59 possible covariate-by-population effects and included in the model, and this model is subsequently fit to the data. Third, the AICc value for this new model is compared to that of the null model. If a reduction in AICc value for the model including the additional covariate of greater than 2 units is observed ($\Delta\text{AICc} \leq 2$), when the old model is compared to the model incorporating the new covariate, that covariate is kept, otherwise it is removed from the model. Moving forward, this process of randomly sampling covariates without replacement, fitting the model to data, and evaluating ΔAICc, (i.e. steps two and three) are repeated until all covariates have been tested for their ability to improve model parsimony (see Figure 5.4).

The result of one round of forward stepwise AICc model building, or fitting the null model and 59 alternative models sequentially, is one realization of a best-fit model based upon the AICc criteria. However, experience indicates that given even small correlations among some

environmental covariates, the order in which covariates are introduced has a subtle influence on the resulting model. Therefore, to more fully explore the uncertainty in model selection, we repeated the forward stepwise AICc process 1,000 times with the order of covariate proposal randomized in each iteration. By evaluating the frequency with which specific covariates appear in best-fit models across these 1,000 realizations, it is possible to determine which covariates are most important in explaining historical variation in Chinook survival. Furthermore, by repeating the stepwise AICc process 1,000 times, we are thoroughly exploring the model space and among these independently built models can determine the single model that has the lowest AICc among the candidate best-fit models.

Markov Chain Monte-Carlo Estimation Methods

The second critical piece of uncertainty in our analysis is estimation uncertainty. Estimation uncertainty describes variation in the estimated value of model parameters, and is a function of how well model parameters are informed by the available data. To estimate uncertainty in coefficients describing the influence of environmental covariates on Chinook survival, we used Bayesian estimation methods. Bayes' Theorem describes the probability of a hypothesis θ, in our case a set of parameter values, given the data, which in our case are both adult spawning abundance ($A_{t,p}$) and juvenile abundance (J_t) observations:

$$P(\theta \mid data) = \frac{P(data \mid \theta) P(\theta)}{\int P(data \mid \theta) P(\theta)} \quad (5.6)$$

The prior probability on logit transformed coefficients was normal with a mean of zero and standard deviation equal to 2.5, as per recommendations by King et al. (2010). Bounded uniform priors were assumed for all other estimated model parameters. Estimated initial (log) abundances 1967-1969 were bounded on the ~U(0, 100) interval, basal stage productivities

($\beta_{s,p,0}$) were bounded on the ~U(-25, 25) interval, and basal stage capacities ($\gamma_{s,p.0}$) bounded on the ~U(-100, 100) interval. Bayesian estimation methods allow the posterior probability distribution for derived and estimated parameters to be calculated, and from those the full range of parameter uncertainty.

Markov Chain Monte-Carlo (MCMC) methods are commonly used numerical algorithms employed to draw samples from the posterior distributions for parameters in Bayesian models (Gelman et al. 2004). We employed the Random Walk Metropolis-Hastings (RW-MH) MCMC algorithm (Hastings 1970, Metropolis et al. 1953) implemented in AD Model Builder (Fournier et al. 2012) to draw samples from posterior distributions of parameters in population dynamics model. The RW-MH MCMC algorithm is a widely applicable MCMC algorithm that accounts for correlations among model parameters. As implemented in ADMB, the RW-MH MCMC algorithm begins by finding the parameter values that maximize the complete data likelihood, or posterior modes, and then uses the estimated covariance matrix for model parameters to create a multivariate proposal distribution. Based upon this multivariate proposal distribution randomly drawn parameter sets, or MCMC jumps, are proposed and either accepted or rejected based upon comparison of the ratio of the proposed posterior density to that of the current state, with a random uniform (0,1) deviate. In this way, the RW-MH MCMC algorithm in ADMB begins as the posterior mode and samples the joint posterior.

MCMC chains were run for 5,000,000 iterations with a thinning rate of 1/1,000 to reduce posterior correlation. The first 30% of the chain was removed as a burn-in period, during which the chain approached the stationary distribution for model parameters. To ensure MCMC results had converged to their stationary distribution, three independent chains were run simultaneously. Model convergence was tested in three separate ways. First, traceplots of MCMC samples were

evaluated for the presence of discernable trends that would indicate a lack of convergence to the true stationary distribution. Second, posterior correlations at differing lags were calculated, to test that there was little autocorrelation. Finally, Gelman and Rubin's convergence diagnostic (Brooks and Gelman 1998, Gelman and Rubin 1992) was used to compare within and among chain variance to determine if all three chains had indeed converged to the same stationary distribution.

Translating Coefficients into Survival Differences

To translate the value of estimated coefficients describing the influence of environmental covariates into predictions for realized changes in survival, we calculated the survival rate for the seven populations from egg, or hatchery release, through adults returning to freshwater under a range of scenarios. Survival rates for each population were calculated by tracking a set number of individuals forward in time across life-stages, assuming no harvest mortality, and using parameter values sampled from the joint posterior for the estimation model. One thousand independent sets of model parameter values were sampled from their joint posterior to preserve posterior correlation, and used to quantify the variation in predictions for the influence of each environmental covariate on survival, arising from estimation uncertainty. Survival rate was calculated as the sum of spawning adults across return years, divided by the number of eggs or hatchery releases. The spawning abundance, used as the basis for calculating survival rates, was the 1970 – 2010 average for the wild-spawning populations (i.e. mainstem Sacramento fall-run, as well as Deer, Mill, and Butte Creek spring-run) and the average release numbers for the most recent 10 years for the Battle Creek (CNFH), Feather River, and American River (Nimbus) hatchery populations. Likewise, the most recent 10-year average was used for capacity of wild

juvenile fall-run Chinook in the Sacramento mainstem and for the total capacity for spring-run and fall-run Chinook rearing in the Sacramento – San Joaquin Delta.

The distribution of survival rate predictions for each population (p), across the 1,000 independent sets of parameter values (i), was first calculated for a base case ($Sbase_{p,i}$). Under the base case the value for all environmental covariates was set at zero, which for z-standardized covariates is equal to the long-term average. Subsequently the covariate-specific survival ($Scov_{p,i,c}$) of each population across the 1,000 parameter sets was determined, as each covariate (c) was sequentially changed to have a value of 1. Covariate-specific survival ($Scov_{p,i,c}$) thus represents the population (p) and sample (i) specific survival rate when covariate c is increased in value to 1 standard deviation above the long-term mean. From this, the percentage difference in survival for each population resulting from an increase in the value of an environmental covariate was calculated as:.

$$\Delta S_{p,i,c} = \frac{\left(S\,\mathrm{cov}_{p,i,c} - Sbase_{p,i}\right)}{Sbase_{p,i}} * 100 \quad (5.7)$$

Results

Model Selection Results

Results of the iterative forward stepwise-AICc model selection (Table 5.3) indicate that the set of environmental covariates (hypotheses) which best describes historical variation in Sacramento Chinook abundance encompasses a wide range of locations within the life cycle, populations, and ecological processes. The most-often AICc-selected covariate was spring air temperature at the city of Sacramento on survival of the Butte Creek population (spring.butte – sacAirTemp.spring) which was selected in 998 of 1,000 best-fit models. This covariate

represents air temperature during juvenile rearing (January – March) at the city of Sacramento, and is included as a surrogate for Butte Creek stream temperature. Additional covariates which were represented in 60% or greater of iteratively built models include: 1) the combined influence of the size of out-migrating spring-run juveniles on the survival of Deer, Mill and Butte Creek spring-run populations (.5.6.7-spring.size.chipps), 2) the combined influence of near-shore upwelling during the period of ocean entry (April – June) upon the survival of the four fall-run populations (.1.2.3.4-upwelling.south.early), and 3) the combined influence of the Pacific Decadal Oscillation during winter (January – May average) of the first year of marine residence (.1.2.3.4.5.6.7-pdo.early) on the survival of all four fall-run and three spring-run populations. The 5th most frequently included covariate was the effect of summer (July – September) air temperature at Sacramento during the brood year, on survival of Butte Creek spring-run Chinook (spring.butte-sacAirTemp.summer). This covariate was included to test hypothesis that high over-summer water temperatures may have a negative impact on the survival and successful spawning of adult spring-run Chinook holding in tributaries.

Covariates describing the influence of water exports on spring and fall-run survival were the 6th, 7th, and 8th most often included. The combined effect of average water exports from the Sacramento – San Joaquin Delta between February and April, quantified by the Dayflow QEXPORTS metric, on survival of spring-run Chinook (.5.6.7-spring.dayflow.export), appeared in 54% of forward stepwise-AICc built models. Similarly, the covariate representing the combined effect of March – May average Sacramento – San Joaquin water exports on the survival of the four fall-run Chinook populations (.1.2.3.4-fall.dayflow.export) was included in 48% of stepwise-AICc built models, with the ratio of water exports to total Delta water inflow (Dayflow: EXPIN) during this same period (.1.2.3.4-fall.dayflow.expin) following closely with a

37% inclusion rate. Other covariates highlighting the influence of water routing and supply in the Sacramento – San Joaquin Delta were included in a smaller subset of stepwise-AICc built models. The influence of average net channel depletion (Dayflow: QCD) between February and April on the grouped spring-run Chinook populations (.5.6.7-spring.dayflow.cd) was included in 22% of the 1,000 stepwise-AICc built models. In addition, the combined influence of the average flow into Georgiana Slough and the Delta Cross Channel (Dayflow: QXGEO) February – April on the spring-run populations (.5.6.7-spring.dayflow.geo) was included in 19% of candidate best-fit models.

While the inclusion rate of specific covariate-by-population effects across the 1,000 stepwise-AICc built models provides an indication of the relative weight of evidence from the data, that each covariate holds some ability to explain historical patterns in survival, we consider the model with the lowest AICc value to have the best predictive ability. The single model with the lowest AICc value represents the most parsimonious fit to the data, explaining the greatest amount of observed variation in adult and juvenile abundance, while estimating the fewest parameters. This lowest AICc or "final" model provides the best basis for predicting future trends in abundance under alternative climate, marine production, and water management scenarios. The final model included 14 covariate-by-population effects, spanning both the freshwater and marine portions of the life cycle (Table 5.4). In addition, the effects incorporated in the final model include both single-population effects as well as shared effects of environmental covariates across multiple populations. In total five of the covariates included in the final (lowest AICc) model were related to survival in the 1st (upriver) stage, six were related to the 2nd stage representing environmental effects on survival through the Sacramento – San Joaquin Delta, two were related to the 3rd stage influencing survival in the nearshore

environment, and only one covariate was related to survival during subsequent years of marine residence.

Of the covariate-by-population effects on upstream survival incorporated in the final model three were related to atmospheric temperature, used as a proxy for tributary-specific water temperatures, and two were related to water flow conditions. The three temperature-related covariate-by-population effects were all based on air temperature at Sacramento, CA and included: 1) the effect of average spring air temperature (January - March) on survival of the fall-run Battle Creek population in the year of emergence (fall.battle.creek - sacAirTemp.spring), 2) the effect of average summer air temperature (July – September) during the brood year on offspring production and oocyte through juvenile survival for the Butte Creek spring-run population (spring.butte - sacAirTemp.summer), and 3) the effect of average spring air temperature (January – March) in the year of emergence on survival of Butte Creek spring-run Chinook (spring.butte - sacAirTemp.spring). The two upstream covariate effects related to water flow conditions included, the influence of average water discharge rates (cfs^{-1}) at Keswick Dam during the period between January and March on the survival of Sacramento mainstem spawning wild fall-run Chinook (fall.sac.mainstem - keswick.discharge), and the effect of average water discharge in Deer Creek between October and December on the brood year survival of spring-run Chinook spawning in that tributary (spring.deer - deer.discharge).

The range of covariates which best describe historical patterns in juvenile Chinook survival through the Sacramento – San Joaquin Delta stage included factors both anthropogenic and natural in origin. Interestingly, the winter (February-April) concentration of sediment (mg/L) measured at Freeport, CA was selected based upon the AICc criteria as an important explanatory covariate for both grouped fall-run (.1.2.3.4-freeport.sed.conc) and spring-run (.5.6.7-

freeport.sed.conc) populations. Two other covariate effects on the combined survival of fall-run Chinook populations which relate to water flow and management in the Sacramento – San Joaquin Delta were also identified in the final model, including average March – May Dayflow metrics for: 1) QCD or net channel depletion for in-delta consumptive use (.1.2.3.4-fall.dayflow.cd), and 2) EXPIN or the ratio of total delta exports to freshwater inflows (.1.2.3.4-fall.dayflow.expin) (CDWR 2014). In addition to sediment concentration, two other covariate effects on the combined survival of the Deer, Mill, and Butte Creek spring-run populations in the Sacramento – San Joaquin Delta were present in the AICc-selected final model. These included the influence of average monthly water exports and diversions from the delta (February – April) as quantified by the Dayflow metric QEXPORTS (CDWR 2014), which represents the sum of Central Valley Project exports, State Water Project exports, Contra Costa Water District diversions, and North Bay Aqueduct exports (.5.6.7-spring.dayflow.export), and the average size of juvenile spring-run Chinook caught in the Chipps Island Trawl (.5.6.7-spring.size.chipps).

Based on the AICc, the final model identified three covariates able to explain Chinook survival in the nearshore region following ocean entry and survival during subsequent years of marine residency. Survival for the four fall-run Chinook populations in the nearshore region was explained in part by upwelling patterns during the spring months (April – June) at the southern NOAA/PFEL monitoring site located at 36°N latitude and 122°W longitude (.1.2.3.4-upwelling.south.early). Additionally, the effect of average wind stress curl during July – December of the year of ocean entry on the survival of all seven combined spring and fall-run populations was included in the final model (.1.2.3.4.5.6.7-curl.late). The last covariate present in the final model linked to broad-scale marine climate patterns was the effect of the average

Pacific Decadal Oscillation Index during the winter of the first year at sea (January – May) on the combined survival of all seven populations (.1.2.3.4.5.6.7-pdo.early).

These 14 population-by-covariate effects, spanning freshwater and marine portions of the Chinook life cycle and all seven analyzed Chinook populations, represent the most parsimonious explanation for historical patterns in Chinook survival and observed juvenile and adult abundance. This final model was used as the basis for the subsequent Bayesian analysis of the effect of each of these covariates and their realized survival influence, and used for predicting future trends in abundance under alternative water management scenarios, predictions for future climate change, and marine production patterns.

Estimation Results

When fit to abundance data, the Bayesian population dynamics model passed all convergence tests. The model fairly accurately predicts the abundance pattern observed for Deer and Mill Creek spring-run populations which exhibit higher adult abundances, relative to the time series, through 1984 followed by a period of lower adult abundance through the mid-1990s, followed by higher relative abundances through 2006 (Figure 5.5). Similarly, the model captured the period of lower spawning abundance of the Butte Creek spring-run population prior to 1985 followed by a pronounced increase in abundance, ending with a relative plateau in the early 2000's (Figure 5.5). Model predictions for both Sacramento mainstem spawning wild fall-run Chinook and Feather River hatchery fall Chinook failed to capture the low returns in 1998 – 1999, but captured the reduction in abundance observed in 2007 – 2008. In general for all seven populations of spring and fall-run Chinook included in the analysis, model predictions did not explicitly capture interannual variation, but explained much of the general trends in abundance across the time series (Figure 5.5).

Posterior distributions for coefficients describing the influence of environmental covariates on survival, as well as those for parameters describing the base survival rate to Sacramento – San Joaquin Delta entry are shown in figure 5.6, with samples from posterior distributions arising from the three separate MCMC chains are drawn in different colors. These results indicate that of the 14 covariates included in the final model, 8 covariates were estimated to have a negative impact on stage-specific productivity (maximum survival rate), 5 were estimated to have a positive influence, and 1 was estimated to have a negative influence on average but with a 95% credible interval range overlapping zero (Figure 5.6 and Table 5.5). The concordance of the parameter medians and credible intervals across the three MCMC chains, along with Gelman-Rubin test statistic values for all parameters ≤ 1.05, indicated that all three chains converged to the same stationary distribution. Model predictions for the value of the basal productivity parameter ($\beta_{s,p,0}$) in the upstream stage, or maximum survival rate to Sacramento – San Joaquin Delta entry indicate large differences in survival between populations, with a distinctly higher survival estimated for hatchery-produced populations (Figure 5.6). It should be noted that for the four wild-spawning populations (i.e. mainstem Sacramento fall-run, and Deer, Mill, and Butte Creek spring runs), this parameter represents the maximum survival rate from egg to Delta entry, whereas for the three hatchery populations (Battle Creek (CNFH), Feather River, and American River (Nimbus) fall-run) this parameter represents the maximum survival rate from hatchery release to Delta entry. The results show that basal productivity or maximum survival rate for the upstream stage is both significantly higher and more variable for the three hatchery-reared populations. Higher maximum survival rates for these populations are to be expected given that they only represent mortality incurred after release, not mortality from fertilization to the date of release. However, the greater variance in maximum survival rate for

the hatchery populations is easily discernable. There is also a geographic trend in survival rates for the wild populations, with populations spawning higher in the watershed (Sacramento mainstem wild) having lower survival, when compared to those spawning in tributaries further down (Figure. 5.6)

The covariates whose survival impact is estimated to be negative include the effect of: 1) water discharge (cfs-1) from Keswick Dam on the mainstem Sacramento spawning fall-run Chinook (fall.sac.mainstem - keswick.discharge), 2) sediment concentration at Freeport, CA (mg/L) on the combined survival of the four fall-run populations (.1.2.3.4-freeport.sed.conc), 3) the export to inflow ratio in the Sacramento – San Joaquin Delta on combine survival of the fall-run populations (.1.2.3.4-fall.dayflow.expin), 4) wind stress curl on the combined survival of all seven populations of spring and fall-run Chinook (.1.2.3.4.5.6.7-curl.late), 5) spring Freeport, CA sediment concentrations on the combined survival of the three spring-run Chinook populations (.5.6.7-freeport.sed.conc), 6) water exports from the Sacramento – San Joaquin Delta on the combined survival of the three spring-run populations (.5.6.7-spring.dayflow.export), 7) the average size of juvenile spring-run Chinook on combined spring-run survival (.5.6.7-spring.size.chipps), and 8) Sacramento air temperature during summer months of the brood year on survival of Butte Creek spring-run Chinook (spring.butte - sacAirTemp.summer).

Five of the covariates were estimated to have positive influence on survival (Table 5.5): 1) upwelling in the nearshore region during spring of the ocean entry year on the combined survival of the fall-run Chinook populations (.1.2.3.4-upwelling.south.early), 2) spring air temperature at Sacramento, CA on the survival of fall-run Battle Creek (CNFH) Chinook (fall.battle.creek - sacAirTemp.spring), 3) spring air temperature at Sacramento, CA on the survival of Butte Creek spring-run Chinook (spring.butte - sacAirTemp.spring), 4) net channel

depletion in the Sacramento – San Joaquin Delta resulting from within-delta consumptive use as quantified by the Dayflow metric QCD on the combined survival of the four fall-run Chinook populations (.1.2.3.4-fall.dayflow.cd), and 5) the magnitude of the Pacific Decadal Oscillation during winter (January – May) of the first year at in the ocean on the combined survival of all seven spring and fall-run Chinook populations (.1.2.3.4.5.6.7-pdo.early). For the 13 covariates classified above as having either a distinct positive or negative effect on survival, the posterior distribution describing the probability of the true value for each coefficient had a 95% credible interval that was completely above or below zero. Although the estimated median value for the coefficient describing the effect of Deer Creek discharge (cfs^{-1}) on Deer Creek spring-run Chinook survival (spring.deer - deer.discharge) is less than zero (i.e. -0.22, Table 5.5) indicating an negative influence on survival, the 95% credible interval overlaps with zero indicating a significant probability (p=0.121) of the covariate having either no influence or a positive influence on survival.

While posterior probability distributions for coefficients representing the influence of each environmental covariate on stage and population-specific productivity ($\beta_{s,p,c}$) describe the model estimate for how much an increase or decrease in the value of that covariate is expected to change stage-specific productivity parameter of the Beverton-Holt equation (Equation 4.2), it is difficult to directly compare these estimated coefficient values for several reasons. First, the basal productivity rate ($\beta_{s,p,0}$) for each stage is population-specific, meaning that the magnitude of estimated coefficients ($\beta_{s,p,c}$) is always relative to the basal productivity rate for the population of interest. Second, coefficient values and basal productivity rates are estimated in logit space to ensure the resultant productivity value is smoothly scaled between 0 and 1 (Equation 4.3), and comparing coefficients and basal productivity rates in logit space may be

difficult to interpret. Therefore, we translated the magnitude of the estimated environmental covariate effects into more easily interpretable changes in survival.

Results of this analysis indicate that several factors can significantly influence survival in the upstream portion of juvenile migration (Figure 5.7 and Table 5.6). Keswick Dam discharge is predicted to reduce egg-to-adult survival by 52.2%, for each increase in discharge rate of 1 SD. Increased air temperatures in the spring months following emergence are expected to increase the survival of Battle Creek (CNFH) fall-run Chinook by 37.5%, although the 95% credible interval for this predictions ranges from a moderate a modest 4.4% increase to a 79.8% increase indicating significant uncertainty in this prediction. Springtime air temperatures are expected to influence the early juvenile survival of Butte Creek spring-run Chinook in a similar direction but to a much greater extent with a predicted 124.7% increase. Conversely, increased summertime air temperatures during the period of adult upstream holding and egg development are expected to reduce survival by 39.4%, indicating that summertime temperatures may be reaching lethal levels or affecting adult fertility. The final environmental variable linked to the upstream stage and early juvenile survival is water discharge in Deer Creek, which is expected to reduce survival for Deer Creek spring-run Chinook by 26.2%. However, it is important to note that there is significant uncertainty in this prediction with an increase in Deer Creek discharge by 1 SD predicted to result in between a 59.4% reduction in survival and a 27% increase in survival 95% of the time.

Later in the life cycle for Sacramento River Chinook, several factors likely influenced juvenile survival in the Sacramento – San Joaquin Delta. A 1 SD increase in the concentration of sediment (mg/L) at Freeport, CA is expected to result in a 37.1% reduction in the survival of the four fall-run Chinook populations. Sediment concentration is predicted to have a slightly larger

influence on survival of the three spring-run populations, with a 54.3% reduction in egg to adult survival. Water exports from the Sacramento – San Joaquin Delta, although quantified through different metrics, are expected to reduce survival of both spring and fall-run juvenile Chinook. An increase in total exports of 1 SD from the 1967-2010 average is predicted to result in a 68.1% reduction in the survival of Deer, Mill, and Butte Creek spring-run Chinook. Similarly, an increase in the ratio of Delta water exports to Delta inflow of 1 SD is expected to reduce survival of the four fall-run populations by 57.8%. Interestingly however, net channel depletion or the quantity of water removed from Delta channels to meet consumptive needs (Dayflow: QCD) is predicted to increase the survival of fall-run Chinook by 43.7%. The final covariate linked to survival of spring-run Chinook in the Sacramento – San Joaquin Delta is the average size of spring-run Chinook in the Chipps Island Trawl survey. Each increase in the average size of juvenile Chinook by 1 SD from the mean (1967-2010) is predicted to reduce survival by 72.9%.

Environmental conditions in the nearshore and marine portions of the Chinook life cycle were also found to have a significant impact on survival to adulthood. An increase in average nearshore upwelling during late spring (April – June) in the region south of San Francisco Bay of 1 SD above the mean, is expected to increase survival to adulthood by 51.2% for the four wild and hatchery-reared fall-run Chinook populations. Also related to marine patterns of nutrient transport and productivity, an increase average wind stress curl during the fall (July – December) of the first year of marine residency was estimated to reduce survival for the seven populations of spring and fall-run Chinook by 39%. The final covariate linked to Chinook survival in the marine environment was the Pacific Decadal Oscillation index during winter (January – May) of the first year of marine residence. An increase in PDO value of 1 SD above the 1967 – 2010 mean is predicted to increase survival of the seven populations of spring and fall-run Chinook by

30%, however there exists significant uncertainty in this prediction with the 95% credible interval ranging from 10.1 - 51% increase in egg or hatchery release to adult survival.

Discussion

This evaluation of the putative environmental drivers of survival for seven populations of spring and fall-run Chinook spawning within the Sacramento River watershed was comprised of two essential components. The first component was model selection or the process of determining the weight of evidence from the data for which subset of the 59 hypothesized covariate-by-population effects were able to best explain historical variation in Chinook salmon survival, and are therefore informative for predicting future trends in abundance. One thousand potential best-fit models were built using forward stepwise based upon AICc as the selection criteria. The percentage of the 1,000 best-fit models resulting from stepwise-AICc building which included a specific covariate provide a good indication of the relative amount of support each of these competing hypotheses had from the adult and juvenile abundance data (Table 5.3). The fact that a range of covariates influencing both grouped and single Chinook populations at all points in the life cycle were present amongst those with a high inclusion rate provide evidence that there is not a single population bottleneck within the life cycle. This indicates that a variety of environmental factors at multiple points within the life cycle play a role in determining interannual survival to adulthood. Of further importance is the observation that both natural covariates, including temperature, water flow, and marine productivity patters, as well as those of anthropogenic origin (i.e. water exports, export/inflow ratio, and water routing) appear amongst the set with the highest inclusion rate. This finding indicates that variation in survival of Sacramento River Chinook population in not driven by natural or anthropogenic processes in

isolation. The final model (Table 5.4), chosen based on having the lowest AICc value amongst the 1,000 candidate best-fit models, likewise includes a range of covariates throughout the life cycle representing both natural and anthropogenic processes are statistically important predictors of survival.

The influence of striped bass (*Morone saxatilis*) on survival of spring-run Chinook was of particular interest given findings by Lindley and Mohr (2003), which indicated that higher future abundances of striped bass were likely to lead to greater extinction potential for winter-run Chinook. While the effect of striped bass on survival on spring-run Chinook was included in 36% candidate best-fit models, it did not appear in the final (lowest AICc) model. When included alongside other covariates in the final model, the estimated effect of striped bass abundance was centered near zero, indicating an inability to estimate a distinctly negative impact on grouped survival of spring-run Chinook. This result indicates that while striped bass abundance does explain some of the variation in spring-run Chinook survival, other explanatory covariates provide a better alternative explanation for historical abundance observations.

The estimated effect that water exports from the Sacramento – San Joaquin Delta on juvenile Chinook survival through this region was also of importance. While the effect of average water export levels on spring-run Chinook survival and the influence of export/inflow ratio on fall-run Chinook survival both appear in the final model, these two covariate effects have a 54% and 37% inclusion rates across the 1,000 candidate best-fit models. The fact that these export-related covariate effects do not appear at the top of the list of most often included covariates, indicates that while they have substantial potential to explain historical patterns in spring and fall-run Chinook survival, as indicated by distinctly negative survival effects whose

95% credible intervals do not overlap zero (Figure 5.7 and Table 5.6), there are other environmental covariate which explain a greater proportion of variation in historical abundance.

The second component of this evaluation was to estimate the direction and magnitude of change in survival rates resulting from variation in each of the covariates in the final model using Bayesian methods. The effect of Sacramento air temperatures on several populations appeared as AICc-selected explanatory covariates for several populations. Sacramento air temperature was employed as a proxy for water temperatures in upstream regions of the Sacramento River watershed for two reasons. First, significant and often linear relationships exist for between stream temperatures and air temperatures in most regions. Second, stream temperature data were not available continuously for the requisite time series (1967 – 2010) for all locations, resulting in the necessity for interpolation based on the relationship with air temperature. Therefore, for consistency in the covariate time-series and to reduce the risk of introducing additional uncertainty into the estimation process, we used air temperatures as covariates in place of interpolated water temperatures. Results indicate a positive influence of increased spring (January - March) air temperatures on the survival of Battle Creek (CNFH) fall-run Chinook and Butte Creek spring-run Chinook. This temperature metric coincides with the period prior to and during which juvenile Chinook are rearing. The estimated positive influence of spring temperatures on Chinook survival could result indirectly from the increase in primary production fostered by increased water temperatures and subsequent effects on food availability. In this way growth potential for juvenile Chinook in freshwater depends indirectly on temperature in the rearing environment through food availability, and directly through effects on metabolism as warmer conditions allow juveniles to approach their bioenergetic optimum. Finally, there is some evidence that acclimation to higher temperatures early in life my facilitate higher thermal

tolerance later in life, although research in this area has primarily focused on Great Lakes rainbow trout and has not been explicitly evaluated in Chinook (Myrick and Chech 1998). While springtime temperatures were estimated to have a positive influence at this point in the lifecycle, it is important to note that higher temperatures experienced later in the lifecycle during summer months may approach upper tolerance limits, resulting in negative survival impacts. However, the effect of increased summertime temperatures on juvenile survival was not evaluated as part of this analysis.

Contrary to the estimated positive effect of spring temperatures, air temperature during the summer months (July-September) of the brood year were found to have a negative impact on the survival of Butte Creek spring-run Chinook (Table 5.6). For Butte Creek spring-run Chinook this time period coincides with the point in the life cycle when adults are holding in freshwater prior to spawning. Prior to the creation of impassable barriers to upstream migration, the life history of spring-run Chinook was adapted to make use of high spring runoff events from snowmelt to migrate upstream into high elevation streams with tolerable temperature regimes where they could successfully mature during the summer months and await spawning when waters cooled to below 14 – 15°C (Williams 2006). However, in Butte Creek mortality rates during the holding period were observed to exceed 20-30% in 2002 and 65% in 2003 during high temperature events (Ward et al. 2003). This is likely the result of the increased metabolic demands for adult spring-run Chinook while holding in freshwater during high temperature events, and the increased rate of disease onset and parasite load observed in other members of the *Oncorhynchus* genus exposed to high temperatures (Kocan et al. 2009).

Water flow conditions during juvenile rearing were also found to be important predictors of Chinook survival. Water discharge rates at Keswick Dam were found to negatively influence

survival of mainstem spawning wild fall-run Chinook, and water discharge in Deer Creek was found to reduce survival of the Deer Creek spring-run population although to a lesser extent (Table 5.6). While it is reasonable to assume that higher discharge rates could lead to greater access to valuable off-channel rearing habitat, water flow conditions additionally have the potential to influence foraging ability by juveniles through the availability of drifting food sources (Neuswanger et al. 2014). Nonetheless the finding that fall-run Chinook survival was negatively influenced by increased water flow contradicts findings by Stevens and Miller (1983) and Newman and Rice (2002). With respect to the influence of water discharge on the survival of Deer Creek spring-run Chinook, this tributary is prone to concentrated high flow events due to flood control levees and a lack of riparian vegetation in its lower reaches (Tompkins 2006). For Deer Creek this may indicate that high water flow rates reduce foraging opportunities for juvenile Chinook, rather than enhancing them, as would be the case in a system with greater floodplain connectivity.

Findings related to the influence of environmental covariates on survival of fall and spring-run Chinook in the Sacramento – San Joaquin Delta are of particular interest in this study. First, the effect of sediment concentration in waters at Freeport, California appeared in the final AICc-selected model, and increases in sediment concentration were estimated to have a substantial negative influence on the survival of both spring and fall-run populations. This finding is contrary to *a priori* expectations that increased sediment concentrations might provide a survival benefit, if they limit the efficacy of visual predators such as striped bass. However, evaluation of data from tagged Chinook using quasi-likelihood mark-recapture models by Newman and Rice (2002) also estimated a negative effect of turbidity in the Sacramento – San Joaquin Delta on survival, but credible intervals for this coefficient describing this effect

overlapped zero and were therefore not significant. We remain limited in our ability to explain the estimated negative effect of sediment concentrations save for the fact that increased sediment influx might be linked to production potential for phytoplankton and the benthic periphyton which form the basis for the aquatic food web.

Similarly, the estimated negative influence of average juvenile spring-run Chinook size on the common survival of the three spring-run populations appears contrary to *a priori* expectations. In the review of size selective mortality in teleost fishes Sogard (1997) found general support for the "bigger is better" hypothesis across taxa. Claiborne et al. (2011) also found that juvenile to adult survival of yearling Chinook from the Willamette River Hatchery increased with size at ocean entry. However, in an evaluation of the effect of size on survival from analysis of scale samples from Chinook returning to the same hatchery, Ewing and Ewing (2002) found either no significant size difference between juveniles at the hatchery and those at ocean entry, or in the case of the 1989 – 1990 brood years evidence for greater survival of smaller individuals. It is important to note that spring-run juvenile size data were unavailable until 1976. As a result we were forced to assume the long-term average for this covariate prior that year which may have influenced our result.

Results of this analysis related to the influence of water exports from the Sacramento – San Joaquin Delta indicate a negative influence of the export/inflow ratio on the combined survival of the four fall-run Chinook populations and a negative influence of increased total Delta exports on the combined survival of spring-run Chinook populations (Table 5.6). Newman and Rice (2002) also found that increased export/inflow ratios resulted in a reduction in survival for Sacramento Chinook (spring-run), although credible intervals for coefficient describing the effect overlapped with zero and so were deemed non-significant. These findings indicate that

higher export rates lead to reduced survival for Sacramento River Chinook on average, however a mechanistic explanation remains elusive. Direct entrainment mortality seems an unlikely mechanism given the success of reclamation and transport procedures, even given increased predation potential at the release site. Changes to water routing may provide a more reasonable explanation for the estimated survival influence of Delta water exports. Higher exports, or export/inflow ratio, result in greater water diversion into the interior delta where survival has been observed to be substantially lower than that in the Sacramento River mainstem (Perry et al. 2010), potentially resulting from an increased encounter rate with predators or prolonged residence in areas with suboptimal feeding opportunities or dissolved oxygen concentrations.

In conjunction with freshwater drivers of survival for spring and fall-run Chinook populations of the Sacramento River watershed, results of this analysis indicate that several attributes of the marine environment have a significant influence on survival. Two covariates related to nearshore and offshore ocean current patterns and resultant nutrient movement within the water column were included as part of the final AICc-selected model. These covariates were the strength of nearshore upwelling and wind stress curl. Nearshore upwelling results in deep, cooler, and nutrient rich waters moving toward the limnetic zone, with onshore transport and convergence fostering higher nearshore productivity during spring and summer. Conversely, wind stress curl is associated with offshore divergent transport (Wells et al. 2008). Our results indicate that increased nearshore upwelling during April – June of the year of ocean entry results in an increase in the combined survival of the four fall-run Chinook populations. Four alternative covariates quantifying upwelling patterns were evaluated as competing hypotheses for fall-run Chinook survival at different locations and quantifying time periods. Covariates were constructed using information from PFEL/NOAA monitoring sites both north and south of San

Francisco Bay and for both the spring (April – June) and fall (July – December) periods. The AICc-selected covariate that appeared in the final model used the upwelling index data for spring time-period and at the southern location. Interestingly, although the effect of upwelling at the southern location in the spring months on the combined survival of spring-run Chinook appeared in 22% of candidate best-fit models, it did not appear in the final (lowest AICc) model, indicating that while upwelling may also be an important predictor of spring-run Chinook survival it appears to explain more variation in fall-run Chinook survival.

Wind stress curl was found to have a negative influence on the combined survival of all seven spring and fall-run Chinook populations. These results are not unexpected given findings by Wells et al. (2007) that indicate greater Chinook growth in the first year of life with increased nearshore upwelling and decreased wind stress curl. Wells et al. (2008) likewise found that reductions in wind stress curl were linked to increased production of rockfish species although they note this may be more related to dispersal of juvenile rockfish. The estimated reduction in survival for Chinook associated with greater wind stress curl is likely explained by trophic interactions, with findings by Macias et al. (2012) indicating that biomass concentrations for phytoplankton and zooplankton are likely to be substantially higher with coastal upwelling as opposed to wind stress curl driven upwelling offshore.

The Pacific Decadal Oscillation (PDO) describes a persisting periodicity in sea surface temperature, mixed layer depth, and strength and direction of ocean currents (Mantua and Hare 2002). Estimates for the influence of the PDO during January – May of the first year at sea indicating for the seven spring and fall-run Chinook populations, indicate increased survival is likely to be observed in during positive PDO events. This result is contrary to findings by Hare et al. (1999) which indicate positive PDO conditions favor production in Alaskan salmon stocks

and disfavor the productivity of West Coast stocks, as well as findings by Wells et al. (2006) which highlight the negative covariation between size of Columbia River Chinook size and PDO values.

Taken together, the results of this analysis indicate that the important factors determining survival for populations of Chinook salmon in the Sacramento River span both freshwater and marine portions of the life cycle and are both natural and anthropogenic in origin. Estimates for demographic parameters and coefficients describing the direction and magnitude of environmental covariate effects on survival may not be used to evaluate future trends in abundance and survival under alternative climate change, ocean production, and water management scenarios. However, when predicting trends in abundance it will be necessary to propagate the uncertainty in parameter estimates forward into the future. This may be done by conducting replicate forward simulations while drawing values for life-cycle model parameters from the joint posterior from the Bayesian analysis. By conducting replicate simulations with independent draws from the joint posterior, both the uncertainty in estimated parameter values and posterior correlations amongst parameter values will be fully represented in future predictions.

Figures

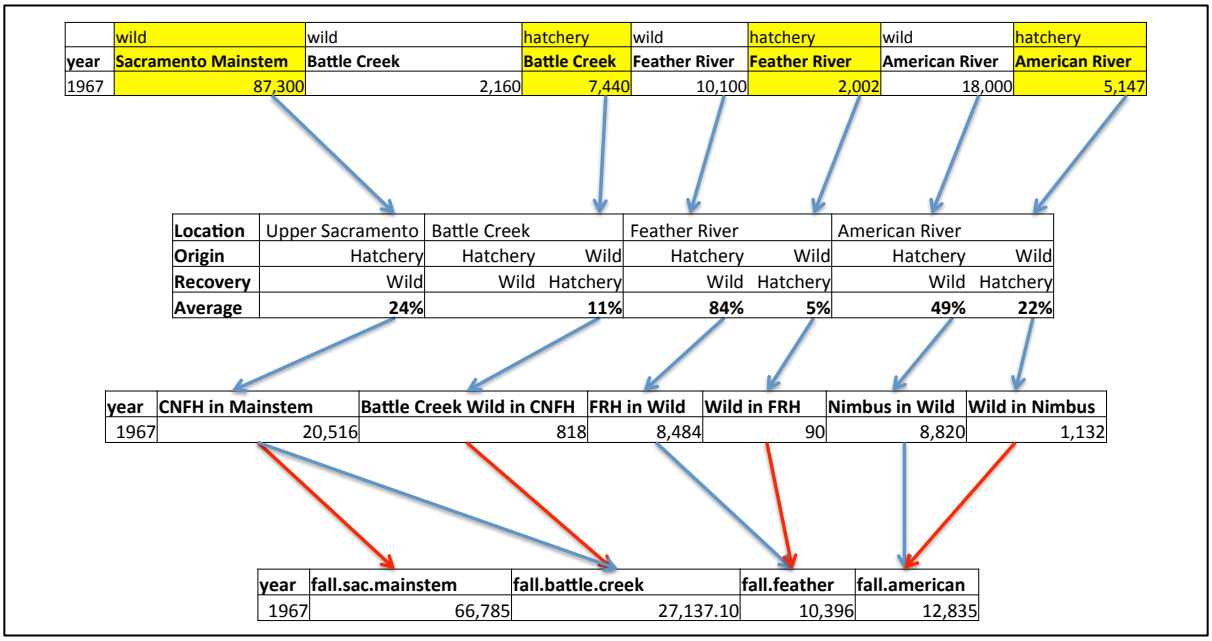

	wild	wild	hatchery	wild	hatchery	wild	hatchery
year	Sacramento Mainstem	Battle Creek	Battle Creek	Feather River	Feather River	American River	American River
1967	87,300	2,160	7,440	10,100	2,002	18,000	5,147

Location	Upper Sacramento	Battle Creek		Feather River		American River	
Origin	Hatchery	Hatchery	Wild	Hatchery	Wild	Hatchery	Wild
Recovery	Wild	Wild	Hatchery	Wild	Hatchery	Wild	Hatchery
Average	24%	11%		84%	5%	49%	22%

year	CNFH in Mainstem	Battle Creek Wild in CNFH	FRH in Wild	Wild in FRH	Nimbus in Wild	Wild in Nimbus
1967	20,516	818	8,484	90	8,820	1,132

year	fall.sac.mainstem	fall.battle.creek	fall.feather	fall.american
1967	66,785	27,137.10	10,396	12,835

Figure 5.1 Empirical schematic showing how the historical abundance of the 1967 population for the four fall-run Chinook populations were reconstructed through additional or removal of the abundance of other stocks.

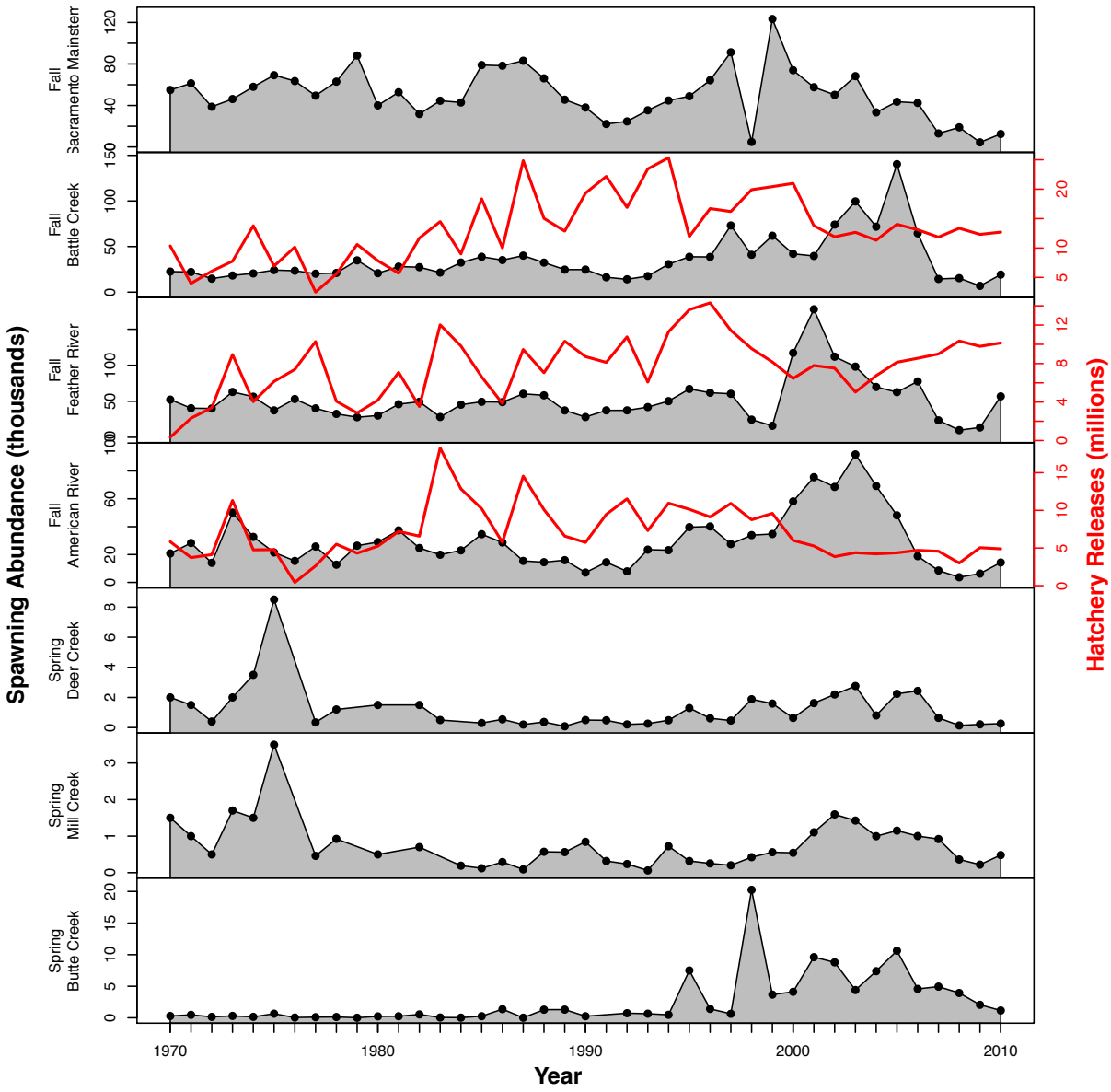

Figure 5.2 Adult abundance (grey area plot) and hatchery release (red line) data for Sacramento River Chinook. Fall-run abundances are reconstructed based upon hatchery-wild stray rate estimates, while spring-run abundances are as reported in GrandTab 2014.

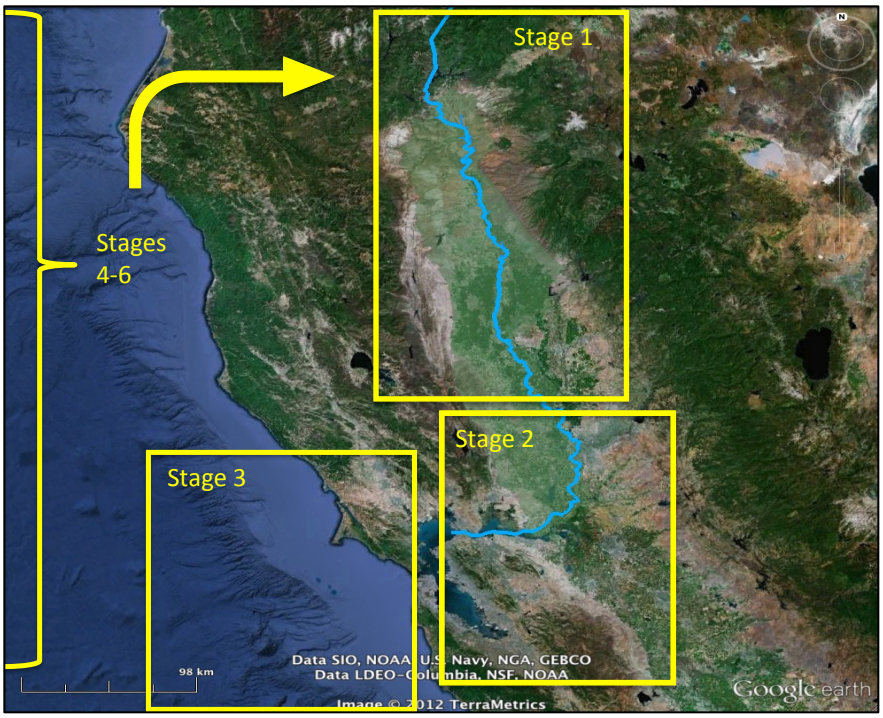

Figure 5.3 Map of estimation model stage structure.

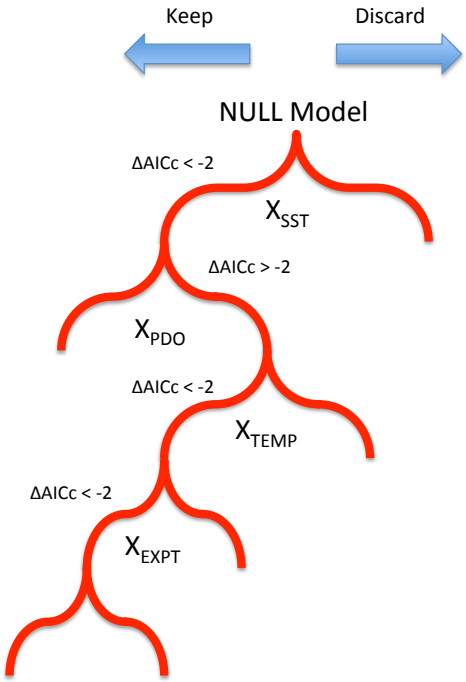

Figure 5.4 Diagram of forward stepwise AICc model building process. Starting from the null model, covariates (X_{TEMP}, X_{PDO} etc.) are sampled at random without replacement from the set of 59 possible hypotheses and included in the statistical model. The model is then fit to abundance data and the difference in AICc values between the old and new models dictates whether that covariate is kept or discarded, and the next iteration begins.

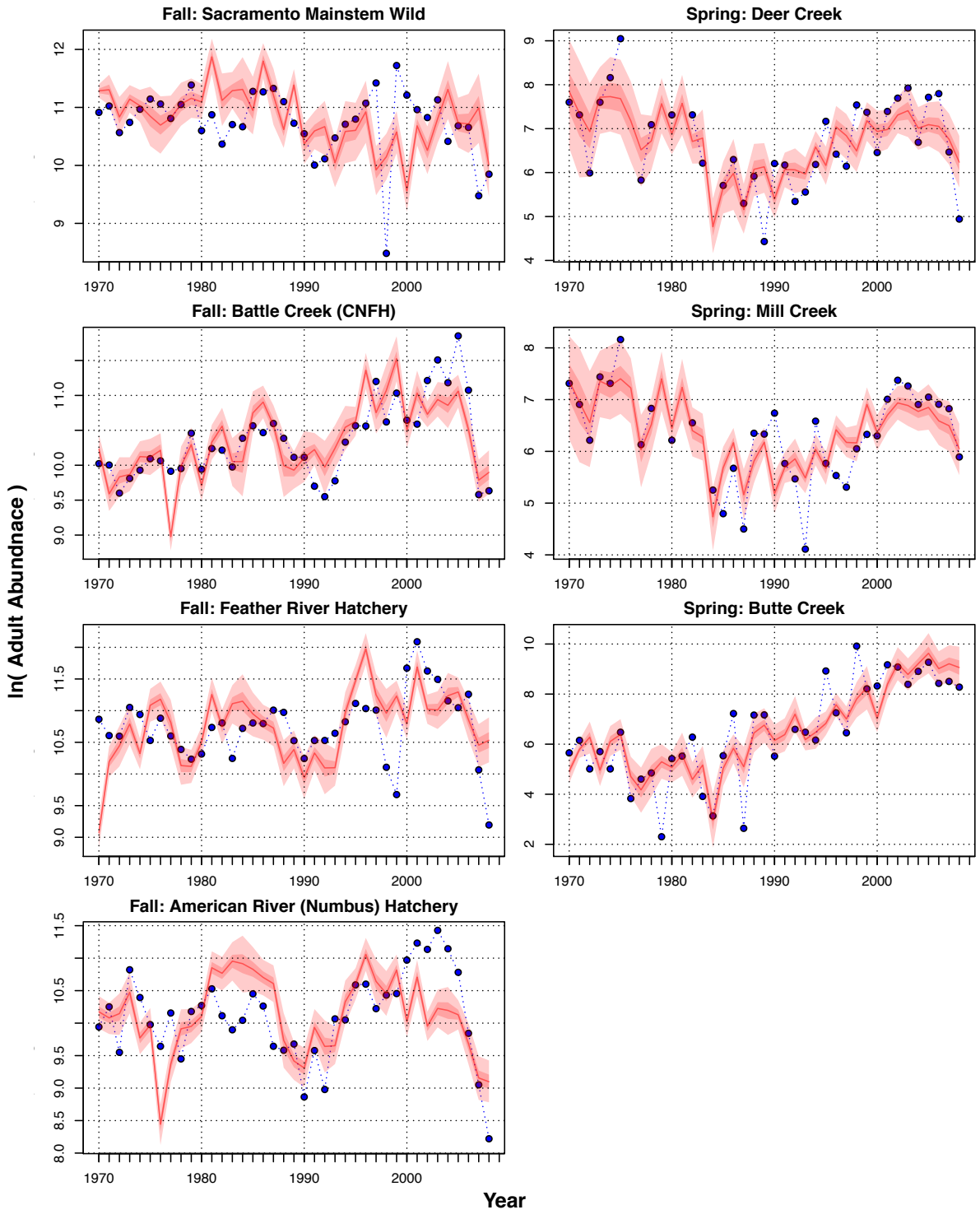

Figure 5.5 Bayesian population dynamics model fit to adult abundance data. Blue points and dashed lines indicate the reconstructed adult abundance in each year on spawning grounds or at hatcheries. Red shaded regions are the 95% and 50% credible intervals, and the red line describes the median of the posterior predictions for abundance in each year. Observed and predicted abundances are presented in natural log space.

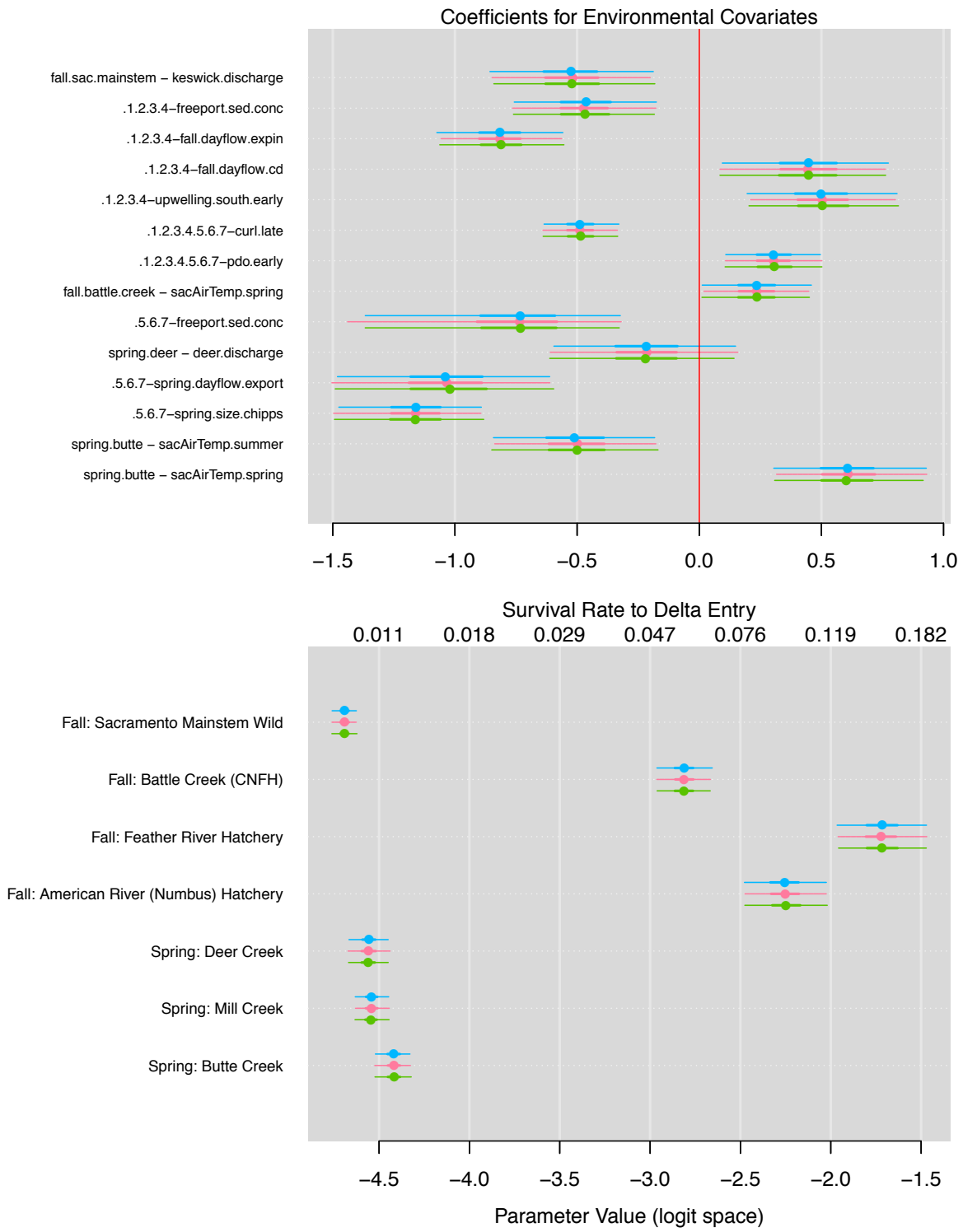

Figure 5.6 Posterior probability distributions for coefficients describing the influence of environmental covariates on survival (top) and the maximum survival rate from egg (or hatchery release) to Sacramento – San Joaquin Delta entry. Caterpillar plots describe the median (dot), 50% credible interval (thick line), and 95% credible interval (thin line) of each posterior. Posteriors from each of the independent MCMC chains are depicted with different colors.

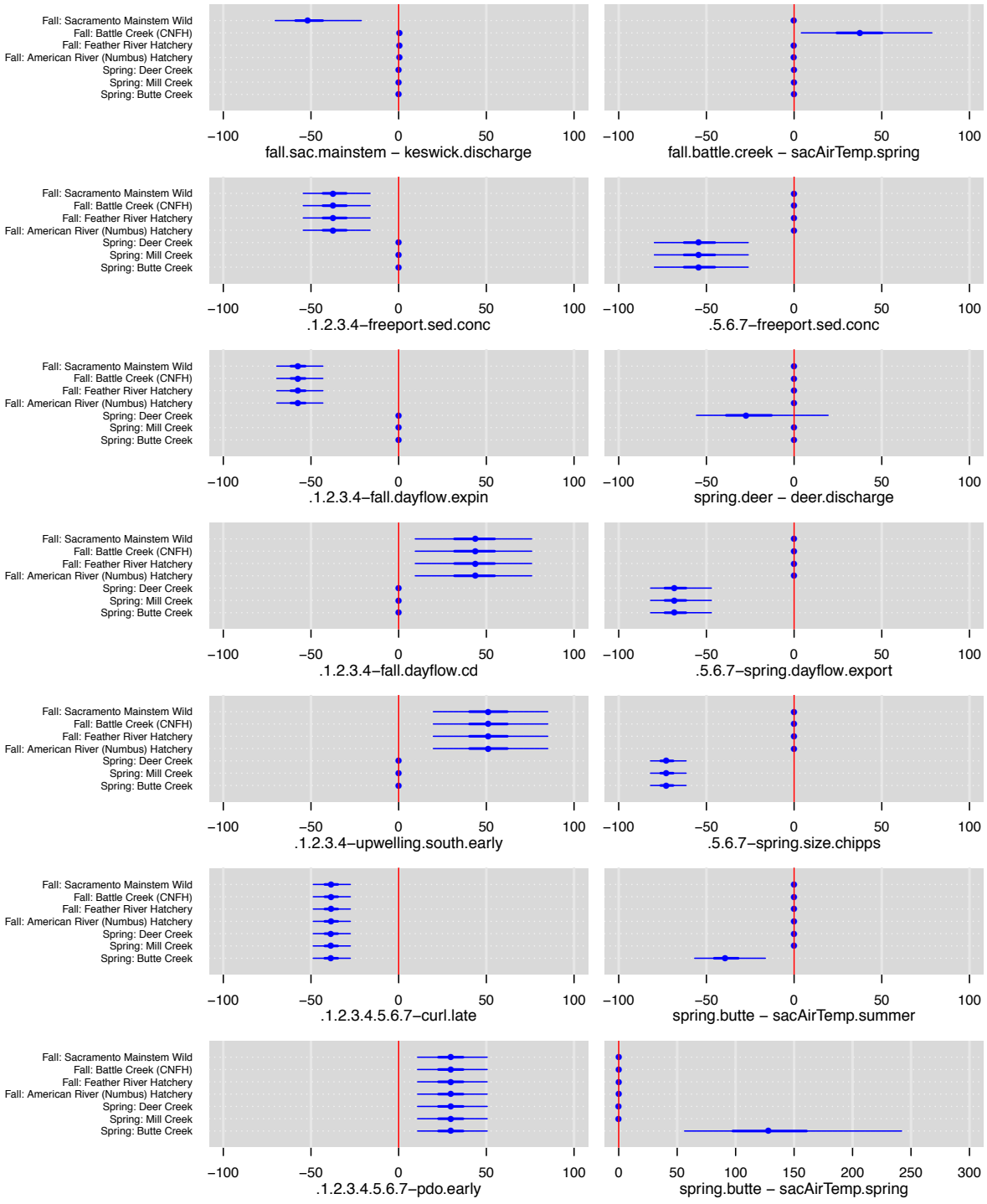

Figure 5.7 Percentage change in egg (or hatchery release) to adult survival resulting from a 1 SD increase in covariate values. Each panel represents the outcome of increasing the value of a specific covariate (listed below the x-axis), with each caterpillar plot describing the effect on each population (y-axis). Plotted values are the difference in survival between a scenario where the covariate value is increased and a base case where all covariates are equal to their long-term mean. Caterpillar plots describe the median (dot), 50% interval (thick line), and 95% interval (thin line) for each survival difference accounting for estimation uncertainty.

Tables

Hypothesis Number	Covariate	Covariate Description	Location	Populations
1	fall.sac.mainstem - sacAirTemp.summer	Sacramento air temperature during summer (July - September) of the brood year	Sacramento, CA	Fall Sacramento Mainstem Wild
2	fall.sac.mainstem - sacAirTemp.spring	Sacramento air temperature during spring (January - March) emergence year	Sacramento, CA	Fall Sacramento Mainstem Wild
3	fall.sac.mainstem - keswick.discharge	Average January - March water discharge (cfs) at Keswick Dam	Keswick Dam	Fall Sacramento Mainstem Wild
4	.1.2.3.4-verona.peak.streamflow	Peak (maximum) streamflow on the Sacramento River mainstem at Verona, CA (January - May)	Verona, Sacramento River	Fall Sacramento Mainstem Wild Fall Battle Creek (CNFH) Hatchery Fall Feather River Hatchery Fall American River (Nimbus) Hatchery
5	.1.2.3.4-yolo.wood.peak.streamflow	Peak (maximum) streamflow into Yolo Bypass at Woodland, CA (January - May)	Into Yolo Bypass at Woodland, CA	Fall Sacramento Mainstem Wild Fall Battle Creek (CNFH) Hatchery Fall Feather River Hatchery Fall American River (Nimbus) Hatchery
6	.1.2.3.4-freeport.sed.conc	Average February - April monthly sediment concentration (mg/L)	Freeport, Sacramento River	Fall Sacramento Mainstem Wild Fall Battle Creek (CNFH) Hatchery Fall Feather River Hatchery Fall American River (Nimbus) Hatchery
7	.1.2.3.4-bass.cpue	Index of Striped Bass abundance as number of striped bass kept	Sacramento - San Joaquin Delta	Fall Sacramento Mainstem Wild Fall Battle Creek (CNFH) Hatchery Fall Feather River Hatchery Fall American River (Nimbus) Hatchery
8	.1.2.3.4-fall.dayflow.geo	Dayflow: Delta Cross Channel and Georgiana Slough Flow Estimate (QXGEO). February - March average	Sacramento - San Joaquin Delta at the Delta Cross Channel and Georgiana Slough	Fall Sacramento Mainstem Wild Fall Battle Creek (CNFH) Hatchery Fall Feather River Hatchery Fall American River (Nimbus) Hatchery
9	.1.2.3.4-fall.dayflow.export	Dayflow: Total Delta Exports and Diversions/Transfers (QEXPORTS). March - May average	Sacramento - San Joaquin Delta	Fall Sacramento Mainstem Wild Fall Battle Creek (CNFH) Hatchery Fall Feather River Hatchery Fall American River (Nimbus) Hatchery
10	.1.2.3.4-fall.dayflow.expin	Dayflow: Export/Inflow Ratio (EXPIN). March - May average	Sacramento - San Joaquin Delta	Fall Sacramento Mainstem Wild Fall Battle Creek (CNFH) Hatchery Fall Feather River Hatchery Fall American River (Nimbus) Hatchery
11	.1.2.3.4-fall.dayflow.cd	Dayflow: Net Channel Depletion (QCD). March - May average	Sacramento - San Joaquin Delta	Fall Sacramento Mainstem Wild Fall Battle Creek (CNFH) Hatchery Fall Feather River Hatchery Fall American River (Nimbus) Hatchery
12	.1.2.3.4-fall.size.chipps	Average size of fall-run Chinook at ocean entry from Chipps Island Trawl	Chipps Island Trawl	Fall Sacramento Mainstem Wild Fall Battle Creek (CNFH) Hatchery Fall Feather River Hatchery Fall American River (Nimbus) Hatchery
13	.1.2.3.4-fall.farallon.temp.early	Average temperature at the Farallon Islands, CA (37° 41.8' N, 122° 59.9' W) during the SPRING months (February - April) BEFORE Chinook ocean entry	Nearshore Region, Farallon Islands, CA	Fall Sacramento Mainstem Wild Fall Battle Creek (CNFH) Hatchery Fall Feather River Hatchery Fall American River (Nimbus) Hatchery
14	.1.2.3.4-fall.farallon.temp.late	Average temperature at the Farallon Islands, CA (37° 41.8' N, 122° 59.9' W) during the SUMMER months (May - July) AFTER Chinook ocean entry	Nearshore Region, Farallon Islands, CA	Fall Sacramento Mainstem Wild Fall Battle Creek (CNFH) Hatchery Fall Feather River Hatchery Fall American River (Nimbus) Hatchery
15	.1.2.3.4-upwelling.north.early	NOAA Index for upwelling at Northern Location (39 N, 125 W), average of SPRING months (April - June)	Nearshore Region	Fall Sacramento Mainstem Wild Fall Battle Creek (CNFH) Hatchery Fall Feather River Hatchery Fall American River (Nimbus) Hatchery
16	.1.2.3.4-upwelling.north.late	NOAA Index for upwelling at Northern Location (39 N, 125 W), average of FALL months (July - December)	Nearshore Region	Fall Sacramento Mainstem Wild Fall Battle Creek (CNFH) Hatchery Fall Feather River Hatchery Fall American River (Nimbus) Hatchery
17	.1.2.3.4-upwelling.south.early	NOAA Index for upwelling at Southern Location (36 N, 122 W), average of SPRING months (April - June)	Nearshore Region	Fall Sacramento Mainstem Wild Fall Battle Creek (CNFH) Hatchery Fall Feather River Hatchery Fall American River (Nimbus) Hatchery
18	.1.2.3.4-upwelling.south.late	NOAA Index for upwelling at Southern Location (36 N, 122 W), average of FALL months (July - December)	Nearshore Region	Fall Sacramento Mainstem Wild Fall Battle Creek (CNFH) Hatchery Fall Feather River Hatchery Fall American River (Nimbus) Hatchery
19	.1.2.3.4.5.6.7-curl.early	NOAA Wind Stress Curl Index for upwelling at Northern Location (39 N, 125 W), average of SUMMER months (April -June)	Nearshore Region	Fall Sacramento Mainstem Wild Fall Battle Creek (CNFH) Hatchery Fall Feather River Hatchery Fall American River (Nimbus) Hatchery Spring Deer Creek Spring Mill Creek Spring Butte Creek
20	.1.2.3.4.5.6.7-curl.late	NOAA Wind Stress Curl for upwelling at Northern Location (39 N, 125 W), average of FALL months (July - December)	Nearshore Region	Fall Sacramento Mainstem Wild Fall Battle Creek (CNFH) Hatchery Fall Feather River Hatchery Fall American River (Nimbus) Hatchery Spring Deer Creek Spring Mill Creek Spring Butte Creek
21	.1.2.3.4.5.6.7-pdo.early	Pacific Decadal Oscillation (PDO), average of January - May monthly indices during first year of mearine residence	Ocean	Fall Sacramento Mainstem Wild Fall Battle Creek (CNFH) Hatchery Fall Feather River Hatchery Fall American River (Nimbus) Hatchery Spring Deer Creek Spring Mill Creek Spring Butte Creek
22	.1.2.3.4.5.6.7-pdo.late	Pacific Decadal Oscillation (PDO), average of October - December monthly indices during first year of mearine residence	Ocean	Fall Sacramento Mainstem Wild Fall Battle Creek (CNFH) Hatchery Fall Feather River Hatchery Fall American River (Nimbus) Hatchery Spring Deer Creek Spring Mill Creek Spring Butte Creek

Hypothesis Number	Covariate	Covariate Description	Location	Populations
23	fall.battle.creek - sacAirTemp.summer	Sacramento air temperature during summer (July - September) of the brood year	Sacramento, CA	Fall Battle Creek (CNFH) Hatchery
24	fall.battle.creek - sacAirTemp.spring	Sacramento air temperature during spring (January - March) emergence year	Sacramento, CA	Fall Battle Creek (CNFH) Hatchery
25	fall.battle.creek - keswick.discharge	Average January - March water discharge (cfs) at Keswick Dam	Keswick Dam	Fall Battle Creek (CNFH) Hatchery
26	fall.battle.creek - battle.discharge	Average January - March water discharge (cfs) on Battle Creek	Cottonwood, Battle Creek	Fall Battle Creek (CNFH) Hatchery
27	fall.battle.creek - battle.peak.gage.ht	Battle Creek peak guage height November - December of brood year	Cottonwood, Battle Creek	Fall Battle Creek (CNFH) Hatchery
28	fall.feather - sacAirTemp.summer	Sacramento air temperature during summer (July - September) of the brood year	Sacramento, CA	Fall Feather River Hatchery
29	fall.feather - sacAirTemp.spring	Sacramento air temperature during spring (January - March) emergence year	Sacramento, CA	Fall Feather River Hatchery
30	fall.feather - keswick.discharge	Average January - March water discharge (cfs) at Keswick Dam	Keswick Dam	Fall Feather River Hatchery
31	fall.feather - feather.oronville.discharge	Average January - March water discharge (cfs) on the Feather River	Oronville, Feather River	Fall Feather River Hatchery
32	fall.american - sacAirTemp.summer	Sacramento air temperature during summer (July - September) of the brood year	Sacramento, CA	Fall American River (Nimbus) Hatchery
33	fall.american - sacAirTemp.spring	Sacramento air temperature during spring (January - March) emergence year	Sacramento, CA	Fall American River (Nimbus) Hatchery
34	fall.american - keswick.discharge	Average January - March water discharge (cfs) at Keswick Dam	Keswick Dam	Fall American River (Nimbus) Hatchery
35	fall.american - american.discharge	Average January - March water discharge (cfs) on the American River	Fair Oaks, American River	Fall American River (Nimbus) Hatchery
36	spring.deer - sacAirTemp.summer	Sacramento air temperature during summer (July - September) of the brood year	Sacramento, CA	Spring Deer Creek
37	spring.deer - sacAirTemp.spring	Sacramento air temperature during spring (January - March) emergence year	Sacramento, CA	Spring Deer Creek
38	.5.6.7-verona.peak.streamflow	Peak (maximum) streamflow on the Sacramento River mainstem at Verona, CA (January - May)	Verona, Sacramento River	Spring Deer Creek Spring Mill Creek Spring Butte Creek
39	.5.6.7-yolo.wood.peak.streamflow	Peak (maximum) streamflow into Yolo Bypass at Woodland, CA (January - May)	Into Yolo Bypass at Woodland, CA	Spring Deer Creek Spring Mill Creek Spring Butte Creek
40	.5.6.7-freeport.sed.conc	Average February - April monthly sediment concentration (mg/L)	Freeport, Sacramento River	Spring Deer Creek Spring Mill Creek Spring Butte Creek
41	.5.6.7-bass.cpue	Index of Striped Bass abundance as number of striped bass kept	Sacramento - San Joaquin Delta	Spring Deer Creek Spring Mill Creek Spring Butte Creek
42	.5.6.7-upwelling.north.early	NOAA Index for upwelling at Northern Location (39 N, 125 W), average of SPRING months (April - June)	Nearshore Region	Spring Deer Creek Spring Mill Creek Spring Butte Creek
43	.5.6.7-upwelling.north.late	NOAA Index for upwelling at Northern Location (39 N, 125 W), average of FALL months (July - December)	Nearshore Region	Spring Deer Creek Spring Mill Creek Spring Butte Creek
44	.5.6.7-upwelling.south.early	NOAA Index for upwelling at Southern Location (36 N, 122 W), average of SPRING months (April - June)	Nearshore Region	Spring Deer Creek Spring Mill Creek Spring Butte Creek
45	.5.6.7-upwelling.south.late	NOAA Index for upwelling at Southern Location (36 N, 122 W), average of FALL months (July - December)	Nearshore Region	Spring Deer Creek Spring Mill Creek Spring Butte Creek
46	spring.deer - deer.discharge	Average October - December water discharge (cfs) at Deer Creek	Vinna, Deer Creek	SpringDeer Creek
47	.5.6.7-spring.dayflow.geo	Dayflow: Delta Cross Channel and Georgiana Slough Flow Estimate (QXGEO). January - March average	Sacramento - San Joaquin Delta at the Delta Cross Channel and Georgiana Slough	Spring Deer Creek Spring Mill Creek Spring Butte Creek
48	.5.6.7-spring.dayflow.export	Dayflow: Total Delta Exports and Diversions/Transfers (QEXPORTS). February - April average	Sacramento - San Joaquin Delta	Spring Deer Creek Spring Mill Creek Spring Butte Creek
49	.5.6.7-spring.dayflow.expin	Dayflow: Export/Inflow Ratio (EXPIN). February - April average	Sacramento - San Joaquin Delta	Spring Deer Creek Spring Mill Creek Spring Butte Creek
50	.5.6.7-spring.dayflow.cd	Dayflow: Net Channel Depletion (QCD). February - April average	Sacramento - San Joaquin Delta	Spring Deer Creek Spring Mill Creek Spring Butte Creek
51	.5.6.7-spring.size.chipps	Average size of spring-run Chinook at ocean entry from Chipps Island Trawl	Chipps Island Trawl	Spring Deer Creek Spring Mill Creek Spring Butte Creek
52	.5.6.7-spring.farallon.temp.early	Temperature at the Farallon Islands, CA (37° 41.8' N, 122° 59.9' W) during the SPRING months (January - March) BEFORE Chinook ocean entry	Nearshore Region	Spring Deer Creek Spring Mill Creek Spring Butte Creek
53	.5.6.7-spring.farallon.temp.late	Temperature at the Farallon Islands, CA (37° 41.8' N, 122° 59.9' W) during the SUMMER months (April - June) AFTER Chinook ocean entry	Nearshore Region, Farallon Islands, CA	Spring Deer Creek Spring Mill Creek Spring Butte Creek
54	spring.mill - sacAirTemp.summer	Sacramento air temperature during summer (July - September) of the brood year	Sacramento, CA	Spring Mill Creek
55	spring.mill - sacAirTemp.spring	Sacramento air temperature during spring (January - March) emergence year	Sacramento, CA	Spring Mill Creek
56	spring.mill - mill.discharge	Average October - December water discharge (cfs) on Mill Creek	Molinos, Mill Creek	Spring Mill Creek
57	spring.butte - sacAirTemp.summer	Sacramento air temperature during summer (July - September) of the brood year	Sacramento, CA	Spring Butte Creek
58	spring.butte - sacAirTemp.spring	Sacramento air temperature during spring (January - March) emergence year	Sacramento, CA	Spring Butte Creek
59	spring.butte - butte.discharge	Average October - December water discharge (cfs) on Butte Creek	Chico, Butte Creek	Spring Butte Creek

Table 5.2 Proportion of observed adult abundance by location estimated from CWT recoveries to be of wild or hatchery origin in 2010 and 2011, and the average used to reconstruct historical abundances.

Location	Origin	Recovery	2010	2011	Average
Upper Sacramento	Hatchery	Wild	20%	27%	**24%**
Battle Creek	Hatchery	Wild			
	Wild	Hatchery	11%	11%	**11%**
Feather River	Hatchery	Wild	78%	90%	**84%**
	Wild	Hatchery	5%	4%	**5%**
American River	Hatchery	Wild	32%	66%	**49%**
	Wild	Hatchery	21%	23%	**22%**

Table 5.3 Model selection results. Percent inclusion rate for environmental covariate effects across 1,000 candidate best-fit models, each resulting from one round of forward stepwise-AICc model building. Note the covariate name includes the single population name, or the numbers for multiple populations upon whose survival the effect of the environmental covariate is shared. For reference population numbers are: 1) fall-run mainstem Sacramento wild-run Chinook, 2) fall-run Battle Creek Coleman National Fish Hatchery produced Chinook, 3) fall-run Feather River Hatchery produced Chinook, 4) fall-run American River Nimbus Hatchery produced Chinook, 5) spring-run Deer Creek wild Chinook, 6) spring-run Mill Creek wild Chinook, and 7) spring-run Butte Creek wild Chinook.

Hypothesis	Covariate	Sum	Percent	Hypothesis	Covariate	Sum	Percent	Hypothesis	Covariate	Sum	Percent
58	spring.butte - sacAirTemp.spring	998	100%	37	spring.deer - sacAirTemp.spring	186	19%	22	.1.2.3.4.5.6.7-pdo.late	11	1%
51	.5.6.7-spring.size.chipps	945	95%	40	.5.6.7-freeport.sed.conc	185	19%	24	fall.battle.creek - sacAirTemp.spring	11	1%
17	.1.2.3.4-upwelling.south.early	783	78%	11	.1.2.3.4-fall.dayflow.cd	182	18%	14	.1.2.3.4-fall.farallon.temp.late	9	1%
21	.1.2.3.4.5.6.7-pdo.early	657	66%	15	.1.2.3.4-upwelling.north.early	169	17%	31	fall.feather - feather.oronville.discharge	9	1%
57	spring.butte - sacAirTemp.summer	571	57%	6	.1.2.3.4-freeport.sed.conc	159	16%	59	spring.butte - butte.discharge	8	1%
48	.5.6.7-spring.dayflow.export	541	54%	56	spring.mill - mill.discharge	131	13%	13	.1.2.3.4-fall.farallon.temp.early	7	1%
9	.1.2.3.4-fall.dayflow.export	484	48%	7	.1.2.3.4-bass.cpue	107	11%	5	.1.2.3.4-yolo.wood.peak.streamflow	3	0%
10	.1.2.3.4-fall.dayflow.expin	374	37%	38	.5.6.7-verona.peak.streamflow	96	10%	16	.1.2.3.4-upwelling.north.late	2	0%
41	.5.6.7-bass.cpue	362	36%	49	.5.6.7-spring.dayflow.expin	95	10%	23	fall.battle.creek - sacAirTemp.summer	2	0%
36	spring.deer - sacAirTemp.summer	359	36%	43	.5.6.7-upwelling.north.late	94	9%	54	spring.mill - sacAirTemp.summer	2	0%
55	spring.mill - sacAirTemp.spring	316	32%	4	.1.2.3.4-verona.peak.streamflow	87	9%	25	fall.battle.creek - keswick.discharge	1	0%
46	spring.deer - deer.discharge	282	28%	3	fall.sac.mainstem - keswick.discharge	85	9%	26	fall.battle.creek - battle.discharge	1	0%
20	.1.2.3.4.5.6.7-curl.late	275	28%	2	fall.sac.mainstem - sacAirTemp.spring	83	8%	27	fall.battle.creek - battle.peak.gage.ht	0	0%
44	.5.6.7-upwelling.south.early	222	22%	29	fall.feather - sacAirTemp.spring	77	8%	28	fall.feather - sacAirTemp.summer	0	0%
50	.5.6.7-spring.dayflow.cd	220	22%	52	.5.6.7-spring.farallon.temp.early	62	6%	30	fall.feather - keswick.discharge	0	0%
18	.1.2.3.4-upwelling.south.late	205	21%	45	.5.6.7-upwelling.south.late	48	5%	32	fall.american - sacAirTemp.summer	0	0%
53	.5.6.7-spring.farallon.temp.late	202	20%	39	.5.6.7-yolo.wood.peak.streamflow	46	5%	33	fall.american - sacAirTemp.spring	0	0%
42	.5.6.7-upwelling.north.early	199	20%	1	fall.sac.mainstem - sacAirTemp.summer	45	5%	34	fall.american - keswick.discharge	0	0%
47	.5.6.7-spring.dayflow.geo	194	19%	12	.1.2.3.4-fall.size.chipps	36	4%	35	fall.american - american.discharge	0	0%
19	.1.2.3.4.5.6.7-curl.early	193	19%	8	.1.2.3.4-fall.dayflow.geo	17	2%				

Table 5.4 Fourteen covariate-by-population effects included in the final AICc-selected model.

Hypothesis Number	Covariate	Covariate Description	Model Stage	Populations
3	fall.sac.mainstem - keswick.discharge	Average January - March water discharge (cfs) at Keswick Dam	Upstream	Fall Sacramento Mair
24	fall.battle.creek - sacAirTemp.spring	Sacramento air temperature during spring (January - March) emergence year	Upstream	Fall Battle Creek (CNF
46	spring.deer - deer.discharge	Average October - December water discharge (cfs) at Deer Creek	Upstream	SpringDeer Creek
57	spring.butte - sacAirTemp.summer	Sacramento air temperature during summer (July - September) of the brood year	Upstream	Spring Butte Creek
58	spring.butte - sacAirTemp.spring	Sacramento air temperature during spring (January - March) emergence year	Upstream	Spring Butte Creek
40	.5.6.7-freeport.sed.conc	Average February - April monthly sediment concentration (mg/L)	Sacramento - San Joaquin Delta	Spring Deer Creek
				Spring Mill Creek
				Spring Butte Creek
48	.5.6.7-spring.dayflow.export	Dayflow: Total Delta Exports and Diversions/Transfers (QEXPORTS). February - April average	Sacramento - San Joaquin Delta	Spring Deer Creek
				Spring Mill Creek
				Spring Butte Creek
51	.5.6.7-spring.size.chipps	Average size of spring-run Chinook at ocean entry from Chipps Island Trawl	Sacramento - San Joaquin Delta	Spring Deer Creek
				Spring Mill Creek
				Spring Butte Creek
6	.1.2.3.4-freeport.sed.conc	Average February - April monthly sediment concentration (mg/L)	Sacramento - San Joaquin Delta	Fall Sacramento Mair
				Fall Battle Creek (CNF
				Fall Feather River Hat
				Fall American River (I
10	.1.2.3.4-fall.dayflow.expin	Dayflow: Export/Inflow Ratio (EXPIN). March - May average	Sacramento - San Joaquin Delta	Fall Sacramento Mair
				Fall Battle Creek (CNF
				Fall Feather River Hat
				Fall American River (I
11	.1.2.3.4-fall.dayflow.cd	Dayflow: Net Channel Depletion (QCD). March - May average	Sacramento - San Joaquin Delta	Fall Sacramento Mair
				Fall Battle Creek (CNF
				Fall Feather River Hat
				Fall American River (I
17	.1.2.3.4-upwelling.south.early	NOAA Index for upwelling at Southern Location (36 N, 122 W), average of SPRING months (April - June)	Nearshore Region	Fall Sacramento Mair
				Fall Battle Creek (CNF
				Fall Feather River Hat
				Fall American River (I
20	.1.2.3.4.5.6.7-curl.late	NOAA Wind Stress Curl for upwelling at Northern Location (39 N, 125 W), average of FALL months (July - December)	Nearshore Region	Fall Sacramento Mair
				Fall Battle Creek (CNF
				Fall Feather River Hat
				Fall American River (I
				Spring Deer Creek
				Spring Mill Creek
				Spring Butte Creek
21	.1.2.3.4.5.6.7-pdo.early	Pacific Decadal Oscillation (PDO), average of January - May monthly indices during first year of mearine residence	1st Ocean Year	Fall Sacramento Mair
				Fall Battle Creek (CNF
				Fall Feather River Hat
				Fall American River (I
				Spring Deer Creek
				Spring Mill Creek
				Spring Butte Creek

Table 5.5 Values for the posterior probability distributions for coefficients describing the influence of environmental covariates ($\boldsymbol{\beta}_{s,p,c}$) on productivity (maximum survival rate).

Covariate	Mean	sd	CV	2.50%	25%	50%	75%	97.50%
fall.sac.mainstem - keswick.discharge	-0.52	0.17	0.32	-0.85	-0.63	-0.52	-0.41	-0.19
.1.2.3.4-freeport.sed.conc	-0.47	0.15	0.32	-0.76	-0.57	-0.47	-0.37	-0.18
.1.2.3.4-fall.dayflow.expin	-0.81	0.13	0.16	-1.06	-0.90	-0.81	-0.73	-0.56
.1.2.3.4-fall.dayflow.cd	0.44	0.17	0.39	0.09	0.33	0.45	0.56	0.77
.1.2.3.4-upwelling.south.early	0.50	0.15	0.31	0.20	0.40	0.50	0.61	0.81
.1.2.3.4.5.6.7-curl.late	-0.49	0.08	0.16	-0.64	-0.54	-0.49	-0.43	-0.33
.1.2.3.4.5.6.7-pdo.early	0.30	0.10	0.33	0.11	0.24	0.31	0.37	0.50
fall.battle.creek - sacAirTemp.spring	0.23	0.11	0.47	0.01	0.16	0.24	0.31	0.45
.5.6.7-freeport.sed.conc	-0.76	0.27	0.35	-1.38	-0.90	-0.73	-0.59	-0.32
spring.deer - deer.discharge	-0.22	0.19	0.87	-0.61	-0.34	-0.22	-0.09	0.15
.5.6.7-spring.dayflow.export	-1.04	0.23	0.22	-1.49	-1.18	-1.03	-0.88	-0.61
.5.6.7-spring.size.chipps	-1.17	0.15	0.13	-1.49	-1.26	-1.16	-1.06	-0.89
spring.butte - sacAirTemp.summer	-0.51	0.17	0.34	-0.84	-0.62	-0.50	-0.39	-0.17
spring.butte - sacAirTemp.spring	0.61	0.16	0.26	0.31	0.50	0.61	0.71	0.93

Table 5.6 Percentage change in egg (or hatchery release) to adult survival resulting from covariate variation. Values in the table are the mean (sd) differences in survival between the base case and a scenario where the value of a specific covariate (row) is increased by 1 standard deviation from the long-term mean.

Covariate	Fall: Sacramento Mainstem Wild	Fall: Battle Creek (CNFH)	Fall: Feather River Hatchery	Fall: American River (Numbus) Hatchery	Spring: Deer Creek	Spring: Mill Creek	Spring: Butte Creek
fall.sac.mainstem - keswick.discharge	-50.2 (12.5)	0.5 (0.1)	0.5 (0.1)	0.5 (0.1)	0 (0)	0 (0)	0 (0)
.1.2.3.4-freeport.sed.conc	-36.5 (10)	-36.5 (10)	-36.5 (10)	-36.5 (10)	0 (0)	0 (0)	0 (0)
.1.2.3.4-fall.dayflow.expin	-57 (6.6)	-57 (6.6)	-57 (6.6)	-57.1 (6.6)	0 (0)	0 (0)	0 (0)
.1.2.3.4-fall.dayflow.cd	43.3 (17.5)	43.3 (17.5)	43.3 (17.5)	43.3 (17.5)	0 (0)	0 (0)	0 (0)
.1.2.3.4-upwelling.south.early	51.1 (16.7)	51.1 (16.7)	51.1 (16.7)	51.1 (16.7)	0 (0)	0 (0)	0 (0)
.1.2.3.4.5.6.7-curl.late	-38.5 (5.4)	-38.5 (5.4)	-38.5 (5.4)	-38.5 (5.4)	-38.5 (5.4)	-38.5 (5.4)	-38.5 (5.4)
.1.2.3.4.5.6.7-pdo.early	29.8 (10.4)	29.8 (10.4)	29.8 (10.4)	29.8 (10.4)	29.8 (10.5)	29.8 (10.5)	29.8 (10.5)
fall.battle.creek - sacAirTemp.spring	-0.2 (0.1)	38.2 (19.4)	-0.2 (0.1)	-0.2 (0.1)	0 (0)	0 (0)	0 (0)
.5.6.7-freeport.sed.conc	0 (0)	0 (0)	0 (0)	0 (0)	-53.8 (13.3)	-53.8 (13.3)	-53.8 (13.3)
spring.deer - deer.discharge	0 (0)	0 (0)	0 (0)	0 (0)	-24.4 (20)	0 (0)	0 (0)
.5.6.7-spring.dayflow.export	0 (0)	0 (0)	0 (0)	0 (0)	-67.2 (9.1)	-67.2 (9.1)	-67.2 (9.1)
.5.6.7-spring.size.chipps	0 (0)	0 (0)	0 (0)	0 (0)	-72.5 (5.3)	-72.5 (5.3)	-72.5 (5.3)
spring.butte - sacAirTemp.summer	0 (0)	0 (0)	0 (0)	0 (0)	0 (0)	0 (0)	-38.4 (10.2)
spring.butte - sacAirTemp.spring	0 (0)	0 (0)	0 (0)	0 (0)	-0.1 (0)	-0.1 (0)	132.8 (47.6)

References

Abbott, J.C., Dunbrack, R.L., and Orr, C.D. 1985. The interaction of size and experience in dominance relationships of juvenile steelhead trout *(Salmo gairdneri)*. Behaviour **92**: 241-253.

Aditya, G., Bhattacharyya, S., Kundu, N., and Saha, G.K. 2005. Frequency-dependent prey-selection of predacious water bugs on *Armigeres subalbatus* immatures. Journal of Vector Borne Diseases **42**(1): 9-14.

Allen, J.A., and Greenwood, J.J.D. 1988. Frequency-dependent selection by predators. Philosophical Transactions of the Royal Society of London. B, Biological Sciences **319**: 485.

Anderson, J.H., Faulds, P.L., Atlas, W.I., Pess, G.R., and Quinn, T.P. 2010. Selection on breeding date and body size in colonizing coho salmon, *Oncorhynchus kisutch*. Molecular Ecology **19**: 2562-2573.

Anderson, J.J., Deas, M., Duffy, P.B., Erickson, D.L., Reisenbichler, R., Rose, K.A., and Smith, P.E. 2009. Independent review of a draft version of the 2009 NMFS OCAP biological opinion. CALFED Sacramento, California.

Baker, M.R., and Schindler, D.E. 2009. Unaccounted mortality in salmon fisheries: non-retention in gillnets and effects on estimates of spawners. Journal of Applied Ecology **46**(4): 752-761.

Baker, M.R., Schindler, D.E., Essington, T.E., and Hilborn, R. 2014. Accounting for escape mortality in fisheries: implications for stock productivity and optimal management. Ecological Applications **24**(1): 55-70.

Bartell, S.M. 1982. Influence of prey abundance on size-selective predation by bluegills. Transactions of the American Fisheries Society **111**(4): 453-461.

Bartholow, J., Heasley, J., Laake, J., Sandelin, J., Coughlan, B.A.K., and Moos, A. 2001. SALMOD: a population model for salmonids: user's manual. Version W3. U.S. Geological Survey, Fort Collins, Colorado.

Battin, J., Wiley, M.W., Ruckelshaus, M.H., Palmer, R.N., Korb, E., Bartz, K.K., and Imaki, H. 2007. Projected impacts of climate change on salmon habitat restoration. Proceedings of the National Academy of Sciences of the United States of America **104**(16): 6720-6725.

Beacham, T.D., and Murray, C.B. 1987. Adaptive variation in body size, age, morphology, egg size, and developmental biology of chum salmon *(Oncorhynchus keta)* in British Columbia. Canadian Journal of Fisheries and Aquatic Sciences **44**: 244-261.

Beacham, T.D., and Murray, C.B. 1989. Variation in developmental biology of sockeye salmon (*Oncorhynchus nerka*) and Chinook salmon (*O. tshawytscha*) in British Columbia. Canadian Journal of Zoology-Revue Canadienne De Zoologie **67**(9): 2081-2089.

Beacham, T.D., and Murray, C.B. 1993. Fecundity and egg size variation in North American Pacific salmon (*Oncorhynchus*). Journal of Fish Biology **42**: 485-508.

Bell, G. 2010. Fluctuating selection: the perpetual renewal of adaptation in variable environments. Philosophical transactions of the Royal Society of London. Series B, Biological sciences **365**(1537): 87-97.

Bernard, D.R. 1983. Variance and bias of catch allocations that use the age composition of escapements. Alaska Department of Fish and Game, Division of Commercial Fisheries,, Anchorage, Alaska.

Berrigan, D. 1991. The allometry of egg size and number in insects. Oikos **60**: 313-321.

Berry, J.F., and Shine, R. 1980. Sexual size dimorphism and sexual selection in turtles (order *Testudines*). Oecologia **44**(2): 185-191.
Beverton, R.J.H., and Holt, S.J. 1957. On the dynamics of exploited fish populations.
Blair, G.R., Rogers, D.E., and Quinn, T.P. 1993. Variation in life history characteristics and morphology of sockeye salmon in the Kvichak River system, Bristol Bay, Alaska. Transactions of the American Fisheries Society **122**: 550-559.
Bolnick, D.I. 2001. Intraspecific competition favours niche width expansion in Drosophila melanogaster. Nature **410**(6827): 463-466.
Branch, T.A., and Hilborn, R. 2010. A general model for reconstructing salmon runs. Canadian Journal of Fisheries and Aquatic Sciences **67**(5): 886-904.
Britton, R.H., and Moser, M.E. 1982. Size specific predation by herons and its effect on the sex-ratio of natural populations of the mosquito fish *Gambusia affinis* Baird and Girard. Oecologia **53**: 146-151.
Brooks, S.P., and Gelman, A. 1998. General methods for monitoring convergence of iterative simulations. Journal of Computational and Graphical Statistics **7**: 434-455.
Burnham, K.P., and Anderson, D.R. 2002. Model selection and multimodel inference : a practical information-theoretic approach. Springer, New York.
California, O.o.t.G.o.t.S.o. 2008. Gov. Schwarzenegger Takes Action to Address Impacts of Vote to Close Commercial and Recreational Salmon Fisheries, Sacramento, CA.
Carlson, S.M., and Quinn, T.P. 2007. Ten years of varying lake level and selection on size-at-maturity in sockeye salmon. Ecology **88**(10): 2620-2629.
Carlson, S.M., Rich, H.B., and Quinn, T.P. 2009. Does variation in selection imposed by bears drive divergence among populations in the size and shape of sockeye salmon? Evolution **63**(5): 1244-1261.
Carlson, S.M., and Seamons, T.R. 2008. A review of quantitative genetic components of fitness in salmonids: implications for adaptation to future change. Evolutionary Applications **1**(2): 222-238.
Carroll, R.J., and Ruppert, D. 1988. Transformation and weighting in regression. Chapman and Hall, New York.
Cavallo, B., Bergman, P.S., and Melgo, J. 2011. Interactive Object-oriented Salmon Simulation (IOS) for the NODOS. Cramer Fish Sciences, Auburn, CA.
Cavallo, B., Merz, J., and Setka, J. 2012. Effects of predator and flow manipulation on Chinook salmon (*Oncorhynchus tshawytscha)* survival in an imperiled estuary. Environmental Biology of Fishes **96**(2-3): 393-403.
Cave, J.D., and Gazey, W.J. 1994. A preseason simulation-model for fisheries on Fraser River sockeye salmon (*Oncorhynchus nerka*). Canadian Journal of Fisheries and Aquatic Sciences **51**(7): 1535-1549.
CDF&W. 2014. GrandTab 2014.04.22: California Central Valley Chinook population report. California Department of Fish and Wildlife.
CDWR. 2014. DAYFLOW Data. *Edited by* C.D.o.W. Resources.
Chasco, B., Hilborn, R., and Punt, A.E. 2007. Run reconstruction of mixed-stock salmon fisheries using age-composition data. Canadian Journal of Fisheries and Aquatic Sciences **64**(11): 1479-1490.
Chen, Y., Chen, L.Q., and Stergiou, K.I. 2003. Impacts of data quantity on fisheries stock assessment. Aquat Sci **65**(1): 92-98.

Claiborne, A.M., Fisher, J.P., Hayes, S.A., and Emmett, R.L. 2011. Size at release, size-selective mortality, and age of maturity of Willamette River Hatchery yearling Chinook salmon. Transactions of the American Fisheries Society **140**(4): 1135-1144.
Clark, J.H., Mcgregor, A., Mecum, R.D., Krasnowski, P., and Carroll, A.M. 2006. The Commercial Salmon Fishery in Alaska. Alaska Fishery Research Bulletin **12**.
Clutton-Brock, T.H., and Harvey, P.H. 1978. Mammals, resources and reproductive strategies. Nature **273**(5659): 191-195.
Conner, J. 1989. Density-dependent sexual selection in the fungus beetle, *Bolitotherus cornutus*. Evolution **43**(7): 1378-1386.
Crump, M.L. 1974. Reproductive strategies in a tropical anuran community.
Cunningham, C.J., Courage, M.G., and Quinn, T.P. 2013. Selecting for the phenotypic optimum: size-related trade-offs between mortality risk and reproductive output in female sockeye salmon. Functional Ecology **27**(5): 1233-1243.
Dann, T.H., Habicht, C., Jasper, J.R., Hoyt, H.A., Barclay, A.W., Templin, W.D., Baker, T.T., West, F.W., and Fair, L.F. 2009. Genetic stock composition of the commercial harvest of sockeye salmon in Bristol Bay, Alaska, 2006-2008. Fishery Manuscript Series 09-06. Alaska Department of Fish and Game, Anchorage, Alaska.
Dann, T.H., Habicht, C., Rogers Olive, S.D., Liller, H.L., Fox, E.K.C., Jasper, J.R., Munro, A.R., Witteveen, M.J., Baker, T.T., Howard, K.G., Volk, E.C., and Templin, W.D. 2012. Stock Composition of Sockeye Salmon Harvests in Fisheries of the Western Alaska Salmon Stock Identification Program (WASSIP), 2006-2008. Alaska Department of Fish and Game, Special Publication. Alaska Department of Fish and Game, Anchorage.
Darwin, C.R. 1874. The descent of man, and selection in relation to sex. Appleton, New York.
Doctor, K.K., and Quinn, T.P. 2009. Potential for adaptation-by-time in sockeye salmon (*Oncorhynchus nerka*): the interactions of body size and in-stream reproductive life span with date of arrival and breeding location. Canadian Journal of Zoology **87**(8): 708-717.
Einum, S., and Fleming, I.A. 2000. Selection against late emergence and small offspring in Atlantic salmon (*Salmo salar*). Evolution **54**: 628-639.
Einum, S., Robertsen, G., and Fleming, I.A. 2008. Adaptive landscapes and density-dependent selection in declining salmonid populations: going beyond numerical responses to human disturbance. Evolutionary Applications **1**(2): 239-251.
Elgar, M.A. 1990. Evolutionary compromise between a few large and many small eggs: comparative evidence in teleost fish. Oikos **59**: 283-287.
Emlen, J.M. 1966. Role of time and energy in food preference. American Naturalist **100**(916): 611-617.
Endler, J.A. 1986. Natural selection in the wild. Princeton University Press, Princeton, N.J.
Ewing, R.D., and Ewing, G.S. 2002. Bimodal length distributions of cultured chinook salmon and the relationship of length modes to adult survival. Aquaculture **209**(1-4): 139-155.
Falconer, D.S. 1981. Introduction to quantitative genetics. Longman, London; New York.
Fitch, H.S. 1985. Variation in clutch and litter size in New World reptiles. University of Kansas Museum of Natural History Miscellaneous Publication(76): 1-76.
Fitzpatrick, B.M., Shook, K., and Izally, R. 2009. Frequency-dependent selection by wild birds promotes polymorphism in model salamanders. BMC Ecology **9**: 12.
Fleming, I.A., and Gross, M.R. 1994. Breeding competition in a pacific salmon (coho: *Oncorhynchus kisutch*): measures of natural and sexual selection. Evolution **48**(3): 637-657.

Fleming, I.A., and Reynolds, J.D. 2004. Salmonid breeding systems. *In* Evolution illuminated: Salmon and their relatives. *Edited by* A.P. Hendry and S.C. Stearns. Oxford University Press, Oxford. pp. 264-294.

Flynn, L., and Hilborn, R. 2003. Identifying the Spatial Distribution of Stocks of Migrating Adult Sockeye Salmon Using Age Composition Data. Alaska Fishery Research Bulletin **10**.

Flynn, L., Punt, A.E., and Hilborn, R. 2006. A hierarchical model for salmon run reconstruction and application to the Bristol Bay sockeye salmon (*Oncorhynchus nerka*) fishery. Canadian Journal of Fisheries and Aquatic Sciences **63**(7): 1564-1577.

Foote, C.J. 1990. An experimental comparison of male and female spawning territoriality in a Pacific salmon. Behaviour **115**(3-4): 283-313.

Fournier, D.A., Sibert, J.R., Majkowski, J., and Hampton, J. 1990. MULTIFAN a likelihood-based method for estimating growth parameters and age composition from multiple length frequency data sets illustrated using data for Southern Bluefin Tuna (*Thunnus maccoyii*). Canadian Journal of Fisheries and Aquatic Sciences **47**(2): 301-317.

Fournier, D.A., Skaug, H.J., Ancheta, J., Ianelli, J., Magnusson, A., Maunder, M.N., Nielsen, A., and Sibert, J. 2012. AD Model Builder: using automatic differentiation for statistical inference of highly parameterized complex nonlinear models. Optimization Methods and Software **27**(2): 233-249.

Gelman, A., Carlin, J.B., Stern, H.S., and Rubin, D.B. 2004. Bayesian data analysis. Chapman & Hall/CRC, Boca Raton, Fla.

Gelman, A., and Rubin, D.B. 1992. Inference from iterative simulation using multiple sequences. Stat Sci **7**: 457-511.

Gende, S.M., Quinn, T.P., Hilborn, R., Hendry, A.P., and Dickerson, B. 2004. Brown bears selectively kill salmon with higher energy content but only in habitats that facilitate choice. Oikos **104**(3): 518-528.

Gende, S.M., Quinn, T.P., and Willson, M.F. 2001. Consumption choice by bears feeding on salmon. Oecologia **127**(3): 372-382.

Gibbons, J.W. 1972. Reproduction, growth, and sexual dimorphism in Canebrake Rattlesnake (*Crotalus horridus atricaudatus*). Copeia(2): 222-&.

Gilbert, J.J., and Williamson, C.E. 1983. Sexual dimorphism in zooplankton (*Copepoda*, *Cladocera*, and *Rotifera*). Annual Review of Ecology and Systematics **14**: 1-33.

Gilhousen, P. 1980. Energy sources and expenditures in Frasier River Canada sockeye salmon *Oncorhynchus nerka* during their spawning migration. International Pacific Salmon Fisheries Commission Bulletin **22**: 1-51.

Good, T.P., Waples, R.S., and Adams, P. 2005. Updated status of federally listed ESUs of West Coast salmon and Steelhead. Northwest Fisheries Science Center

Southwest Fisheries Science Center, Seattle, Washington

Santa Cruz, California.

Grant, P.R., and Grant, B.R. 2002. Unpredictable evolution in a 30-year study of Darwin's finches. Science **296**(5568): 707-711.

Gross, M.R. 1985. Disruptive selection for alternative life histories in salmon. Nature **313**(5997): 47-48.

Gustafson, R.G., Waples, R.S., Myers, J.M., Weitkamp, L.A., Bryant, G.J., Johnson, O.W., and Hard, J.J. 2007. Pacific salmon extinctions: Quantifying lost and remaining diversity. Conservation Biology **21**(4): 1009-1020.

Habicht, C., Seeb, L.W., Myers, K.W., Farley, E.V., and Seeb, J.E. 2010. Summer-fall distribution of stocks of immature sockeye salmon in the Bering Sea as revealed by single-nucleotide polymorphisms. Transactions of the American Fisheries Society **139**(4): 1171-1191.

Hansson, L.A., Nicolle, A., Brodersen, J., Romare, P., Brönmark, C., and Skov, C. 2007. Consequences of fish predation, migration, and juvenile ontogeny on zooplankton spring dynamics. Limnology and Oceanography **52**: 696-706.

Hare, S.R., and Mantua, N.J. 2000. Empirical evidence for North Pacific regime shifts in 1977 and 1989. Prog Oceanogr **47**(2-4): 103-145.

Hare, S.R., Mantua, N.J., and Francis, R.C. 1999. Inverse production regimes: Alaska and West Coast Pacific salmon. Fisheries **24**(1): 6-14.

Hastings, W.K. 1970. Monte Carlo sampling methods using Markov chains and their applications. Biometrika **57**: 97-109.

Hauser, L., Baird, M., Hilborn, R., Seeb, L.W., and Seeb, J.E. 2011. An empirical comparison of SNPs and microsatellites for parentage and kinship assignment in a wild sockeye salmon (*Oncorhynchus nerka*) population. Molecular ecology resources **11**: 150-161.

Hauser, L., and Seeb, J.E. 2008. Advances in molecular technology and their impact on fisheries genetics. Fish and Fisheries **9**: 473-486.

Healey, M.C. 1982. Timing and relative intensity of size-selective mortality of juvenile chum salmon *(Oncorhynchus keta)* during early sea life. Canadian Journal of Fisheries and Aquatic Sciences **39**: 952-957.

Healey, M.C. 1987. The adaptive significance of age and size at maturity in female sockeye salmon (*Oncorhynchus nerka*). Canadian Special Publication of Fisheries and Aquatic Sciences **96**: 110-117.

Heath, D.D., Fox, C.W., and Heath, J.W. 1999. Maternal effects on offspring size: variation through early development of chinook salmon. Evolution **53**: 1605-1611.

Hendrix, A.N., Hilborn, R., Kimmerer, W., and Lessard, R. in prep. Modeling the influence of historical factors on population dynamics of salmon: the OBAN model.

Hendrix, N., Danner, E., Greene, C.M., Imaki, H., and Lindley, S.T. 2014. Life cycle modeling framework for Sacramento River Winter-run Chinook salmon. NOAA Technical Memorandum.

Hendry, A.P., Berg, O.K., and Quinn, T.P. 1999. Condition dependence and adaptation-by-time: breeding date, life history, and energy allocation within a population of salmon. Oikos **85**(3): 499-514.

Hilborn, R. 2012. The evolution of quantitative marine fisheries management 1985-2010. Natural Resource Modeling **25**(1): 122-144.

Hilborn, R., and Mangel, M. 1997. The ecological detective: confronting models with data. Princeton University Press, Princeton, NJ.

Hilborn, R., Maunder, M., Parma, A., Ernst, B., Payne, J., and Starr, P. 2003a. COLERAINE: a generalized age-structured stock assessment model. School of Aquatic and Fishery Sciences, University of Washington, Seattle, Washington.

Hilborn, R., Quinn, T.P., Schindler, D.E., and Rogers, D.E. 2003b. Biocomplexity and fisheries sustainability. Proceedings of the National Academy of Sciences of the United States of America **100**(11): 6564-6568.

Hilborn, R., and Walters, C.J. 1992. Quantitative fisheries stock assessment : choice, dynamics, and uncertainty. Chapman and Hall, New York.

Hoekstra, H.E., Hoekstra, J.M., Berrigan, D., Vignieri, S.N., Hoang, A., Hill, C.E., Beerli, P., and Kingsolver, J.G. 2001. Strength and tempo of directional selection in the wild. Proceedings of the National Academy of Sciences of the United States of America **98**(16): 9157-9160.

Holtby, L.B., and Healey, M.C. 1986. Selection for adult size in female coho salmon (*Oncorhynchus kisutch*). Canadian Journal of Fisheries and Aquatic Sciences **43**(10): 1946-1959.

Honea, J.M., Jorgensen, J.C., McClure, M.M., Cooney, T.D., Engie, K., Holzer, D.M., and Hilborn, R. 2009. Evaluating habitat effects on population status: influence of habitat restoration on spring-run Chinook salmon. Freshwater Biology **54**(7): 1576-1592.

Honek, A. 1993. Intraspecific variation in body size and fecundity in insects - a general relationship. Oikos **66**(3): 483-492.

Huber, E.R., and Carlson, S.M. in review. Temporal trends of California Central Valley fall run Chinook salmon hatchery release practices.

Hughes, A.L., and Hughes, M.K. 1986. Paternal investment and sexual size simorphism in North American passerines. Oikos **46**(2): 171-175.

Hulsmann, S., Rinke, K., and Mooij, W.M. 2005. A quantitative test of the size efficiency hypothesis by means of a physiologically structured model. Oikos **110**(1): 43-54.

Jann, P., Blanckenhorn, W.U., and Ward, P.I. 2000. Temporal and microspatial variation in the intensities of natural and sexual selection in the yellow dung fly Scathophaga stercoraria. Journal of Evolutionary Biology **13**(6): 927-938.

Johnson, J.K. 1990. Regional overview of coded wire tagging of anadromous salmon and steelhead in Northwest America. Am. Fish. Soc. Symp **7**: 127-133.

Johnson, K.F., Monnahan, C.C., McGilliard, C.R., Vert-pre, K.A., Anderson, S.C., Cunningham, C.J., Hurtado-Ferro, F., Licandeo, R.R., Muradian, M.L., Ono, K., Szuwalski, C.S., Valero, J.L., Whitten, A.R., and Punt, A.E. 2014. Time-varying natural mortality in fisheries stock assessment models: identifying a default approach. ICES Journal of Marine Science.

Joshi, A., and Mueller, L.D. 1996. Density-dependent natural selection in Drosophila: Trade-offs between larval food acquisition and utilization. Evolutionary Ecology **10**(5): 463-474.

Kendall, N.W., Hard, J.J., and Quinn, T.P. 2009. Quantifying six decades of fishery selection for size and age at maturity in sockeye salmon. Evolutionary Applications **2**(4): 523-536.

Kendall, N.W., and Quinn, T.P. 2009. Effects of population-specific variation in age and length on fishery selection and exploitation rates of sockeye salmon (*Oncorhynchus nerka*). Canadian Journal of Fisheries and Aquatic Sciences **66**(6): 896-908.

Kesavaraju, B., Alto, B.W., Lounibos, L.P., and Juliano, S.A. 2007. Behavioural responses of larval container mosquitoes to a size-selective predator. Ecological Entomology **32**: 262-272.

King, R., Morgan, B., Gimenez, O., and Brooks, S. 2010. Bayesian analysis for population ecology. CRC Press.

Kingsolver, J.G., and Diamond, S.E. 2011. Phenotypic selection in natural populations: what limits directional selection? American Naturalist **177**(3): 346-357.

Kingsolver, J.G., Hoekstra, H.E., Hoekstra, J.M., Berrigan, D., Vignieri, S.N., Hill, C.E., Hoang, A., Gibert, P., and Beerli, P. 2001. The strength of phenotypic selection in natural populations. American Naturalist **157**(3): 245-261.

Kinnison, M.T., Unwin, M.J., and Quinn, T.P. 1998. Growth and salinity tolerance of juvenile chinook salmon (*Oncorhynchus tshawytscha*) from two introduced New Zealand populations. Canadian Journal of Zoology **76**: 2219-2226.

Knapp, G., Guetttabi, M., and Goldsmith, S. 2013. The Economic Importance of the Bristol Bay Salmon Industry. Institude of Social and Economic Research, University of Alaska Anchorage, Anchorage, Alaska.

Kocan, R., Hershberger, P., Sanders, G., and Winton, J. 2009. Effects of temperature on disease progression and swimming stamina in Ichthyophonus-infected rainbow trout, Oncorhynchus mykiss (Walbaum). J. Fish Dis. **32**(10): 835-843.

Kope, R.G., and Botsford, L.W. 1990. Determination of Factors Affecting Recruitment of Chinook Salmon Oncorhynchus-Tshawytscha in Central California. Fishery Bulletin **88**(2): 257-269.

Kormos, B., Palmer-Zwahlen, M., and Low, A. 2012. Recover of coded-wire tags from Chinook salmon in California's Central Valley escapement and ocean harvest 2010. Fisheries Branch Administrative Report. California Deparment of Fish and Game, Sacramento, Calfornia.

Lapointe, M., Eaton, B., Driscoll, S., and Latulippe. 2000. Modelling the probability of salmonid egg pocket scour due to floods. Canadian Journal of Fisheries and Aquatic Sciences **57**: 1120-1130.

Law, R. 2000. Fishing, selection, and phenotypic evolution. ICES Journal of Marine Science **57**(3): 659-668.

Leather, S.R. 1988. Size, reproductive potential and fecundity in insects: Things aren't as simple as they seem. Oikos **51**(3): 386-389.

Leftwich, P.T., Edward, D.A., Alphey, L., Gage, M.J.G., and Chapman, T. 2012. Variation in adult sex ratio alters the association between courtship, mating frequency and paternity in the lek-forming fruitfly Ceratitis capitata. Journal of Evolutionary Biology **25**(9): 1732-1740.

Levin, B.R., Antonovics, J., and Sharma, H. 1988. Frequency-dependent selection in bacterial populations. Philosophical Transactions of the Royal Society B: Biological Sciences **319**(1196): 459-472.

Lin, J., Quinn, T.P., Hilborn, R., and Hauser, L. 2008. Fine-scale differentiation between sockeye salmon ecotypes and the effect of phenotype on straying. Heredity **101**(4): 341-350.

Lindley, S.T., Grimes, C.B., Mohr, M.S., Peterson, W., Stein, J., Anderson, J.T., Botsford, L.W., Bottom, D.L., Busack, C.A., Collier, T.K., Ferguson, J., Garza, J.C., Grover, A.M., Hankin, D.G., Kope, R.G., Lawson, P.W., Low, A., Macfarlane, R.B., Moore, K., Palmer-Zwahlen, M., Schwing, F.B., Smith, J., Tracy, C., Webb, R., Wells, B.K., and Williams, T.H. 2009. What caused the Sacramento River fall Chinook stock collapse? Pre-publication report to the Pacific Fishery Management Council.

Lindley, S.T., and Mohr, M.S. 2003. Modeling the effect of striped bass (*Morone saxatilis*) on the population viability of Sacramento River winter-run chinook salmon (*Oncorhynchus tshawytscha*). Fishery Bulletin **101**(2): 321-331.

Lindley, S.T., Schick, R., May, B.P., Anderson, J.J., Greene, S., Hanson, C., Low, A., Mcewan, D., Macfarlane, R.B., Swanson, C., Ln, L., and Evans, D.L. 2004. Population structure of threatened and endangered Chinook salmon ESUs in California's Central Valley Basin. Analysis.

MacArthur, R.H. 1962. Some generalized theorems of natural selection. Proceedings of the National Academy of Sciences of the United States of America **48**(11): 1893.
MacArthur, R.H., and Pianka, E.R. 1966. On optimal use of a patchy environment. American Naturalist **100**(916): 603-609.
Macias, D., Franks, P.J.S., Ohman, M.D., and Landry, M.R. 2012. Modeling the effects of coastal wind- and wind-stress curl-driven upwellings on plankton dynamics in the Southern California current system. J. Mar. Syst. **94**: 107-119.
Magnusson, A., and Hilborn, R. 2007. What makes fisheries data informative? Fish and Fisheries **8**(4): 337-358.
Mantua, N.J., and Hare, S.R. 2002. The Pacific decadal oscillation. Journal of Oceanography **58**(1): 35-44.
Mathews, S.B. 1968. An estimate of ocean mortality of Bristol Bay sockeye salmon three years at sea. Journal of the Fisheries Research Board of Canada **25**: 1219-1227.
Maunder, M.N., Deriso, R.B., and Hanson, C.H. 2015. Use of state-space population dynamics models in hypothesis testing: advantages over simple log-linear regressions for modeling survival, illustrated with application to longfin smelt (Spirinchus thaleichthys). Fisheries Research **164**: 102-111.
McAllister, M.K., and Ianelli, J.N. 1997. Bayesian stock assessment using catch-age data and the sampling - Importance resampling algorithm. Canadian Journal of Fisheries and Aquatic Sciences **54**(2): 284-300.
McGlauflin, M.T., Schindler, D.E., Seeb, L.W., Smith, C.T., Habicht, C., and Seeb, J.E. 2011. Spawning Habitat and Geography Influence Population Structure and Juvenile Migration Timing of Sockeye Salmon in the Wood River Lakes, Alaska. Transactions of the American Fisheries Society **140**(3): 763-782.
McPhee, M.V., and Quinn, T.P. 1998. Factors affecting the duration of nest defense and reproductive lifespan of female sockeye salmon, *Oncorhynchus nerka*. Environmental Biology of Fishes **51**: 369-375.
Megrey, B.A. 1989. Review and comparison of age-structured stock assessment models from theoretical and applied points of view. *In* Mathematical Analysis of Fish Stock Dynamics. *Edited by* E.F. Edwards and B.A. Megrey. American Fisheries Society, Bethesda, Maryland. pp. 8-48.
Menard, J., and Miller, J.C. 1997. Report to the Alaska Board of Fisheries on the stock composition of sockeye salmon catches within east side Bristol Bay fishing districts, 1983-1995. Regional Information Rep. 2A97-31. Alaska Department of Fish and Game, Division of Commercial Fisheries Management and Development, Anchorage, Alaska.
Metropolis, N., Rosenbluth, A.W., Rosenbluth, M.N., Teller, A.H., and Teller, E. 1953. Equations of state calculations by fast computing machines. Journal of Chemical Physics **21**: 1087-1092.
Michel, C.J. 2010. River and estuarine survival and migration of yearling Sacramento River Chinook salmon (*Oncorhynchus tshawytscha*) smolts and the influence of environment, University of California, Santa Cruz, Santa Cruz, California.
Milner, J.M., Albon, S.D., Illius, A.W., Pemberton, J.M., and Clutton-Brock, T.H. 1999. Repeated selection of morphometric traits in the Soay sheep on St Kilda. Journal of Animal Ecology **68**(3): 472-488.

Minard, R.E., and Meacham, C.P. 1987. Sockeye salmon (*Oncorhynchus nerka*) management in Bristol Bay, Alaska. Canadian Special Publication of Fisheries and Aquatic Sciences **96**: 336-342.
Moorcroft, P.R., Albon, S.D., Pemberton, J.M., Stevenson, I.R., and Clutton-Brock, T.H. 1996. Density-dependent selection in a fluctuating ungulate population. Proceedings of the Royal Society of London. Series B, Biological sciences **263**(1366): 31-38.
Moore, J.W., and Schindler, D.E. 2004. Nutrient export from freshwater ecosystems by anadromous sockeye salmon (Oncorhynchus nerka). Canadian Journal of Fisheries and Aquatic Sciences **61**(9): 1582-1589.
Mossman, A.S. 1958. Selective predation of glaucous-winged gulls upon adult red salmon. Ecology **39**: 482-486.
Moussalli, E., and Hilborn, R. 1986. Optimal Stock Size and Harvest Rate in Multistage Life-History Models. Canadian Journal of Fisheries and Aquatic Sciences **43**(1): 135-141.
Mueller, L.D. 1997. Theoretical and empirical examination of density-dependent selection. Annual Review of Ecology and Systematics **28**: 269-288.
Murray, C.B., and McPhail, J.D. 1988. Effect of incubation-temperature on the development of 5 species of Pacific salmon (*Oncorhynchus*) embryos and alevins. Canadian Journal of Zoology-Revue Canadienne De Zoologie **66**(1): 266-273.
Myrick, C.A., and Chech, J.J. 1998. Temperature effects on Chinook salmon and Steelhead: a review focusing on California's Central Valley populations. *In* Bay-Delta Modeling Forum.
Neuswanger, J., Wipfli, M.S., Rosenberger, A.E., and Hughes, N.F. 2014. Mechanisms of drift-feeding behavior in juvenile Chinook salmon and the role of inedible debris in a clear-water Alaskan stream. Environmental Biology of Fishes **97**(5): 489-503.
Newman, K.B., and Brandes, P.L. 2010. Hierarchical Modeling of Juvenile Chinook Salmon Survival as a Function of Sacramento-San Joaquin Delta Water Exports. North American Journal of Fisheries Management **30**(1): 157-169.
Newman, K.B., and Rice, J. 2002. Modeling the survival of Chinook salmon smolts outmigrating through the lower Sacramento River system. Journal of the American Statistical Association **97**(460): 983-993.
NMFS. 2009. Biological opinion and conference opinion on the long-term operations of the Central Valley Project and State Water Project. National Marine Fisheries Service, Southwest Region.
NRC. 2010. A scientific assessment of alternatives for reducing water management effects on threatened and endangered fishes in California's Bay Delta. National Research Council Committee on Sustainable Water and Environmental Management in the California Bay-Delta, Washington, D. C.
O'Reilly, P.T., Herbinger, C., and Wright, J.M. 1998. Analysis of parentage determination in Atlantic salmon (*Salmo salar*) using microsatellites. Anim. Genet. **29**(5): 363-370.
Olendorf, R., Rodd, F.H., Punzalan, D., Houde, A.E., Hurt, C., Reznick, D.N., and Hughes, K.A. 2006. Frequency-dependent survival in natural guppy populations. Nature **441**: 633-636.
Olsen, E.M., Heino, M., Lilly, G.R., Morgan, M.J., Brattey, J., Ernande, B., and Dieckmann, U. 2004. Maturation trends indicative of rapid evolution preceded the collapse of northern cod. Nature **428**(6986): 932-935.
Olsson, M.M., and Shine, R. 1997. The seasonal timing of oviposition in sand lizards (*Lacerta agilis*): why early clutches are better. Journal of Evolutionary Biology **10**: 369-381.

Ono, K., Licandeo, R., Muradian, M.L., Cunningham, C.J., Anderson, S.C., Hurtado-Ferro, F., Johnson, K.F., McGilliard, C.R., Monnahan, C.C., Szuwalski, C.S., Valero, J.L., Vert-Pre, K.A., Whitten, A.R., and Punt, A.E. 2014. The importance of length and age composition data in statistical age-structured models for marine species. ICES Journal of Marine Science.

Owen-Smith, N., and Mills, M.G.L. 2008. Shifting prey selection generates contrasting herbivore dynamics within a large-mammal predator-prey web. Ecology **89**(4): 1120-1133.

Palmer-Zwahlen, M., and Kormos, B. 2013. Recovery of coded-wire tags from Chinook salmon in California's Central Valley escapement and ocean harvest in 2011. Fisheries Branch Administrative Report. California Department of Fish and Wildlife, Sacramento, California.

Partridge, L. 1988. The rare-male effect: what is its evolutionary significance? Philosophical Transactions of the Royal Society B: Biological Sciences **319**(1196): 525-539.

Perry, R.W., Skalski, J.R., Brandes, P.L., Sandstrom, P.T., Klimley, A.P., Ammann, A., and MacFarlane, B. 2010. Estimating survival and migration route probabilities of juvenile Chinook salmon in the Sacramento-San Joaquin River Delta. North American Journal of Fisheries Management **30**(1): 142-156.

Pianka, E.R. 1970. R-selection and K-selection. American Naturalist **104**(940): 592-&.

Potter, E.C.E., Crozier, W.W., Schon, P.J., Nicholson, M.D., Maxwell, D.L., Prevost, E., Erkinaro, J., Gudbergsson, G., Karlsson, L., Hansen, L.P., MacLean, J.C., Maoileidigh, N.O., and Prusov, S. 2004. Estimating and forecasting pre-fishery abundance of Atlantic salmon (Salmo salar L.) in the Northeast Atlantic for the management of mixed-stock fisheries. ICES Journal of Marine Science **61**(8): 1359-1369.

Poytress, W.R., Gruber, J.J., Carrillo, F.D., and Voss, S.D. 2014. Compendium report of Red Bluff Diversion Dam rotary trap juvenile anadromous fish production indices for years 2002-2012. Report of U.S. Fish and Wildlife Service to California Department of Fish and Wildlife and US Bureau of Reclamation.

Preziosi, R.F., Fairbairn, D.J., Roff, D.A., and Brennan, J.M. 1996. Body size and fecundity in the waterstrider *Aquarius remigis*: A test of Darwin's fecundity advantage hypothesis. Oecologia **108**(3): 424-431.

Prugh, L.R. 2005. Coyote prey selection and community stability during a decline in food supply. Oikos **110**(2): 253-264.

Punzalan, D., Rodd, F.H., and Rowe, L. 2010. Temporally variable multivariate sexual selection on sexually dimorphic traits in a wild insect population. The American naturalist **175**(4): 401-414.

Pyper, B.J., and Peterman, R.M. 1999. Relationship among adult body length, abundance, and ocean temperature for British Columbia and Alaska sockeye salmon (*Oncorhynchus nerka*), 1967-1997. Canadian Journal of Fisheries and Aquatic Sciences **56**(10): 1716-1720.

Pyper, B.J., Peterman, R.M., Lapointe, M.F., and Walters, C.J. 1999. Patterns of covariation in length and age at maturity of British Columbia and Alaska sockeye salmon (*Oncorhynchus nerka*) stocks. Canadian Journal of Fisheries and Aquatic Sciences **56**: 1046-1057.

Quinn, T.P. 2005. The behavior and ecology of Pacific salmon and trout. University of Washington Press, Seattle.

Quinn, T.P., and Buck, G.B. 2001. Size- and sex-selective mortality of adult sockeye salmon: Bears, gulls, and fish out of water. Transactions of the American Fisheries Society **130**(6): 995-1005.
Quinn, T.P., Carlson, S.M., Gende, S.M., and Rich, H.B. 2009. Transportation of Pacific salmon carcasses from streams to riparian forests by bears. Canadian Journal of Zoology **87**: 195-203.
Quinn, T.P., and Foote, C.J. 1994. The effects of body size and sexual dimorphism on the reproductive behavior of sockeye salmon, *Oncorhynchus nerka*. Animal Behaviour **48**(4): 751-761.
Quinn, T.P., Gende, S.M., Ruggerone, G.T., and Rogers, D.E. 2003. Density-dependent predation by brown bears (*Ursus arctos*) on sockeye salmon (*Oncorhynchus nerka*). Canadian Journal of Fisheries and Aquatic Sciences **60**(5): 553-562.
Quinn, T.P., Hendry, A.P., and Buck, G.B. 2001a. Balancing natural and sexual selection in sockeye salmon: interactions between body size, reproductive opportunity and vulnerability to predation by bears. Evolutionary Ecology Research **3**: 917-937.
Quinn, T.P., Hendry, A.P., and Wetzel, L.A. 1995. The influence of life history trade-offs and the size of incubation gravels on egg size variation in sockeye salmon (*Oncorhynchus nerka*). Oikos **74**(3): 425-438.
Quinn, T.P., and Kinnison, M.T. 1999. Size-selective and sex-selective predation by brown bears on sockeye salmon. Oecologia **121**(2): 273-282.
Quinn, T.P., Stewart, I.J., and Boatright, C.P. 2006. Experimental evidence of homing to site of incubation by mature sockeye salmon, *Oncorhynchus nerka*. Animal Behaviour **72**(4): 941-949.
Quinn, T.P., Wetzel, L., Bishop, S., Overberg, K., and Rogers, D.E. 2001c. Influence of breeding habitat on bear predation and age at maturity and sexual dimorphism of sockeye salmon populations. Canadian Journal of Zoology-Revue Canadienne De Zoologie **79**: 1782-1793 ST - Influence of breeding habitat on b.
Randa, L.A., Cooper, D.M., Meserve, P.L., and Yunger, J.A. 2009. Prey switching of sympatric canids in response to variable prey abundance. J Mammal **90**(3): 594-603.
Reimchen, T.E. 2000. Some ecological and evolutionary aspects of bear-salmon interactions in coastal British Columbia. Canadian Journal of Zoology **78**(3): 448-457.
Restrepo, V.R., and Legault, C.M. 1995. Approximations for solving the catch equation when it involves a plus group. Fishery Bulletin **93**(2): 308-314.
Reznick, D., and Endler, J.A. 1982. The impact of predation on life-history evolution in Trinidadian guppies (*Poecilia reticulata*). Evolution **36**(1): 160-177.
Rich, H.B., Jr, Carlson, S.M., Chasco, B.E., Briggs, K.C., and Quinn, T.P. 2006. Movements of male sockeye salmon, *Oncorhynchus nerka*, on spawning grounds: the effects of in-stream residency, density, and body size. Animal Behaviour **71**: 971-981.
Ricker, W.E. 1976. Review of the rate of growth and mortality of Pacific salmon in salt water, and noncatch mortality caused by fishing. Journal of the Fisheries Research Board of Canada **33**: 1483-1525.
Rieseberg, L.H., Widmer, A., Arntz, A.M., and Burke, J.M. 2002. Directional selection is the primary cause of phenotypic diversification. Proceedings of the National Academy of Sciences of the United States of America **99**(19): 12242-12245.
Roff, D.A. 1992. The evolution of life histories: theory and analysis. Chapman and Hall, New York.

Rose, K.A., Anderson, J.J., McClure, M.M., and Ruggerone, G.T. 2011. Salmonid integrated life cycle models workshop: Report of the independent review pannel. Delta Science Program.

Ruckelshaus, M.H., Levin, P., Johnson, J.B., and Kareiva, P.M. 2002. The Pacific salmon wars: What science brings to the challenge of recovering species. Annual Review of Ecology and Systematics **33**: 665-706.

Ruggerone, G.T., Hanson, R., and Rogers, D.E. 2000. Selective predation by brown bears (*Ursus arctos*) foraging on spawning sockeye salmon (*Oncorhynchus nerka*). Canadian Journal of Zoology **78**(6): 974-981.

Ryan, T.P. 1997. Modern regression methods. Wiley, New York.

Scheuerell, M.D., Hilborn, R., Ruckelshaus, M.H., Bartz, K.K., Lagueux, K.M., Haas, A.D., and Rawson, K. 2006. The Shiraz model: a tool for incorporating anthropogenic effects and fish-habitat relationships in conservation planning. Canadian Journal of Fisheries and Aquatic Sciences **63**(7): 1596-1607.

Schnute, J., and Sibert, J. 1983. The salmon terminal fishery: a practical, comprehensive timing model. Canadian Journal of Fisheries and Aquatic Sciences **40**(7): 835-853.

Schnute, J.T., and Haigh, R. 2007. Compositional analysis of catch curve data, with an application to Sebastes maliger. Ices Journal of Marine Science **64**(2): 218-233.

Schuett-Hames, D.E., Peterson, N.P., Conrad, R., and Quinn, T.P. 2000. Patterns of gravel scour and fill after spawning by chum salmon in a western Washington stream. North American Journal of Fisheries Management **20**: 610-617.

Seamons, T.R., Bentzen, P., and Quinn, T.P. 2007. DNA parentage analysis reveals inter-annual variation in selection: results from 19 consecutive brood years in steelhead trout. Evolutionary Ecology Research **9**: 409-431.

Semlitsch, R.D., and Gibbons, J.W. 1982. Body size dimorphism and sexual selection in two species of water snakes. Copeia(4): 974-976.

Serbezov, D., Bernatchez, L., Olsen, E.M., and Vøllestad, L.A. 2010. Mating patterns and determinants of individual reproductive success in brown trout (*Salmo trutta*) revealed by parentage analysis of an entire stream living population. Molecular Ecology **19**: 3193-3205.

Shaklee, J.B., Beacham, T.D., Seeb, L., and White, B.A. 1999. Managing fisheries using genetic data: case studies from four species of Pacific salmon. Fisheries Research **43**(1-3): 45-78.

Shaw, R.D. 1998. An archaeology of the Central Yupik: A regional overview for the Yukon-Kuskokwim Delta, northern Bristol Bay, and Nunivak Island. Arct. Anthropol. **35**(1): 234-246.

Shigemiya, Y. 2004. Reversible frequency-dependent predation of a puffer, *Takifugu niphobles* (Pisces : Tetraodontidae), related to spatial distribution of colour-polymorphic prey. Biol. J. Linnean Soc. **81**(2): 197-202.

Shine, R. 1979. Sexual selection and sexual dimorphism in the Amphibia. Copeia(2): 297-306.

Shine, R. 1988. The evolution of large body size in remales: A critique of Darwin's fecundity advantage model. American Naturalist **131**(1): 124-131.

Shine, R., LeMaster, M.P., Moore, I.T., Olsson, M.M., and Mason, R.T. 2001. Bumpus in the snake den: effects of sex, size, and body condition on mortality of red-sided garter snakes. Ecology **55**: 598-604.

Siepielski, A.M., DiBattista, J.D., and Carlson, S.M. 2009. It's about time: the temporal dynamics of phenotypic selection in the wild. Ecology letters **12**(11): 1261-1276.

Siepielski, A.M., DiBattista, J.D., Evans, J.A., and Carlson, S.M. 2011. Differences in the temporal dynamics of phenotypic selection among fitness components in the wild. Proceedings. Biological sciences / The Royal Society **278**(1711): 1572-1580.

Sims, S.E. 1982. Algorithms for solving the catch equation forward and backward in time. Canadian Journal of Fisheries and Aquatic Sciences **39**(1): 197-202.

Sinervo, B., and Licht, P. 1991. Proximate constraints on the evolution of egg size, number, and total clutch mass in lizards. Science **252**: 1300-1302.

Sinervo, B., Svensson, E., and Comendant, T. 2000. Density cycles and an offspring quantity and quality game driven by natural selection. Nature **406**(6799): 985-988.

Smith, C.C., and Fretwell, S.D. 1974. The optimal balance between size and number of offspring. American Naturalist **108**: 499-506.

Smith, M.J. 2010. Genetics provide a forty-five year retrospective of sockeye salmon (*Oncorhynchus nerka*) harvest compositions in Bristol Bay, Alaska, School of Aquatic and Fishery Sciences, University of Washington, Seattle, Washington.

Smith, M.J., Pascal, C.E., Grauvogel, Z., Habicht, C., Seeb, J.E., and Seeb, L.W. 2011. Multiplex preamplification PCR and microsatellite validation enables accurate single nucleotide polymorphism genotyping of historical fish scales. Molecular ecology resources **11 Suppl 1**: 268-277.

Sogard, S.M. 1997. Size-selective mortality in the juvenile stage of teleost fishes: A review. Bulletin of Marine Science **60**(3): 1129-1157.

Sokal, R.R., and Rohlf, F.J. 1981. Biometry : the principles and practice of statistics in biological research. W. H. Freeman, San Francisco.

Sommer, T., Harrell, B., Nobriga, M., Brown, R., Moyle, P., Kimmerer, W., and Schemel, L. 2001a. California's Yolo Bypass: Evidence that flood control can be compatible with fisheries, wetlands, wildlife, and agriculture. Fisheries **26**(8): 6-16.

Sommer, T.R., Nobriga, M.L., Harrell, W.C., Batham, W., and Kimmerer, W.J. 2001b. Floodplain rearing of juvenile chinook salmon: evidence of enhanced growth and survival. Canadian Journal of Fisheries and Aquatic Sciences **58**(2): 325-333.

Starr, P., and Hilborn, R. 1988. Reconstruction of Harvest Rates and Stock Contribution in Gauntlet Salmon Fisheries - Application to British-Columbia and Washington Sockeye (Oncorhynchus-Nerka). Canadian Journal of Fisheries and Aquatic Sciences **45**(12): 2216-2229.

Stearns, S.C. 1992. The evolution of life histories. Oxford University Press, Oxford.

Steen, R.P., and Quinn, T.P. 1999. Egg burial depth by sockeye salmon (*Oncorhynchus nerka*): implications for survival of embryos and natural selection on female body size. Canadian Journal of Zoology **77**: 836-841.

Stevens, D.E., and Miller, L.W. 1983. Effects of river flow on abundance of young Chinook salmon, American Shad, Longfin Smelt, and Delta Smelt in the Sacramento-San Joaquin River system. North American Journal of Fisheries Management **3**: 425-437.

Straty, R.R. 1975. Migratory routes of adult sockeye salmon Oncorhynchus nerka in the eastern Bering Sea and Bristol Bay. NOAA (National Oceanic and Atmospheric Administration) Technical Report NMFS (National Marine Fisheries Service) SSRF (Special Scientific Report Fisheries) **690**: 1-32.

Svensson, E. 1997. Natural selection on avian breeding time: causality, fecundity-dependent, and fecundity-independent selection. Evolution **51**: 1276-1283.

Taberlet, P., Griffin, S., Goossens, B., Questiau, S., Manceau, V., Escaravage, N., Waits, L.P., and Bouvet, J. 1996. Reliable genotyping of samples with very low DNA quantities using PCR. Nucleic Acids Res **24**(16): 3189-3194.

Templin, W.D., Collie, J.S., and Quinn, T.J.I. 1996. Run reconstruction of the wild pink salmon fishery in Prince William Sound, 1990-1991. American Fisheries Society Symposium; Proceedings of the Exxon Valdez oil spill symposium **18**: 499-508.

Thornhill, R., and Alcock, J. 1983. The evolution of insect mating systems. Harvard University Press, Cambridge, Mass.

Tomkins, J.L., and Brown, G.S. 2004. Population density drives the local evolution of a threshold dimorphism. Nature **431**(7012): 1099-1103.

Tompkins, M.R. 2006. Floodplain connectivity and river corridor complexity: Implications for river restoration and planning for floodplain management, University of California, Berkley.

Trexler, J.C., Tempe, R.C., and Travis, J. 1994. Size-selective predation of sailfin mollies by two species of heron. Oikos **69**: 250-258.

van den Berghe, E.P., and Gross, M.R. 1989. Natural selection resulting from female breeding competition in a pacific salmon (coho: *Oncorhynchus kisutch*). Evolution **43**: 125-140.

Veuille, M. 1980. Sexual-behavior and evolution of sexual dimorphism in body size in *Jaera* (Isopoda Asellota). Biol. J. Linnean Soc. **13**(1): 89-100.

Ward, P.D., McReynolds, T.R., and Garman, C.E. 2003. Butte Creek spring-run Chinook salmon, *Oncorhynchus tshawytscha* pre-spawn mortality evaluation, 2003. Inland Fisheries Administrative Report. California Department of Fish and Game, Chico, California.

Weber, E.D., and Fausch, K.D. 2005. Competition between hatchery-reared and wild juvenile Chinook salmon in enclosures in the Sacramento River, California. Transactions of the American Fisheries Society **134**(1): 44-58.

Wells, B.K., Field, J.C., Thayer, J.A., Grimes, C.B., Bograd, S.J., Sydeman, W.J., Schwing, F.B., and Hewitt, R. 2008. Untangling the relationships among climate, prey and top predators in an ocean ecosystem. Marine Ecology-Progress Series **364**: 15-29.

Wells, B.K., Grimes, C.B., Field, J.C., and Reiss, C.S. 2006. Covariation between the average lengths of mature coho (*Oncorhynchus kisutch*) and Chinook salmon (*O. tshawytscha*) and the ocean environment. Fisheries Oceanography **15**(1): 67-79.

Wells, B.K., Grimes, C.B., and Waldvogel, J.B. 2007. Quantifying the effects of wind, upwelling, curl, sea surface temperature and sea level height on growth and maturation of a California Chinook salmon (Oncorhynchus tshawytscha) population. Fisheries Oceanography **16**(4): 363-382.

West, C.J., and Larkin, P.A. 1987. Evidence for size-selective mortality of juvenile sockeye salmon (*Oncorhynchus nerka)* in Babine Lake, British Columbia. Canadian Journal of Fisheries and Aquatic Sciences **44**: 712-721.

Wetzel, C.R., and Punt, A.E. 2011. Performance of a fisheries catch-at-age model (Stock Synthesis) in data-limited situations. Mar. Freshw. Res. **62**(8): 927-936.

Williams, J.G. 2006. Central valley salmon: a perspective on Chinook and steelhead in the Central Valley of California. San Francisco Estuary & Watershed Science **4**(3).

Woolbright, L.L. 1983. Sexual selection and size dimorphism in anuran amphibia. American Naturalist **121**(1): 110-119.

Young, K.A. 2005. Life-history variation and allometry for sexual size dimorphism in Pacific salmon and trout. Proceeding of the Royal Society of London B **272**: 167-172.

Zabel, R.W., Scheuerell, M.D., McClure, M.M., and Williams, J.G. 2006. The interplay between climate variability and density dependence in the population viability of Chinook salmon. Conservation Biology **20**(1): 190-200.

Zar, J.H. 2010. Biostatistical analysis. Prentice-Hall/Pearson, Upper Saddle River, N.J.

Zeh, D.W. 1987. Aggression, density, and sexual dimorphism in Chernetid Pseudoscorpions (Arachnida, Pseudoscorpionida). Evolution **41**(5): 1072-1087.

Zeug, S.C., Albertson, L.K., Lenihan, H., Hardy, J., and Cardinale, B. 2011. Predictors of Chinook salmon extirpation in California's Central Valley. Fisheries Manag Ecol **18**(1): 61-71.

Zeug, S.C., Bergman, P.S., Cavallo, B.J., and Jones, K.S. 2012. Application of a Life Cycle Simulation Model to Evaluate Impacts of Water Management and Conservation Actions on an Endangered Population of Chinook Salmon. Environ. Model. Assess. **17**(5): 455-467.